SAIMM

THE SOUTHERN AFRICAN INSTITUTE OF MINING AND METALLURGY

VOLUME 119 NO. 7 JULY 2019

CAPACI OCCASIO

FOUNDED 1894

125 YEARS 1894 - 2019

UNIVERSITEIT iYUNIVESITHI STELLENBOSCH UNIVERSITY

100 1918 · 2018

ENGINEERING EZOBUNJINELI INGENIEURSWESE

UNIVERSITY OF THE WITWATERSRAND, JOHANNESBURG

CHE MET SCHOOL OF CHEMICAL AND METALLURGICAL ENGINEERING

Dave Tudor

The SAIMM bids farewell to Dave Tudor, Editor of the SAIMM *Journal* and Chair of the Publications Committee, who is relocating to the UK.

Dave hails from Oswestry, a historic market town in Shropshire, England, close to the Welsh border. He graduated from the University of Manchester Institute of Science and Technology (UMIST) with a degree in Chemical Engineering, and began his career with Anglo American in Zambia, where he worked at the Rokana smelter in Kitwe and the lead-zinc operation at Broken Hill (now Kabwe). Returning to the UK in 1977, he held a variety of positions – as a process engineer, an industrial engineer with Michelin Tyre, works manager of a custom powder milling operation, and as an expatriate recruitment officer for the Zambian mining industry. He moved to Canada in 1982 for a short spell with Hudson Bay Mining and Smelting, and then returned to Africa to join Anglo's Gold and Uranium Division at Vaal Reefs, moving successively to Freegold North, Amcoal (now Anglo Coal) New Vaal Colliery, and to the Johannesburg head office in 1997, from where he retired in 2003.

Dave's ten years as Editor have seen a number of far-reaching changes in the way the SAIMM *Journal* is produced and distributed, which have considerably enhanced the impact and accreditation of the *Journal*. Journal papers dating back to 1969, as well as conference proceedings, are now freely available on the SAIMM website to anyone, in line with one of the main strategic objectives of the SAIMM – to disseminate scientific and technical information to the benefit of the mining and metallurgical industries. There is an initiative currently underway to scan and upload all of the remaining historical copies of the *Journal* (dating from 1894). This is supported by the Carnegie Foundation (as part of their effort to get a wider range of African journals online) and Sabinet. Open access to older historical material will provide a rich source of information to readers who otherwise would have struggled to obtain it.

The reviewing process has been migrated to the Open Journal System (OJS), resulting in a substantially paper-free process to manage progress from submission to publication. Indexing of our *Journal* in the Directory of Open Access Journals (DOAJ benefits the Institute and its members through increased dissemination, and hence a wider audience for published papers and better visibility for the authors. The recent year-on-year improvement in our *Journal* Impact Factor and source-normalized impact per paper (SNIP) factor is a clear indication that the SAIMM *Journal* is finding a wider readership with each passing year.

The SAIMM *Journal* is listed in the OneMine global mining database, the Web of Science, Scopus, the African Journal Archive, and the Scientific Electronic Library Online (SciELO) SA, South Africa's premier open-access (free to access and to publish) searchable full-text journal database. Our *Journal* was accepted into the Directory of Open Access Journals (DOAJ) early in 2018. Accreditation with the Academy of Science of South Africa (ASSAf) and SciELO SA ensures that papers published in our *Journal* are recognized by the Department of Higher Education and Training (DHET) and are eligible for subsidization, a feature that is very important to academia in Southern Africa.

Together, these initiatives have raised the profile of the SAIMM *Journal* and contributed to it being recognized as one of the most respected mining technical publications in the world, ranked as a 'premier journal' by the international Society of Mining Professors (SOMP).

Dave has been a Fellow of the SAIMM since 2009, and in August 2017 he was elected Honorary Life Fellow.

The SAIMM extends its deepest thanks to Dave for his tireless devotion and enthusiasm. We shall miss him, and we wish him and his family everything of the best.

OFFICE BEARERS AND COUNCIL FOR THE 2018/2019 SESSION

Honorary President

Mxolisi Mgojo
President, Minerals Council South Africa

Honorary Vice Presidents

Gwede Mantashe
Minister of Mineral Resources, South Africa

Rob Davies
Minister of Trade and Industry, South Africa

Mmamoloko Kubayi-Ngubane
Minister of Science and Technology, South Africa

President

A.S. Macfarlane

President Elect

M.I. Mthenjane

Senior Vice President

Z. Botha

Junior Vice President

V.G. Duke

Incoming Junior Vice President

I.J. Geldenhuys

Immediate Past President

S. Ndlovu

Co-opted to Office Bearers

R.T. Jones

Honorary Treasurer

V.G. Duke

Ordinary Members on Council

I.J. Geldenhuys
C.C. Holtzhausen
W.C. Joughin
G.R. Lane
E. Matinde
H. Musiyarira
G. Njowa
S.M Rupprecht
N. Singh
A.G. Smith
M.H. Solomon
D. Tudor
A.T. van Zyl
E.J. Walls

Past Presidents Serving on Council

N.A. Barcza
R.D. Beck
J.R. Dixon
M. Dworzanowski
H.E. James
R.T. Jones
G.V.R. Landman
C. Musingwini
J.L. Porter
S.J. Ramokgopa
M.H. Rogers
D.A.J. Ross-Watt
G.L. Smith
W.H. van Niekerk
R.P.H. Willis

G.R. Lane–TPC Mining Chairperson
Z. Botha–TPC Metallurgy Chairperson

K.M. Letsoalo–YPC Chairperson
G. Dabula–YPC Vice Chairperson

Branch Chairpersons

Botswana	Vacant
DRC	S. Maleba
Johannesburg	D.F. Jensen
Namibia	N.M. Namate
Northern Cape	F.C. Nieuwenhuys
Pretoria	R.J. Mostert
Western Cape	L.S. Bbosa
Zambia	D. Muma
Zimbabwe	C. Sadomba
Zululand	C.W. Mienie

PAST PRESIDENTS

*Deceased

* W. Bettel (1894–1895)
* A.F. Crosse (1895–1896)
* W.R. Feldtmann (1896–1897)
* C. Butters (1897–1898)
* J. Loevy (1898–1899)
* J.R. Williams (1899–1903)
* S.H. Pearce (1903–1904)
* W.A. Caldecott (1904–1905)
* W. Cullen (1905–1906)
* E.H. Johnson (1906–1907)
* J. Yates (1907–1908)
* R.G. Bevington (1908–1909)
* A. McA. Johnston (1909–1910)
* J. Moir (1910–1911)
* C.B. Saner (1911–1912)
* W.R. Dowling (1912–1913)
* A. Richardson (1913–1914)
* G.H. Stanley (1914–1915)
* J.E. Thomas (1915–1916)
* J.A. Wilkinson (1916–1917)
* G. Hildick-Smith (1917–1918)
* H.S. Meyer (1918–1919)
* J. Gray (1919–1920)
* J. Chilton (1920–1921)
* F. Wartenweiler (1921–1922)
* G.A. Watermeyer (1922–1923)
* F.W. Watson (1923–1924)
* C.J. Gray (1924–1925)
* H.A. White (1925–1926)
* H.R. Adam (1926–1927)
* Sir Robert Kotze (1927–1928)
* J.A. Woodburn (1928–1929)
* H. Pirow (1929–1930)
* J. Henderson (1930–1931)
* A. King (1931–1932)
* V. Nimmo-Dewar (1932–1933)
* P.N. Lategan (1933–1934)
* E.C. Ranson (1934–1935)
* R.A. Flugge-De-Smidt (1935–1936)
* T.K. Prentice (1936–1937)
* R.S.G. Stokes (1937–1938)
* P.E. Hall (1938–1939)
* E.H.A. Joseph (1939–1940)
* J.H. Dobson (1940–1941)
* Theo Meyer (1941–1942)
* John V. Muller (1942–1943)
* C. Biccard Jeppe (1943–1944)
* P.J. Louis Bok (1944–1945)
* J.T. McIntyre (1945–1946)
* M. Falcon (1946–1947)
* A. Clemens (1947–1948)
* F.G. Hill (1948–1949)
* O.A.E. Jackson (1949–1950)
* W.E. Gooday (1950–1951)
* C.J. Irving (1951–1952)
* D.D. Stitt (1952–1953)
* M.C.G. Meyer (1953–1954)
* L.A. Bushell (1954–1955)
* H. Britten (1955–1956)
* Wm. Bleloch (1956–1957)
* H. Simon (1957–1958)
* M. Barcza (1958–1959)
* R.J. Adamson (1959–1960)
* W.S. Findlay (1960–1961)
* D.G. Maxwell (1961–1962)
* J. de V. Lambrechts (1962–1963)
* J.F. Reid (1963–1964)
* D.M. Jamieson (1964–1965)
* H.E. Cross (1965–1966)
* D. Gordon Jones (1966–1967)
* P. Lambooy (1967–1968)
* R.C.J. Goode (1968–1969)
* J.K.E. Douglas (1969–1970)
* V.C. Robinson (1970–1971)
* D.D. Howat (1971–1972)
* J.P. Hugo (1972–1973)
* P.W.J. van Rensburg (1973–1974)
* R.P. Plewman (1974–1975)
* R.E. Robinson (1975–1976)
* M.D.G. Salamon (1976–1977)
* P.A. Von Wielligh (1977–1978)
* M.G. Atmore (1978–1979)
* D.A. Viljoen (1979–1980)
* P.R. Jochens (1980–1981)

G.Y. Nisbet (1981–1982)
A.N. Brown (1982–1983)

* R.P. King (1983–1984)

J.D. Austin (1984–1985)
H.E. James (1985–1986)
H. Wagner (1986–1987)

* B.C. Alberts (1987–1988)
* C.E. Fivaz (1988–1989)
* O.K.H. Steffen (1989–1990)
* H.G. Mosenthal (1990–1991)

R.D. Beck (1991–1992)

* J.P. Hoffman (1992–1993)
* H. Scott-Russell (1993–1994)

J.A. Cruise (1994–1995)
D.A.J. Ross-Watt (1995–1996)
N.A. Barcza (1996–1997)

* R.P. Mohring (1997–1998)

J.R. Dixon (1998–1999)
M.H. Rogers (1999–2000)
L.A. Cramer (2000–2001)

* A.A.B. Douglas (2001–2002)

S.J. Ramokgopa (2002-2003)
T.R. Stacey (2003–2004)
F.M.G. Egerton (2004–2005)
W.H. van Niekerk (2005–2006)
R.P.H. Willis (2006–2007)
R.G.B. Pickering (2007–2008)
A.M. Garbers-Craig (2008–2009)
J.C. Ngoma (2009–2010)
G.V.R. Landman (2010–2011)
J.N. van der Merwe (2011–2012)
G.L. Smith (2012–2013)
M. Dworzanowski (2013–2014)
J.L. Porter (2014–2015)
R.T. Jones (2015–2016)
C. Musingwini (2016–2017)
S. Ndlovu (2017–2018)

Honorary Legal Advisers
Scop Incorporated

Auditors
Genesis Chartered Accountants

Secretaries
The Southern African Institute of Mining and Metallurgy
Fifth Floor, Minerals Council South Africa
5 Hollard Street, Johannesburg 2001 • P.O. Box 61127, Marshalltown 2107
Telephone (011) 834-1273/7 • Fax (011) 838-5923 or (011) 833-8156
E-mail: journal@saimm.co.za

Editorial Board
R.D. Beck
P. den Hoed
B. Genc
R.T. Jones
W.C. Joughin
H. Lodewijks
C. Musingwini
S. Ndlovu
J.H. Potgieter
N. Rampersad
T.R. Stacey
M. Tlala

Editorial Consultant
D. Tudor

Typeset and Published by
The Southern African Institute of Mining and Metallurgy
P.O. Box 61127
Marshalltown 2107
Telephone (011) 834-1273/7
Fax (011) 838-5923
E-mail: journal@saimm.co.za

Printed by
Camera Press, Johannesburg

Advertising Representative
Barbara Spence
Avenue Advertising
Telephone (011) 463-7940
E-mail: barbara@avenue.co.za

ISSN 2225-6253 (print)
ISSN 2411-9717 (online)

Directory of Open Access Journals

THE INSTITUTE, AS A BODY, IS NOT RESPONSIBLE FOR THE STATEMENTS AND OPINIONS ADVANCED IN ANY OF ITS PUBLICATIONS.

Copyright© 2018 by The Southern African Institute of Mining and Metallurgy. All rights reserved. Multiple copying of the contents of this publication or parts thereof without permission is in breach of copyright, but permission is hereby given for the copying of titles and abstracts of papers and names of authors. Permission to copy illustrations and short extracts from the text of individual contributions is usually given upon written application to the Institute, provided that the source (and where appropriate, the copyright) is acknowledged. Apart from any fair dealing for the purposes of review or criticism under ***The Copyright Act no. 98, 1978, Section 12,*** of the Republic of South Africa, a single copy of an article may be supplied by a library for the purposes of research or private study. No part of this publication may be reproduced, stored in a retrieval system, or transmitted in any form or by any means without the prior permission of the publishers. ***Multiple copying of the contents of the publication without permission is always illegal.***

U.S. Copyright Law applicable to users In the U.S.A.
The appearance of the statement of copyright at the bottom of the first page of an article appearing in this journal indicates that the copyright holder consents to the making of copies of the article for personal or internal use. This consent is given on condition that the copier pays the stated fee for each copy of a paper beyond that permitted by Section 107 or 108 of the U.S. Copyright Law. The fee is to be paid through the Copyright Clearance Center, Inc., Operations Center, P.O. Box 765, Schenectady, New York 12301, U.S.A. This consent does not extend to other kinds of copying, such as copying for general distribution, for advertising or promotional purposes, for creating new collective works, or for resale.

SAIMM
THE SOUTHERN AFRICAN INSTITUTE OF MINING AND METALLURGY
FOUNDED 1894
125 YEARS 1894 - 2019

VOLUME 119 NO. 7 JULY 2019

Contents

Journal Comment: The Public Funding of Research
by R.L. Paul. iv

President's Corner: The uprising of the Youth
by A.S. Macfarlane . . . . . v–vii

Why the small-span small-pillar (sssp) concept for underground mining?
F.S.A. de Frey. . . . . viii–ix

STUDENT PAPERS

Hydrothermal preparation of biochar from spent coffee grounds, and its application for the removal of cadmium from coal tailings leachate
E. Fosso-Kankeu, R. Weideman, D. Moyakhe, F.B. Waanders, M. Le Roux, and Q.P. Campbell. 607

Biochar prepared from spent coffee grounds was pre-treated by surfactant impregnation with sodium dodecyl sulphate, and the adsorption behaviour and capacity for removal of cadmium from solution by both the untreated biochar were determined through adsorption isotherms, transport kinetics, and thermodynamic studies. The pre-treated biochar showed potential as an adsorbent and could be considered for use in the treatment of metal-polluted effluents.

Determination of optimal fragmentation curves for a surface diamond mine
K.M. Phamotse and A.S. Nhleko. 613

Optimum fragmentation after blasting must be achieved to produce a run-of-mine (ROM) feed that does not choke the crusher and cause delays in production. The Kuz-Ram model is used to predict the fragmentation at the mine. Results showed that the blast design parameters, as well as the execution of the drilling and blasting, may be the cause of the fragmentation problems. It was concluded that the blast design parameters need to be reviewed.

Developing a mining plan for restarting the operation at Uis mine
J.H. Maritz and S. Uludag. 621

A mining plan was required for phase 1 of the Uis Tin Project. The mine design criteria were determined and used as input to generate the mine design by utilizing professional engineering software. A 5-year production schedule was developed and the mobile mining equipment requirements calculated, and recommendations made for implementing the 5-year mining plan.

Optimization of the cycle time to increase productivity at Ruashi Mining
I.N.M. Nday and H. Thomas. 631

An on-site investigation was conducted to determine the actual cycle time components of queuing time, loading time, hauling time, and dumping time of the articulated dump trucks. By applying Systems Thinking to the cycle time, man-made constraints in the actual cycle time were identified and recommendations to mitigate them were suggested to optimize the cycle time.

International Advisory Board
R. Dimitrakopoulos, McGill University, Canada
D. Dreisinger, University of British Columbia, Canada
M. Dworzanowski, Consulting Metallurgical Engineer, France
E. Esterhuizen, NIOSH Research Organization, USA
H. Mitri, McGill University, Canada
M.J. Nicol, Murdoch University, Australia
E. Topal, Curtin University, Australia
D. Vogt, University of Exeter, United Kingdom

SAIMM
THE SOUTHERN AFRICAN INSTITUTE OF MINING AND METALLURGY
FOUNDED 1894
125 YEARS 1894 - 2019
VOLUME 119 NO. 7 JULY 2019

PAPERS OF GENERAL INTEREST

The state of mine closure in South Africa – what the numbers say
I. Watson and M. Olalde 639

A list of mine closure certificates applied for between 2011 and 2016 and a list of certificates granted over the same period for all nine regions of South Africa were obtained. Analysis of this data showed that the mine closure system as implemented in South Africa is largely ineffective. Furthermore, the issuing of closure certificates varies significantly among the regional offices, with the success rate for applications being generally low and issuing of certificates taking an extended period.

Stability considerations for slopes excavated in fine hard soils/soft rocks at Cobre Las Cruces mine, Sevilla, Spain
S. Cooper, M.D. Rodriguez, J.M. Galera, and V. Pozo 647

At Cobre Las Cruces mine, a combination of substantially soft rock and more competent, older lithologies presents substantial challenges in maintenance of slope stability and, therefore, operative safety at the mine site. This paper describes the fundamental design, excavation, and monitoring measures implemented to maintain safe production and the lessons learnt during the mine development.

The effects of froth depth and impeller speed on gas dispersion properties and metallurgical performance of an industrial self-aerated flotation machine
H. Naghavi, A. Dehghani, and M. Karimi 661

A factorial experimental design was used to study how the gas dispersion properties, froth retention time, and flotation performance respond to changes in froth depth and impeller speed. The interaction effects of the froth depth and impeller speed were also established, which allowed a strategy to be developed for operating self-aerated flotation machines, based on varying the froth depth and impeller speed with regard to the cell duty.

A proposed preliminary model for monitoring hearing conservation programmes in the mining sector in South Africa
N. Moroe, K. Khoza-Shangase, M. Madahana, and O. Nyandoro 671

Occupational noise-induced hearing loss (ONIHL) is classified as the leading work-related disability in the mining industry. This study proposes the use of a feedback-based noise monitoring model as a tool for monitoring and managing ONIHL in the mining sector in South Africa. The model could also form part of an early intervention and management strategy for of ONIHL in the workplace.

Coal pillar strength analysis based on size at the time of failure
J.N. van der Merwe 681

The paper describes an investigation where the rate of pillar scaling was applied to the pillars in the data bases of failed and unfailed pillars. An equation for pillar strength which predicts significantly greater pillar strength than the previous statistical analyses was developed. It was concluded that the lower strengths found by previous statistical analyses are due to the incorrect pillar width being used, and that by adjusting the pillar sizes to compensate for scaling, more credible results that correspond to direct testing are obtained.

The Public Funding of Research

The *Journal* this month is referred to as the 'Student Edition', as the papers are the published output of students registered for university degrees in various minerals-related subjects across Southern Africa. As one might expect, the topics of the research cover a broad spectrum ranging from mine planning, optimization of mining operations, productivity, safety, mineral processing, environmental treatment of wastewaters, to even the recycling of electronic scrap.

Our universities face increasing financial pressure brought about by a number of factors which include government pressure to withhold or cap annual fee increases, the promise of free tertiary education for all those who passed the National Senior Certificate with a university entrance, and the lowering of the bar for university entrance by the scrapping of the list of 'designated subjects' by the government in March 2018 (which increased the number of students qualifying for university entrance by 18 000 compared to the previous year[1]).

Obviously, universities are expected to develop balanced and sustainable annual operating and capital budgets, but this is not an easy task given the aforementioned financial pressures. Faculties such as Science and Engineering have to cope with added pressures, as they must provide laboratory facilities for undergraduate and postgraduate teaching and research purposes. Particularly in the area of postgraduate research, students and staff are required to prepare numerous research proposals for public and private funding necessary for the students to live and the university to provide the facilities, equipment, and operating costs to conduct the research.

As members of the SAIMM, we can take some pleasure in reading the student papers in this issue of the *Journal* covering such a breadth of subject material, and feeling that the human resource capability required to sustain the mining industry is already in the making. But we should not be complacent.

And so it is with some interest that I read an article in the Johannesburg Star newspaper of 27 February 2019 which was reporting on research conducted at the University of Pretoria (UP) into the public funding of research. The article starts with the statement that: 'The government has outlined new policy objectives around science, technology and innovation. These are in draft form and will soon appear in a new White Paper. The vision of the policy is the use of science and technology to drive the sustainable and inclusive development of South Africa.'

Excellent – I can't wait to read the White Paper. The article then continues with a summary of the UP research, and I must quote from the newspaper article as I have not seen the actual PhD research report from UP. They key points are as follows (I quote verbatim):

- There are seven councils which collectively consume 55% of government's research budget. [The science councils of relevance to the mining industry would be the Council for Geoscience, Mintek, and the CSIR].
- Work recently completed for the National Treasury reveals that since 2003, science councils have become expensive and often unproductive institutions……It is clear from the trend that in 2014 the science councils became the most expensive performers in the system, and are now almost three times the unit cost of universities.
- The problem is that the model used to create these science councils is outdated. Today, universities fulfil many of the councils' roles at a much lower cost and also add value by simultaneously training postgraduate students.
- Our work suggests that closing under-performing science councils could achieve two important goals. First, the public budget for R&D will be enhanced because at least a portion of the R6 billion funding can be redirected to universities and the private sector. Second, the country's ability to absorb new technologies and knowledge will be strengthened.
- The analysis for National Treasury was done using the programme evaluation approach of Performance Expenditure Reviews……The Treasury review involved benchmarking the public-funded R&D system. The findings suggested that the science councils are unproductive and need to be either closed or their resources redirected.

I was not aware of this performance review conducted by, or on behalf of, the National Treasury. It is not quite clear to me whether it is openly stated in the Treasury review that science councils should be 'either closed or their resources redirected', or whether this was inferred by the authors of the UP research (I suspect the latter). Either way, the statement is blunt and uncompromising – most un-government-like, if you know what I mean. Was I the only one sleeping on my watch? Or did most of you miss this too?

Our science councils were established at a completely different time in South Africa's history, undoubtedly fulfilled their mandate at that time, and some have achieved an international reputation for their research output. But time and reputation do not stand still – financial pressures have not been kind to similar public research organizations in the USA, Canada, the UK, and elsewhere, which were created to service the mining aspirations of those countries. Should South Africa not take a strong dose of introspection and re-evaluate the value added by these science councils in relation to other options of using the public funds? Of course we should. The debate on this subject should move into the public domain, and be conducted openly, honestly, dispassionately, objectively, and scientifically. We expect nothing less.

R.L. Paul

[1]https://www.dailymaverick.co.za/article/2019-01-07-increase-in-2018-matric-bachelors-passes-means-universities-headed-for-a-perfect-storm/

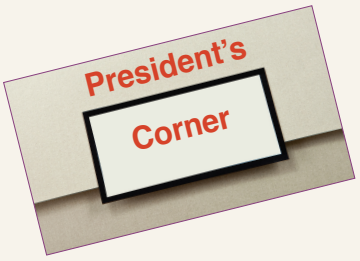

The uprising of the Youth

Although this edition is for the month of July, at the time of writing we are approaching the public holiday of Youth Day.

As we should all know, Youth Day in South Africa, celebrated on 16 June, is a public holiday that commemorates an event which resulted in a wave of protests across the country, known as the Soweto uprising of 1976. On this day, between 3000 and 10 000 protestors mobilized by the South African Students Movements Action Committee, and supported by the Black Consciousness Movement' marched peacefully to demonstrate and protest against the government-of-the-day's directive to make the Afrikaans language alongside English the compulsory medium of instruction in schools in 1974.

The marchers, on their way to Orlando stadium, were met by heavily armed police who attempted to blockade the march, and then opened fire on the protestors. In this conflict, 13 year-old Hector Peterson was one of the first to be shot dead, and the image of him being carried by Mbuyisa Makhubo has become the tragic and pathetic symbol of the uprising. Consequential to this day, police estimated that 150 protestors were killed, but other estimates escalate this number to as many as 700.

This dreadful day in South African history has its roots in the Bantu Education system developed by the apartheid regime that came to power in 1948 and which culminated in the Bantu Education Act of 1953, which created a separate education system for 'blacks', as designed by H.F. Verwoerd who postulated 'There is no place for (the African) in the European community above the level of certain forms of labour. It is of no avail for him to receive a training which has, as its aim, absorption in the European community'.

In retrospect, one can but marvel at the courage of the protestors, who felt with deep conviction, the need to dictate their own future, as opposed to it being dictated to them. One can also only feel a sense of national shame that such a thing could have happened.

Obviously, our South African Youth Day must continue to reflect on the events of 1976, because, as Marcus Garvey stated, 'A people without the knowledge of their past history, origin and culture is like a tree without roots'. Michelle Obama said 'You may not always have a comfortable life, and you will not always be able to solve all of the world's problems at once, but don't ever underestimate the importance you can have because history has shown us that courage can be contagious and hope can take on a life of its own'.

However, we must also use the day (and every day) to ensure our youth are, on the one hand given a sustainable world to live in, while at the same time afforded the opportunity to shape their own future, and that of the world. The dues that we, as a society, have to pay for the past need to be invested in the future of today's youth.

International Youth Day is celebrated on 12 August, and is an awareness day designated by the General Assembly of the United Nations in 1999. It serves as an annual celebration of the role of young women and men as essential partners in change, and an opportunity to raise awareness of challenges and problems facing the world's youth.

This year's theme is 'Transforming Education' to highlight efforts to make education more inclusive and accessible for all youth, including efforts by youth themselves. This is a far cry from the events and causes of the 1976 uprising in South Africa, as it calls on the youth themselves to create their own future. The theme is rooted in Goal 4 of the 2030 Agenda for Sustainable Development which is 'to ensure inclusive and equitable quality education and promote lifelong learning opportunities for all'. The aim of the day is to examine how governments, young people, and youth-led and youth-focused organizations, as well as other stakeholders, are transforming education so that it becomes a powerful tool to achieve the 2030 Agenda for Sustainable Development.

This is all against the reality that there are currently 1.8 billion young people between the ages of 10 and 24 in the world, which is the largest youth population ever. However, one in ten of the world's children live in conflict zones, and 24 million of them are out of school. Political instability, labour market challenges, and limited space for political and civil participation have led to the increasing isolation of youth in societies.

In South Africa, our youth unemployment rate, according to Stats SA, stands at a staggering 55.2% as at the end of March 2019, with the overall official unemployment rate at 27.6%. Stats SA estimated graduate unemployment in 2018 to stand at 33.5%.

Closer to home, there are various unconfirmed estimates that, in the mining industry in South Africa, there are up to 300 qualified mining engineers who are unemployed. A similar situation exists with geologists.

So what can we take away from this, apart from deep depression, and how can we as an Institute and an industry support Goal 4? Let's consider this firstly from the supply and demand side, for the mining industry.

Firstly, on the supply side, there seems to be a dichotomy in that we have so many young people, many of whom are competent and capable of embracing Industrial Revolution 4.0, and qualified, but whose qualifications may not be appropriate for the modernized industry. This could either be because the qualifications are out of date and irrelevant, or because the industry is not ready for change in terms of the skills and development programmes it will require.

On the other hand, it may merely be an oversupply of qualified people into a market that is not hungry for these skills, because of the state of the industry. This reflects an out-of-synch situation between the pipeline of graduates created in upswings in the cycle and the reduced requirements of offtake because of downswings during the creation of the pipeline. While the industry is at the behest of the commodity cycle, this means that either the cycles need to be better matched, or that alternative career paths be made available, either in manufacturing, research, or entrepreneurship.

In terms of qualifications, there are numerous examples of where this is definitely the case, where Certificates of Competency in particular require modernizing to take account of digital developments and technologies, and where syllabi at tertiary institutions and training organizations require updating. In some cases, such as at Wits, this has already started, but in the case of certificates and TVET qualifications, there is an urgent need for attention.

Developing this change is a tedious process, which requires dedicated volunteers on the one hand to step forward and say 'Ï will help with that', while on the other hand requiring that bureaucratic processes do not stand in the way of progress.

The SAIMM established the Scholarship Trust Fund, in 2002. Since 2004, contributions of R3 million have been dispersed to needy university students who do not have bursaries – unfortunately, an increasing number year-on-year. This helps them with tuition, meals, supplies, travel, accommodation *etc*. Members are encouraged to continue to support this needy cause, and the Institute will continue to find ways in which more funds can be raised.

Clearly, the area of basic education requires urgent attention in terms of relevance, accessibility, affordability, and quality, but that is a matter which requires a collective will to prioritize and fix, in a national discussion.

On the demand side, industry readiness for IR4.0 and the kind of training and development, and career paths that are required is an area requiring attention, where new work structures and career pathways need to be developed so that these are relevant, value adding, and lead to retention of skills.

In these areas, it is pleasing that the Young Professionals Council of the SAIMM has been active, both in terms of university course modernization and with the origination of a new graduate development programme, which still is to be rolled out to Council and industry.

Our industry is facing many challenges in terms of productivity, cost, profitability, and health and safety. Additionally, it faces ever-increasing pressure to create a sustainable post-mining landscape that embraces the surrounding communities and identifies opportunities for local industrialization and agri-business development.

These challenges demand many new skills sets, including social sciences, economics, data science, and information management. They also require effort in research and development, and innovation,

and the resources to effect this. Significantly, this requires the industry to identify new and appropriate career paths in these areas, and the development of a hunger to utilize these skills to allow the mining companies to become the modern corporate citizens that they aspire to be.

In the R&D space, we need to engender a culture of innovation and change, and there are no better people to drive this than our inquisitive millennials, who should be encouraged to challenge the status quo every step of the way. This can be done either by examination of the internal culture of organizations, or through structures and processes that allow these ideas to flow through to real change and implementation.

Companies, whether mining and mineral processing companies, universities, research institutions, equipment manufacturers, financial institutions, and consulting companies operating in the mining space should embrace the youth through establishing internships and creating opportunities for innovation and development.

As a practical example, it would be wise for the Mining Qualifications Authority to divert monies currently allocated to undergraduate studies to the funding of internships and research, to be conducted by the very people who were funded to study at undergraduate level, but who now are unemployed.

A further area where the YPC is active is that of entrepreneurship and leadership. Despite their aspirations, not all young mining professionals can become mine owners or CEOs. Alternative opportunities for young people with entrepreneurial appetites should include establishing new companies in the mining supply chain, an area strongly supported by the Mining Charter 3 requirements and by the Departments of Labour, Science, Technology, and Higher Education, and Trade and Industry. While the YPC has driven this vision through the Entrepreneurship in the Minerals Industry Conference series (with this year's event on 31 July), they should be encouraged through wide support, but also driven by a collective effort to encourage and develop entrepreneurs through incubation processes and facilities. This collective effort should include mining companies, mining equipment manufacturers, MEMSA, SAMPEC, and the state departments mentioned above, all in the name of enterprise development.

The SAIMM will continue to support the YPC, but even more so, and every member of the Institute is encouraged to support them, their mentorship programme, the scholarship trust fund, and in any way that will make a difference.

Our youth are the leaders of the future. One thing is for certain, and that is that the future will be very different from the present. We must now prepare the ground so that, together with our youth, we can co-create the future while embracing their vision of the future.

A.S. Macfarlane
President, SAIMM

Why the small-span small-pillar (sssp) concept for underground mining?

Introduction

By this time it is common knowledge that seismic events pose major risks for mineworkers, mines, and the public in the mining areas. The qualification and/or quantification of these risks to my mind are immaterial. The main objective should be to eliminate or control the causes of rockfalls and seismic events to the best of our ability. The mining fraternity should give more attention to removing or managing the causes of rockfalls and seismic events instead of mitigating the results.

Having worked on Crown Mines and East Rand Proprietary Mine, which was at that time (1952 to 1977) the deepest mine in the world, and being involved in rescue work underground after seismic events, I took a personal interest in this phenomenon.

After a considerable amount of research and following the development of the mines' efforts to address the problem of seismic events, I came to the conclusion as a production manager that *the major cause of seismic events was the excessive spans that were created during the stoping operations*. The challenge was to find a mining method (layout) that would enable the mines to keep spans between pillars to the minimum without jeopardizing profitability because of an unacceptable extraction ratio.

After the rock mechanics published their findings that a pillar in quartzite with a size to width ratio of 10:1 for a stoping width of 1 m should be indestructible, I put forward the idea of a pillar and stall method to the then Chamber of Mines Research Organisation.

The formation of a mine seismicity expert panel

This is a very commendable thought, provided it does not become another exercise in which a large amount of money is spent on the detail and intricacies of the different theories that are constantly being put forward for further investigation, which would be another of those nice-to-know exercises without presenting a real add-on value.

Why the small-span small-pillar concept?

The sssp method of mining comprises an array of small pillars left as support with the minimum span between pillars.

The cutting of pillars and stalls is looked upon as an unnecessary exercise, which will interfere with productivity and the extraction ratio of the orebody.

When this mining layout was compared with other known layouts for deep mines it proved to be the better layout, and in most cases where it has been accepted as practice in the platinum mines it has been found to be working well, with the added advantage of mechanized mining and fewer production delays due to 'backbreaks'.

To describe the progress of the SSSP concept I will set it out in chronological order, together with a brief summary of the findings and conclusions.

1993

Letter to the Government Mining Engineer dated 26 February 1993, written by F.S.A. de Frey. Reports on fatal accidents caused by seismic events on gold mines in the Carletonville area.

Conclusions:

The challenge is therefore to prevent seismic events or at least control the occurrence of seismic events by maintaining the state of equilibrium and stability in the mine at all times.

'If a board and pillar system can maintain the above stability, mining of the VCR and carbon leader at the same time should present no major problems.'

Letter from CSIR Mining Technology dated 4 May 1993.

'*I believe that your idea does warrant further attention and investigation, and that you should carry out the modeling yourself.*' [Signed] Duncan Adams.

Letter from J.A. Ryder dated 17 June 1993. Using BEPIL modelling.

'*4.1 The concept of using a dense array of strong squat pillars in mining at great depth has a number of extremely attractive features: minimal regional disturbance to the rockmass, with consequent low closure, ERR and field stress levels, and tolerable pillar foundation stress levels. Imponderables such as nature of hangingwall fracturing and incidence of damaging seismicity might best be evaluated on an actual field trial basis*'.

1995

Authors' reply to discussion on *Design of pillar systems in South Africa* by M.U. Ozbay, J.A. Ryder, and A.J. Jager. *Journal of the South African Institute of Mining and Metallurgy*, July/August 1995.

'*We agree wholeheartedly that further research, together with carefully planned field trials, is warranted in pursuit of this potentially highly rewarding concep*t.'

1997

Report from G.S. Esterhuizen, dated 20 June 1997. Using MINSIM-D stress analysis program.

Conclusions:

'It is concluded that bord and pillar layout at a depth of 3000 m will have minimal effects on the surrounding rock mass ... The proposed bord and pillar layout will result in extremely low levels of energy release rate, will have no destabilizing effects on geological structures, barring local instability. The layout will allow pre-development of tunnels at depths of 25 m 30 m below the reef. These tunnels will be safe from stresses induced by unmined geological structures on the reef plane.'

1998

A.R. Leach. Numerical evaluation of room and pillar mining methods in deep level mining. Completed as part of Deep-mine Task 3.2.1. CSIR Division of Mining Technology, Johannesburg, 31 December 1998.

Leach expressed doubts about the rock condition in close proximity to the sidewalls of the pillars. He concluded that it should not exceed the depth of 6 m in any normal longwall at depth.

1999

F.S.A. de Frey. Evaluation of bord and pillar as a mine design alternative for ultra-deep mines. Report on Deepmine task 3.2.1, March 1999. Submitted to F. Viera.

De Frey found that taking all the critical factors into consideration the only real problem would be the difficulty of ventilating mini-backstopes until the next holing for through ventilation is established. This was applicable only when the mining method was up-dip strike face stoping. Using overhand strike mining did not present a problem and is at present (2009) being successfully applied at the Amplats Waterval platinum mine.

2002

'Examine the criteria for establishing the small span small pillar concept as a safe mining method in deep mines'. SIMRAC GAP 828, January 2002

De Frey, Handley, and Webber expanded on the findings of the Deepmine project. So much time and effort was spent on proving that it was feasible to design a mine based on the sssp concept that the advantages of the *design from a seismic event* point of view did not get the necessary attention, and to my mind the real advantage was clouded by a lot of mining issues. In the end it was concluded that sssp compared very favourably on all the critical issues but that the main issue might be the possibility of pillar failures.

De Frey is of the opinion that this argument carries no weight if you compare all the other advantages from a seismic event point of view. It could only provide safer conditions from a seismic event or rockfall point of view.

2008

B.P. Watson *et al*. Merensky pillar strength formulae based on back-analysis of pillar failures at Impala Platinum. *Journal of the South African Institute of Mining and Metallurgy*, volume 108, August 2008.

The authors did an excellent job but to my mind are still only concentrating on the strength of the pillars and not giving the necessary attention to the effect of the spans between the pillars and their effect on the strength of the pillars.

F.S.A. de Frey
Mine Engineering Consultant

TAKE CONTROL OF YOUR WATER

There's nothing worse than an unknown variable and there's nothing more variable than water. Floods, torrential downpours, moving water from A to B – it can very quickly get out of control. That's why the Weir Minerals team works tirelessly with sites to design tailored dewatering solutions. We use our expertise in both process and products to maximise efficiency and help you take control of your water.

Learn more at dewateringsolutions.weir

Copyright © 2019, Weir Minerals Australia Limited. All rights reserved.

WEIR

DEWATERING SOLUTIONS
Minerals
www.minerals.weir
www.weirafricastore.com

Hydrothermal preparation of biochar from spent coffee grounds, and its application for the removal of cadmium from coal tailings leachate

E. Fosso-Kankeu[1*], R. Weideman[1], D. Moyakhe[1], F.B. Waanders[1], M. Le Roux[2], and Q.P. Campbell[2]

[*]Paper written on project work carried out in partial fulfilment of B.Eng (Chemical Engineering) degree

Affiliation:
[1]Water Pollution Monitoring and Remediation Initiatives Research Group in the School of Chemical and Minerals Engineering of the North West University, Potchefstroom, South Africa.
[2]Coal beneficiation Research Group in the School of Chemical and Minerals Engineering of the North West University, Potchefstroom, South Africa.

Correspondence to:
E. Fosso-Kankeu

Email:
Elvis.FossoKankeu@nwu.ac.za
elvisfosso.ef@gmail.com

Dates:
Received: 19 Nov. 2018
Revised: 28 Feb. 2019
Accepted: 7 Mar. 2019
Published: July 2019

How to cite:
Fosso-Kankeu, E., Weideman, R., Moyakhe, D., Waanders, F.B., Le Roux, M., and Campbell, Q.P. Hydrothermal preparation of biochar from spent coffee grounds, and its application for the removal of cadmium from coal tailings leachate.
The Southern African Insitute of Mining and Metallurgy

DOI ID:
http://dx.doi.org/10.17159/2411-9717/449/2019

ORCiD ID:
E. Fosso-Kankeu
https://orchid.org/0000-0002-7710-4401

Synopsis

Spent coffee grounds were transformed into biochar using a hydrothermal method. Some of the biochar product was pre-treated through surfactant impregnation with sodium dodecyl sulphate (SDS) to enhance its adsorption capacity. The non-treated(NT) and pre-treated(PT) biochars were characterized using FTIR spectroscopy and SEM-EDS analyses, which revealed that the products had the potential for adsorption of heavy metals from solution and confirmed the successful impregnation of biochar with SDS surfactant. The two adsorbents were then used for the removal of cadmium from solution and the adsorption behavior and capacity determined through adsorption isotherm, kinetic, and thermodynamic studies. It was found that the cadmium was adsorbed in several concentric layers on the surface of the adsorbents through a chemisorption mechanism. The PT biochar was identified as a superior adsorbent, with a capacity of q_e = 10.67 mg/g compared to the NT biochar with q_e = 4.82 mg/g. The adsorption of cadmium onto the PT biochar was further determined to be spontaneous and endothermic. It was therefore concluded that the PT biochar shows potential as an adsorbent and could be considered for implementation in the treatment of metal-polluted effluents.

Keywords
spent coffee grounds, biochar, surfactant impregnation, cadmium, coal tailings leachate, adsorption.

Introduction

Coal mining operations are notorious for producing large amounts of waste tailings, which are disposed of in the form of a slurry on tailings dams. This inadvertently contributes towards environmental problems (Jin, Mansour, and Thomas, 2017). Heavy metals are one of the most common pollutants that originate from solid mine waste disposal facilities, and these can leach into groundwater supplies, contaminating them and rendering the water unsuited for human consumption (Salomons, 1995). Cadmium occurs in conjunction with metalliferous ores and can cause severe damage to agricultural soils and drinking water supplies in the vicinity of mining sites (Dudka *et al.*, 1995). It has a tendency to migrate into the surrounding vegetation, which in turn can cause harm to humans and animals when consumed (Marquez *et al.*, 2018).

Precipitation and coagulation methods are widely used to remove heavy metals from aqueous solutions. The drawback of these processes is that they generates large amounts of low-density aerated sludge, which give rise to dewatering and disposal problems (Fu and Wang, 2011). Membrane filtration is another very effective method for removing heavy metals from wastewater. A huge disadvantage of this technology is the high costs involved. That said, the method is still widely considered due to it is simplicity and flexibility in plant design and operation (Fu and Wang, 2011). Other methods for the removal of heavy metals from solutions include ion exchange, electrodeposition, reverse osmosis, and electroplating (Redwscu and Nicolae, 2012). The implementation of all these processes is hindered by the high capital and/or operational costs involved.

Adsorption is an effective and economical way to remove heavy metals from wastewater. Due to adsorption being reversible in some cases, it is possible to regenerate the adsorbent by stripping of the

adsorbed species and re-using it (Fu and Wang, 2011). Activated carbon (AC) is a widely used adsorbent for the removal of heavy metals from solution in the wastewater treatment sector (Jusoh *et al*., 2007; Kang *et al*., 2008). The main concern with activated carbon is that it remains an expensive material, with prices still on the increase.

An alternative adsorption method makes use of biochar for the removal of heavy metals from wastewater. The benefits of using biochar include its low production costs, availability of a wide range of feedstocks, diversity of the biochar with each type of feedstock, and mechanical and thermal stability (Mohan *et al*., 2015). Biochar can be produced using organic materials as a feedstock. One of these materials is spent coffee grounds. Over 120 million bags of coffee are produced worldwide each year , which correspond to 7 Mt of coffee waste (Zuorro and Lavecchia, 2012). These spent coffee grounds have no commercial value and are usually sent to compost facilities for disposal (Zuorro and Lavecchia, 2012). This makes spent coffee grounds an abundant feedstock available for the production of biochar. To improve the adsorption capabilities of the char, sodium dodecyl sulphate (SDS) is impregnated on the surface of the char by means of a physico-chemical pretreatment process. The addition of SDS will increase the amount of potential bonds on the char's surface, which may lead to an improvement of its sorption capacity (Fosso-Kankeu *et al*., 2017a).

Experimental

Biochar production

A slurry of spent coffee grounds was prepared for a 3 vol% biomass loading. The slurry was mixed with reverse osmosis (RO) water to produce 60 L of solution. RO water is used instead of tap water to prevent damage to the stainless steel inside the reactor due to the high chlorine content of normal tap water. The slurry was then soaked overnight.

The hydrothermal liquefaction (HTL) reactor tanks were filled with 60 L of slurry, sealed, and pressurized with nitrogen gas (baseline 5.0 bar) to 90 bar, and the reactor temperature was increased to 305°C. As soon as the reactor reached target temperature the flow of slurry from the tanks to the reactor was set to 120 L/h. This gave the slurry a residence time of 10 minutes inside the 20 L reactor vessel.

After all the slurry had flowed through the reactor it was switched off and left to cool overnight. The tanks were then depressurized and the product was sampled.

The HTL plant product is a mixture of an aqueous oil phase and biochar solid phase. The biocrude was separated from the aqueous phase by pressure filtration. The filtered biocrude was then dissolved in acetone to separate it from the biochar. This was done by reacting the biocrude in a 1 L Erlenmeyer flask with 1 L acetone for 48 hours on a magnetic stirrer. This process was repeated to ensure maximum removal of oil from the char, which increased the porosity of the biochar. The product biochar was finally separated from the acetone solution in a Büchner filter and dried for 12 hours at 105°C. The dried biochar was crushed to a particle size less than 250 µm using a ceramic mill.

Biochar pre-treatment

The biochar was impregnated with sodium dodecyl sulphate (SDS) by adding 10 g of biochar to 1 L SDS solution (10 g/L); the mixture was incubated and stirred at 120 r/min for 24 hours at 60°C. The solution was then filtered by Büchner filtration. The biochar was then dried at 65°C for 12 hours, and the dried biochar was crushed to finer particles using a ceramic bowl.

Characterization of the biochar

Both biochars were characterized by Fourier transform infrared spectroscopy (FTIR) using an IRAffinity-1S instrument from Shimadzu. The spectrometer had a spectral range from 4000 to 400 cm^{-1}. This process was used to identify the functional groups of the biochars. The surface morphology of each adsorbent was determined using scanning electron microscopy (SEM) photography (TESCAN, VEGA SEM) under a 20 kV electron acceleration voltage coupled with energy-dispersive X-ray spectroscopy (EDS) for elemental analysis (Fosso-Kankeu *et al*., 2015).

Adsorption experiments

All the adsorption experiments were carried out in a batch system. The biochar dosage was fixed at 0.2 g per 50 mL solution. The adsorption capabilities of treated and untreated biochar were tested, thus two sets of adsorbents were tested for each experiment. The variables tested included the sorption contact time, initial cadmium concentration, and water temperature. Finally, coal tailings leachates were used to determine the real-time adsorption behaviour of the biochar.

Effect of contact time

A 250 mL flask containing 0.2 g adsorbent and 50 ppm cadmium in 50 mL of aqueous solution was incubated at 25°C. The flask was continuously stirred by shaking it at a speed of 120 r/min for 15, 30, 45, 60, 120, 180, and 240 minutes to assess the effect of time on the adsorption of cadmium onto the different biochars.

Effect of initial cadmium concentration

The second set of experiments was carried out to determine the adsorption capability of the biochars at different initial cadmium concentrations. The same set-up was repeated, only this time using a one-hour residence time for the chars in the solution while varying the initial cadmium concentration from 10 ppm to 70 ppm at 10 ppm intervals.

Effect of temperature

The process was again repeated with a residence time of one hour and initial cadmium concentration of 50 ppm. The temperature of the solution was increased to 35°C, 45°C, and 55°C.

Adsorption of cadmium from the coal tailings leachate

The last set of adsorption experiments was carried out to determine the biochar adsorption capability when exposed to a multi-metal solution. The total metal concentration of a coal tailings leachate was adjusted to 100, 200, and 250 ppm and spiked with cadmium (30 ppm). These solutions were exposed to 0.2 g of the various biochars and the adsorption process was carried out as described in the first set of adsorption experiments while keeping the contact time at 1 hour.

After the adsorption process, an aliquot of 20 mL solution was then placed in 50 mL centrifuge tubes. The tubes were centrifuged at 4000 r/min for 10 minutes, after which the biochar was separated from the solution. The supernatant solution was then poured into a new tube for analysis by inductively coupled plasma – optical emission spectrometry (ICP-OES) (ICP Expert II, Agilent Technologies 720 to determine the concentration of the residual cadmium in solution.

Results and discussion

Characterization of adsorbents

FTIR spectra

The spectra of the treated and untreated biochars (Figure 1) show almost the same pattern of peaks. Significant peaks were observed in the range 2100–2200 cm^{-1}, which can be ascribed to the presence of adsorbent group $C \equiv C$ deriving from the alkyne functional group. The peak at 2650 cm^{-1} suggests the formation of formic acid dominated by the carboxylic group, which plays an important role in the binding of metals. Important binding groups such as C-H stretch and C=O can relate and play significant roles during the adsorption process (Kantcheva, 2003).

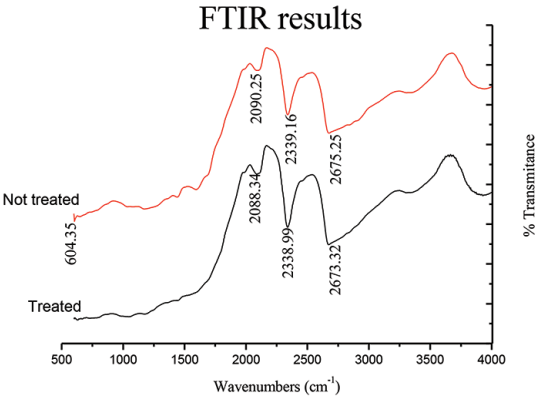

Figure 1—FTIR spectra of untreated and treated biochar

SEM-EDS

SEM-EDS analysis was done to determine if the treatment with SDS was successful by comparing the surface areas available for adsorption on the two biochars. The results of these analyses are shown in Figures 2 and 3 and Tables I and II.

A comparison of the elemental weight percentages between the NT biochar and PT biochar, as indicated in Tables I and II, shows an increase in sodium from $0\%_{wt}$ to $0.3\%_{wt}$ and for sulphur from 0.12%wt to $1.44\%_{wt}$. This indicated that the impregnation with SDS was a success, leaving the PT biochar with a coarser outer surface compared to the NT biochar. This change in surface structure can be attributed mainly to sulphur loading onto the biochar.

Adsorption effectiveness

Figure 4 shows the SEM-EDS spectra of the NT and PT biochars after exposure to cadmium in solution. When these spectra are compared with those for the pure biochars in Figures 2 and 3 respectively, the presence of cadmium in the spectra is clear. This confirms the ability of both biochars to adsorb cadmium from an aqueous solution.

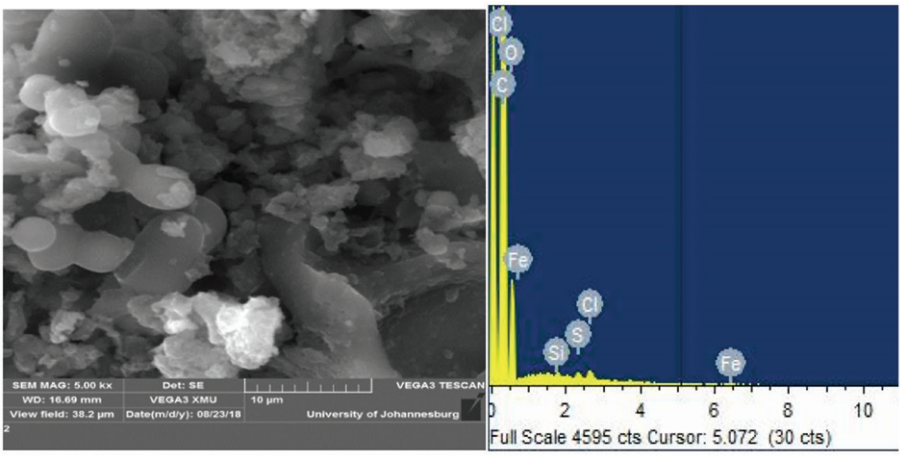

Figure 2—SEM-EDS of NT biochar

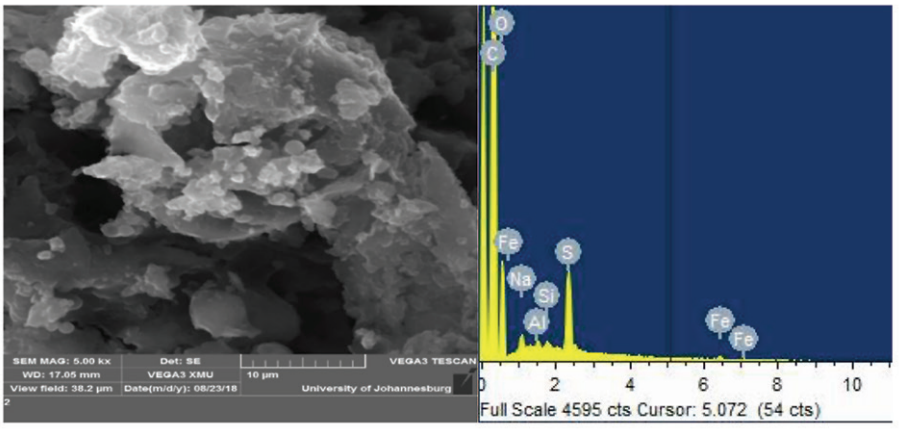

Figure 3—SEM-EDS of PT biochar

Table I

EDS results NT biochar

Element	Weight %	Atomic %
C	82.67	86.61
O	16.80	13.21
Si	0.06	0.03
S	0.12	0.05
Cl	0.2	0.07
Fe K	0.14	0.03

Table II

EDS results of PT biochar

Element	Weight %	Atomic %
C	82.91	87.31
O	14.97	11.83
Na	0.30	0.17
Al	0.08	0.04
Si	0.09	0.04
S K	1.44	0.57
Fe K	0.21	0.05

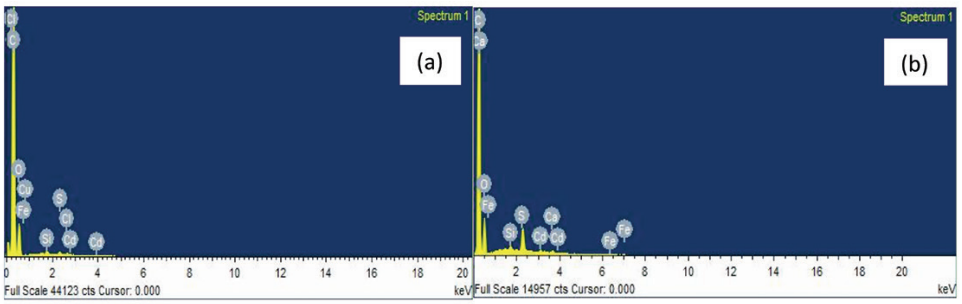

Figure 4—SEM-EDS of (a) NT biochar and (b) PT biochar post cadmium exposure

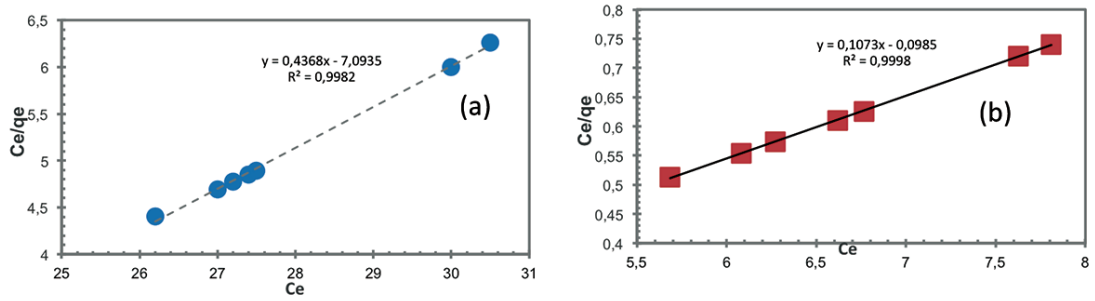

Figure 5—Validation of the Langmuir isotherm model for adsorption of Cd onto (a) NT biochar and (b) PT biochar

Isotherm and kinetic models

The Langmuir and Freundlich isotherms were used to determine the adsorption mechanisms of the two biochars. This was done by determining the equilibrium concentration of cadmium after one hour of adsorption, starting at various initial cadmium concentrations, and plotting either C_e/q_e *vs* C_e or log q_e *vs* log C_e, for the two different isotherms respectively.

Figure 5 shows the Langmuir plots for (a) the NT biochar and (b) the PT biochar. From the strong linear relationship of both graphs, the slope and intercept were used to determine the Langmuir constants q_m and b. These are reported in Table III.

To validate the Freundlich isotherm model, Figures 6a and 6b were constructed by plotting log(q_e) as a function of log (C_e); the Freundlich isotherm parameters n and k_f were determined from the slope and intercept of the plots respectively. The values obtained are reported in Table III.

From Table III, it can be observed that the coefficient of determination (R^2) in both instances is close to unity, therefore the Langmuir and the Freundlich isotherm models fit the cadmium adsorption equilibrium data for both the treated and untreated biochars. This implies that cadmium attaches to the binding groups on the surface of the chars as well as inside the pores (homogeneous and heterogeneous surfaces) (Yao *et al.*, 2014; Fosso-Kankeu, 2016).

Table III

Langmuir and Freundlich constants

Adsorbent	Langmuir isotherm			Freundlich isotherm		
	q_m (mg/g)	b	R^2	n	k_f	R^2
NT biochar	2.29	-0.062	0.9982	-0.75	457.9	0.9985
PT biochar	9.3197	-1.0893	0.9998	-6.4	14.6	0.9972

Kinetic rate experiments were conducted to validate the pseudo-first and pseudo-second-order kinetics. The adsorption data over time was considered and the kinetic parameters for a pseudo-first-order kinetic model and a pseudo-second-order kinetic model were determined by plotting $ln(q_e - q_t)$ *vs* t and t/q *vs* t (Figures 7a and b), respectively. The kinetic parameters are reported in Table IV.

The ability of the model to predict the adsorption behaviour of the biochar can be determined by considering the coefficient of determination (R^2). From Table IV, it is clear that the pseudo-second-order model fits the kinetics of both biochar samples, while the pseudo-first-order model is not suitable for the prediction of the reaction kinetics. This implies that the adsorption of cadmium on both adsorbents took place through a chemisorption mechanism.

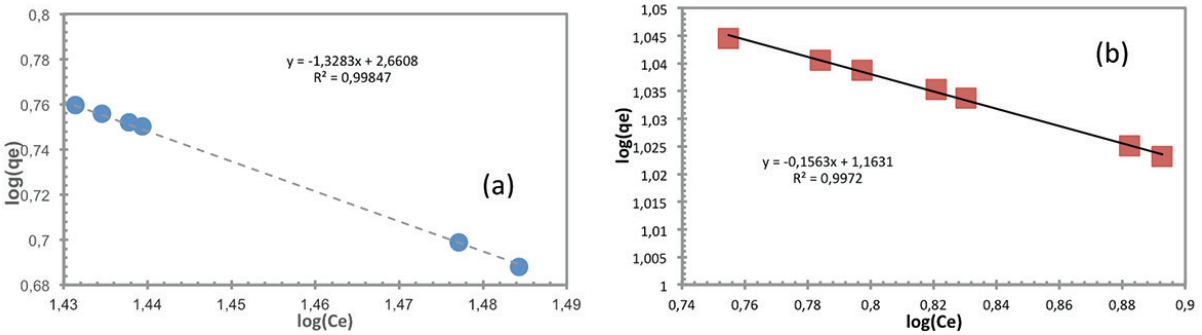

Figure 6—Validation of the Freundlich isotherm model for adsorption of Cd onto (a) NT biochar and (b) PT biochar

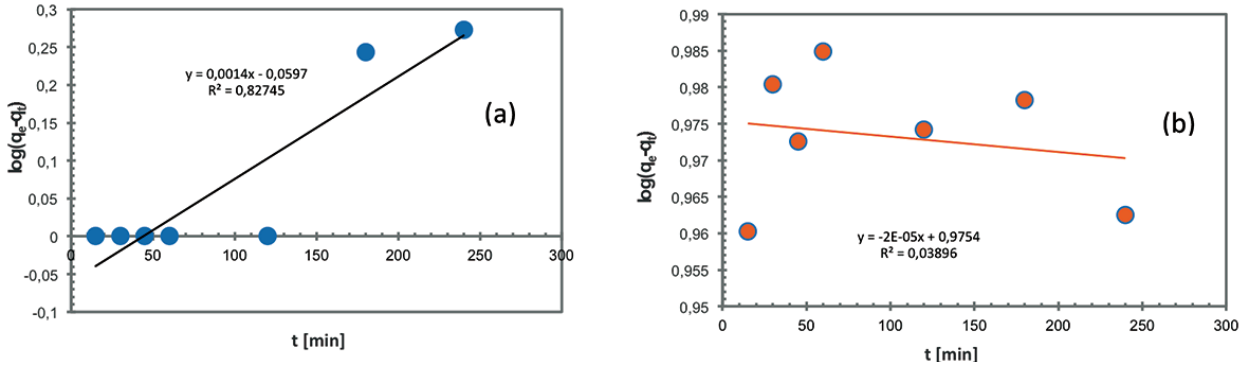

Figure 7—Validation of the pseudo-first-order isotherm model for adsorption of Cd onto (a) NT biochar and (b) PT biochar

Table IV

Pseudo-first and second-order constants

Adsorbent	Pseudo-first-order kinetics			Pseudo-second-order kinetics		
	q_e (mg/g)	K_1	R²	q_e (mg/g)	K_2	R²
NT biochar	0.8716	-0.0032	0.8275	4.8239	-0.0277	0.9953
PT biochar	9.449	0.00005	0.039	10.6724	-0.0803	0.9995

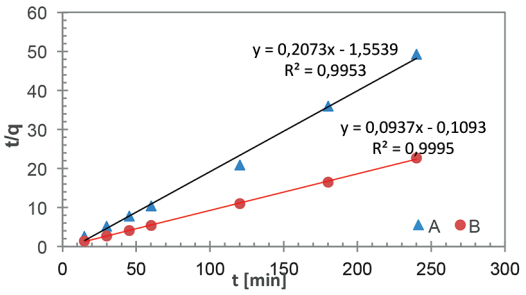

Figure 8—Validation of the pseudo-second-order isotherm model for adsorption of Cd onto (A) NT biochar and (B) PT biochar with SDS

The pseudo-second-order adsorption capacities clearly show that the PT biochar had a higher adsorption capacity, more than double the adsorption capacity of the NT biochar. This shows that the impregnation with SDS was successful, with q_e = 10.67 mg/g compared to the NT biochar with q_e = 4.82 mg/g. These results are similar to previous studies reported (Fosso-Kankeu *et al.*, 2017a).

Thermodynamic study

To evaluate the thermodynamic properties of the biochar, batch adsorption experiments were conducted at three different temperatures (35°C, 45°C, and 55°C).

To calculate the enthalpy change, entropy change, and Gibbs free energy the van't Hoff equation was used:

$$lnK_a = -\frac{\Delta G^o}{RT} = -\frac{\Delta H^o}{RT} + \frac{\Delta S^o}{R}$$

To determine the thermodynamic properties of the biochar, Figure 9 was constructed by plotting ln (*qe*/*Ce*) *vs* 1/*T*.

The positive values of the Gibbs free energy of the NT biochar indicate that the adsorption of cadmium on the char was not spontaneous in nature, which is in contrast with the PT biochar where it is clearly spontaneous. In a similar way, it can be showned that in both cases the adsorption of cadmium was endothermic in nature due to the large positive enthalpy values, confirming that the adsorption of cadmium on NT biochar and PT biochar occurred through a chemisorption mechanism (Fosso-Kankeu *et al.*, 2017b). The positive entropy values obtained for the PT biochar suggest randomness in the solid/liquid interface where there are a few structural changes in the adsorbent and adsorbate for the adsorption of Cd.

Application of biochar for the treatment of coal tailings leachate

Samples of 100, 200, and 250 ppm dissolved metals in coal leachate were spiked with 30 ppm cadmium then exposed to the different biochars for adsorption. The results are shown in Figure 10.

As seen from Figure 10, at a 100 ppm metal concentration the adsorbent showed the highest affinity for cadmium adsorption from the solution. With increasing total metal concentration the adsorbents' ability to adsorb cadmium decreased significantly due to competition for binding sites on the adsorbents by other metals present in solution . This trend was shown by both the NT and the PT biochar. It is, however, clear that the PT biochar outperformed the NT biochar for each metallic feed concentration,

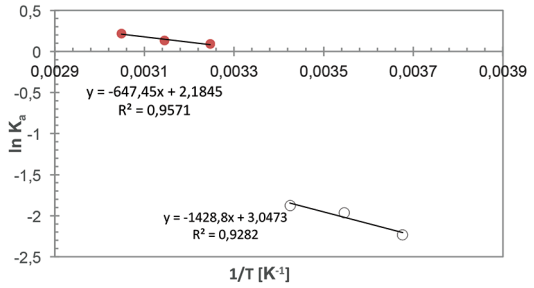

Figure 9—Thermodynamic analysis of the adsorption of Cd with (X) NT biochar, and (Y) PT biochar with SDS

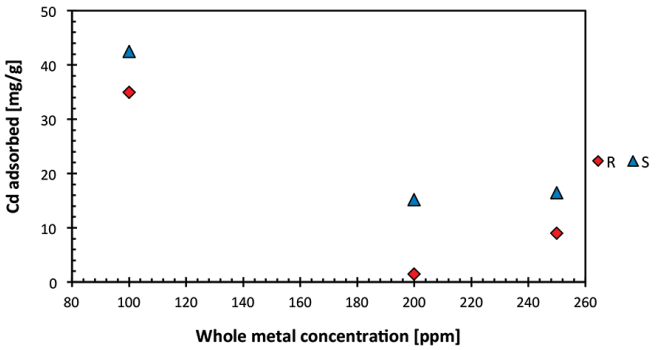

Figure 10—Effect of whole solution concentration on the adsorption of Cd with (R) NT biochar, and (S) PT biochar with SDS

validating the use of SDS impregnation in the removal of cadmium from aqueous mine tailings solutions.

Conclusion

Spent coffee grounds were successfully converted into biochar using hydrothermal methods. It was proven by SEM-EDS that SDS surfactant impregnation of the biochar is possible, creating suitable binding groups that can be identified with FTIR analysis. The isothermal study revealed that the adsorption process occurred through a combination of homogeneous and heterogeneous mechanisms, while the kinetic study confirms the suitability of the pseudo-second-order model for the prediction of the adsorption capacity, allowing the PT biochar to be recognized as the best adsorbent, with a capacity of q_e = 10.67 mg/g compared to the NT biochar with a capacity of q_e = 4.82 mg/g. The thermodynamic study showed that the adsorption of cadmium on the PT biochar was a spontaneous process which took place through a chemisorption mechanism. Application of the biochars to coal tailings leachate was more successful at lower total metal feed concentrations, with the PT biochar outperforming the NT biochar. Spent coffee grounds, which is seen as a waste product in most societies, could therefore be beneficiated to form biochar and applied for effective treatment of mine wastewater contaminated with cadmium.

Acknowledgements

The authors appreciate the sponsorship from North-West University, the contributions of Mr N. Lemmer from the North-West University, as well as Ms Nomsa Baloyi and Mr Edward Malenga from the University of Johannesburg.

References

Cheng, S., Liu, G., Zhou, C., and Sun, R. 2018. Chemical speciation and risk assesment of cadmium in soils around a typical coal mining area of China. *Ecotoxicology and Environmental Safety*, vol. 160. pp. 67–74.

Dudka, S., Piotrowska, M., Chlopecka, A., and Witek, T. 1995. Trace-metal contamination of soils and crop plants by the mining and smelting industry in upper Silesie, South Poland. *Journal of Geochemical Exploration*, vol. 52, no. 1–2. pp. 237–250.

Fosso-Kankeu, E., Mittal H., Waanders, F., and Ray, S.S. 2017b. Thermodynamic properties and adsorption behaviour of hydrogel nanocomposites for cadmium removal from mine effluents. *Journal of Industrial and Engineering Chemistry*, vol. 48. pp. 151–161.

Fosso-Kankeu, E., Waanders, F., Lemmer, N., and Steyn, R.H. 2017a. Surfactant Impregnated bentonite clay for the removal of heavy metals from solution. *Proceedings of the 9th International Conference on Advances in Science, Engineering, Technology & Waste Management* (ASET WM-17), Parys, South Africa, 27-28 November 2017. Waanders, F., Fosso-Kankeu, E., Topcuoglu, B., Plaisent, M., and Thaweesak, Y. (eds). pp. 54–63.

Fosso-Kankeu, E., Waanders, F., and Fourie, C.L. 2016. Adsorption of Congo Red by surfactant-impregnated bentonite clay. *Desalination and Water Treatment*, vol. 57. pp. 27663–27671. doi: 10.1080/19443994.2016.1177599

Fosso-Kankeu, E., Mittal, H., Mishra, S.B., and Mishra, A.K. 2015. Gum ghatti and acrylic acid based biodegradable hydrogels for the effective adsorption of cationic dyes. *Journal of Industrial and Engineering Chemistry*, vol. 22, pp.171–178.

Fu, F. and Wang, Q. 2011. Removal of heavy metal ions from wastewater: a review. *Journal of Environmental Management*, vol. 92. pp. 407–418.

Jin, H.P., Mansour, E., and Thomas, B. 2017. A practical testing approach to predict the geochemical hazards of in-pit coal mine tailings and rejects. CATENA, vol. 148. pp. 3–10.

Jusoh, A., Shiung, L.S., Ali, N., and Noor, M.J.M.M. 2007. A simulation study of the removal efficiency of granular activated carbon on cadmium and lead. *Desalination*, vol. 206. pp. 9–16.

Kang, K.C., Kim, S.S., Choi, J.W., and Kwon, S.H. 2008. Sorption of Cu^{2+} and Cd^{2+} onto acid- and base-pre-treated granular activated carbon and activated carbon fiber samples. *Journal of Industrial and Engineering Chemistry*, vol. 14. pp. 131–135.

Kantcheva, M. 2003. FT-IR spectroscopic investigation of the reactivity of NOx species adsorbed on Cu^{2+}/ZrO_2 and $CuSO_4/ZrO_2$ catalysts toward decane. *Applied Catalysis B: Environmental*, vol. 42. pp. 89–109.

Marquez, J., Pourret, O., Faucon, M., Weber, S., Hoang, T., and Martinez, E. 2018. Effect of cadmium, copper, and lead on the growth of rice in the coal mining region of Quang Ninh, Cam-Pha (Vietnam). *Sustainability*, vol. 10, no. 6. p. 1758. doi: 10.3390/su10061758

Mohan, D., Prachi, S., Ankur, S., Phillip, H.S., and Charles, P.J. 2015. Lead sorptive removal using magnetic and nonmagnetic fast pyrolysis energy cane biochars . *Journal of Colloid and Interface Science*, vol. 448. pp. 513–528.

Redwscu, A. and Nicolae, A. 2012. Adsorption of Zn, Cu and Cd from waste waters by means of maghemite nanoparticles. *UPB Scientific Bulletin, Series B: Chemistry and Materials Science*, vol. 74. pp. 255–264.

Salomons, W. 1995. Environmental impact of metals derived from mining activities: Processes, predictions, prevention. *Journal of Geochemical Exploration*, vol. 52. pp. 5–23.

Yao, Y., Gao, B., Fang, J., Zhang, M., Chen, H., Zhou, Y., Creamer, A.E., Sun, Y., and Yang, L. 2014. Characterization and environmental applications of clay-biochar composites. *Chemical Engineering Journal*, vol. 242. pp. 136–143.

Zuorro, A. and Lavecchia, R. 2012. Spent coffee grounds as a valuable source of phenolic compounds and bioenergy. *Journal of Cleaner Production*, vol. 34. pp. 49–56. ◆

Table V

Thermodynamic properties

Adsorbent	*Ka*	Temperature (K)	Δ*G* (kJ/mol)	Δ*S* (J/mol/K)	Δ*H* (kJ/mol)
NT biochar	0.1071	308	4075.79	25.3	11879
	0.1406	318	3822.43		
	0.1532	328	3569.08		
PT biochar	1.0941	308	-210.98	18.2	5382
	1.1420	318	-392.60		
	1.2443	328	-574.21		

Determination of optimal fragmentation curves for a surface diamond mine

K.M. Phamotse[1]* and A.S. Nhleko[1]

***Paper written on project work carried out in partial fulfilment of BSc (Mining Engineering) degree**

Affiliation:
[1]School of Mining Engineering, University of the Witwatersrand, South Africa.

Correspondence to:
K.M. Phamotse

Email:
kmphamotse@gmail.com

Dates:
Received: 22 Nov. 2018
Revised: 26 Mar. 2018
Accepted: 5 Sep. 2018
Published: July 2019

How to cite:
Phamotse, K.M. and Nhleko, A.S. Determination of optimal fragmentation curves for a surface diamond mine. The Southern African Insitute of Mining and Metallurgy

DOI ID:
http://dx.doi.org/10.17159/2411-9717/494/2019

ORCiD ID:
Phamotse, K.M.
https://orchid.org/0000-0002-0256-7508

Synopsis

Liqhobong Mining Development Company (LMDC) has been experiencing problems with boulders after blasting where the fragment sizes exceed the maximum of 800 mm as per mine standard. As a result, the mine has employed various methods to improve the fragmentation. The goal is to produce a run-of-mine (ROM) feed that does not choke the crusher and cause delays in production. In order to achieve this goal, fragmentation distribution within the fines and coarse envelope must be optimized through effective planning of blasting activities and accurate execution.

The mine determined the fines-coarse envelope within which the entire crushing system can handle fragments using Split Desktop software. It is expected that both the predicted and actual fragmentation curves lie within that envelope for optimal fragmentation. The Kuz-Ram model with blast design parameters of 2.6 m for burden, 2.8 m for spacing, and 127 mm hole diameter was used to predict the fragmentation. The results show that the blast design parameters may need altering to achieve optimum fragmentation. Furthermore, the execution of the drilling and blasting may be the cause of the fragmentation problems. The mean fragmentation size (X_{50}) differs greatly, unlike the uniformity index (n)s values which are relatively close to each other (0.6 to 2.2). The mean squared error (MSE) values have a large range. A proposed solution is a modified burden, spacing, and hole diameter. It is concluded that blast design parameters need to be reviewed in order to obtain correct predictions.

Keywords
fragmentation analysis, blasting, Kuz-Ram model, open pit mining, particle size distribution.

Introduction

Fragmentation has an impact on the mine production cycle which comprises, *inter alia*, drilling, blasting, loading, hauling, and crushing. Correct fragmentation as set by the plant design is important as it reduces the time lost due to secondary blasting and/or loading difficulties. In this paper we analyse blast results at Liqhobong Mining Development Company (LMDC) in Lesotho for a period of six months. This project was undertaken to observe the trends from the blasts and to identify whether any discrepancies exist in the overall blast information. The period under study included 16 blasts.

There are both controllable and uncontrollable factors that affect fragmentation. The controllable factors are blast design parameters such as burden, spacing, hole diameter, stemming length, and initiation timing. The uncontrollable factors are rock properties such as uniaxial compressive strength (UCS) and geological discontinuities within the rock mass. The mine's requirement is that blasted fragments do not exceed 800 mm. However, the mine was not able to meet the desired fragmentation profile. Various principles have been adopted to address this challenge by modifying the blast design parameters, such as use of rules of thumb and the Kuz-Ram model.

At LMDC, fragmentation distribution has been a problem since mining began in 2017. This was evident in the fact that, after blasting, there were rocks larger than 800 mm (the maximum size on the feed grizzly). This was addressed by employing a predictive model for fragmentation (the Kuz-Ram model), which revealed some flaws since the prediction still exceeded the designed fines-coarse envelope for the mine. The flaws were, however, not taken into account in anticipation that the prediction would match the actual fragmentation results obtained using Split Desktop software.

For drilling and blasting design purposes, 'rules of thumb' are normally used but at LMDC they were not effective. Therefore, it was important to derive a solution to achieve optimal fragmentation as this would reduce delays in the mine production cycle.

Determination of optimal fragmentation curves for a surface diamond mine

Mining method

The mine employs a conventional open-pit mining method consisting of drill, blast, load, and haul phases. The pit design is based on a split shell concept in order to prolong waste stripping as much as possible while providing a double ramp system to mitigate the risk of failing ramps. The ore is mined by five split shells, namely: cut 1, cut 2 north, cut 2 south, cut 3 north, and cut 3 south (Figure 1). Every split shell has its own ramp system, but where the north cut meets the south cut the ramps will join to form a concentric system. Figure 1 depicts a sectional view of the different mining cuts. Cut 1 is currently being mined.

Problem statement

The mine was experiencing problems due to post-blast fragments greater than 800 mm, considered as 'boulders' based on processing plant requirements. The generation of boulders results in production delays, since the boulders need to be reduced in size using a mechanical rock-breaker. The mine predicts fragmentation using the Kuz-Ram fragmentation model, which is a commonly used method to predict blast fragmentation (Cunningham, 2005; Strelec, Gazdek, and Mesek, 2011; Adebola, Ajayi, and Elijah, 2016; Gheibi, *et al.*, 2009). However, the data from the Kuz-Ram analysis is not recorded for every blast. Prior to the generation of boulders, the mine did not develop prediction models for every blast as it was assumed that the blast design parameters were appropriate, on the basis of trial blasts. Nevertheless, the mine attempts to predict fragmentation correctly within the fines-coarse envelope as per the plant design. The fines-coarse envelope was determined by the use of particle size distribution (PSD) during trial blasts to determine how the kimberlite at the mine responded to crushing. The fines-coarse envelope is a result of the extremities of the particle size distribution curves that were smoothed out, which resulted in two curves. The mine found a positive correlation between the predicted and the actual fragmentation curves. The inability to predict fragmentation correctly may be attributed to the use of estimated parameters such rock density, UCS, and rock mass description (RMD). Even though these parameters are used to determine the rock factor, 'A', at LMDC there is no constant 'A' factor used. The 'A' factor is recalculated for every blast prediction. Other features that affect the 'A' factor are the joint plane spacing (JPS) and joint plane orientation (JPO), which are determined visually by the responsible person on duty. Thus, the values obtained may differ as the determination of JPO and JPS is subjective. This may introduce discrepancies to the input data, depending on the experience of the observer. Furthermore, the UCS values for the different kimberlite types are assumed to be uniform across the mine. Figure 2 shows an example of fragmentation curves that are used to analyse how fine or coarse blasted material is for an ore block. The block is assigned a code as shown in Figure 3 where, for example, O2603C1P19 is read as the elevation of 2603 m above mean sea level, cut 1, block number P19.

The Kuz-Ram fragmentation model is used to predict fragmentation size distribution. It is important to note that on the graph, fragment sizes range from 0.1 mm to 1000 mm. This does not limit the predicted and actual fragment sizes to the graph constraints. This is shown in Table I, with size fragments in millimetres and percentage passing data for O2603C1P19 of up to 4000 mm.

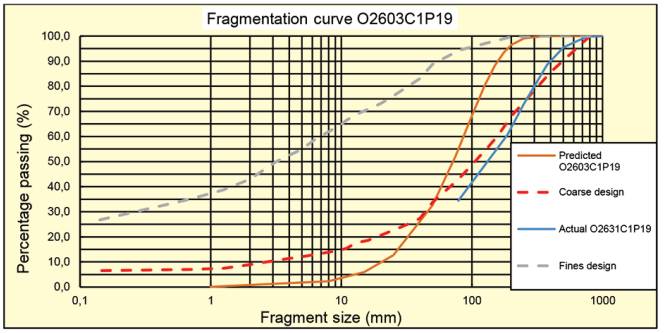

Figure 2—Fragmentation curves: actual, predicted, and fines-coarse design for the crusher

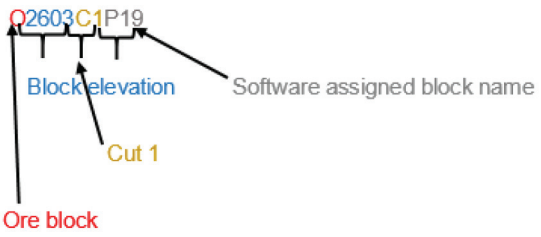

Figure 3—Block identification code

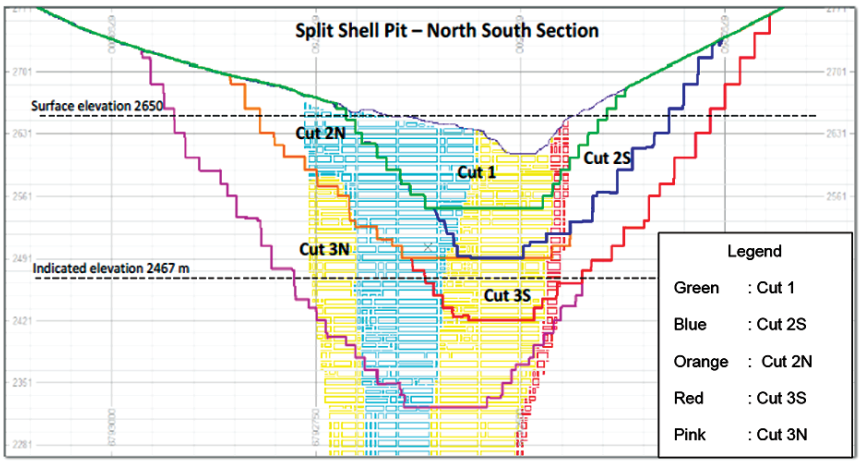

Figure 1—Sectional view of split shell design at LMDC (Firestone Diamonds plc, 2015)

Table I

Predicted and actual size data for O2603C1P19

Predicted O2603C1P19		Actual O2603C1P19	
Size (mm)	% passing	Size (mm)	% passing
4000	100.00	1000	100.00
2000	100.00	750	99.70
1000	100.00	500	95.50
750	100.00	375	88.50
500	100.00	250	73.00
350	100.00	187	60.70
250	100.00	78.70	34.40
200	99.60	-	-
175	99.00	-	-
150	97.50	-	-
125	94.00	-	-
100	86.80	-	-
75	73.50	-	-
50	51.80	-	-
25	23.10	-	-
15	11.70	-	-
8	4.80	-	-
1	0.20	-	-

Crusher design fragmentation results are shown in Figure 2 as an envelope formed by fines design and coarse design curves developed by the use of PSD. Therefore, if the predicted and actual fragmentation curves fall within the fines-coarse envelope this indicates that the ideal/desired fragmentation profile is achieved. The actual and predicted fragmentation curves shown in Figure 2 do not fit into the fines-coarse envelope. Both the actual and predicted curves are closer to the coarse side, hence there is a greater probability of boulders forming. It is important to note that the values shown in Figure 2 may exceed the maximum values on the graph as shown in Table I. This raises the question '*Will the analysis of previous blast information correctly predict an optimal fragmentation curve*?'

Objectives

The objectives of this research study were to:

- Use descriptive statistics to analyse data based on previous actual and predicted fragmentation curves
- Identify controllable blast design parameters that affect the shape of predicted fragmentation curves
- Fit fragmentation curves within the fines and coarse design curves so as to deem them 'ideal' for the crusher.

Literature review

The orebody and rock conditions at every mine are unique, therefore, each mine should have tailored solutions to allow for optimal orebody extraction. Fragmentation control is a challenging task since there are many parameters to take into account, which include rock structure, burden, spacing, hole diameter, bench height, and initiation timing. The challenges are caused by the fact that rock is generally neither homogeneous nor isotropic. For the purposes of this study, we analyse only the factors that cause deviations between planned and actual blast design parameters. This investigation was conducted through image analysis, the Kuz-Ram fragmentation model, and descriptive statistics.

Background to fragmentation models developed

Many researchers have successfully managed to derive solutions on how to design drilling and blasting parameters that will result in optimum fragmentation. In 1933, Rosin and Rammler developed a model to predict particle size distribution during blasting, known as the Rosin-Rammler particle size distribution model (Vesilind, 1980). The Rosin-Rammler distribution is identical to the Weibull density distribution that describes material failure and fatigue phenomena (Alderliesten, 2013). This size distribution has been very important in rock fragmentation studies as it outlines size distribution as a percentage passing curve. Spathis (2013) conducted a study on a three-parameter rock fragmentation distribution, which is developed under the Swebrec function. The model acts as a fit for measured mass percentage passing distributions along with the Weibull (Rosin-Rammler) distribution that is exemplified in the Kuz-Ram model (Spathis, 2013). This three-parameter model has the added advantage of fitting the fines region on cumulative mass percentage passing curves for fragmentation (Spathis, 2013). Cunningham (2005) developed the widely used Kuz-Ram fragmentation model. This model is a combination of Kuznetov's empirical equation and the Rosin-Rammler size distribution model. Gonzalez and Montoro (1993) developed image analysis software, based on the Kuz-Ram fragmentation model, to analyse fragmentation of blasted material by measuring the spatial relationship between fragmented material and the actual size of the fragmented material.

Kuz-Ram fragmentation model

The Kuz-Ram model provides a technique to predict the distribution of fragments in terms of the percentage mass passing through a grizzly screen. This is done by using mathematical equations developed by Cunningham, using Kuznetsov's empirical equation and the Rossin-Ramler distribution, to quantify fragmented rock. There are limitations to the Kuz-Ram fragmentation model as it is an empirical way to predict fragmentation. These limitations are that there are parameters that not taken into account, the measurement of fragmentation is limited, and it is challenging to scale blasting effects (Cunningham, 2005). These limitations may make it difficult to accurately determine what is to be seen in a practical sense. Another major limitation with the Kuz-Ram fragmentation model is that it is heavily dependent on the Rossin-Rammler equation, which underestimates fines (Ouchterlony, Sanchidrian, and Moser, 2016). This is further proof that the Kuz-Ram model may not be representative of what happens in reality. Equation [1] denotes the formula for determining mean fragmentation size (X_{50}) developed by Kuznetsov in 1973. The mean fragmentation size is simply an estimate that gives an overview of the outcome resulting from blast design parameters for an operative prediction process (Adebola, Ajayi, and Elijah, 2016).

$$X_{50} = A.\frac{Q^{1/6}}{k^{0.8}} \times \left(\frac{115}{RWS}\right)^{0.633} \quad [1]$$

where

X_{50}: Mean fragment size (cm)
RWS: Relative weight strength
K: Powder factor (specific charge – above grade) in (kg/m^3)
A: Rock factor.

The uniformity index (n) is used to determine how even the breakage of rock is expected to be, based mainly on parameters

employed during drilling (Cunningham, 2005). Equation [2] shows how the uniformity index is calculated. The uniformity index indicates the uniformity of the fragment sizes and ranges between 0.6 and 2.2 for a well fragmented blast (Adebola, Ajayi, and Elijah, 2016).

$$n = \left[2.2 - 14\left(\frac{B}{D}\right)\right]\left[0.5\left(1 + \frac{S}{B}\right)\right]^{0.5}\left[1 - \frac{W}{B}\right]\left[\frac{L}{H}\right] \quad [2]$$

where

B: Burden (m)
D: Hole diameter (mm)
S: Spacing (m)
W: Standard deviation of drilling accuracy (m)
L: Total length of drilled hole (m)
H: Bench height (m).

Then, using the uniformity index (n) and mean fragment size [X_{50}] the percentage passing can be determined using Equation [3] (Adebola, Ajayi, and Elijah, 2016):

$$Percentage\ passing\ (\%) = 100 - \left[100 * e^{-0.693*\left(\frac{meshsize}{X_{50}}\right)^n}\right] \quad [3]$$

Descriptive statistics

Descriptive statistics are used to describe the key features of data in a study. Descriptive statistics are also used to summarize large data-sets in order to make an informed analysis. They include the mean, mode, median, skewness, and kurtosis of a data-set. In this paper, descriptive statistics are used to obtain an in-depth analysis of fragmentation results. The descriptive statistics that were necessary to finding a solution to the mine's problem are the mean, median, mode, range, standard deviation, variance, and box-and-whisker plot.

Box-and-whisker plots (box plots)

The box plot is a five-number summary comprising the minimum, first quartile (Q_1), median, third quartile (Q_3), and maximum values. Box plots aid in understanding the characteristics of data distribution and the level of the distribution of the values from the data. The data is organized into a box and two lines referred to as whiskers.

Estimators

Estimators are used in statistics as a measure of efficiency. There are two main estimators used; the bias and the mean squared error (MSE). The bias is described as the difference between the average value of the estimator and the actual or true value (the mean of the true value). The standard error is simply an estimator of the standard deviation (Holton, 2014). The MSE combines the concepts of bias and the standard error. Ideally, a MSE should be close to zero, implying that there is a good fit of data. In other words, the smaller the MSE value, the closer the fit is to the data. To calculate the MSE, Equation [4] is used (Holton, 2014).

$$MSE = E([H - \theta]^2) \quad [4]$$

where

E: Estimator
H: Standard error
θ: Bias.

Results and analysis

Table II summarizes the descriptive statistics obtained for all 16 blast results analysed on the fragmentation size distribution. The reason for collecting 16 sets of data was to make an informed decision on the trends in the behaviour of blasted rock.

Three classes of data are analysed, namely:

- Comparison of ideal and actual fragmentation with skewness of zero
- Comparison of ideal and actual fragmentation with different skewness values
- Comparison of predicted and actual fragmentation.

These classes arose because the mine initially used trial and error to design blasts, and later adopted the Kuz-Ram fragmentation model to predict blasts outcomes in terms of fragmentation size distribution. The 'ideal', predicted, and actual curves are all expected to fit within the fines-coarse envelope as

Table II

Summary of the descriptive statistics for 16 blasts

Blast ID	Mean	Median	Mode	Minimum	Maximum	Variance	Standard deviation	Standard error	Skewness
O2603C1P3	88.53	98.73	100.00	43.17	100.00	368.98	19.21	6.40	-2.02
O2603C1P12	57.51	57.67	-	9.72	100.00	788.68	28.08	6.81	-0.05
O2603C1P19	78.83	88.50	-	34.43	100.00	589.50	24.46	9.25	-1.11
O2589C1P1	47.65	44.33	-	2.07	100.00	1073.06	32.76	8.19	0.34
O2659C1P19	85.39	94.58	100.00	46.43	100.00	386.49	19.66	7.43	-1.57
O2659C1T1	74.11	77.84	-	37.36	100.00	566.08	23.79	8.99	-0.43
O2603C1P26	55.07	51.90	-	13.62	100.00	679.42	26.07	6.32	0.34
O2603C1P10	41.90	35.19	-	1.54	100.00	1042.65	32.29	8.34	0.65
O2603C1P31	44.84	43.16	-	4.28	95.58	954.45	30.96	6.32	0.22
O2617C1P16	32.40	24.01	-	2.69	100.00	805.68	28.38	6.69	1.46
O2603C1P25	50.00	50.00	-	20.00	80.00	900.00	30.00	17.32	0.00
O2603C1P20	50.00	50.00	-	20.00	80.00	900.00	30.00	17.32	0.00
O2617C1P26	50.00	50.00	-	20.00	80.00	900.00	30.00	17.32	0.00
O2617C1T2	50.00	50.00	-	20.00	80.00	900.00	30.00	17.32	0.00
O2645C1P8	50.00	50.00	-	20.00	80.00	900.00	30.00	17.32	0.00
O2617C1P44	67.52	69.66	-	18.50	100.00	801.30	28.31	6.67	-0.31
Averages	54.61	58.47	150.00	19.61	93.47	784.77	28.01	10.50	-0.05

per the plant design and crushing capabilities. Table III shows the blast design parameters that are used at the mine and which are used as input parameters for the Kuz-Ram fragmentation model.

Comparison of ideal and actual fragmentation with skewness of zero

This class of data has only three data-sets recorded for the actual blast. Therefore, it is expected that the results may be inaccurate because the fewer the data-points, the less accurate the results will be. This data recorded a skewness of zero and the mean and median values were the same. Identical mean and median values could imply that the fragments are distributed normally; however, this could be incorrect as there is no mode to confirm that. The skewness of zero implies that the data is a normal distribution even though this is not true. given that the data contains only three points. The results from this data-set cannot be regarded as a true representation of the fragmentation distribution.

Blast ID O2603C1P25

The size fragments fall within the mine standards of a minimum of 0.1 mm and a maximum of 1000 mm. These extremes are put in place even though the lowest crushing size is 10 mm and the largest grizzly at the run of mine (ROM) tip is 800 mm, as 1000 mm is manageable by a rock-breaker (pecker) and 0.1 mm diamonds can still be recovered if they are of gem quality. The percentage passing values are determined from the graphs as 20% smaller than 37.54, 50% at 178.15 mm or less, and 80% at 437.87 mm or less. All the fragments pass through the 800 mm grizzly, signifying an absence of boulders for this specific blast. However, the problem is the fact that the size fragments do not fall within the crusher fines-coarse design.

Figure 4 shows the data plotted using a logarithmic (log) scale. A log scale was used because it tends to respond well to skewness near large values and shows the percentage well (Robbins, 2013). The 'ideal' curve on the graph was calculated using the midpoints of the fines and coarse envelope to determine, on average, the 'ideal' fragmentation curve that is to be expected. The predicted curve was obtained using the Kuz-Ram fragmentation model and the actual curve data was obtained photographically by the use of Split Desktop software. The bias for the data is 1.08, which yields a MSE of 301.15. The large positive MSE indicates a difference between the actual and 'ideal' curves. The large MSE value might be due to the fact that the 'ideal' and actual curves have different ranges of 78.95 and 60.00 respectively for their percentage passing values. This causes inaccuracies in the analysis of the data.

Table III

Blast design parameters used at LMDC

Blast design information	
Hole diameter (mm)	127
Burden (m)	2.6
Spacing (m)	2.8
Bench height (m)	14
Sub-drill (m)	0.8
Stemming (m)	2.5
Stemming material	Tailings
Pattern layout	Staggered
Explosives	Emulsion (HEF100)
Timing – Spacing (ms)	33

Comparison of ideal and actual fragmentation with different skewness values

These results have more than three data-points for the actual blast results, which is expected to yield a more accurate representation of the fragmentation. Blast identity O2603C1P31 is analysed.

Blast ID O2603C1P31

The fragments do not lie within the acceptable size range of 0.1 mm–1000 mm. The data is further analysed in Figure 5 to ascertain if it fits within the fines-coarse envelope.

In Figure 5, there are values that extend beyond the fragment size of 1000 mm for the 'ideal' curve, although the upper limit shown on the curve is 1000 mm. This means that some data is missing from the graph and this may cause inaccurate results. At 80% percentage passing, fragments less than 500 mm passed through. At 50% passing, fragments less than 200 mm passed through and at 20%, fragments less than 50 mm. The bias for the data-set is 6.17, which yields a MSE of 78.11. The skewness is 0.22, hence the data-set is positively skewed. The value of the MSE is large in this case as a result of the large bias, thus the bias was over-estimated. The actual curve strays further away from the coarse curve, indicating that boulders are present.

Comparison of predicted and actual fragmentation

For this class of data, the predicted curves that were plotted using the Kuz-Ram fragmentation model and actual fragmentation profile are comparable. Since the Kuz-Ram fragmentation model was used, the X_{50} and n values are shown, calculated using Equations [1] and [2], respectively. These two values are critical as they are the main input values when calculating percentage passing using Equation [3].

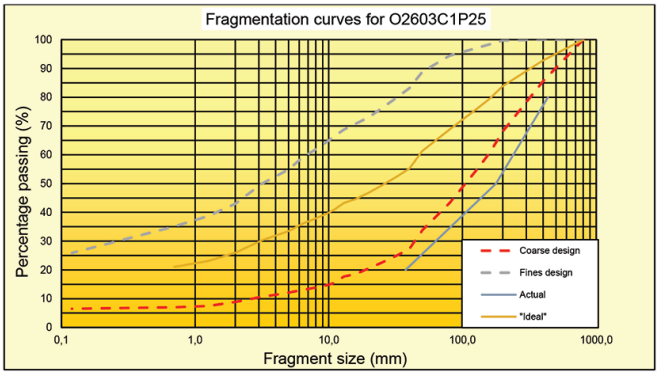

Figure 4—Fragmentation curves for O2603C1P25

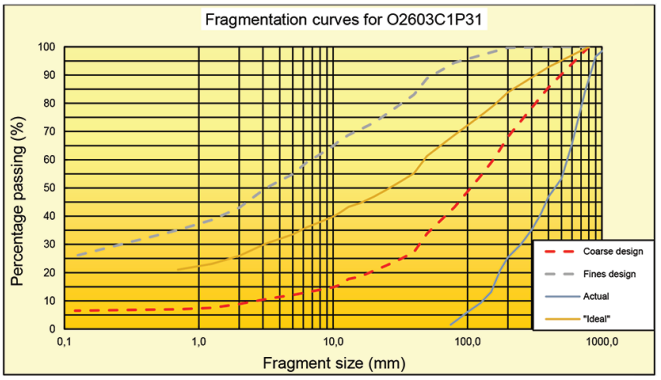

Figure 5—Fragmentation curves for O2603C1P31

Blast ID O2603C1P12

The prediction shows a range of sizes from 1 mm to 4000 mm and the actual data a range from 1 mm to 2000 mm. For both data-sets, the size fragments indicate the presence of boulders. The predicted data indicates a mean size of 47.7 mm and a uniformity index of 1.54. At 80%, 50%, and 20% passing, fragments less than 75 mm, 50 mm, and 25 mm passed through, respectively. The uniformity index lies within the acceptable range of 0.6 and 2.2.

The predicted curve in Figure 6 is flat at the beginning, denoting 100% passing from 200 mm to 4000 mm. It is important to note that the predicted curve does not lie entirely within the fines-coarse envelope. The reason for the top falling outside the envelope is the very large fragment sizes that are predicted. The actual curve lies within the fines-coarse envelope for smaller fragments, but outside it for the larger fragments, which could be due to the powder factor of 1.76 kg/m^3. This introduces the impact/effect of the explosives utilized on the profile of the rock blasted. It is important to note that the rock properties value used in the prediction parameters was an average value for the whole mine, therefore it may not be an accurate representation of the true rock properties in the blast area. The bias for the data-set is 19.44, which yields a MSE of 443.98. The data-set is negatively skewed (skewness is –0.05). The value of the MSE is large as a result of a large bias, thus the bias was over-estimated.

Box-and-whisker plots

Box-and-whisker plots were constructed for each blast to determine the spread of the percentage passing. For this analysis, pure descriptive statistics are used. The data analysed is for the actual fragments in order to determine how the fragments were spread out.

Blast ID O2603C1P25

In Figure 7, both the upper quartile and lower quartiles have a difference of 15.00. The data shows an even spread in terms of percentage passing for the fragments. However, this does not mean that the fragments are 'ideal' as the minimum is 20.00 and the maximum is 80.00, which means that the spread of the range of the fragments themselves is not large (it is 60). This value of 60 compared to the median of 50 shows that the data is not as evenly distributed as it seems.

Blast ID O2603C1P31

In Figure 8, the upper quartile and lower quartile have a difference of 24.77 and 9.67 respectively. This difference manifests in two whiskers, the whisker for the upper quartile being twice as long as that for the lower quartile. The long whisker could be an indication that there are very large fragments compared to the rest of the data. This is in addition to the fact that the median is 43.16, indicating that the majority of the fragments fall within the lower 50% of the data but there are more coarse fragments than fine fragments.

Blast ID O2603C1P12

From Figure 9, the data seems to be relatively evenly distributed. However, the median is 57.67, and the differences between the Q1 and the minimum, and the maximum and Q3 values, are 27.79 and 20.28 respectively. The 7.51 difference between the two values shows that the spread of fragments for this blast is relatively even for the top 50% and the bottom 50% of the data.

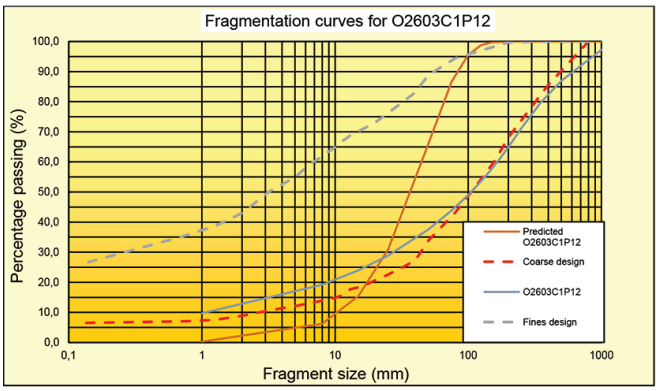

Figure 6—Fragmentation curves for O2603C1P12

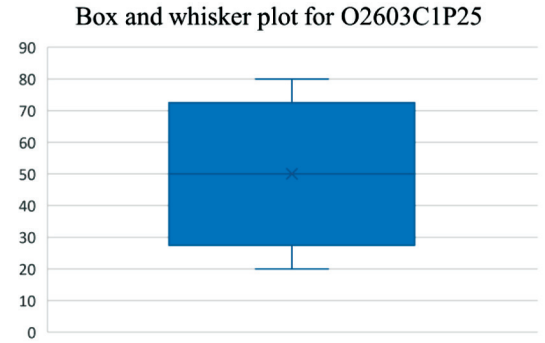

Figure 7—Box-and-whisker plot for O2603C1P25

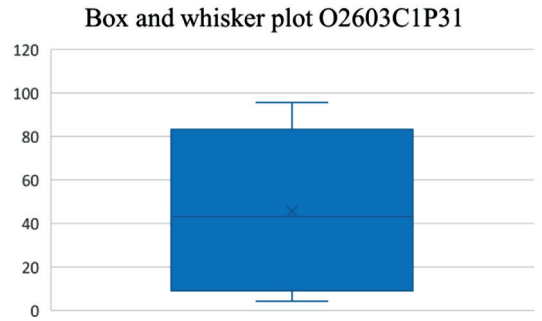

Figure 8—Boxand-whisker plot for O2603C1P31

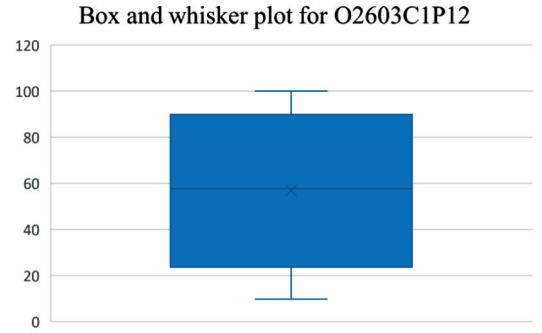

Figure 9—Box-and-whisker plot for O2603C1P12

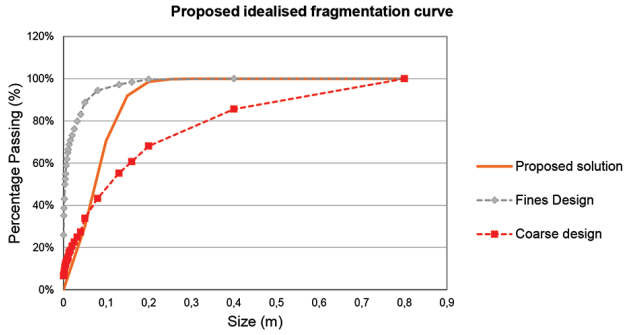

Figure 10—Proposed model for fragmentation curve

Proposed solution

The limitations with the Kuz-Ram fragmentation model have led, in this case, to the determination of a proposed solution where only one parameter can be altered at a time. The focus was mainly on controllable blasting factors as some of the other limitations with the Kuz-Ram fragmentation model would be difficult to surmount. Figure 10 shows a proposed prediction curve and the parameters that were modified to achieve the desired fragmentation results. At 99.70% passing, the graph indicates a size of 200 mm and from thereon 100% passing all the way to 800 mm. At 33.80% passing, the graph indicates a size of 50 mm. The percentage passing less than 33.80% extends beyond the coarse envelope. The difference between the percentage passing within the fines-coarse envelope is 65.90%, with sizes ranging from 200 mm to 800 mm at 100% passing. This is an improved prediction design compared with the current results obtained by the mine. This improved prediction meets the requirements to fit the model into the fines-coarse envelope. It is, however, subject to testing. This improved design was achieved by changing the burden from 2.60 m to 2.80 m and the spacing from 2.80 m to 3.00 m. The spacing to burden ratio was 1.07. This improved design assists the mine in fitting its predicted model into the constraints of the plant design (fines-coarse envelope).

Conclusions

The research study showed that the gap between the predicted and actual curves differs for the same blast, which is the first indication that the desired fragmentation will not be achieved. In cases where no fragmentation curves were drawn, the ranges for the fragments also differ from those that are supposed to fit into the fines-coarse envelope. These discrepancies between what is expected and what actually happens make it difficult to identify the parameters that need to be adjusted to meet the mine standards.

The MSE between the expected and predicted results is large for all the blasts, which means that the drilling and blasting crews do not follow the correct procedures and end up doing what is required in order to complete a blast to schedule.

A slight increase in the powder factor made a difference to the 'actual' curves, which shows that the rock mass to be blasted must be studied thoroughly in order to calculate the correct powder factor. There is no tailor-made solution to designing blasts, but each mine must determine its own blast design parameters by trial and error until the desired result is achieved.

The results from the Kuz-Ram fragmentation model prove further that the explosives used and the rock properties play a significant role in determining how well fragmented the rock will be. The calculation for the mean fragmentation size is strongly dependent on the rock properties which, in this case, may be incorrect due to the subjective (visual) determination of rock properties like the JPO and JPS. The theoretical calculation of the uniformity index, on the other hand, fell within the accepted range for all three blasts. This is dependent on the mine's blast design parameters, which is further proof that the blast design parameters are suited for the mine.

More than two prediction parameters should be used at the mine and there should be quality checks and assurances for the whole process that leads up to rock being fragmented. Furthermore, the mine should keep a good record of blasts. Good record-keeping is important to assist in improving the prediction models and the actual fragmentation curves. The calculations for the predictions should be done well before every single blast in order to be able to identify trends.

References

Adebola, J.M., Ajayi, O.D., and Elijah, O.P. 2016. Rock fragmentation prediction using Kuz-Ram model. *Journal of Environment and Earth Science*, vol. 6, no. 5. pp. 111–113. https://www.iiste.org/Journals/index.php/JEES/article/download/30610/31442+&cd=1&hl=en&ct=clnk&gl=za [accessed 16 March 2018].

Alderliesten, M. 2013. Mean particle diameters. Part VII. The Rosin-Rammler size distribution: Physical and mathematical properties and relationships to moment-ratio defined mean particle diameters. *Particle & Particle Systems Characterisation*, vol. 30, no. 3. pp. 244–257. https://onlinelibrary.wiley.com/doi/abs/10.1002/ppsc.201200021 [accessed 16 March 2018].

Cunningham, C.V.B. 2005. The Kuz-Ram fragmentation model – 20 years on. European Federation of Explosive Engineers, Brighton. https://miningandblasting.files.wordpress.com/2009/09/the-kuz-ram-fragmentation-model-e28093-20-years-on.pdf [accessed 30 April 2018].

Firestone Diamonds plc. 2015. Diamond Resource and Reserve Report. London.

Gheibi, S., Aghababaei, H., Hoseinie, S.H., and Yashar, P. 2009. Modified Kuz-Ram fragmentation model and its use at the Sungun Copper Mine. *International Journal of Rock Mechanics*, vol. 46, no. 6. pp. 967–973. https://www.researchgate.net/publication/208032337_Modified_Kuz-Ram_fragmentation_model_and_its_use_at_the_Sungun_Copper_Mine/amp [accessed 28 June 2019].

Gonzalez, E. and Montoro, J. 1993. New analytical methods to evaluate fragmentation based on image analysis. *Rock Fragmentation by Blasting*. Balkema, Rossmanith, H. (ed.). Rotterdam. pp. 309–316.

Holton, G.A. 2014. Value-at-Risk: Theory and Practice. 2nd edn. Belmont, Holton, GA.

Ouchterlony, F., Sanchidrian, J., and Moser, P. 2016. Percentile fragment size predictions for blasted rock and the fragmentation-energy fan. *Rock Mechanics and Rock Engineering*, vol. 50, no. 4. pp. 751–779. https://link.springer.com/article/10.1007/s00603-016-1094-x [accessed 28 June 2019].

Robbins, N. 2013. Data driven journalism. http://datadrivenjournalism.net/resources/when_should_i_use_logarithmic_scales_in_my_charts_and_graphs [accessed 10 May 2018].

Spathis, A.T. 2013. A three parameter rock fragmentation distribution. *Measurement and Analysis of Blast Fragmentation*. Sanchidrián, J.A. and Singh, A.K. (eds.). Taylor & Francis, London. pp. 73-86.

Strelec, S., Gazdek, M., and Mesek, J. 2011. Blasting design for obtaining desired fragmentation. *Technical Gazette*, vol. 18, no. 1. pp. 79–86. https://hrcak.srce.hr/file/98636&ved=2ahUKEwi2rJWCyJnjAhUa1AKHcPoCHsQFjACegQIAhAB&usg=AOvVaw1E35VnKBQeCCeZwWSs1tHw&cshid=1562185270284 [accessed 8 June 2019].

Vesilind, P.A. 1980. The Rosin-Rammler particle size distribution. *Resource Recovery and Conservation*. Elsevier, Amsterdam. pp. 275-277. https://www.sciencedirect.com/science/article/pii/0304396780900074 [accessed 10 April 2018]. ◆

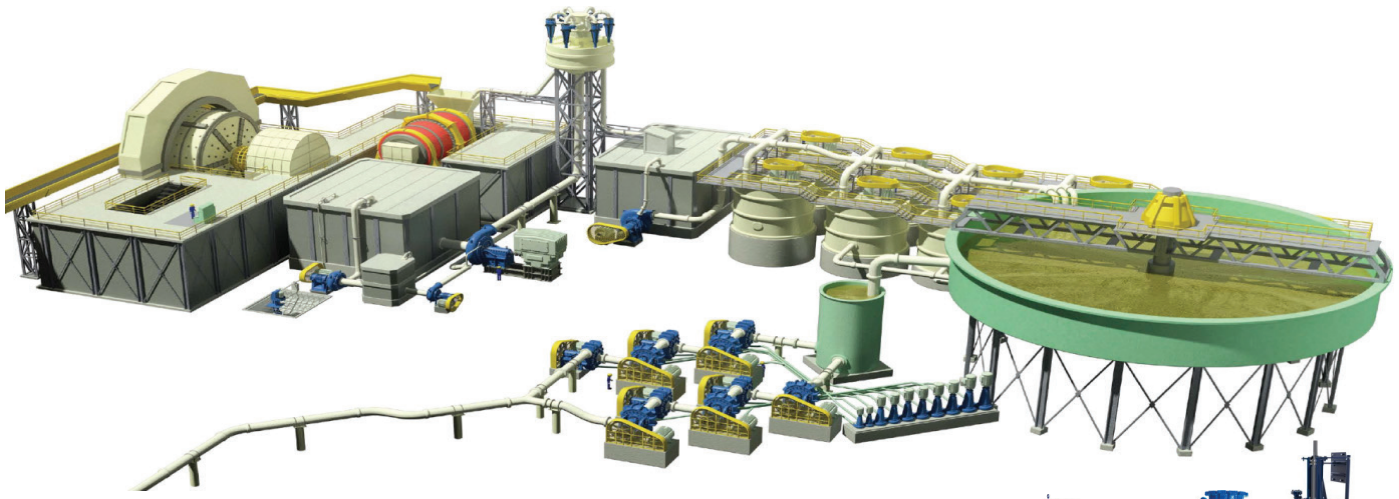

Single-source supplier: your partner for pumps, valves and service

KSB is one of the world's leading supplier of Pumps , Valves and related Systems. Wherever there are fluids to be transported, controlled or shut off, customers globally rely on our products.

WATER
INDUSTRY
WASTE WATER
ENERGY
MINING
BUILDING SERVICES

KSB in South Africa has branches in all the major centres as well as West Africa, East Africa, Namibia and Zambia, ensuring a bigger footprint.

www.ksbpumps.co.za

› Our technology. Your success.
Pumps • Valves • Service

Our Technology. Your Success.
Your B-BBEE Level 1 Partner

KSB

SAMREC
THE SOUTH AFRICAN CODE FOR THE REPORTING OF EXPLORATION RESULTS, MINERAL RESOURCES AND MINERAL RESERVES

SAMCODES
THE SOUTH AFRICAN MINERAL REPORTING CODES

SAMVAL
THE SOUTH AFRICAN CODE FOR THE REPORTING OF MINERAL ASSET VALUATIONS

SAIMM YPC
YOUNG PROFESSIONALS COUNCIL

Introduction to THE SAMREC AND SAMVAL CODES

Saturday · 21 September 2019

Mandela Mining Precinct, Auckland Park, Johannesburg

PRESENTER

Professor Rupprecht
University of Johannesburg

Lecture Outline

The object of the Lecture is to supply the participants with the basics of the SAMREC and SAMVAL Codes. The purpose of the 3-hour lecture is to supply young professionals with the opportunity to broaden their mining knowledge of general mining issues.

The lecture intends to provide the professional with a better understanding and appreciation of the South African reporting codes. Sufficient detail will also enable the mining engineer to benefit from this lecture as real issue are raised during the course of the 3 hour lecture. The lecture will be broken into four (4) - 30 minute sessions structured to comprise of a basic introduction of the Codes and key definitions and principles. The second and third session will introduce the SAMREC and SAMVAL Codes and their application in Public Reporting. The final session will provide a number of case studies thereby enabling participants to fully benefit from the sessions.

Developing a mining plan for restarting the operation at Uis mine

J.H. Maritz[1]* and S. Uludag[1]

***Paper written on project work carried out in partial fulfilment of B.Eng (Mining Engineering) degree**

Affiliation:
[1]University of Pretoria, South Africa.

Correspondence to:
J.H. Maritz

Email:
henko.maritz@gmail.com

Dates:
Received: 12 Dec. 2018
Revised: 18 Apr. 2018
Accepted: 24 Apr. 2019
Published: July 2019

How to cite:
Maritz, J.H. and Uludag, S. Developing a mining plan for restarting the operation at Uis mine.
The Southern African Insitute of Mining and Metallurgy

DOI ID:
http://dx.doi.org/10.17159/2411-9717/536/2019

ORCiD ID:
J.H. Maritz
https://orchid.org/0000-0002-5046-8934

Synopsis

AfriTin Mining Limited plans to reopen the Uis tin mine in Namibia and establish a pilot processing plant for phase 1 of the Uis tin project, which is scheduled to commence in the last quarter of 2018 . A mining plan is required for phase 1 to supply the new pilot processing plant with 500 kt of run-of-mine ore per annum, for a period of 5 years. New geological mapping and three-dimensional modelling of the mining area were utilized to identify the most optimal mining locations that require low initial waste stripping. An open-pit mining method was selected to target the surface outcrops of the pegmatite orebodies. The mine design criteria were determined and used as input to generate the mine design by utilizing professional engineering software. The mine design was optimized and an overall stripping ratio of 0.81 was achieved. A 5-year production schedule was developed for the mine design according to quarterly periods of three months. A fixed production target of 125 kt of ore was assigned to the quarterly periods, and a ramp-up production target of 65 kt of ore was assigned for the first period. The mobile mining equipment requirements were calculated, and recommendations were made for implementing the 5-year mining plan.

Keywords
mining plan, mine design criteria, production schedule, optimal, stripping ratio.

Introduction

AfriTin Mining Limited is the owner of the Uis tin project in Namibia and plans to reopen the Uis tin mine, which is located near the town of Uis, approximately 164 km north of Swakopmund. The Uis tin mine was owned and operated by Imkor Tin, a subsidiary of Iscor South Africa. Mining commenced in 1958, and the operation was closed in 1991. Steffen Robertson & Kirsten (SRK) defined the life of mine (LOM) plan for the historical Uis mine in 1989. The SRK report estimated the historical resources and reserves, which consisted of sixteen cassiterite-bearing pegmatite orebodies. SRK developed the most economical pit designs to provide the highest average tin grade at the lowest practical waste stripping ratio. Exploration data from the SRK report of 1989 was used extensively throughout this study, since no new exploration drilling has been conducted. The pegmatites are present as large, subvertical and outcropping veins up to 100 m in thickness. Once phase 1 is operational, mining will be conducted using conventional open pit mining methods. Initial production will be from exposed pegmatite veins in the old mine workings. AfriTin plans to establish a pilot processing plant by the end of 2018 to beneficiate run-of-mine ore at a rate of 500 kt per annum.

Project background

Phase 1 of the project required a mining plan for the reopening of the mine. This study focused on developing the phase 1 mining plan to supply the pilot processing plant with run-of-mine ore at a rate of 500 kt/a for a period of five years. The mining plan included a detailed mine design and production schedule for the phase 1 operation. The mining locations with the lowest stripping ratios were identified, and the opportunities and constraints of the historical pit excavations were considered in the mine design.

A detailed production schedule was developed for the optimal pit designs. The production schedule precisely identifies when and where mining must take place within the mine design to meet the required tonnages. The mining plan also provides recommendations for the required mobile mining equipment based on the production schedule.

Developing a mining plan for restarting the operation at Uis mine

Objectives and methodology

The following objectives were formulated.

- Develop the mine design criteria by utilizing historical information and a research-based approach
- Analyse the topographical surface and the geological block model of the mining area to identify alternative mining locations that will yield maximum grade
- Generate optimal pit designs for the V1 and V2 pegmatite orebodies with the lowest practical waste stripping ratio by utilizing professional mine design software
- Develop an optimal mining sequence that minimizes waste stripping by extracting the outcropping veins first, and strategically mining at locations that yield easy ore extraction
- Develop the waste and ore hauling routes using professional mine design software and satellite images
- Establish the most suitable mobile mining equipment fleet that minimizes hauling distances by utilizing first-principle calculations.

The research for this study was conducted on each of the mine design criteria. Furthermore, reports and articles related to the historical mining and processing operation were studied and the mine was visited to investigate the historical pits. Suitable mining methods for the operation were considered and compared. The ore definition and modifying factors associated with the mineable resource were determined. The company provided a three-dimensional geological model as input to the mining plan. The mining layout, mining limits, and pit design were developed using professional mine design software in cooperation with the mining engineer of AfriTin. The locations for the overburden dumps were determined and the hauling routes were designed. Subsequently, a mine production schedule was generated, again using proprietary scheduling software. The mobile mining equipment requirements were modelled based on the results of the mine production schedule. Finally, directives related to the management of the mining operation were established.

Scope of study

The mining plan is limited to the V1 and V2 pegmatite orebodies, which have been determined as the target for phase 1. This study focuses only on the primary mineral, cassiterite, and does not include any recommendations for secondary minerals contained in the V1 and V2 pegmatites. The methodology for developing the mining plan is applicable only to similar open-pit mining operations. The mining plan includes a mine design, production schedule, and recommendations for mobile mining equipment. A financial analysis is not included in this study.

Literature review

Geology and mineralization

The SRK (1989) historical estimates determined that the V1 and V2 pegmatite orebodies comprised approximately 50% of the total mineable reserves. The V1 and V2 pegmatites were reported with a tin grade of approximately 0.139%, which is higher than the overall reserve grade. The stripping ratios for the V1 and V2 pegmatites are economically favourable compared with the other pegmatites (Steffen Robertson & Kirsten, 1989).

The lack of digital information regarding the V1 and V2 pegmatites gave rise to a new mapping of both orebodies, conducted by AfriTin. High-resolution geological mapping and three-dimensional modelling of the V1 and V2 orebodies were completed at the beginning of 2018. The mapping exercise gave more confidence in the data that was used in the mine plan. One of the more important outcomes of the mapping was the extension of the V2 pegmatite to the southwest of the pit, enabling the extent of the V1 and V2 pegmatites orebodies to be accurately identified for planning purposes. The map of the V1 and V2 pegmatites is shown in Figure 1.

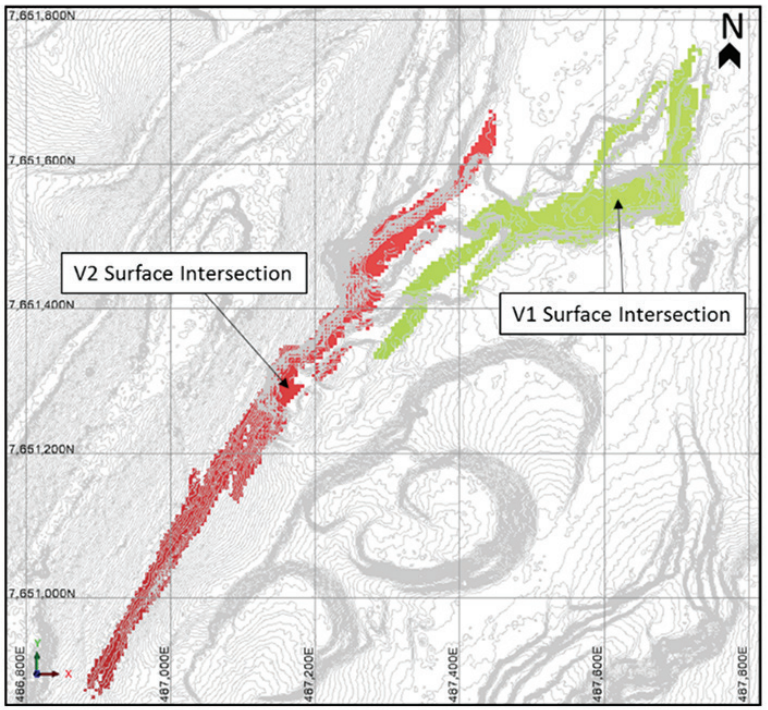

Figure 1—Mapped outcrops of the V1 and V2 pegmatites and 1 m contour intervals of the surface

Geotechnical considerations

The SRK report of 1989 provided the historical pit parameters and stated that the ground conditions at the Uis tin mine are stable under these parameters. The following is a list of the historical pit parameters (Steffen Robertson & Kirsten, 1989):

- Mining bench heights for V1/V2 pit are 15 m
- Road and ramp widths are 20 m
- Maximum road gradient is 10%
- Minimum working width at pit floor is 20 m
- Minimum cutback working width from toe to crest is 40 m.

The old V1/V2 pit design done by SRK in 1989 used slope angles of 60° for pegmatite and between 44° and 53.5° for waste rock (The MSA Group, 2017). According to the SRK report of 1989, the slope stability at these angles was good and no slope failure incidents were reported.

A digital terrain model (DTM) was used to inspect various historical mining locations within the V1/V2 pit. Measurements of the maximum slope angles were taken and compared to the theoretical pit parameters to prove the validity of the historical information. Figure 2 illustrates how the DTM measurements were taken. From inspection of the V1/V2 pit, it was found that most of the pit was mined at a slope angle between 55° and 60°.

Hydrogeological considerations

The area of the Uis Tin Mine has a very dry climate and the groundwater recharge is relatively low. The mining area does not receive much rain and the groundwater recharge is dependent on run-off in the Omaruru River (van Wyk, 2018). When mining for phase 1 takes place at elevations below the actual groundwater level, groundwater inflow into the pits is not considered a major risk and only limited pumping may be required due to the low groundwater recharge of the area. It is recommended that groundwater inflow should be monitored when mining for phase 1 starts, although no risk is expected.

Environmental considerations

According to the Environmental Impact Assessment study done in 2013, the Uis project can commence with the re-opening of the Uis tin mine provided that all the recommended control and mitigatory measures are in place. The following are the key findings of the EIA report (Jenneker and Williams, 2013).

- The geographical area where Uis tin mine is located is not considered a sensitive biodiverse area.
- Some negative impacts that can affect the Uis project have been identified, but these will not necessarily have any deleterious effect on the surrounding environment's biodiversity.
- The development of the Uis mine will create much-needed job opportunities, especially during the construction and operational phases. The mine will have a positive influence on the town of Uis and will contribute to the economy of Namibia.
- If the mining company maintains close interaction with the local authorities it can be expected that there will be no negative socio-economic impacts on the town of Uis.
- It is important that all the mitigating measures that were mentioned in the report are adhered to and included in a legal agreement between the relevant parties.

Economic considerations

The price and cost parameters in Table I were used to determine a financial model that calculated the break-even waste stripping ratio (BESR) for phase 1. Stripping ratio is defined as the amount of waste to ore that is removed. The BESR is the stripping ratio where the cost of production equals the income from sales. Exceeding the BESR during any specific operational period will result in an operating loss.

The BESR can be calculated by equating the cost of production to the income from sales:

$$\text{Cost of production} = \text{Net income from sale} \quad [1]$$

using the following symbols:

C_M = Mining cost per ton of concentrate
C_C = Concentrator cost per ton of concentrate
C_L = Logistics cost per ton of concentrate
C_O = Overhead costs per ton of concentrate
C_Y = Royalty per ton of concentrate
C_S = Sales commission per ton of concentrate
C_T = Treatment charges per ton of concentrate
I_G = Gross income per ton of concentrate

Table I

Price and cost parameters used for calculation of the break-even waste stripping ratio (Afritin, 2018a)

Parameter	Value
Gross income (US$/t concentrate)	12 600
Mining cost (US$/t)	2.55
Concentrator cost per ton processed (US$/t)	5.82
Logistics cost (US$/t concentrate)	150
Overhead cost per tonne of concentrate (US$/t)	1228
Royalty (US$/t concentrate)	343
Sales commission (US$/t concentrate)	378
Treatment charges (US$/t concentrate)	654
Run-of-mine Sn feed grade	0.136%
Concentrate Sn grade	60%
Overall recovery of Sn metal	60%

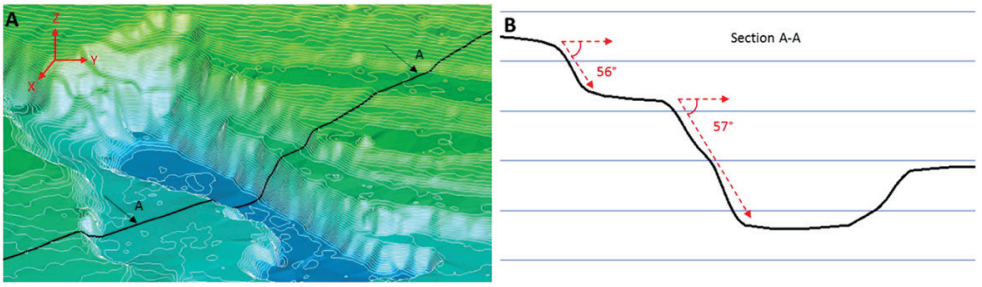

Figure 2—Position of section line (A) and cross-section view of the V1/V2 pit (B)

BESR = Break-even waste stripping ratio
C_m = Mining cost per ton mined
C_{cp} = Concentrator cost per ton processed
G_f = Run-of-mine feed grade
R_m = Overall Sn metal recovery
G_c = Concentrate Sn grade (%)

Equation [1] can be rewritten as:

$$C_M + C_c + C_L + C_O = I_G - C_S - C_T - C_Y \quad [2]$$

where:

$$\text{Mining cost per ton of ore} = (1 + \text{BESR}) * C_m \quad [3]$$

The mining cost per ton of concentrate:

$$C_M = \frac{\text{Mining cost per ton of ore}}{\text{Concentrate tons produced per ton of ore}} \quad [4]$$

$$C_M = \frac{(1 - \text{BESR}) * C_m}{(G_f * R_m)/G_c}$$

The concentrator cost per ton of concentrate:

$$C_C = \frac{C_{cp}}{(G_f * R_m)/G_c} \quad [5]$$

By solving for break-even waste stripping ratio:

$$\text{BESR} = \frac{\left(I_G - C_S - C_T - C_c/\left(\frac{G_f * R_m}{G_c}\right) - C_L - C_O - C_Y\right) * (G_f * R_m)/G_c}{C_m} - 1 \quad [6]$$

A BESR of 1.97 was calculated, which means that for every unit of ore mined, 1.97 times the equivalent unit of waste can be mined to break even. The BESR was used as a mine design criterion to determine the limit of the open pit mine design.

Results and discussion

Mining method

The first mining phase at Uis tin mine will implement an open pit mining method at preselected mining locations that target the V1 and V2 pegmatite surface outcrops. The V1 and V2 pegmatite orebodies will be mined by two separate open pits. The open pit mine process cycle consists of drilling and blasting to break and expose the ore, followed by loading, hauling, and dumping of the broken ore

Ore and waste determination

In this study 'ore' is defined as the pegmatite rock, from both the V1 and V2 pegmatite bodies, that consists of valuable mineralized material. 'Waste' is defined as the schist host rock surrounding the V1 and V2 pegmatite bodies. It should be noted that all the material outside the pegmatite bodies, within the geological model, is assumed to be waste rock. A cut-off grade method is normally used to distinguish between ore and waste material. However, due to the nature of the ore and waste rock, a simpler approach was used. The ore and waste rock have distinct colours which make them easy to identify in the pit. The visual difference between the ore and waste rock is illustrated in Figure 3.

Mine design criteria

The information gathered from the literature review was investigated to conclude the mine design criteria. The mine design criteria were used as input to the mine design for phase 1 at the Uis tin mine.

Digital terrain model (DTM)

A digital terrain model (DTM) for the Uis mining area was generated by combining a stereo pair of satellite images and 12 control points from a differential GPS survey that was conducted within the mining area. The DTM shown in Figure 4 is accurate to 1 m in the X, Y, and Z dimensions and was utilized to develop the mine design.

Geological model

The geological model for the V1 and V2 pegmatite bodies is shown in Figure 5. This three-dimensional geological model served as a reference point for the mine design process. The pegmatite envelopes in the geological model were used to determine the extent of the mine design. A relative density of 2.66 t/m³ was assigned to both the waste and ore material in the geological model. An average grade of 0.139% Sn was assigned to both the V1 and V2 pegmatite bodies. The geological model was used for the tonnage calculations for both waste and ore.

Figure 3—Contact between the pegmatite and schist and their distinct colour (Afritin, 2018b)

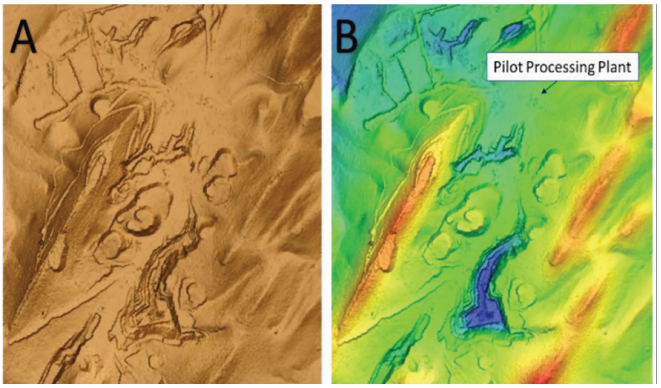

Figure 4—(A) Plan view of the digital terrain model. (B) The DTM coloured according to elevation changes, together with the location of the pilot processing plant

Figure 5—The geological model of the V1 and V2 pegmatites extrapolated beneath the contoured map of the surface

Geological and mining losses

The life-of-mine report by SRK (1989) assumed zero geological and mining losses, based on historical operating data and experience. For this study, it is also assumed that the geological and mining losses will be zero, as it is not expected that the nature of the ore deposit would have changed over the past three decades.

Production scheduling constraints

The production schedule was developed by assuming that the production from the different mining stages within the pit designs will proceed in a bench-by-bench fashion, starting at the top bench and moving downwards. There is a possible opportunity to split production between multiple levels within a single mining stage. However, the production schedule did not include this possibility, which resulted in a more conservative overburden stripping profile.

Pit design parameters

The historical pit parameters from the SRK report of 1989 were compared with the digital measurements of the old pit workings. It was found that the maximum slope angles were between 50° and 60°. The historical pit parameters were used together with new open-pit standards from AfriTin to determine the new pit design parameters.

It was assumed that relatively small mining equipment, such as excavators and articulated dump trucks (ADTs), will be used for phase 1 mining. The following is a list of the new parameters used the V1 and V2 pit designs:

- Mining bench heights are 10 m
- Mining bench widths (berms) are 7 m
- The overall pit slope angle is 55° (crest-to-crest)
- Road and ramp widths are 15 m
- Maximum road gradient is 12.5%
- Minimum working width at pit floor is 20 m.

The pit parameters were modelled in a simple design and are illustrated in Figure 6 to better understand and visualize the terms.

Break-even stripping ratio

The BESR of 1.97 was calculated by utilizing the financial model. The BESR was used as a benchmark for both the mine design and the production schedule. The maximum stripping ratio of the mining sequence must not exceed the BESR.

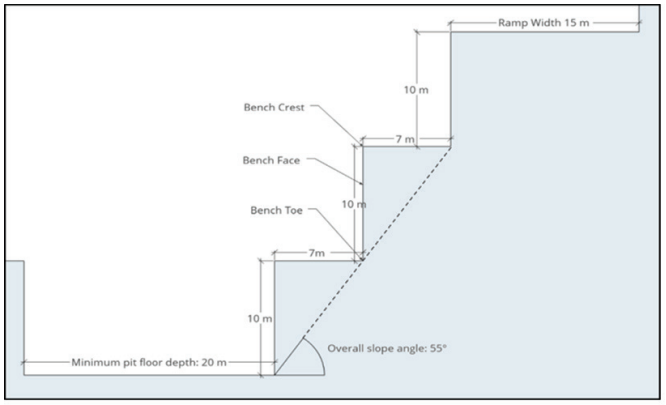

Figure 6—Illustration of the open pit bench design parameters for the V1 and V2 pit design

Number of mining areas

The nature of the V1 and V2 pegmatite orebodies allows for the simultaneous development of two different open pits. This decreases the production risk compared to a single pit, should an incident occur that stops mining activities within the pit, and allows for more flexible grade control. The two mining areas are illustrated in Figure 7.

Mine design

The pit designs for both the V1 and V2 pegmatite orebodies were generated with professional mine design software. The pit designs were optimized to reduce the overall stripping ratio while still adhering to the tonnage requirements of the 5-year mining plan. The pit designs were generated according to five different stages that represent the sequence for mining the two open pits.

The V1 and V2 pegmatite outcrops on the surface are illustrated in Figure 8, together with the pit designs for both the V1 and V2 pegmatite bodies.

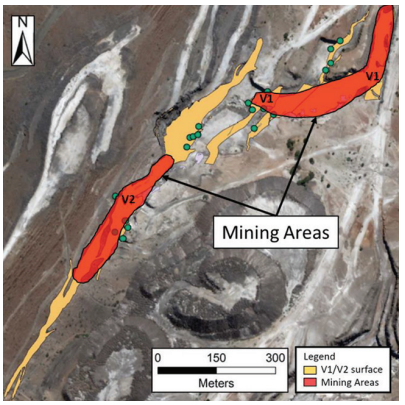

Figure 7—Two mining areas illustrated on the geological map of the V1 and V2 pegmatite orebodies (Afritin, 2018b)

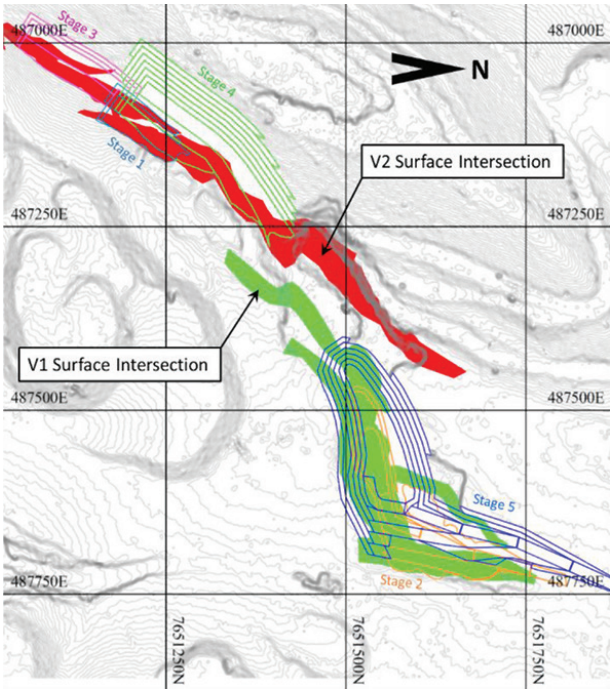

Figure 8—Overview of the mine design and the mapped V1 and V2 pegmatite surface outcrops

The pit design for the V2 pegmatite orebody was generated with three different stages as illustrated in Figure 9. The surface outcrops of the V2 pegmatite orebody are targeted in stage 1 and stage 3 of the pit design.

Stage 4 of the pit design will serve as a pushback with a higher incremental waste stripping ratio. The pit designs for both stage 1 and stage 3 have a total of three 10 m benches and the design for stage 4 has seven 10 m benches. Access roads for drilling machines will be developed on the hill to the northwest side of the pit.

The section line A-A was generated perpendicular to the strike of the V2 pegmatite orebody. This section line was used to generate a vertical section view of the V2 pit design as illustrated in Figure 10. The pit design for stage 1 was generated mostly within the V2 pegmatite orebody, which resulted in a low waste stripping ratio. The waste stripping ratio increases during the stage 4 pushback since more waste is contained within the boundary of the pit. The southeastern boundaries of the pits were generated along the contact line between the V2 pegmatite orebody and the waste rock to reduce the waste stripping ratio.

The pit design for the V1 pegmatite orebody was generated with two different stages as illustrated in Figure 11. The stage 2 design was targeted at the outlines of the historical mining excavations with the objective of deepening the historical excavations at a low waste stripping ratio. Stage 5 will serve as a pushback for stage 2 to access the ore at increasing depth. The pit design for stage 2 was generated with two 10 m benches and the design for stage 5 has a total of five 10 m benches.

The location of the access ramps was determined by utilizing the historical access ramps since the development of these access ramps will require less waste removal.

Figure 12 illustrates the stage 2 pit design generated within the boundary of the V1 pegmatite orebody to ensure a low waste tripping ratio. The stage 5 pit design was generated to access the ore at increasing depth and requires more waste removal during the pushback.

The geological block model, surface digital terrain model (DTM), and the pit designs for the different mining stages were integrated into one model as illustrated in Figure 13. This model

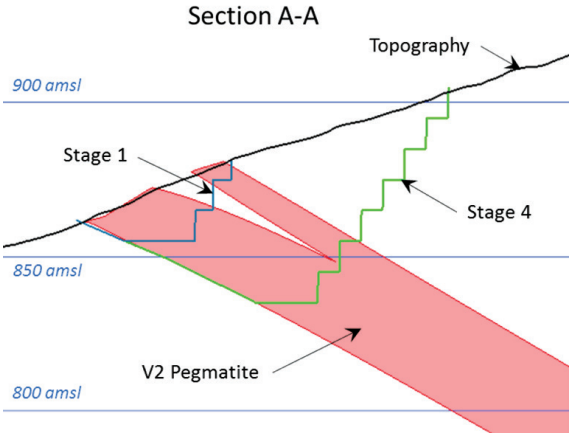

Figure 10—Section view along the line A-A illustrating the outlines of the pit designs for both stage 1 and stage 4 relative to the V2 pegmatite orebody

was used to calculate the ore and waste volumes and tonnages for each mining stage. The calculated volumes and tonnages are summarized in Table II, together with the waste stripping ratio for each mining stage.

Since a low overall waste stripping ratio of 0.81 was achieved for phase 1, it has proved beneficial to implement the method of targeting the surface outcrops of the pegmatite bodies during the first stages of mining, followed by incremental pushbacks to allow access to the deepening pegmatite orebodies. The pit designs for the V1 and V2 pegmatite orebodies will give access to a total of approximately 2 751 440 t of ore throughout phase 1.

The objective of the phase 1 mining plan is to deliver ore to the pilot processing plant at a rate of 500 000 t/a for a period of five years. Therefore, phase 1 must deliver a total of 2.5 Mt of ore to the pilot processing plant. The pit designs that were generated will be sufficient for phase 1 since an excess of 251 440 t of ore can be delivered to accommodate for potential losses.

It should be noted that the information in Table II is not compliant with the SAMREC Code due to the lack of drill-hole information from the mineral exploration phase. It is possible that

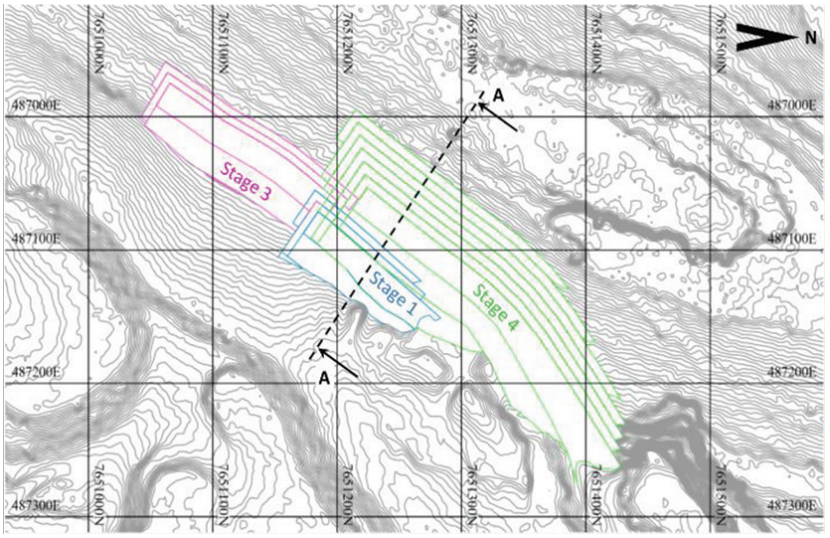

Figure 9—An overview of the V2 pegmatite pit design and the boundaries of the different stages together with the contour map of the surface topography

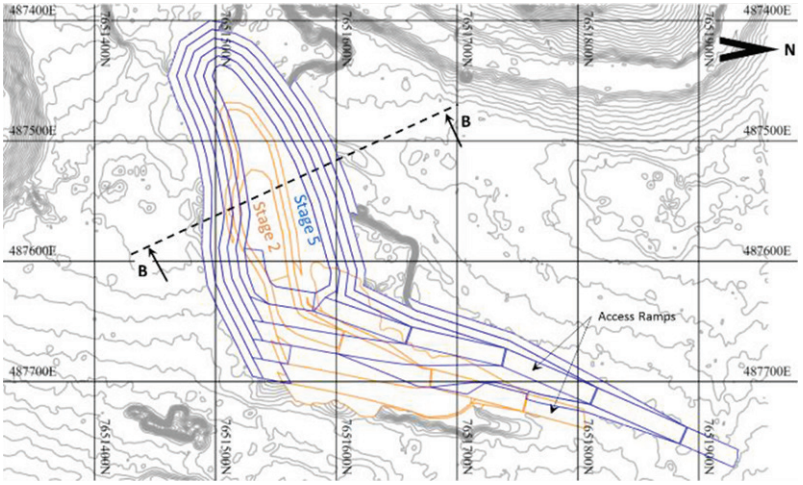

Figure 11—An overview of the V1 pegmatite pit design illustrating the boundaries of the different stages together with the contour map of the surface topography

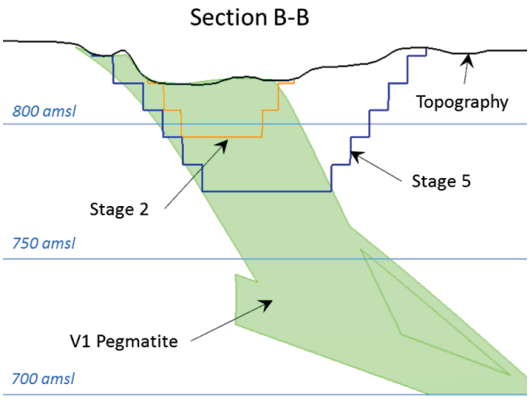

Figure 12—Section view along the line B-B illustrating the outlines of the pit design for both stages 2 and stages 5 relative to the V1 pegmatite orebody

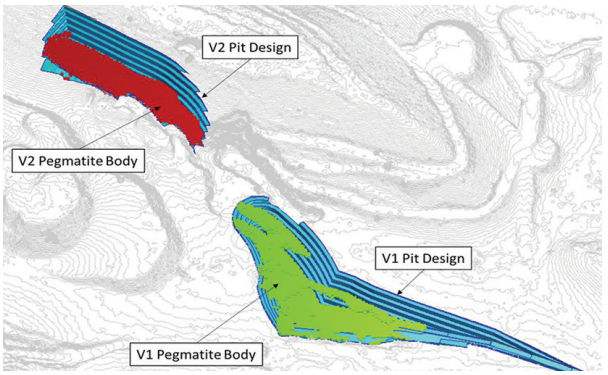

Figure 13—An overview of the geological model of the V1 and V2 pegmatite bodies contained within the final boundaries of the pit designs and the surface topography

Table II

Summary of the volumes and tonnages for both ore and waste for each mining stage per pegmatite orebody

Pegmatite body	Mining Stage	Volume (m³)		Tons (t)		SR
		Ore	Waste	Ore	Waste	
V1	2	157.813	50.500	419.783	134.330	0.32
	5	427.500	415.938	1 137.150	1 106.395	0.97
	1	59.438	9.438	158.105	25.105	0.16
V2	3	72.250	34.813	192.185	92.603	0.48
	4	317.375	327.125	844.218	870.153	1.03
Total		1 034.376	837.814	2 751.440	2 228.585	0.81

the *in situ* pegmatite bodies differ from the modelled pegmatite bodies. Therefore, the pit designs were generated to deliver excess ore tonnages to minimize the risk of the *in situ* orebody deviating from the modelled orebody.

Production sequence and schedule

Specialist mine modelling software was used to develop a mining production schedule for the mine designs. The mine production was scheduled according to quarterly periods of three months, with mining assumed to commence on 1 October 2018. A fixed production target of 125 000 t of ore was assigned to the quarterly periods. It is assumed that the gradual ramp-up to steady state production will take approximately one period (three months). Therefore, the production target for the first period was scheduled at 62 500 t of ore to allow for the gradual ramp-up to steady-state production. The production target split is 57%/43% for the V1 and V2 pits respectively. The ratio of the split was developed based on the ore tonnages contained within each pit design shell.

The initial mining stage for both the V1 and V2 pit designs was generated to target a low waste (overburden) stripping ratio. It should be noted that the low waste stripping ratios of the initial stages do not imply that the overall waste stripping ratio for the initial periods of the production schedule will be low, since the

production schedule was developed by utilizing the initial mining stages to accommodate for the simultaneous removal of the overburden of the later stages.

Stage 4 and stage 5 of the mine design have higher stripping ratios than the initial stages since more waste removal is required to access the ore at increasing depth. Therefore, the required waste removal for stages 4 and 5 will commence simultaneously with the initial mining stages. Figure 14 illustrates that the waste stripping ratio for the first nine quarters is significantly higher than the overall stripping ratio of 0.81.

The graph in Figure 15 illustrates the mining sequence of the ore and overburden during each stage. The required overburden removal for stages 4 and 5 will commence well in advance of the planned ore mining for stages 4 and 5, as illustrated in Figure 15. Stages 1, 2, and 3 will be completely mined out within the first nine quarters, and during this period a relatively large amount of overburden from stages 4 and 5 will also be removed.

The production schedule and the mine designs were integrated into a three-dimensional scheduling model that provides yearly representations of the mining progress in terms of the face positions, as illustrated in Figure 16. The scheduling model visually represents the mining sequence and clearly identifies where mining activities will take place within the pit designs throughout phase 1. The different colours in Figure 16 represent the different mining stages and illustrate how the ore and overburden extraction will progress. The model also proved the validity of the production schedule in terms of adhering to the spatial constraints of the mine design.

Overburden and waste disposal

The historical waste dumps on the eastern side of the V1 and V2 pits will be used for the waste disposal during phase 1. The historical waste dumps are situated relatively close to the new pit designs for both the V1 and V2 pegmatite bodies and require little development. The routes leading from the pits to the waste dump location are shown in Figure 17.

Mobile mining equipment requirements

The required number of haul trucks and drill rigs was determined by first-principle calculations based on the data of the phase 1 production schedule. Hauling routes leading to the waste dump

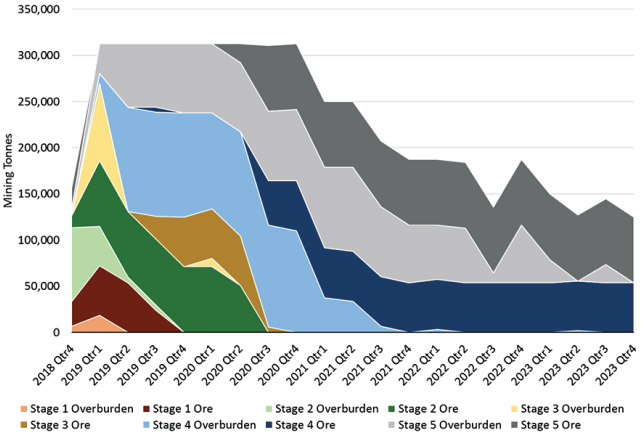

Figure 15—Graph of mining sequence in terms of the overburden and ore tons per stag

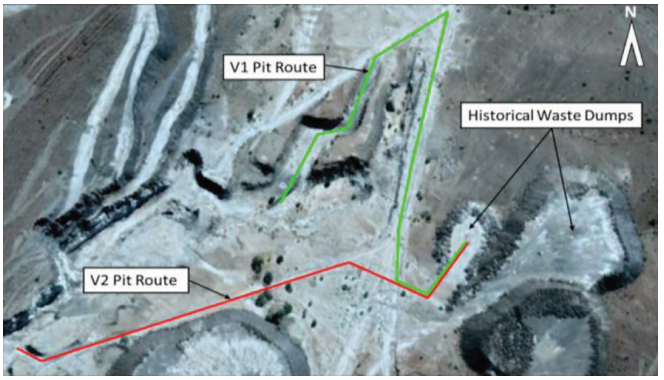

Figure 16—Satellite image of the historical waste dumps and the marked routes from the V1 and V2 pits to the waste dumps (Google Earth, 2018)

and the pilot processing plant were generated for both the V1 and V2 pit designs as shown in Figure 18. The distances and inclinations of the hauling routes were determined and used to calculate the average cycle times of a typical 25 t haul truck. The number of cycles a waste and ore truck can complete per quarter is calculated in Table III.

Typical drilling parameters for the ground conditions at the Uis tin mine are provided in Table IV.

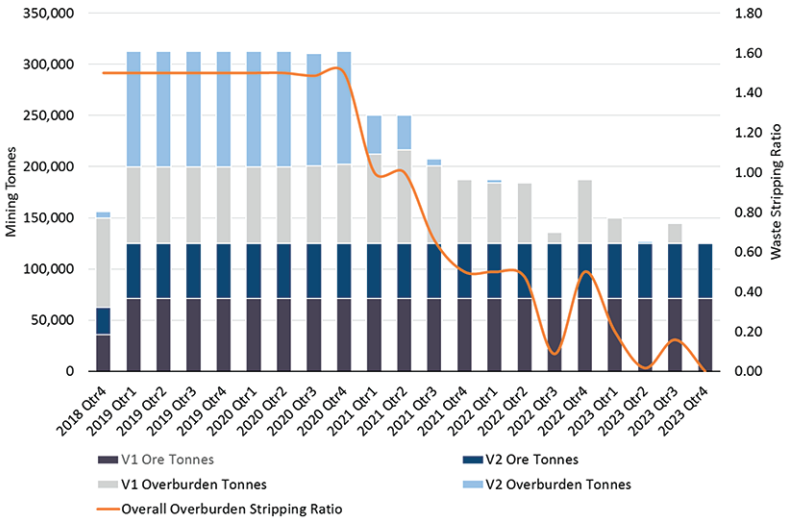

Figure 14—Quarterly tonnage profile and waste stripping ratio of the mining production schedule

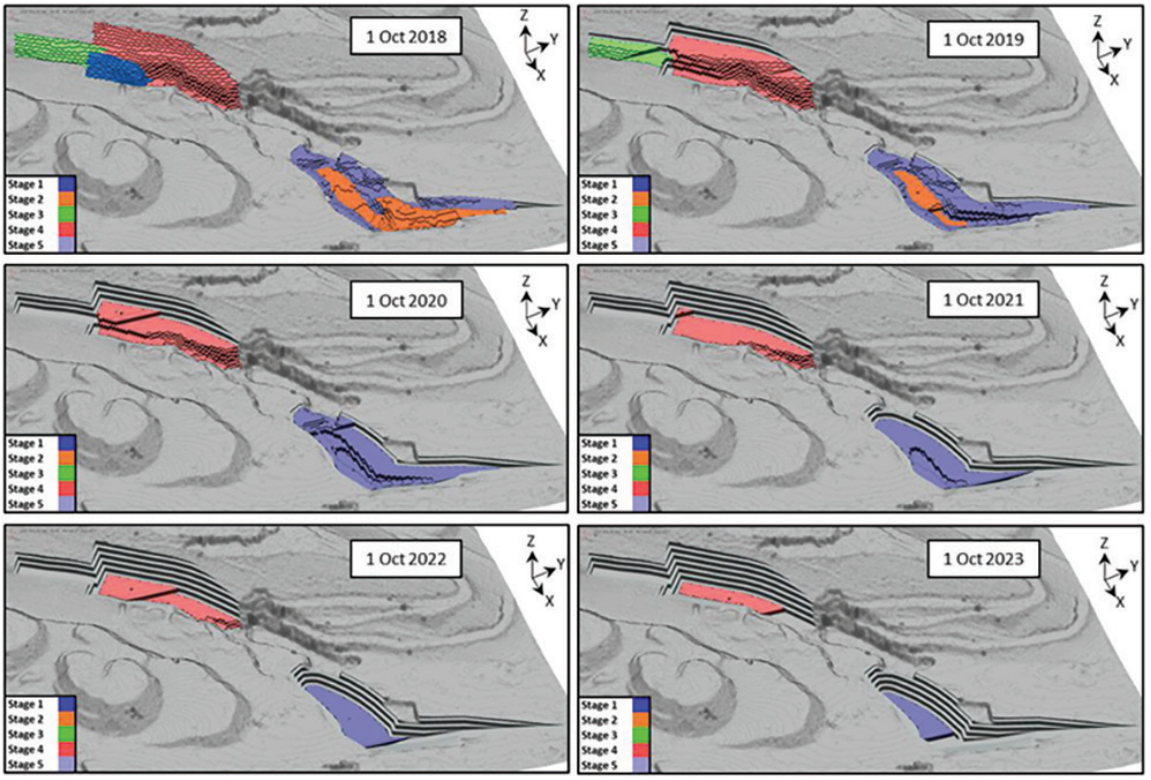

Figure 17—Satellite image of the historical waste dumps and the routes from the V1 and V2 pits to the waste dumps (Google Earth, 2018)

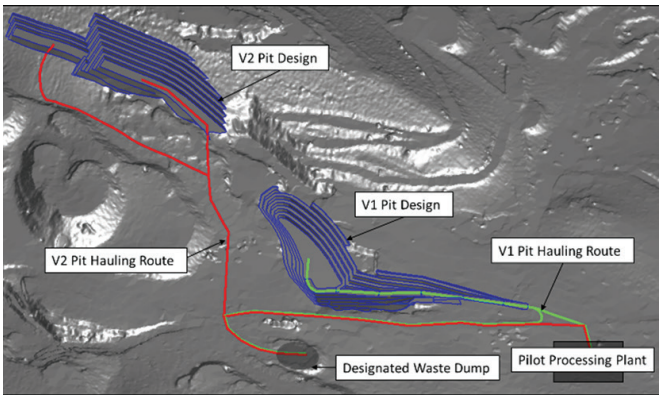

Figure 18—Overview of the V1 and V2 pit hauling routes leading to the waste dump and pilot processing plant

Table III

Mining and hauling parameters per quarter period for both the V1 and V2 pit operations (Afritin, 2018a)

Truck operating parameters	Units	V1 pit	V2 pit
Shift hours per day	h	10	10
Days per quarter	d	91	91
Availability	%	75%	75%
Utilization	%	70%	70%
Operating hours per quarter	h	584	584
Truck payload	t	25	25
Fill factor	%	90%	90%
Tons per truck cycle	t	22.5	22.5
Average cycle time (ore)	min	7.7	8.8
Average cycle time (waste)	min	11.2	7.3
Possible cycles per truck per quarter (ore)	Cycles	4 559	4 002
Possible cycles per truck per quarter (waste)	Cycles	3 121	4 775

Table IV

Drilling parameters used to calculate the required number of trucks (Afritin, 2018a)

Drilling parameters	Units	Value
Relative density (RD) of ore *in situ*	t/m³	2.66
Relative density (RD) of waste *in situ*	t/m³	2.66
Burden	m	2.5
Spacing	m	2.5
Blast-hole length	m	10
Area coverage per blast hole	m²	6.25
In situ volume per blast hole	m³	62.5
Drilling metres per *in situ* volume	m/m³	0.16
Average drilling metres per month per rig	m/month	10 000
Average drilling metres per quarter per rig	m/quarter	30 000

The abovementioned parameters were used to calculate the number of haul trucks and drill rigs required per quarter based on the production schedule for phase 1. Figure 19 shows the calculated equipment requirements per quarter.

Conclusions

The average stripping ratio was optimized by generating initial mining stages along the surface outcrops of the V1 and V2 pegmatite orebodies, followed by incremental pushback stages. The designs for the initial mining stages were generated with low average stripping ratios and the subsequent pushback stages were generated with higher average stripping ratios. This development strategy allows for a fast production ramp-up and limited mining infrastructure. The pre-stripping waste requirements of the pushback mining stages were significantly larger than those for the initial mining stages. The production

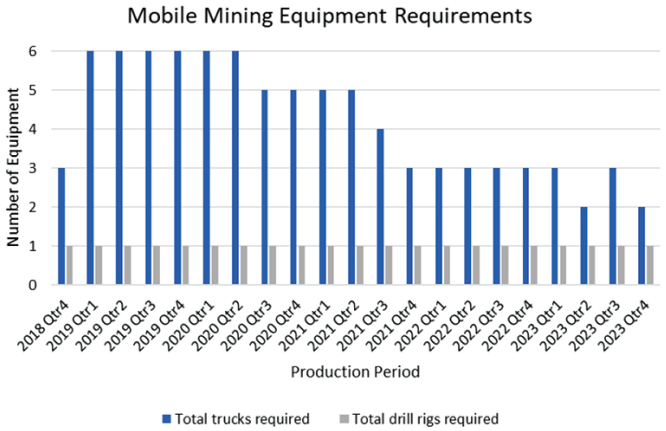

Figure 19—Number of haul trucks and drill rigs required per quarter

schedule was developed by allowing the pre-stripping of the pushback stages to commence simultaneously with the initial mining stages, which resulted in the first periods of the production scheduling having a higher stripping ratio than the average stripping ratio. The mine design and production schedule were successfully optimized to ensure that the maximum stripping ratio per quarter does not exceed the break-even stripping ratio. The mobile mining equipment requirements were determined to ensure that the mining plan can be executed adequately.

The optimized mine design and production schedule presented in this study provide a recommended long-term framework for the phase 1 mining operation at the Uis tin mine. Once phase 1 is operational, the optimized 5-year mining plan will supply the pilot plant with ore at a rate of 500 000 t/a while maintaining an average waste to ore stripping ratio of less than 1.0.

Recommendations

It is recommended that the mine design and production schedule should be implemented in the phase 1 mining plan at the Uis tin mine. Exploration drilling should be conducted to improve the confidence in the geological data and the phase 1 mining plan should be revised and updated accordingly.

References

Afritin. 2018a. Afritin unit cost model v6. Illovo, South Africa.

Afritin. 2018b. High-resolution geological mapping and 3D modelling of the V1/V2 pegmatite, Uis Tin Mine. Illovo, South Africa.

Jenneker, A. and Williams, W. 2013. Environmental Impact Assessment for the re-commissioning of the Uis Tin and Tantalum Mine. EnviroSolutions, Manassas, VA.

Steffen Robertson & Kirsten. 1989. Life of mine plan for Uis Tin Mine. Sandton, South Africa.

The MSA Group. 2017. Competent Person's Report for Uis tin project, Namibia. Randburg, South Africa

Van Wyk, B. 2018. Uis tin mine: An appraisal of water supply alternatives for the pilot plant., BVW Groundwater Consulting Services, Namibia. ◆

Learn more:
www.geobrugg.com/rockfall

GEOBRUGG®
BRUGG
Safety is our nature

Why choose Geobrugg?

- For the most valuable asset in life - our safety
- High tensile steel mesh
- Blast resistant
- Different mesh types for different ground conditions
- Proven static and dynamic performance
- Cutting edge corrosion protection
- Tailor-made sheet sizes

Geobrugg Southern Africa (Pty) Ltd | Unit 3 Block B Honeydew Business Park | 1503 Citrus Street | Honeydew 2170 | South Africa | T +27 11 794 3248 | info@geobrugg.com | www.geobrugg.com

Optimization of the cycle time to increase productivity at Ruashi Mining

I.N.M. Nday[1]* and H. Thomas[1]

*Paper written on project work carried out in partial fulfilment of BSc.Eng (Mining Engineering) degree

Affiliation:
[1]University of the Witwatersrand, South Africa.

Correspondence to:
I.N.M. Nday

Email:
isaacndayone@gmail.com

Dates:
Received: 6 Feb. 2019
Revised: 5 Apr. 2019
Accepted: 16 Apr. 2019
Published: July 2019

How to cite:
Nday, I.N.M. and Thomas, H. Optimization of the cycle time to increase productivity at Ruashi Mining.
The Southern African Insitute of Mining and Metallurgy

DOI ID:
http://dx.doi.org/10.17159/2411-9717/624/2019

ORCiD ID:
I.N.M. Nday
https://orchid.org/0000-0003-1802-3609

Synopsis

The optimization of the cycle time to increase productivity at Ruashi Mining was an on-site project investigation conducted from December 2017 to January 2018. The main objective of the investigation was to determine the actual cycle time components. These comprise the queuing time, loading time, hauling time, and dumping time of ADTs (articulated dump trucks). Data was also collected on two hydraulic shovels to identify where these could be optimized. The actual cycle time obtained was compared to the theoretical cycle time to ascertain the constraints, which affect productivity. By applying Systems Thinking to the cycle time, man-made constraints of the actual cycle time were identified and recommendations to mitigate them suggested to optimize the cycle time. However, rainfall is a natural constraint that adversely affects the actual cycle time, and which cannot be mitigated.

In addition, both the theoretical and actual cycle time were analysed, as well as the theoretical and actual productivity for the year 2017. Based on the findings, conclusions and recommendations were made to optimize the cycle time.

Keywords
opencast mining, cycle time, optimization, productivity.

Introduction

The aim of the project was to increase Ruashi Mining's productivity by 39%, from about 7.537 Mt of broken material mined to 12..367 Mt targeted in 2017.

Background

Ruashi Mining is a copper (main commodity), cobalt (by-product), and acid producer located in the Democratic Republic of Congo (DRC), 10 km from the city of Lubumbashi. Figure 1 shows the location of the Ruashi Mining open pit.

Ruashi Mining started production in 1911 and in 2005 the mine was registered as a DRC company owned by Metorex Group Limited. In November 2013, the Chinese company Jinchua Group International Resources Co. Ltd. bought a majority stake in the business. Ruashi Mining currently produces 38 000 t of copper and 4400 t of cobalt per annum. The company has contracted NB Mining (a contract mining company) to transport its ore. To optimize the productivity of the mine, considering ore flow delivery at Ruashi Mining, the cycle time is the indicator used in this project. The cycle time components were recorded on site using a stopwatch.

Problem statement

There are many ways in which the productivity of a mine can be optimized, one way being by decreasing the actual cycle time. At Ruashi Mining there are constraints affecting and extending the cycle as shown in Figure 2. The constraints need to be identified and eliminated or mitigated to optimize the cycle time, which will increase productivity in terms of the tonnage of broken rock transported per annum.

Literature survey

To structure this project, a Master's project on the optimization of the haulage cycle model for open pit mining using a simulator and a context-based alert system was reviewed.

By utilizing mining software, simulations of an actual system in a process can be generated. Parameters of the simulation can be modified several times with the aim of looking for the ultimate optimization model. In this way it is possible to save costs, resources, and time.

Optimization of the cycle time to increase productivity at Ruashi Mining

Figure 1—Location of Ruashi Mining in the southern part of the DRC (Google Earth, 2018)

Excavator type	ADT type	Excess minutes
For 6.2 m³	B40D:	1.51 min
	B50D:	4.13 min
For 5.5 m³	B40D:	2.08 min
	B50D:	4.23 min

Figure 2—Excess minutes in the cycle time per excavator and ADT type

Furthermore, an As-Is and a To-Be model were developed to represent the haulage route of an open pit mining operation so that the cycle time can be optimized. Values generated with the As-Is model were subsequently adjusted in the To-Be. This model could be used for other mines, taking into account their parameters such as the production, geology, and haulage equipment.

The main goal of the project was to develop a methodology to improve productivity, reduce unproductive time, increase truck and shovel utilization, and reduce the queuing time for shovels and the crusher by applying simulation techniques, without incurring any additional investment.

In addition, the As-Is model allowed for the representation of a mine operating at a particular time, and the To-Be model showed how the operation would look after certain adjustments. (Vasquez Coronado, 2014).

Ercelebi and Bascetin (2009) developed a model based on closed queuing network theory that can be utilized to determine the optimal number of trucks working with each shovel in the system. In addition, using a linear programming model they determined how the ADTs should be dispatched to the shovels. The case study was conducted at the Orhaneli open pit coal mine in Turkey. Ercelebi and Bascetin stated that productivity of the equipment is an important factor in the profitability and that shovel-truck systems are the most common in open pit mining. The aim of developing a model was to maximize productivity and hence increase production, which in turn will result in cost reduction and increased profitability.

At Ruashi Mining ADTs do not arrive at the shovel at consistent times, nor does it take the same amount of time for shovels to load trucks. Therefore, the randomness of arrival times of ADTs at the shovel results in queuing time or the shovel being idle while waiting for ADTs to arrive.

A linear programming model (LPM) assumes no ADTs queuing under ideal conditions with maximum shovel utilization. LPM minimizes the number of ADTs required for the shovel utilization without ADTs queuing and is equivalent to maximizing the overall production rate.

Lane (2018) stated that a fundamental understanding of the mining system is vital to maximizing operational output. Systems Thinking is a management discipline used to comprehend different components constituting a system and to examine how these components link and interact to contribute to the overall system efficiency.

The mining system comprises different activities that interlink and when the optimum performance of each activity is obtained, the targeted throughput can be produced. An underperforminig activity compromises the total throughput. Therefore, it is imperative to thoroughly understand the mining system to identify a constraining activity in that system and optimize it to improve the mining output. It is worth noting that, optimizing a non-constraint activity will not have as great an impact on the overall throughput as optimizing a constraint (Goldratt, n.d.).

The Theory of Constraints is a methodology for identifying the most important constraint that compromises the mine throughput and then systematically improving that constraint until it is no longer the limiting factor. Sets of tools provided by the Theory of Constraints to maximize the mine throughput are:

1. The five focusing steps (used to identify and eliminate constraints) as shown in Figure 3.
2. The thinking processes (used to analyse and resolve problems).

These are designed with cause-and-effect tools. Firstly, identify the cause of undesirable effects, and secondly eliminate them without creating new ones. Thinking processes answers three questions:

- What needs to be optimized?
- What should it be optimized to?
- What actions will lead to the optimization?

3. Throughput accounting (a method for measuring performance and guiding management decisions) (Goldratt, n.d.).

Catoca Mining Society (CMS) is an opencast diamond mine which was assessed with the purpose of productivity optimization. The production rates at the mine were neither constant nor did they follow the designed or planned output. As a strategy to overcome the issue, the mine increased the unit

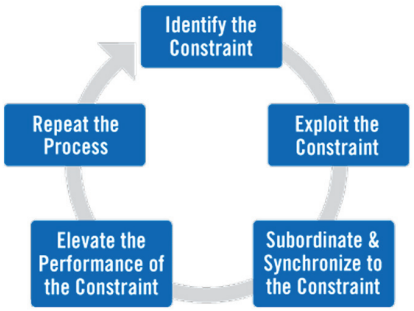

Figure 3—Five focusing steps to identify and eliminate constraints

numbers for both excavators and haulage to operate at maximum efficiency. The operational conditions such as the weather, breakdowns, and maintenance were to be considered because these conditions could disrupt the hauling and loading operation.

Achieving shovel productivity is dependent on having adequate ADT coverage to minimize shovel delays. In addition, the availability of the shovel and ADT system is a crucial parameter to consider, as it dictates the utilization and subsequently the output (productivity) of the system.

The parameters affecting the loading/haulage cycle were identified and simulated accordingly to determine the optimum operation cycle. Furthermore, the results have shown that for a distance of 2.7 km, six ADTs should be used for optimal efficiency (Vemba, 2004).

Mkhatshwa (2009) investigated the Mamatwan opencast manganese mine in South Africa, which was failing to reach its daily production target. This was due to factors such as road conditions, and poor matching of ADTs and shovels. Mkhatshwa further stated that properly designed haul roads result in minimum traffic congestion and thus increase the production efficiency of the ADTs.

Mkhatshwa also stated that by correctly matching the equipment, production can be improved by minimzsing the loading time and obtaining 95% loading of ADTs. In practice, it is impossible to achieve a 100% load for the ADTs.

On-site investigation

The on-site investigation included the time spent at the Ruashi Mining, under NB Mining. The purpose was to investigate the mining operations, to identify constraints and to collect cycle time data to determine the total actual cycle time for optimization to be realized.

Interpretation of data

The interpretation of the data (analysis and results) included statistical calculations to find the average loading, hauling, and manoeuvring time (dumping and queuing times). The actual cycle time was then compared to the theoretical cycle time and the excess times were determined for each cycle time component.

Systems Thinking applied to optimize the cycle time

Approach to optimize the cycle time

By definition, Systems Thinking is a management discipline used to comprehend different components constituting a system and examine how these components link and interact to contribute to the overall system efficiency (Lane, 2018). Figure 4 shows the cycle time system with individual activities.

The cycle time system consists of different activities; namely, the loading time, travelling time with ADTs loaded, queuing time at the run-of-mine (ROM) pad, dumping time at the ROM pad stockpiles, hauling time with ADTs unloaded, and queuing time at the loading point. For an optimal cycle time to be achieved, the abovementioned activities must be performing efficiently. Therefore, to optimize the cycle time, the constraining activity must be identified and mitigated.

Constraint identified in the cycle time system

By considering the cycle time as a system, and knowing that every system has a constraint, it is imperative to identify the constraint(s) in the cycle time system to be able to optimize that system.

From the on-site investigation and data analysis, the following constraints were identified:

- Work ethics of the operators (operators stopping the ADTs to discuss trivial matters, *e.g.* sport, for a short period of time)
- Mine road conditions
- Condition of equipment
- Long queuing time of the ADTs at the shovel.

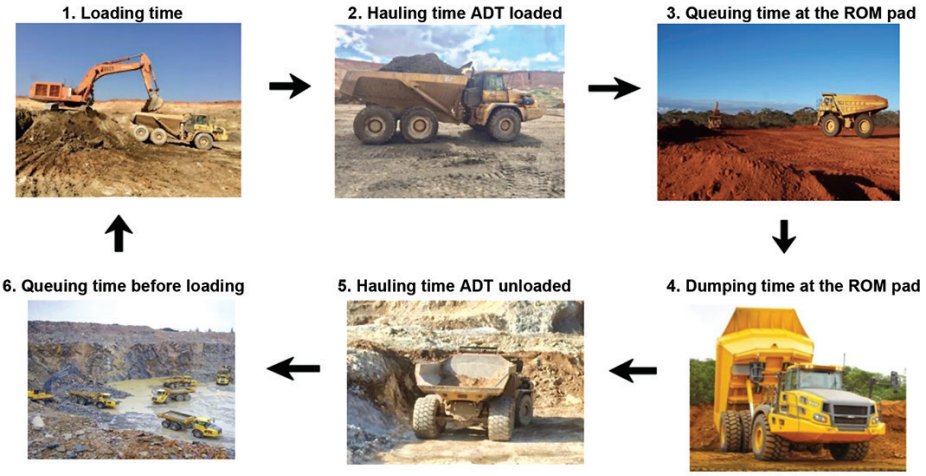

Figure 4—The cycle time system with individual activities

To optimize the cycle time, these activities must be mitigated, starting with the most important and proceeding to the least important. Furthermore, to optimize the present cycle time, there is a need to be aware of the theoretical cycle time, which would be compared to the actual cycle time.

On-site data analysis

The data collected on-site was analysed and used for the calculation of the actual cycle time to be optimized. The analysis included:

- Queuing time
- Hauling time
- Dumping time
- Production data.

The production data collected revealed a failure to reach the daily production target as well as the monthly target of excavated material (ore and waste) to be delivered to different destinations. To add value to Ruashi Mining, there must be consistent ore delivery to the ROM pad.

Figure 5 shows Ruashi Mining's monthly production for the year 2017. The targeted production was met or surpassed in only 4 out of the 12 months. As a result, the 2017 Ruashi Mining annual production target was not achieved.

Influence of rainfall

The southern part of the DRC has a tropical climate, with the rains from mid-November to the beginning of April. Consequently, open pit mining operations are affected negatively during this period.

- ADT hauling speed is decreased
- Mud accumulayes on the mine roads and in the open pit
- During heavy rain, the operations stop due to safety concerns and access issues. The Ruashi open pit contains talc, which becomes slippery when wet. Consequently, it is dangerous to operate mining equipment under such conditions.

However, Ruashi Mining continues to operate during this period because of ore stockpiled at the ROM pad. Figure 6 shows the monthly production for the year 2017–2018, highlighting the effect of rainfall on production.

The monthly production achieved (orange trendline) is below the targeted production (blue trendline) from mid-November 2017 to the beginning of April 2018.

Theoretical cycle time calculation

The average cycle time is obtained as follows:

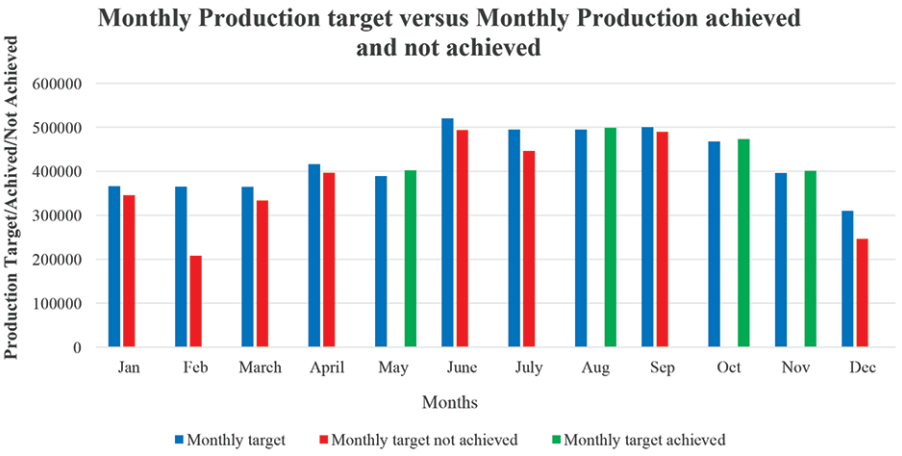

Figure 5—Monthly production *versus* target at Ruashi Mining

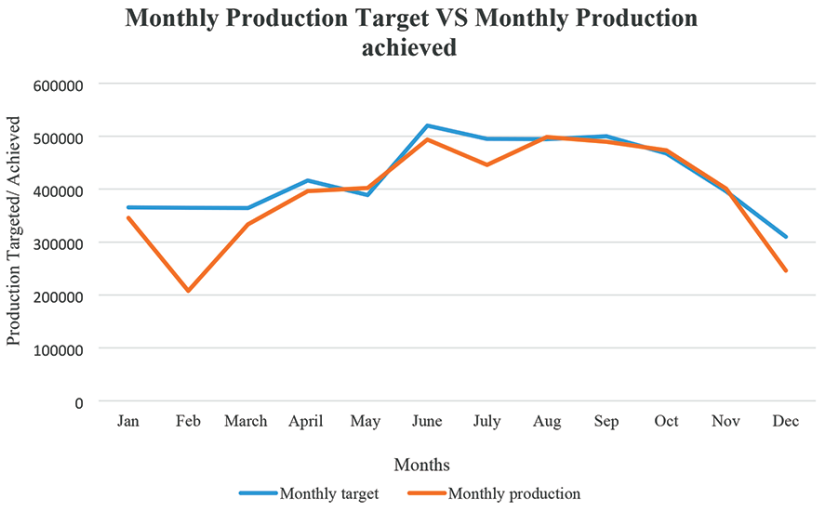

Figure 6—Effect of the the rainfall season on monthly production at Ruashi Mining

Cycle time = Loading time + hauling time (ADT loaded) + Dumping time (raise and lower time) + hauling time (ADT unloading) + Queueing time [1]

Theoretical queuing time results

When the cycle time is ideal, there are no constraints compromising an operation. By reviewing the paper by Ercelebi and Bascetin (2009), it could be concluded that in an ideal cycle time there is no queuing of the ADTs at the shovel.

Theoretical loading time results

The loading time is the sum of the times (in minutes and seconds) for the number of passes. For this project, the loading times were recorded for the two Hitachi shovels, namely the Hitachi EX 1200-6 and Hitachi EX 870 LCR-3.

Struck capacity of B40D	18.5 m³
Struck capacity of B50D	22 m³
EX 870 LCR-3 capacity	5.5 m³
EX 1200-6 capacity	6.2 m³

Equation 2. Loading time

No. of passes = Loading time (min) ÷ Shovel cycle time (min) [2]

- EX 1200-6 = 28.3 seconds = 0.4717 minutes
- EX 870 LCR-3 = 29 seconds = 0.4833 minutes.

Theoretical hauling time results

$$\text{Hauling time} = \frac{\text{Set distance}}{\text{Speed of haulers}} \quad [3]$$

- ADTs are required to travel on a flat surface at 40 km/h
- ADTs are required to travel up the ramp of 10° (grade = 10°; tan (10°) × 100% = 17.63%) at a speed of 12 km/h, and down the ramp at a speed of 20 km/h
- Assume the rolling resistance (based on the road conditions observed from the on-site investigation) to be 4%
- Total resistance force = Grade + Rolling resistance = 21.63% (approx. 22%).

Figure 7 depicts the rim pull chart used to determine the speed of the BELL B40D ADTs. The overall B40D weight was 66 851 kg, which is used on the left-hand side graph. An arrow intercepts the 22% total resistance force and another arrow intercepts the gear in red on the right-hand side graph. A speed of 7 km/h is determined from the graph, so that the total hauling time (going and returning) could be determined:

$$\text{Total hauling time} = \frac{2.93\ \text{km}}{7\ \text{km/h}} = 0.4185\ \text{h (25.11 mintes)}$$

The hauling time that the B40D should take to travel from the open pit to the ROM pad and return to the pit is 25.11 minutes. Figure 8 depicts the rim pull chart for the B50D; the grade and the rolling resistance remain constant as for the B40D.

The B50D speed was determined to be 6.5 km/h from the B50D rim pull chart, as seen in Figure 8. The overall B50D weight was 79 920 kg. The blue arrow is used to illustrate how the speed was determined.

$$\text{Total hauling time} = \frac{2.93\ \text{km}}{6.5\ \text{km/h}} = 0.4508\ \text{h (27.05 minutes)}$$

The hauling time that the B50D should take to travel from the open pit to the ROM pad and return to the open-pit is 27.05 minutes.

Theoretical dumping time results

The dumping time at the ROM pad includes the raising and lowering of the bucket.

- Dumping time B40D: 13.0 + 7.6 = 20.6 seconds = 0.3433 minutes [4a]
- Dumping time B50D: 11.2 + 9.9 = 21.1 seconds = 0.3517 minutes. [4b]

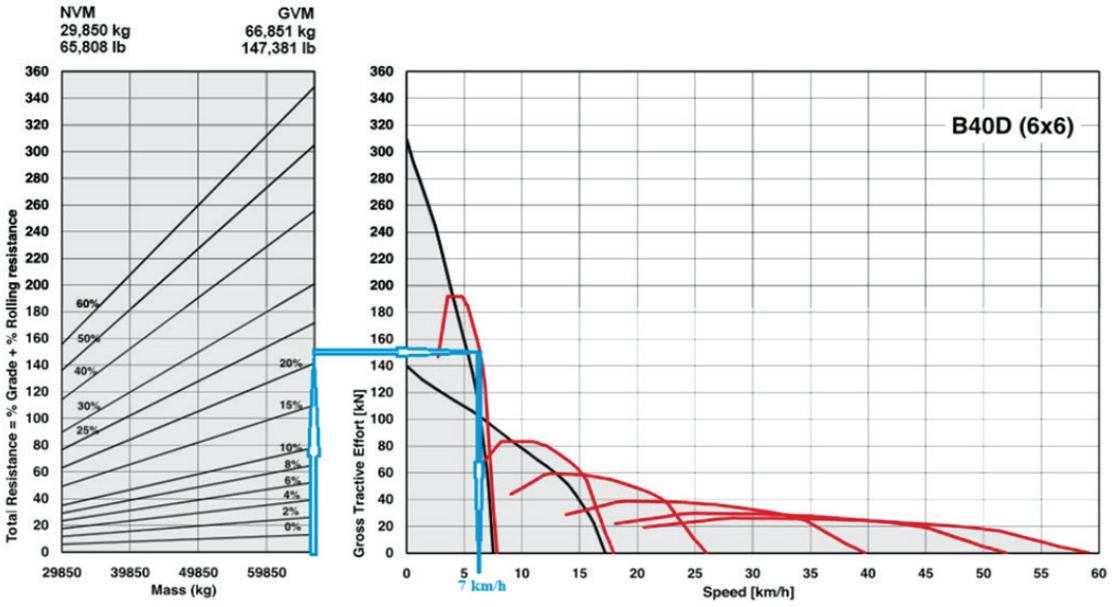

Figure 7—Rim pull chart for the B40D

Optimization of the cycle time to increase productivity at Ruashi Mining

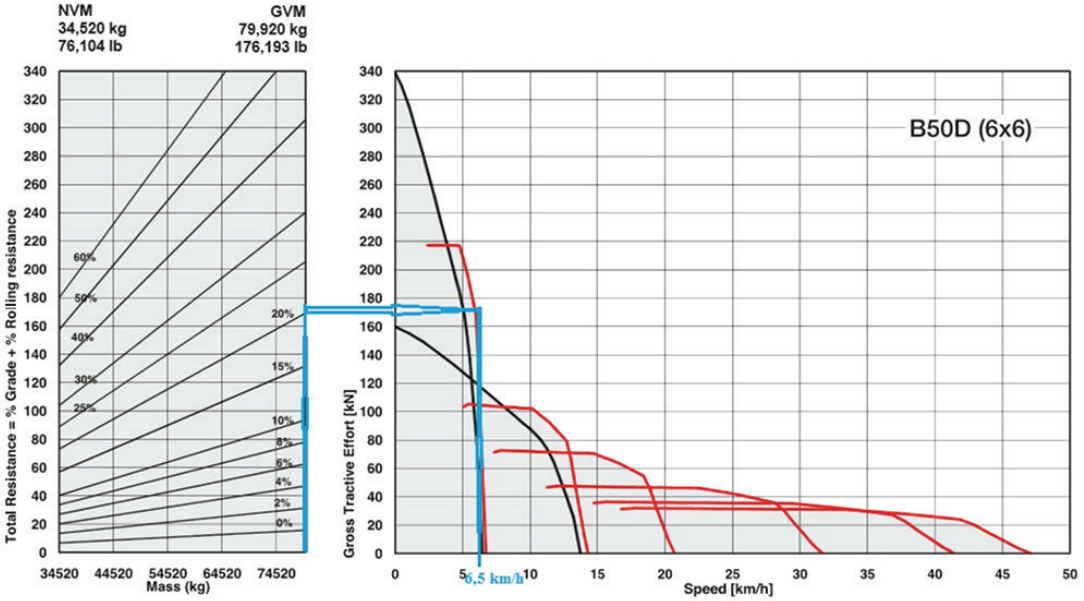

Figure 8—Rim pull chart for the B50D

Table I

Theoretical cycle time results

	Average time			Average time	
	40 t	50 t		40 t	50 t
Queuing time (min)	0	0	Queuing time (min)	0	0
Loading time (min) EX 870 LCR-3	0.4833	0.4833	Loading time (min) EX 1200	0.4717	0.4717
Hauling time (min)	25.11	27.05	Hauling time (min)	25.11	27.05
Dumping time (min)	0.3433	0.3517	Dumping time (min)	0.3433	0.3517
Average theoretical cycle time (min)	25.937	27.885	Average theoretical cycle time (min)	25.925	27.873

Table II

Actual cycle times for different shovels and payloads

	Average time			Average time	
	40 t	50 t		40 t	50 t
Queuing time (min)	03:36.0	03:36.0	Queuing time (min)	03:36.0	03:36.0
Loading time (min) EX 870 LCR-3	02:01.0	02:12.2	Loading time (min) EX 1200	01:43.6	02:00.5
Hauling time (min)	21:59.4	25:59.5	Hauling time (min)	21:59.4	25:59.5
Dumping time (min)	00:25.2	00:24.3	Dumping time (min)	00:25.2	00:24.3
Average theoretical cycle time (min)	28:01.6	32:11.7	Average theoretical cycle time (min)	27:44.2	32:00.0

Theoretical cycle time results

The theoretical cycle time is the ideal cycle time. Table I shows the theoretical cycle time results after calculating different components making up the total theoretical cycle time.

Different shovels give different loading times, depending on their capacities when loading ADTs of different payloads. This will result in different theoretical cycle times, as can be seen in Table I.

Actual cycle time calculations

The actual cycle time was calculated from the data collected on site using a stopwatch. A summary of the actual cycle time components is shown in Table II.

It is worth noting that the loading time data was collected for two different shovels, and that affects the actual cycle times.

Theoretical cycle time versus actual cycle time analysis

The main differences between the theoretical and actual cycle times are in the input assumptions.

The purpose of calculating the theoretical (ideal) cycle time was to determine the benchmark to optimize the actual cycle time. In addition, the theoretical cycle time was calculated with the data obtained from the manufacturer's specification booklets, whereas the actual cycle time was calculated with data collected on site. Figure 9 shows the chart comparing the actual and theoretical cycle time of a Hitachi EX 1200-6 shovel.

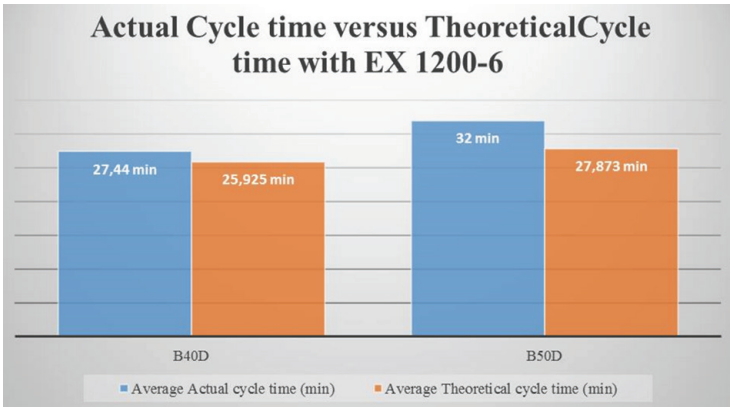

Figure 9—Actual *versus* theoretical cycle time for the EX 1200-6

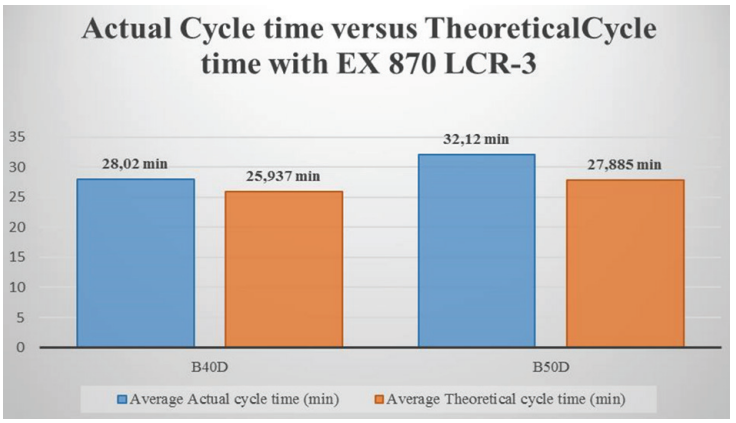

Figure 10—Actual *versus* theoretical cycle time for the EX 870 LCR-3

As expected, the actual cycle time is longer than the theoretical cycle time. For the B40D, the difference in cycle time is 1.52 minutes and for the B50D the difference is 4.13 minutes. By mitigating the constraints identified, the cycle time will be optimized, and the actual cycle time will be reduced to a time equal to or better than the theoretical cycle time. Figure 10 shows the actual *versus* theoretical cycle time for a Hitachi shovel EX 870 LCR-3.

From Figure 10, with a Hitachi 870 LCR-3, the difference in the cycle time of the B40D is 2.08 minutes and that for the B50D is 4.24 minutes. There is also a need to optimize this cycle time as the gap (largely caused by the queuing time) between the theoretical and the actual cycle time is significant.

Production calculation

Production data interpretation

The production data to be analysed was collected on the mine. Shift data:

- Two shifts per day
- Eleven hours per shift (ideal scenario)
- Nine effective working hours per shift, *i.e.* 18 effective working hours per day.

Planned versus actual production per annum

Equations [5] to [7] are used to calculate the annual production (planned and achieved) in 2017. By knowing the planned tons production per ADT and the number of trucks operating on the mine, the calculations could be done as follows:

$$\text{Cycles per hour} = \text{Cycle time (min)} \div 60 \quad [5]$$

$$\text{Tons per annum (t)} = \text{Tons per day} \times \text{Number of days per annum} \quad [6]$$

$$\text{Tons per annum (t)} = \text{Tons per day} \times \text{Number of days per annum} \quad [7]$$

ADTs and shovels have surpassed the required working hours, which has become a constraint as identified during the on-site investigation. Consequently, unpredictable breakdowns occur, which affect the machine availability and utilization as shown in Table III.

As a result, there was a 39.06% shortfall in production in 2017–2018, with 4 830 403.91 t of unmoved material being the outcome of the longer cycle time due to the constraints.

Conclusions

There are two types of constraints identified in the production mining cycle. There are man-made constraints identified through Systems Thinking analysis (*i.e.* the mine roads and condition of equipment, lack of work ethic from the operators, bucket fill

Table III

Comparative production calculation results (predicted actuals) for each truck type matched with each shovel

	Annual planned production				Annual actual production			
	EX 870 LCR-3		EX 1200-6		EX 870 LCR-3		EX 1200-6	
	B40D	B50D	B40D	B50D	B40D	B50D	B40D	B50D
Payload (t)	40	50	40	50	40	50	40	50
Bucket fill factor (FF)	0.9	0.9	0.9	0.9	0.9	0.9	0.9	0.9
Availability (Av)	0.8	0.8	0.8	0.8	0.75	0.75	0.75	0.75
Utilization (Uti)	0.7	0.7	0.7	0.7	0.6	0.6	0.6	0.6
Cycle time (min)	25.94	27.89	27.44	27.87	28.02	32.12	25.93	32
Cycles per hour	2.31	2.15	2.19	2.15	2.14	1.87	2.31	1.88
Production (t/h)	46.63	54.21	44.08	54.25	34.69	37.83	37.49	37.97
Available number of ADTs	11	5	11	5	11	5	11	5
Production of all ADTs	512.94	271.06	484.90	271.26	381.58	189.13	412.34	189.84
Effective shift hours per day	22				18			
Tons produced per day	11 284.63	5 963.43	10 667.76	5 967.71	6 868.52	3 404.42	7 422.14	3 417.19
Number of days per annum	365				357			
Tons produced per annum	4 118 888.51	2 176 651.13	3 893 730.61	2 178 213.13	2 452 062.53	1 215 378.27	2 649 702.74	1 219 935.94
Total tons produced	12 367 483.39				7 537 079.47			
Production shortfall (t)	4 830 403.91							
Difference (%)	39.06							

factor of the shovel, and the queuing of ADTs at the shovel). There is also a naturally occurring constraint, which is the rainfall from mid-November to the beginning of April. This constraint cannot be mitigated.

From the analysis of the results, the actual cycle time of a B40D ADT can be reduced by 8% (from 28.02 minutes to 25.94 minutes) when used with the Hitachi 870 LCR-3 shovel. Moreover, the actual cycle time for the B50D ADT can be reduced by 13.2% (from 32.12 minutes to 27.89 minutes) using the Hitachi 870 LCR-3. When excavating with the Hitachi 1200-6 shovel, the actual cycle time can be reduced by 5.5% (from 27.44 minutes to 25.94 minutes) for the B40D ADT and by 12.9% (from 32 minutes to 27.87 minutes) for the B50D ADT.

Finally, a reduction in cycle time increases production as it can achieve a higher tonnage per hour and per shift. The production can be increased with the same resources and fixed costs by optimizing the productivity through Systems Thinking. Eventually, the increase in the financial performance of the mine may extend the life of mine (LOM) as it will allow access to previously uneconomical reserves. Ultimately, the positive impact on the country will be tangible through royalties, taxes, and the economy.

Recommendations

- Scheduled mine roads and equipment maintenance. Mine roads must be regularly maintained, especially during the rainy season, to allow smooth running of the mine operations
- Empowering the workers would be an effective way to overcome their poor work ethic, by demonstrating the impact their work has on the overall mine operation and output. Proving to workers how losing minutes discussing trivial matters adversely affects the daily, monthly, and yearly cycle time, therefore, the productivity (Lane, 2018)
- It was observed from the on-site investigation and proven by data analysis that the inconsistency in the loading time data must have been caused by the shovel bucket filling factor. NB Mining must reinforce its operator-training programme so that the operators have the competency to operate the shovels at full efficiency
- The following formula can be used to calculate the number of trucks required per shovel. This will reduce the queuing time of the ADTs at the shovel. For the purpose of this calculation, the actual hauling and loading cycle times are used because they are based on the data collected on-site.

$$\begin{aligned}\text{No of trucks required per shovel} &= 1+\frac{\text{Hauling cycles time (minutes)}}{\text{Loading cycle time (minutes)}}\\ &= 1+\frac{21.59}{2.01}=10.74\approx 11_{\text{ADTs(EX 870 LCR}-3\text{ loading B40D)}}\\ &= 1+\frac{25.60}{2.12}=12.07\approx 13_{\text{ ADTs(EX 870 LCR}-3\text{ loading B50D)}}\\ &= 1+\frac{21.59}{1.44}=14.99\approx 15_{\text{ ADTs(EX 1200}-6\text{ loading B40D)}}\\ &= 1+\frac{25.60}{2.00}=12.80\approx 13_{\text{ ADTs(EX 1200}-6\text{ loading B50D)}}\end{aligned} \quad [8]$$

Future studies can be conducted on:

- Application of Systems Thinking in mining to optimize a mine's throughput
- Adding value to a mine by saving costs on diesel when implementing 'stop-start systems' on ADTs.

References

Goldratt, E. Not dated. Theory of Constraints – Lean Manufacturing. https://www.leanproduction.com/theory-of-constraints.html [accessed 29 March 2018].

Vasquez Coronado, P.P. 2014. Optimization of the haulage cycle model for open pit mining using a discrete-event simulator and a context-based alert system. The University of Arizona. http://hdl.handle.net/10150/321594

Ercelebi, S. and Bascetin, A. 2009. Optimization of shovel-truck system for surface mining. *Journal of the Southern African Institute of Mining and Metallurgy*, vol. 109. pp. 434–437.

Lane, G. 2018. Systems Thinking for mining. Industrial and Research Seminar II. University of the Witwatersrand, Johannesburg.

Mkhatshwa, S. 2009. Optimization of the loading and hauling fleet at Mamatwan open pit mine. *Journal of the Southern African Institute of Mining and Metallurgy*, vol. 109. pp. 225–226.

Vemba, M. 2004. Loading and transport system at SMC – Optimization. *Journal of the South African Institute of Mining and Metallurgy*, vol. 104. pp. 141–146. ◆

The state of mine closure in South Africa – what the numbers say

I. Watson[1] and M. Olalde[2]

Affiliation:
[1]University of the Witwatersrand, South Africa.
[2]Freelance Journalist, South Africa.

Correspondence to:
I. Watson

Email:
Ingrid.watson@wits.ac.za

Dates:
Received: 18 Sep. 2018
Revised: 14 Jan. 2019
Accepted: 15 Feb. 2019
Published: July 2019

How to cite:
Watson, I. and Olalde, M.
The state of mine closure in South Africa – what the numbers say.
The Southern African Insitute of Mining and Metallurgy

DOI ID:
http://dx.doi.org/10.17159/2411-9717/331/2019

ORCiD ID:
I. Watson
https://orchid.org/0000-0001-5350-3734

Synopsis

The consequences of ineffective mine closure in South Africa are evident from the number of abandoned mines and operations on extended care-and-maintenance, the on-selling of mines to less well-resourced companies to close, and increasing illegal mining activities. However, the data to substantiate these observations and provide insight into the underlying issues has not been available. Through the Promotion of Access to Information Act, a list of mine closure certificates applied for between 2011 and 2016 and a list of certificates granted over the same period for all nine regions of South Africa was obtained. From the analysis of this data, we show that the mine closure system as implemented in South Africa is largely ineffective. Although closure certificates are being granted, these are for prospecting sites and small-scale mines, which have a relatively small environmental impact. No large mines of any environmental significance were relinquished over the period under review, with very few applying for closure certificates. Furthermore, the issuing of closure certificates varies significantly between regional offices, with the success rate for applications being generally low and issuing of certificates taking an extended period.

Keywords
mine closure, certification, legal process.

Introduction

There are a number of concerns with the mine closure process as practiced in South Africa, and these have largely been laid at the door of government. Alberts *et al.* (2017) stress that the legislation generally conforms to international best practice. However, the system is 'complex and unwieldy', involving various pieces of legislation and different government departments with overlapping requirements and different interpretations of the law. A further area of concern is the capacity and competence of government to implement legislation. The '*shortage of relevant mine closure skills and knowledge within the regulator*' was identified by van Druten and Bekker (2017) as a key contributor to unsuccessful closure. Lack of capacity and resources within the regulator has also been highlighted by Botham, Kelso, and Annegarn (2011) and Milaras, McKay, and Ahmed (2014). A recent study of the mineral application process by Corruption Watch (2017) indicates that positions in the regulator have been frozen for many years, leading to a shortage of staff, and that unqualified individuals have been appointed. There is also the perceived reluctance of government to grant closure in order to limit transfer of the liability to the state and delay the inevitable job losses.

Notwithstanding this, there is also the inability and seeming lack of motivation from the side of mining companies to successfully rehabilitate and close mines. Closure often involves the management of difficult environmental issues, such as acid mine drainage (AMD), which are difficult to quantify and predict (van Druten and Bekker, 2017) and costly to manage. Closure costs are often underestimated by mining companies (Botham, Kelso, and Annegarn 2011). With the assumption that closure certificates are not being granted and the lack of concrete relinquishment criteria, some mines are not applying for closure. Milaras, McKay, and Ahmed (2014, p.10) quote a professional working in mine closure in South Africa:

> '*The requirement to reduce mitigated risk to zero is unattainable, and since it cannot be achieved, no mines are getting closure permits. This means that the best possible practices are being rejected, and since undertaking best practice brings no reward, mines are not bothering to do their best.*'

Contributing to this perspective is the requirement for perpetual liability included in recent amendments to closure legislation, in terms of which a mining company will continue to remain liable

for environmental pollution regardless of having been issued with a closure certificate. Industry argues that there is thus no incentive to obtain closure certificates (Alberts *et al.*, 2017). An alternative to closing a mine when it is no longer profitable is on-selling, the transfer of mining rights to a lower cost producer. This is a common practice in South Africa (Humby, 2014) and from a resource efficiency perspective, makes sense. Legislation allows for such a transfer provided that consent is obtained from the Minister of Mineral Resources and that the new holder is capable of carrying out and complying with the obligations and the terms and conditions of the right in question. This is often a preferred option for government as it limits the number of job losses. However, it has implications for the eventual rehabilitation and closure of these mines, which is left to less well-resourced companies mining now-marginal deposits. The current case of Blyvooruitzicht near Carletonville (Humby, 2014) is an example of the consequences of this. As stated by Humby (2014, p. 8):

> *This "pass-the-parcel" approach to the custodianship of the closure plan, where the "gift" ends up in the hands of the weakest, seriously undermines the value and integrity of the forward planning approach to mine closure. Where the last link in the chain of mining companies operating a site then fails to apply for a closure certificate, it also undermines the rule of law.*

Although we understand what some of the problems may be, there is no country-wide, data-based perspective of the current state of mine closure in South Africa. A key indicator of the success of the mine closure process is the number of closure certificates issued (the number of mines relinquished). The granting of a closure certificate implies that a mining company has adequately rehabilitated the mine site in line with a closure plan and to the satisfaction of the regulator. A closure certificate allows a mining company to reclaim its financial provision and move on to other projects, and the land to be used for other productive purposes. This is the outcome of the mine closure process. During 2016, data on closure certificates issued across all nine regions of South Africa between 2011 and 2016 was obtained. This data, reviewed here, provides an insight into the state of mine closure in South Africa. Prior to discussing the data, an overview is presented of mining in South Africa and the legal process to obtain closure.

Mining in South Africa

South Africa has a mature mining industry that dates back to the 1860s with the discovery of significant diamond and gold deposits. Since then, a great number of other commodities have been exploited, including iron ore, chromium, manganese, coal, and platinum, the latter two, along with gold, making the largest contribution to the economy (Minerals Council South Africa, 2018). The major mineral deposits, high-value commodities, and operating mines in South Africa are clustered in six of its nine provinces: the Northern Cape, North West, Limpopo, Mpumalanga, Free State, and Gauteng (Table I). Even though the percentage contribution of mining in Gauteng to the provincial GDP is relatively low (2.3%) it is a substantial amount (R22.34 billion) and should be viewed against other economic activities in Gauteng, the industrial heartland of South Africa, and the historical importance of gold mining in this province. The bulk of South Africa's mineral production is from large-scale mining. However, there are also a number of small-scale operators mining a range of commodities, predominantly construction materials and, in the Northern Cape and North West provinces, diamonds (Ledwaba and Mutemeri, 2017). Data on small-scale mining is limited.

Modern mining transformed the South African economy, and by 1980 it contributed 21% of South Africa's GDP, second to manufacturing. Although mining still makes a significant contribution, adding R334 billion to the economy in 2017, its role has decreased, contributing 6.8% of the GDP (Minerals Council South Africa, 2018). This reduction is attributed, in part, to the closure of mines. Statistics presented by the Department of Water and Sanitation (July 2017) indicate that there are almost double the number of closed coal, gold and base metal mines in South Africa (n = 2787) than operational mines (n = 1654[1]), yet very few of these, if any, have received closure certificates.

The environmental and social impacts of mining depend largely on the commodity mined, its location, and the type of mining practiced. Acid mine drainage (AMD) is a major concern in the gold and coal mining sectors in South Africa. The Mpumalanga Highveld, as well as being the focus of large-scale coal mining, is also home to South Africa's most productive agricultural land and a key water catchment (Hermanus *et al.*, 2015). Platinum mining in Limpopo and the North West coincides with rural communal land and has seen intensive intra-community struggles (Mnwana, 2015; Hermanus *et al.*, 2015).

[1]This figure differs slightly from that mentioned in Table I. This may be due to the use of data from different years and reinforces the later finding on access to and quality of data.

Table I

Mining in South Africa, per province (source: Minerals Council South Africa, 2018; DMR D1 2016a database)

Province	Main commodities	Mining contribution to provincial GDP 2016 (%)	Mining GDP 2010 (R billion – nominal terms 2016)	Number of operating large-scale mines in 2016 (Total = 1741)
Northern Cape	Diamonds, iron ore, manganese	31.1	52.34	302
North West	PGMs, gold, diamonds	28.4	17.27	341
Limpopo	Coal, PGMs, iron ore	27.9	55.51	142
Mpumalanga	Coal and PGMs	24.8	49.93	219
Free State	Gold, diamonds	12.6	18.06	77
Gauteng	Gold	2.3	22.34	167
KwaZulu-Natal	Coal, construction materials	1.9	8.30	133
Eastern Cape	Construction materials	0.3	0.60	171
Western Cape	Construction materials, marine diamonds	0.2	0.95	189

Mining authorization and closure

Closure planning has been a requirement in South Africa since the Minerals Act of 1991, which stipulated that an environmental management programme (EMP) be submitted, rehabilitation be undertaken, financial provision made, and an application submitted for a closure certificate (Swart, 2003). Following this, and since the first democratic elections in 1994, there has been significant legal reform, including to mining and environmental legislation. This is continuing, as detailed by Alberts *et al.* (2017). The following is a summary of the current requirements to obtain a license and then close a mine, as is relevant to this paper.

The granting of mining authorizations, regulation of operations, and issuing of closure certificates is governed by the Department of Mineral Resources (DMR), predominantly through the Mineral and Petroleum Resources Development Act (MPRDA) and the National Environmental Management Act (NEMA), although other departments (most notably Environmental Affairs and Water and Sanitation) and various pieces of legislation are also relevant. While the regulation of mining is a national competence, it is operationalized by nine regional offices, largely aligning to the provinces.

In order to prospect and exploit a mineral resource, the MPRDA requires an application for a prospecting right, a mining right or a mining permit, as outlined in Table II. An application for a right or permit must be accompanied by an application for an environmental authorization, which includes the submission of an environmental assessment, environmental management plan, and closure plan, as well as sufficient financial provision for rehabilitation and closure. Over the life of the operation, the mine is expected to annually assess and update the financial provision and submit an audit report on its adequacy. An annual rehabilitation plan should also be completed.

In line with global best practice, the closure process is seen as extending throughout the life of an operation, with upfront planning for closure required. The MPRDA closure principles require ongoing assessment and management of environmental impacts, compliance with safety and health requirements, that residual and latent environmental impacts are identified and quantified, land be rehabilitated, as far as is practicable, to its natural state or to a predetermined and agreed standard or land use which conforms with the concept of sustainable development, and that this be done efficiently and cost-effectively.

The final application procedure for a closure certificate is complex, involves a number of different statutes and guidance documents (Alberts *et al.*, 2017) and is currently being amended. Having previously been regulated almost entirely through the MPRDA by the DMR, as of 20 November 2015 it is also managed in line with NEMA and its regulations, but still principally by the DMR. Currently a closure certificate is required from the DMR, and the process to obtain this involves meeting requirements from both pieces of legislation. In terms of the MPRDA an application should be made to the Regional Manager and must be accompanied by a final rehabilitation, decommissioning, and mine closure plan, an environmental risk report, and a performance assessment of the closure plan. This should be done within 180 days of the end of mining or prospecting activities. In line with NEMA and its regulations, an environmental authorization, involving a basic assessment, should be obtained. This, together with an environmental audit of the closure plan and EMP, should be submitted. There is clearly overlap between these requirements, and the assumption is that a single process, meeting the requirements of both pieces of legislation (and the NEMA financial provision regulations) will be undertaken.

A closure certificate will be issued only if the Chief Inspector of Mines (responsible for health and safety) and other relevant government departments (particularly Water and Sanitation and Environmental Affairs) have confirmed in writing that the provisions pertaining to health and safety and management regarding pollution of water resources, the pumping and treatment of extraneous water, and compliance with the conditions of the environmental authorization have been addressed. These authorities have 60 days in which to respond.

A closure certificate allows companies to relinquish the mine. Historically, under the Minerals Act of 1991, an unconditional closure certificate was issued in terms of section 12, provided all the conditions stipulated in the Act had been complied with and the objectives of the closure plan met (Dixon, 2003). In terms of the MPRDA, the holder remains responsible for any environmental liability until a closure certificate has been obtained. However, recent requirements of NEMA introduce the concept of perpetual liability (Alberts *et al.*, 2017), where responsibility is allocated to the mining company notwithstanding the issuing of a closure certificate by the Minister responsible for mineral resources. This highlights the strengthening of legislation to hold mining accountable for pollution impacts and the minimization of state liability; understandable given their experience of dealing with post-closure acid mine drainage decant from the Witwatersrand basins and combusting coal mines in Mpumalanga. The Minister is entitled to retain a portion of the financial provision for latent and residual impacts.

In South Africa there are a number of mines on care and maintenance due to their inability to secure a government-issued

Table II

Types of mineral authorizations granted in terms of the MPRDA

Prospecting right, in terms of Section 17 of MPRDA • No limit to physical extent of the right • Valid for a period up to 5 years. It may be renewed once for a period not exceeding 3 years
Mining right, in terms of Section 23 of MPRDA • No limit to the physical extent of the right • Valid for up to 30 years and may be renewed for further periods each of which may not exceed 30 years • This right is issued for large-scale mining
Mining permit, in terms of Section 27 of MPRDA • Granted for an area not exceeding 5 hectares • Valid for a period of two years and may be renewed three times for a period of up to a year each (*i.e.* an additional 3 years) • Typically granted for small-scale mines

closure certificate (Milaras, McKay, and Ahmed, 2014). Care and maintenance has traditionally been seen as an alternative to closing mines and has occasionally resulted in abandonment. An attempt to regulate care and maintenance was made in the 2015 Financial Provision Regulations under NEMA, which required mining companies to make an application for mines to be put on care and maintenance, which could be valid for a period not exceeding five years, after which it should be reviewed. However, this requirement has subsequently been removed from the 2017 draft regulations, leaving care and maintenance unregulated.

Data and methodology

Data on mine closure is not in the public domain. In August 2015, one of the authors applied for and obtained access to this information in terms of the Promotion of Access to Information Act of 2000 (PAIA). Access was requested to a list of all closure applications made between 1 July 2012 and 1 July 2015 and a list of all closure certificates granted in the same period, across the country.

A second source of data used in this paper comes from a Parliamentary question submitted by the Democratic Alliances' shadow minister for minerals, James Lorimer, and answered on 22 April 2016. The shadow minister asked (a) *How many mine closure certificates were issued in the (i) 2011-12, (ii) 2012-13, (iii) 2013-14, (iv) 2014-15 and (v) 2015-16 financial years, and (b) what was the (i) name and (ii) location of each mine that was issued with a closure certificate, and (c) on what date was each specified certificate issued*?

The two data-sets were combined and entered into spreadsheets. The data was reviewed and any duplications removed. Judging from discrepancies between the two data sources, both data-sets are incomplete, although by small margins. Together this represents the most complete set to date of closure certificates granted in South Africa, for the period 2011 to 2016.

The certificates granted were grouped by region and type of authorization, and where relevant, compared with the DMR D1 spreadsheets of operating mines (for 2005 to 2014) to identify the commodity mined. Not all authorizations were identifiable as prospecting rights, mining rights, or mining permits. These are grouped as 'unlisted sites'. As the type of right or permit cannot be identified, unlisted sites are excluded from the analysis and conclusions drawn about prospecting rights, mining permits, and mining rights. Some of the original unlisted sites have been followed up with the license holders, who were able to confirm what type of authorization they were. These were reallocated accordingly.

Results

Access to and quality of data

The first finding relates to the availability and quality of data on mine closure. Data is held by the DMR and requires a legal process to access, granted through PAIA. The process is relatively straightforward, requiring the completion of a form with a description of the documentation required. However, in this case there was a delay in acquiring the data. Approval was granted by the national office of the DMR, yet it took approximately 21 months to obtain all the information from the provincial departments. Even after approval, not all the requested information was received (see Table III for summary of what was received and openAFRICA (2018) for the data). The Western Cape did not provide any data, and in some cases data exceeding the timeframe requested was provided. Information on closure applications made was provided for only four regions and by the Springbok office of the Northern Cape, which provided data on all applications made since 2004. The North West Province data included applications made since 2008.

The format and level of detail of data provided differ between regions. While all regions provided at least the company name and permit/right reference number, other regions' lists were more detailed and included property names and dates. One region provided copies of the closure certificates. Data from the Western Cape was obtained through the parliamentary question. From this data it appears that instead of converting old order rights to new order rights, as required by the legislation, the Western Cape regional office issued these with closure certificates, influencing the data.

From the exercise of accessing the data, it would appear that not even government has a national overview of mine closure in South Africa. The lack of readily available and complete data limits monitoring of closure and informed decision-making, contributing to perceptions which are not always helpful.

Closure certificates are being granted

As illustrated in Table IV, closure certificates are being granted

Table III

Information received from PAIA request

Region	Data obtained?	
	List of closure applications	List of closure certificates granted
Northern Cape (Springbok and Kimberley offices)	No (Kimberley) Yes (2004-2015, Springbok)	Yes (2012–2015)
North West	Yes (2008–2015)	Yes (2012–2015)
Limpopo	Yes (2012–2015)	Yes (2012–2015)
Mpumalanga	No	Yes (2012-2017)
Free State	No	Yes (2012–2015)
Gauteng	Yes (2012–2015)	Yes (2012–2015)
KwaZulu-Natal	Yes (2012–2015)	Yes (2012–2015)
Eastern Cape	No	Yes (2012–2015, incomplete)
Western Cape	No	No

Table IV

Closure certificates issued for prospecting rights, mining permits, mining rights, and unlisted sites, per region (2011–2016)

Region	Large-scale mines		Small-scale mines – mining permits	Prospecting rights	Unlisted sites	Total per region	% per region
	Mining rights (excl. road works)	Mining rights for road works					
Northern Cape	3	0	87	42	11	143	18%
North West	3	6	59	39	24	131	16%
Limpopo	0	0	65	77	3	145	18%
Mpumalanga	0	0	6	4	0	10	1%
Free State	1	45	63	99	13	221	28%
Gauteng	0	0	10	5	0	15	2%
KwaZulu-Natal	0	0	33	21	5	59	7%
Eastern Cape	0	0	29	0	12	41	5%
Western Cape	20	6	11	1	0	38	5%
Total per type	27	57	363	288	68	803	100%
% per type	3%	7%	45%	36%	9%	100%	-

across all regions and for all types of permits and rights. As would be expected given the validity period of mining permits and prospecting rights, the bulk of certificates have been granted for these (363 and 288 respectively). For a number (n = 68) there is no indication of the type of right or permit (unlisted). A total of 84 (27 + 57) mining rights were relinquished during the period under review.

The granting of closure certificates varies among regions. Comparing different regions provides an interesting perspective, particularly for Mpumalanga and Gauteng. Both regions host significant large-scale mining activities (refer to Table I) yet have granted only 10 and 15 closure certificates, respectively, over the five-year period. Very few certificates have been granted for mining permits and prospecting rights and none to large-scale mines. The commodities mined in these regions (largely gold and coal) are linked to significant environmental pollution in the form of AMD, and many coal mines in Mpumalanga are opencast, making them more difficult and expensive to rehabilitate. These are also some of the oldest mining areas in South Africa. The situation is similar for large-scale mines in Limpopo, where no closure certificates have been granted in the study period. Based on this data, it would appear that large-scale operations mining commodities that have a significant environmental impact are not being relinquished.

Closure of large-scale mines

The majority of the mining rights relinquished (n = 57) are for the closure of works associated with road construction and maintenance (*e.g.* borrow pits), which are issued to the South African National Road Agency Ltd (SANRAL) or provincial authorities responsible for public road construction and maintenance. These organs of state are exempt from having to apply for prospecting or mining rights or mining permits for activities to remove any mineral for the construction and maintenance of dams, harbours, roads, and railway lines. However, they do follow a process to ensure the information is captured on the South African Mineral Resources Administration System (SAMRAD) and are issued with the appropriate permit, for which they must eventually apply for closure in terms of Section 43 of the MPRDA – the 57 certificates issued during this time period.

The remaining 27 closure certificates for mining rights (3% of all certificates issued) went to large-scale mines that are not related to road works. Of these, 20 were granted in the Western Cape, a region with minimal significant mining activities (according to the DMR's D1 2016 list of operational mines, the Western Cape has no operational coal, gold, or platinum mines). Analysis of the certificates issued in the Western Cape revealed that 11 were for old order rights (it appears that closure certificates were issued when converting old order to new mining rights following the implementation of the MPRDA). The remaining nine are for operations mining construction materials, largely sand.

The other three regions that issued closure certificates for mining rights, and where mining is an important contributor to the economy, were the Free State, Northern Cape, and North West, as elaborated below.

Region – Free State

1. On 26 June 2013 a closure certificate was granted to Invest In Property (Pty) Ltd for mining right 180MR at the remaining extent of Kalkfontein A 13, district Boshof. This mine does not appear on the DMR list of operating mines (D1) from 2005 to 2013, and no other reference to it could be found. It is thus unclear what the commodity is. Other commodities mined in this area are diamonds and salt.

Region – North West

2. On 15 October 2013, a closure certificate was issued to Etruscan Diamonds (Pty) Ltd for mining right 38MR located at remaining extent of the farm Klipgat 18 IQ, Ventersdorp. This was a diamond mine (according to DMR D1 2006 database).
3. On 18 January 2013, a closure certificate was issued to Wynand Johannes Visser for mining right 212MR (in conjunction with 6/2/2/2674) located on certain portion of the farm Christiana Town and Town Lands 326 HO, Christiana. This was a diamond mine (according to DMR D1 2006 database)

4. On 3 September 2014, a closure certificate was issued to Carel-Lo-Andries Botha for mining right 443MR located at remaining extent of the farm Webb 159 HO, Wolmaransstad. It is unclear what commodity was mined as this does not appear on the DMR operating mines database (D1) from 2005 to 2013. This is an alluvial diamond mining area.

Region – Northern Cape

5. Lafarge Gypsum Holdings (Pty) Ltd applied for a closure certificate of mining right number 508 in the Springbok region on 12 March 2015 and was granted the certificate on 15 June 2016. This is gypsum mine (DMR D1 database).
6. De Beers Consolidated Mines applied for a closure certificate for mining right 514 in the Springbok region on 23 August 2013 and was granted the certificate on 9 June 2015. This was a diamond mine.
7. JK Plant Hire cc was issued a closure certificate on 17 April 2013 for its mining right (NC 30/5/1/2/2/211 MR) on Portion 2 of the farm Morgenzon no. 35 and portion 12 of the farm Slypklip in the Kimberley region. No reference to the mining right could be found in the D1 database; however, JK Plant Hire holds another mining right, for diamonds (on the farm Mazelsfontein in the Northern Cape). Based on this, and the location of the right, it is assumed that the commodity mined was diamonds.

At least three, possibly six, of these closure certificates are for the closure of alluvial diamond mines. When taken together with the closure certificates granted for sand mining in the Western Cape, one can again conclude that, for large-scale mines, only those with a relatively low environmental impact are being relinquished.

Closure of small-scale mines and prospecting permits

Almost half the closure certificates granted over the five-year period have been to the holders of mining permits (n = 363) for small-scale mining operations. Unfortunately, there is very little reliable data on the number of operating small-scale mines. Unverified data presented by the DMR puts the number of permits at 3574 (Department of Mineral Resources, 2016b). If this is the case, and given the period for which permits are valid (two years, renewable for up to five years), the number of closure certificates granted seems very low.

There is no consolidated database on the number of prospecting permits issued by the DMR. Prospecting permits can either be converted to a mining right or closed. Although prospecting permits have been issued with closure certificates (n = 288), the number also appears very low.

Closure applications in five regions

The data on applications for closure certificates is limited, with only five regions supplying this information. As indicated, in some cases the data obtained extended beyond the period (*e.g.* North West and the Springbok office of the Northern Cape), with some provinces listing all closure certificates granted in the period (*i.e.* for applications made prior to 2012) and others including only certificates granted for applications made since 2012. Table V summarizes this data, but due to information limited to the period 2012 to 2015, and indicates the success rate for applications made *during the period under review that were granted during this period*. However, we know from Table IV that more closure certificates were issued than are indicated here. These were for applications made prior to 2012.

With the exception of the Springbok office of the Northern Cape, very few applications made *during the period under review were granted during this period*, indicating that processing closure applications takes time and that even though some closure certificates are being granted, many are not. The relatively high application success rate in the Northern Cape may be due to the nature of mining in this region, where alluvial diamond mining predominates.

It is unclear what the status is of the mines and permits where closure certificates have been applied for but have not been granted. As described by Milaras, McKay, and Ahmed (2014), these may be under care and maintenance. As regards the applications for closure of mining rights (including for road works), very few applications were made *during the period under review*, with only four being granted *during this period*. Again, additional data for all regions over a longer time period is needed to better understand the practice here.

Conclusion

The data confirms that mine closure in South Africa is problematic, with many questions remaining unanswered.

It is clear that closure certificates are not being issued as envisaged by the legislation, particularly for large-scale mines. For a closure certificate to be granted, a mine must be rehabilitated to an agreed standard by the rights holder and an application for closure made. There is currently insufficient data to determine the extent to which this is happening and how much of the problem sits with mining companies. The lack of

Table V

Applications for closure certificates made and certificates granted between 2012 and 2015, for regions where complete information was provided

Region	For all types of rights and permits (2012–2015)			For mining right only (incl. for road works)	
	Applications for closure	Closure granted for applications made	Success rate	Applications for closure	Closure granted for applications made
Northern Cape (Springbok office only)	97	53	56%	2	2
North West	334	81	24%	9	2
Limpopo	227	59	26%	0	0
Gauteng	33	16	48%	3	0
KwaZulu Natal	52	15	29%	0	0

applications for closure and the low application success rate may be an indication of the difficulty in successfully rehabilitating large mines, confirmation of the extended time needed to do this, and the perception that, with underfunded financial provision, it is easier and cheaper to put a mine on indefinite care and maintenance or sell it to avoid closure.

As regards government's role, the lack of transparency, incomplete data, regional inconsistencies, and low number of certificates issued for all types of rights points to problems within the DMR. This supports previous findings by Botham, Kelso, and Annegarn, (2011), Milaras, McKay, and Ahmed (2014), van Druten and Bekker (2017), and Corruption Watch (2017) regarding the capacity and competence of the regulator, resulting in the inability, and perhaps unwillingness, of officials to make the judgement call that rehabilitation is sufficient.

A recommended first step in addressing these concerns is to better understand the current closure certification process through access to additional data. Reliable, complete, detailed, and comparable data from all regions over a longer time period should be analysed to increase the validity of findings and focus responses and further research. Government's acceptance of the PAIA applications to obtain the data reviewed in this paper has set a precedent for further data requests. It would also be in the regulator's interest to establish a national-level database with this information, to assist with monitoring the implementation and effectiveness of the new closure regulations.

The ongoing review of the financial provision regulations offers an opportunity to engage with currently willing regulators to compel further transparency that could advance this line of study. Additionally, an integral part of this amendment process should be to better align the regulations towards providing a business incentive for responsible closure and the use of best practices. Finally, collaboration with government at this stage could act as a springboard toward increased national dialogue on these ever-salient issues surrounding mine closure and post-mining land use.

Acknowledgement

The authors acknowledge funding from the National Research Foundation, Thuthuka Funding Instrument.

References

Alberts, R., Wessels, J.A., Morrison-Saunders, A., McHenry, M.P., Sequeira, A.R., Mtegha, H., and Doepel, D. 2017. Complexities with extractive industries regulation on the African continent: What has 'best practice' legislation delivered in South Africa? *The Extractive Industries and Society*, vol. 4, no. 2. pp. 267–277

Botham, N.D., Kelso, C.J., and Annegarn, H.J. 2011. Best practice in acquiring a mine closure certificate – a critical analysis of the De Beers Oaks Diamond Mine, Limpopo, South Africa. *Proceedings of the Sixth International Conference on Mine Closure – Mine Site Reclamation,* Lake Louise, Alberta, Canada, 18-21 September 2011. Vol. 2. Fourie, A., Tibbet, M., and Beersing, A. (eds.), Australian Centre for Geomechanics, Perth. pp. 401–410

Corruption Watch. 2017. Mining for sustainable development research programme. Johannesburg, South Africa

Dixon, C. 2003. Mine closure from a legal perspective: Do the provisions of the new Mineral and Petroleum Resources Development Act and draft Regulations make closure legally attainable? *Journal of the South African Institute of Mining and Metallurgy*, vol. 103, no. 8. pp. 483–488.

Hermanus, M., Walker, J., Watson, I., and Barker, O. 2015. Impact of the South African Minerals and Petroleum Resources Development Act on levels of mining, land utility and people. *TRAVAIL, Capital et Société*, vol. 48, no. 1–2. pp. 10–38

Humby, T.L. 2014. Facilitating dereliction? How the South African legal regulatory framework enables mining companies to circumvent closure duties. *Proceedings of the Ninth International Conference on Mine Closure*, Sandton, South Africa. Weiersbye, I.M., Fourie A., and Tibbet, M. (eds). Australian Centre for Geomechanics, Perth.

Ledwaba, P. and Mutemeri, N. 2017. Preliminary study on artisanal and small-scale mining in South Africa. Report prepared for Open Society Foundation for South Africa, by the Centre for Sustainability in Mining and Industry, University of the Witwatersrand.

Milaras, M., McKay, T.J., and Ahmed, F. 2014. Mine closure in South Africa: A survey of current professional thinking and practice. *Proceedings of the Ninth International Conference on Ming Closure*, Sandton, South Africa. Weiersbye, I.M., Fourie, A., and Tibbet, M. (eds). Australian Centre for Geomechanics, Perth.

Minerals Council South Africa. 2018. Facts and Figures 2017. http://www.mineralscouncil.org.za/industry-news/publications/facts-and-figures

Mnwana, S. 2015. Mining and 'community' struggles on the platinum belt: A case of Sefikile village in the North West Province, South Africa. *The Extractive Industries and Society*, vol. 2, no. 3. pp. 500–508.

openAFRICA. 2018. Oxpeckers Investigative Environmental Journalism Centre. https://africaopendata.org/organization/oxpeckers-investigative-environmental-journalism

Republic of South Africa. Department of Mineral Resources. 2004. Directory D1/2004. Operating mines and quarries and mineral processing plants in the Republic of South Africa, 2004.

Republic of South Africa. 2005. Directory D1/2005. Operating mines and quarries and mineral processing plants in the Republic of South Africa, 2005.

Republic of South Africa. 2006. Directory D1/2006. Operating mines and quarries and mineral processing plants in the Republic of South Africa, 2006.

Republic of South Africa. 2007. Directory D1/2007. Operating mines and quarries and mineral processing plants in the Republic of South Africa, 2007.

Republic of South Africa. 2009. Directory D1/2009. Operating mines and quarries and mineral processing plants in the Republic of South Africa, 2009.

Republic of South Africa. 2010. Directory D1/2010. Operating mines and quarries and mineral processing plants in the Republic of South Africa, 2010.

Republic of South Africa. 2011. Directory D1/2011. Operating mines and quarries and mineral processing plants in the Republic of South Africa, 2011.

Republic of South Africa. 2012. Directory D1/2012. Operating mines and quarries and mineral processing plants in the Republic of South Africa, 2012.

Republic of South Africa. 2013. Directory D1/2013. Operating mines and quarries and mineral processing plants in the Republic of South Africa, 2013.

Republic of South Africa. 2014. Directory D1/2014. Operating mines and quarries and mineral processing plants in the Republic of South Africa, 2014.

Republic of South Africa. 2016a. Directory D1/2016. Operating mines and quarries and mineral processing plants in the Republic of South Africa, 2016.

Republic of South Africa. 2016b. Department of Mineral Resources. , Report of SSM database successful projects. Unpublished report.

Swart, E. 2003. The South African legislative framework for mine closure. *Journal of the South African Institute of Mining and Metallurgy*, vol. 103, no. 8. pp. 489–492.

Van Druten, E.S. and Bekker, M.C. 2017. Towards an inclusive model to address unsuccessful mine closures in South Africa. *Journal of the Southern African Institute of Mining and Metallurgy*, vol. 117, no. 5. pp. 485–490. ◆

As a trusted partner to the world's largest mining and minerals processing companies around the world, CiDRA professionals collaborate with their customers to apply highly differentiated process optimization solutions that take efficiency, recovery and throughput to new heights.

When it comes to requiring the most innovative integrated technologies that provide mission critical information previously unattainable from existing technologies, you can rely on CiDRA.

CiDRA®
Minerals Processing

CiDRA Minerals Processing Inc.
Felix Project Management and Consulting Services C.C.
South Africa • jfelix@cidra.com • Phone: +27.11.900.1386
cidra.com/minerals-processing

SAIMM
THE SOUTHERN AFRICAN INSTITUTE OF MINING AND METALLURGY

In collaboration with the MMMA

TAILING STORAGE CONFERENCE 2020

Investing in a Sustainable Future

12–13 February 2020

Birchwood Hotel & OR Tambo Conference Centre
Johannesburg, South Africa

BACKGROUND

Engineers designing tailing storage facilities are faced with a number of new challenges resulting from the encroachment of both formal and informal housing projects, legislation pertaining to water usage and pollution control, shortages of water for processing, and the requirements for tailing dam closure.

This has resulted in the introduction of new designs for construction of more stable dams, alternative deposition methods, the introduction of non-permeable linings, and the capping of dams to encourage rehabilitation and minimize dust pollution. The shortage of water in Southern Africa has necessitated changes in dam design to minimize water usage by either reducing the amount of water to the dam or increasing the amount of water recovered.

Understandably, new legislation has been passed to regulate the construction and operation of tailing storage facilities. This knowledge resides with few specialists in the industry, and the operators on the mines are sometimes unaware of the consequences of these changes for their operations. In many cases the operations engineer has been misinformed and the need has arisen to get the parties together to discuss the implications of the changes.

Reprocessing of existing tailings adds to the complexity of operating a tailing storage facility, and many new operators have little or no reference material to assist them when planning a retreatment project.

For further information contact
Camielah Jardine
Head of Conferencing • SAIMM
Tel: (011) 834-1273/7
Fax: (011) 833-8156 or (011) 838-5923
E-mail: camielah@saimm.co.za
Website: http://www.saimm.co.za

Stability considerations for slopes excavated in fine hard soils/soft rocks at Cobre Las Cruces mine, Sevilla, Spain

S. Cooper[1], M.D. Rodriguez[1], J.M. Galera[1], and V. Pozo[2]

Affiliation:
[1]Universidad Politécnica de Madrid.
[2]Subterra Ingeniería.

Correspondence to:
S. Cooper

Email:
stephen.cooper@fqml.com

Dates:
Received: 13 Sep. 2018
Revised: 17 Jan. 2019
Accepted: 15 Feb. 2019
Published: July 2019

How to cite:
S. Cooper, M.D. Rodriguez, J.M. Galera, and V. Pozo
Stability considerations for slopes excavated in fine hard soils/soft rocks at Cobre Las Cruces mine, Sevilla, Spain.
The Southern African Insitute of Mining and Metallurgy

DOI ID:
http://dx.doi.org/10.17159/2411-9717/322/2019

Synopsis

Cobre Las Cruces mine extracts copper minerals from a VMS deposit located in the well-known Iberian Pyrite Belt (IPB). As an open pit, it is distinguished geologically from other IPB mines by the presence of around 150 m of Tertiary soft marls, known locally as the Guadalquivir Blue Marls, followed by a regionally important aquifer. Below the marls and aquifer the mineralization is hosted by rocks typical of the Palaeozoic within the IPB, comprising gossan, tuffs, slates, and sulphides.

This combination of a substantially soft rock and more competent, older (but still occasionally problematic) Palaeozoic lithologies constitutes a unique geological framework and presents substantial challenges in maintenance of slope stability, and therefore operational safety, at the mine site. This paper describes the fundamental design, excavation, and monitoring measures implemented at the mine to maintain safe production, and the lessons learnt during the mine development.

Keywords
pit design, slope stability, monitoring.

Introduction

As a modern Spanish mine, Las Cruces is committed to the use of best available technology and practices with the aim of guaranteeing the production of ore in a safe environment. From a practical perspective, this implies the realization of a high quality pit design, ongoing geotechnical mapping of exposed slopes to ensure conformity with design, and use of leading geotechnical surveillance technology to complement visual observations. The focus of this article is to illustrate how, at a mine site with potentially problematic soil/rock conditions, multiple advanced techniques employed from design stage analysis through to final pit configuration and vigilance, were combined to achieve an overall control of the ground conditions. In Figure 1 the layout of the pit is shown, illustrating development at the beginning of 2015.

Mine description

The mine is an open pit measuring 1600 m by 900 m (final pit shell) with a maximum depth of 250 m. The mine extracts copper sulphides from the same volcano-sedimentary Palaeozoic deposit as the Rio Tinto and Aznalcollar mines. The ore is overlain by 140–150 m of the tertiary soft marls known as the Guadalquivir Blue Marls (Oteo, 2000). Below these marls there is a sandy formation that constitutes, together with the weathered top part of the Palaeozoic, a known aquifer denominated 'Niebla-Posadas'. Regionally, the water table is located around 30 m below the surface. Finally the Palaeozoic, in which the mineralization is hosted, is defined by slates, tuffs, and porphyric rocks.

To access the mineralization a pre-stripping excavation of the marls is required. These marls constitute a problematic unit from a geotechnical point of view as they present weak strength and low deformational parameters. This concern (associated with a lack of experience of such excavations in the Guadalquivir marls) strongly conditioned the original pit geometry, which was defined by an overall slope of 28° from the surface down to 150 m depth. In the Palaeozoic strata, a general slope of 45° was adopted.

The marls are highly impermeable (k = 10^{-9} to 10^{-10} m/s) and so, without some form of hydromechanical coupling, a flow-based analysis would predict only a small pore pressure drop due to flow towards the pit. An additional aspect that required consideration and inclusion at the design stage was the incorporation of a perimetral drainage system. The system was based on well points drilled directly into the aquifer and pumping commenced prior to pit excavation, to minimize environmental impacts and improve geotechnical behaviour as excavation progressed.

Figure 1—Actual layout of the pit (2015)

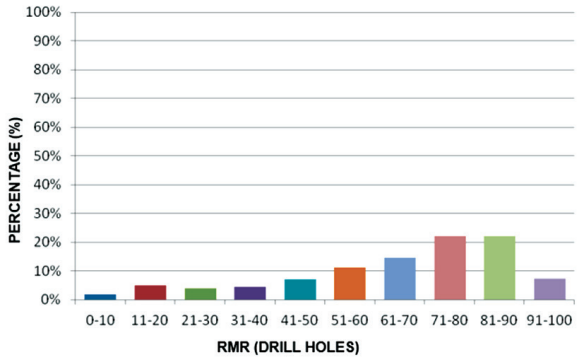

Figure 2—RMR statistical distribution for the gossan (leached component of mineralization)

Geological and geotechnical characterization at the mine

Initial characterization of the rocks was by dedicated geotechnical drilling and laboratory testing. Use was also made of geological drilling undertaken to assess the orebody characteristics.

As part of a standard operating procedure, geotechnical logging of key geological mineral resource boreholes was undertaken (over 45 000 m of drilling prior to pit development). Additional complementary drilling of over 700 m of purely geotechnical boreholes was carried out in order to target explicit unknowns and improve the characterization of the surrounding host rocks. These boreholes were logged and analysed in detail. Figure 2 shows an example of the RMR histogram compiled for the mine´s gossan zone (with an average thickness between 10 m and 20 m, commencing at around 150 m depth) highlighting the RMR statistical distribution for this lithology using the drill-hole database. This RMR characterization was further improved following processing of in-pit mapping once stripping exposed this lithotype.

Summarizing all the existing data, Table I shows the stratigraphy of the mine from top to bottom, including the typical thickness of each unit.

Figure 3 shows the detailed stratigraphy of the Tertiary strata that overlie the ore. Figure 4 shows the evolution of the UCS with depth, with distinction made between pre-excavation

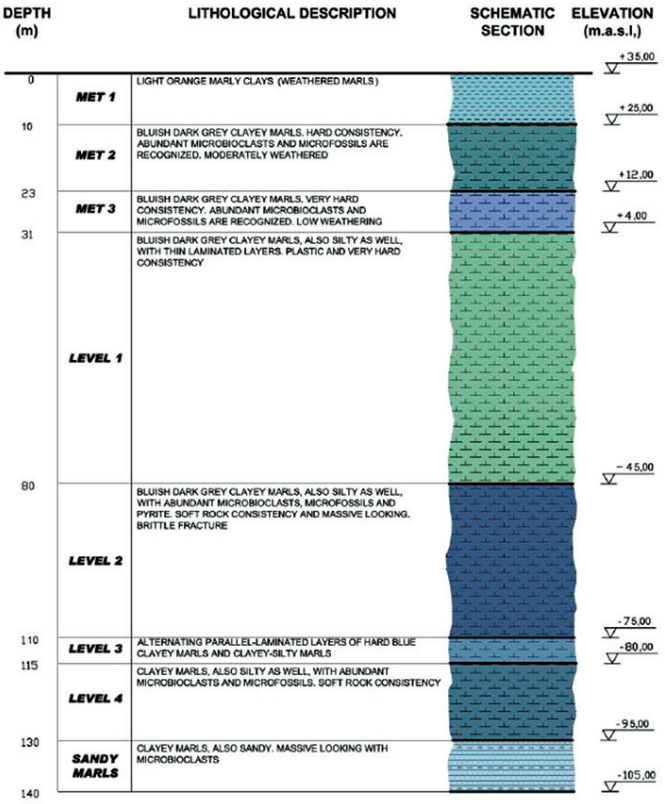

Figure 3—Lithological description of the marls with depth, according to weathering condition and geotechnical characteristics

Table I

Depth and thickness of various lithologies within the pit at Las Cruces mine

Lithology	Description	Designation	Typical depth (top, m)	Typical depth (base, m)	Thickness (m)
Weathered marls	Brown, highly weathered Brown mottled blue, weathered. Blue mottled brown, moderately weathered	MET1 MET2 MET3	0 10 23	10 23 31	10 13 9
Fresh marls	Blue, very weak, without observable weathering Blue, weak, without observable weathering Blue, weak, without observable weathering Sandy marls, transition zone to aquifer	LEVEL 1 LEVEL 2 LEVEL 3 SANDY MARLS	31 80 110 120	80 110 120 125	49 30 10 5
Aquifer	Partially cemented sands	AQU	125	140	15
Gossan	Yellow-reddish leached sulphide-derived hard rock	GOSSAN	140	155	
Sulphides	Massive or sem- massive sulphides, 'hard' rock	SULPHIDE	155	250	
Tuffs,	Volcanic host rocks	TUFF	140	-	Surrounds orebody
Shales	Metamorphic host rock	SXM	140	-	Surrounds orebody

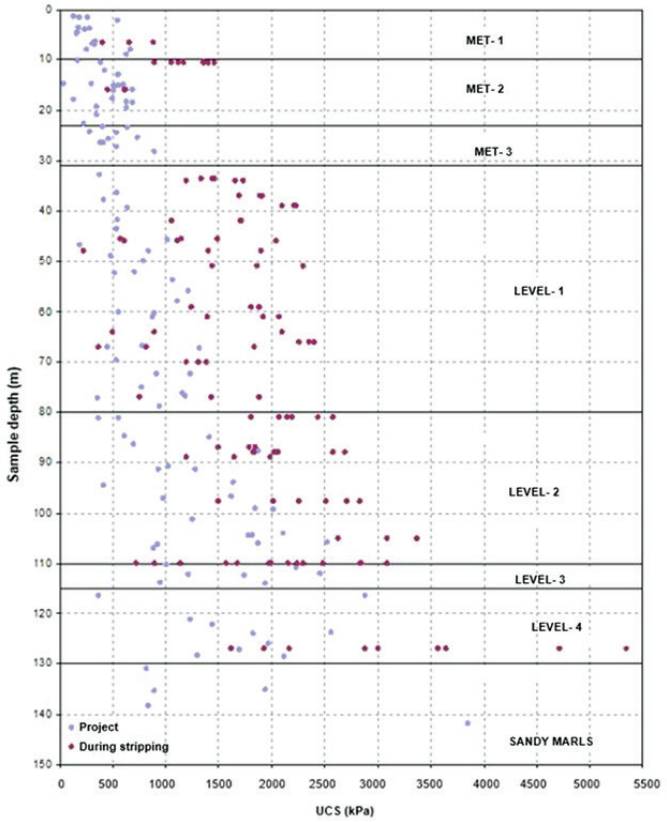

Figure 4—Lithological profile of the pre-stripping materials with compressive strengths (Galera *et al*., 2009b). Note increases in UCS values on the less disturbed bulk samples obtained during stripping (in red)

tests undertaken on samples from drill-holes, and tests on bulk samples obtained in the field during excavation, which were considered to be less disturbed. Table II shows the main geomechanical values for each horizon.

Below the marls and aquifer the mineralization is hosted by the rocks typical of the Palaeozoic within the Iberian Pyrite Belt. For the purposes of geotechnical evaluation the following lithologies were established: gossan, tuffs, slates, and sulphides. Geologically, these lithologies can be further sub-categorized with respect to their geochemistry. Table III includes strength and deformability values for the existing lithologies in the Palaeozoic.

Initial design (2003)

Using the geomechanical data from the site investigation based on boreholes and laboratory and *in situ* testing, an initial design of the slopes was undertaken for the mine using final pit shell configurations to provide a geometry for a 2D limit state analysis, applying the Rocscience geotechnical programme SLIDE as well as FLAC2D finite difference code for deformation analysis.

In fundamental terms, the limit state programme SLIDE undertakes systematic calculations of various slip circle configurations, discretely separating the geometry into slices to determine the least favourable situation with respect to balance of forces. Deformations are not considered in this type of analysis. Instead, the programme calculates the ultimate limit state condition of the slope, utilizing the geotechnical characterization of the soils and rock to determine the maximum resistance provided by the overall rock mass, comparing the sum of these values against the stresses induced by the weight of the rock mass in order to determine a safety factor for stability.

Table II

Geomechanical values for each geotechnical horizon – Tertiary

Description	Horizon	Depth (m)	σ_{ci} (kp/cm²)	m_i	s	*c* (kp/cm²)	ϕ (°)	γp (t/m³)	γ (t/m³)	ω (%)	PI (%)	*E* (MPa)
Highly weathered marls	MET-1	0-10	3.5	2	1	1.10	22	2.714	1.415	30.3	34.3	28.03
Moderately weathered marls	MET-2	10-23	3.8	4	1	1.50	21	2. 714	1.459	28.5	30.2	56.20
Slightly weathered marls	MET-3	23-31	3.8	4	0.07	1.50	21	2.714	1.496	27.1	30.8	47.58
Unweathered marls (low strength)	LEVEL-1	31-80	4.0	6	0.05	2.1	20	2.714	1.528	25.5	38.1	106.11
Unweathered marls (medium strength)	LEVEL-2	80-110	4.0	6	0.05	2.7	18	2.714	1.585	24.2	39.1	156.53
Unweathered marls (high strength)	LEVEL-4	115–130	6.0	6	0.01	2.8	18	2.714	1.579	24.2	38.5	233.61

Symbols
- Uniaxial Compressive Strength (UCS) σ_{ci}
- Hoek and Brown constitutive moderl parameters m_i, s
- Cohesion c
- Friction angle ϕ
- Apparent density γ_p
- Dry density γ
- Moisture content ω
- Plasticity Index *PI*
- Young's modules *E*

Table III

Geomechanical values for each geotechnical horizon – Paleozoic

Group	Intact Rock					Joints					
		Elastic		Plastic		Strike		Peak		Residual	
	ρ (kN/m³)	Ei (MPa)	v	σ_{ci} (MPa)	mi	Dip (°)	Dir (°)	Jc (kPa)	Jϕ (°)	Jc (KPa)	Jϕ (°)
Gossan	28.90	20.00	0.25	19.3	7.23	–	–	–	–	–	–
Tuffs	23.00	8.200	0.25	16.0	8.24	–	–	–	–	–	–
Shales	24.00	22.500	0.20	4.4	4.78	70	004	130	22	0	22
Sulphides	44.0	80.000	0.20	115.0	12.85	–	–	–	–	–	–

Symbols
- Dry density ρ
- Young's modules (intact) E_i
- Poisson's modules *V*
- Uniaxial Compressive Strength (UCS) σ_{ci}
- Hoek and Brown constitutive moderl parameters m_i,
- Joint cohesion J_c
- Joint friction Jϕ

Stability considerations for slopes excavated in fine hard soils/soft rocks

FLAC2D finite difference code was utilized to obtain information on localized overstresses, to better determine the transition from peak to residual resistance conditions and in order to determine deformation magnitudes for subsequent interpretation of displacement monitoring data from instrumentation in the field.

Figures 5 and 6 show typical examples of slope stability analysis at the mine; the first to determine the ultimate limit state using the method of slices, the second using finite difference stress-strain analysis software to determine deformation magnitudes.

It should be stressed that with this initial design the mine operated successfully for 3 years, until a refinement process commenced in 2007. Figure 7 shows the relatively good condition of the pit in late 2007, one year after commencement of pre-stripping operations.

Key points of the 2003 initial design

- The use of limit state equilibrium analysis software to determine the minimum safety factor required for compliance with legislative requirements. Spanish mining law ITC 07-01-03 stipulates minimum safety factors of 1.2 for non-seismic conditions and 1.1 for seismic conditions, with those seismic conditions being established by the country geographic register for earthquake potential
- Assumption of overlying homogenous marls subject to non-structural failure mechanisms

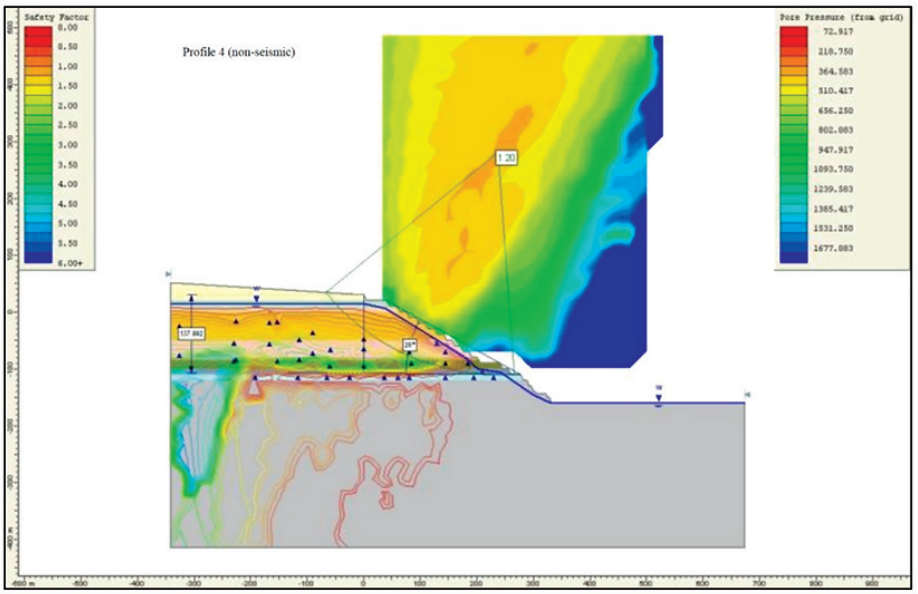

Figure 5—Stability analysis using ROCSCIENCE SLIDE 5.0 showing incorporated pore pressure contours, highlighting conformity with non-seismic safety factor requirements in accordance with Spanish seismic resistance guidence (NCSE-02)

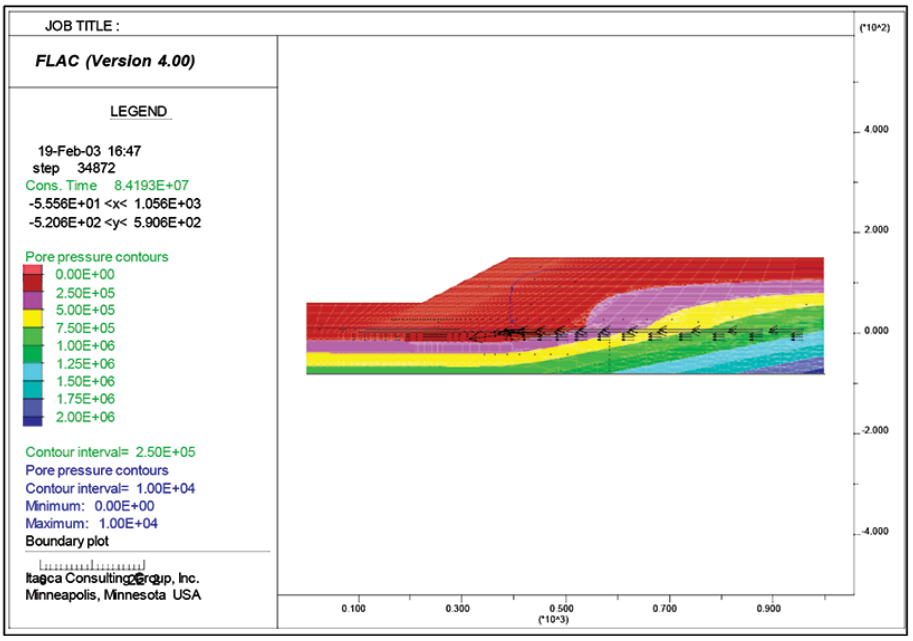

Figure 6—Initial design, determination of pore pressure development in FLAC v4.00 for subsequent use with the SLIDE analysis

Figure 7—Condition of pit in 2007. The base level -55mAOD is dark in colour, showing the moist condition of the intact marls when first exposed

- Use of FLAC v4.00 to generate pore pressures associated with pre-strip pumping of the SDR (system of drainage and reinjection) network. The SDR network comprised a ring of perimetral drainage wells designed to draw water away from the pit, to be returned to the ground *via* re-injection at a considerable distance from the mine. The beneficial drawdown effect created by this drainage system needed to be considered within the FLAC analysis
- Strain-softening characteristics incorporated into marl parameters. A particular early concern regarding the marls was the high ratio between peak and residual resistance parameters. This varied with respect to the depth and weathering condition of the marls; however, typical peak friction angles were determined from laboratory tests (triaxial and shear box) at 21°, while the residual friction angles for the same marls were as low as 7° with deformations at less than 3%.

Pit vigilance

The slopes were intensively monitored from the very first stages of pre-striping. The instrumentation implemented was based on two types of measurement: deformation (using inclinometers and topographical surveys) and pore pressure measurement using vibrating-wire piezometers. These piezometer installations were initially sand-packed constructed, although during mining development and trialling in non-essential zones, the construction methodology was switched to grouted piezometers in later years, which proved quicker to equilibrate and easier to install.

Topographical monitoring (the GeoMoS monitoring system)

Slope surface movement was monitored using a GeoMoS topographical system. An early version of the system was installed during the first stages of pre-stripping, enabling movements to be catalogued and compared with determined velocity alert levels. These levels are shown in Table IV, while Figure 8 shows an example of the topographical prism survey on the perimeter of the pit as well as inside it, on the operational ramp.

Over the years the system has been overhauled to increase reliability and measurement frequency (as high as one reading every 20 minutes of well over 100 prisms). In 2014 two more advanced systems were purchased; a pit slope scan from one of these is showed in Figure 9. The first of these systems was placed on the south side of phase 3 of the pit to reduce distances to prisms in newer phases and thereby increase precision. The most recently installed system represented a significant jump in the technology, enabling direct laser-based measurement of the slope surfaces (eliminating the need to install prisms in potentially unstable slopes). This system, near-analogous to a more expensive radar system, was installed within the Palaeozoic to monitor slopes during the extraction of an unanticipated high-grade ore zone in contact with problematic shales. The purchase costs of the system were justified by it enabling the operations team to guarantee personnel safety while extracting substantial additional ore not contemplated in the original pit configuration.

Table IV

Established alert levels at the mine

Level	Displacement velocity (mm/d)	Likely cause	Action
Attention	1	Long-term decompression from pore pressure dissipation	Visual inspection, increase local inclinometer measurement frequency.
Alert	3	Short-term decompression from rapid principal stress rotation (localized pit stripping) / potential. instability	As above plus recheck design with local geometrics. Consider likely progress pattern and the necessity of cessation of activities in zone.
Emergency	10	Instability.	As above plus cessation of activities in zone.

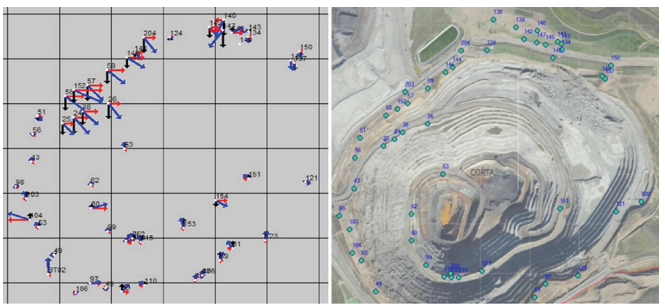

Figure 8—Example of daily pit prism displacement monitoring

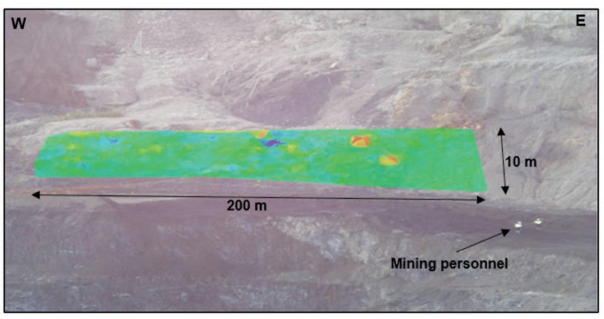

Figure 9—Direct slope scan showing areas of movement

In-ground monitoring

Over the mining facility (including both pit and dumps) a matrix of piezometers and inclinometers was installed. The number of instruments increased proportionally with the mine development from the early stages to the current configuration of 72 piezometers and over 50 inclinometers.

Piezometers

Piezometric levels were monitored to ensure that pore pressures did not exceed levels where the slope stability safety factors could be considered to be compromised. Figure 10 shows an example of the ongoing monitoring of the pore pressure around the pit. Figure 11 provides a plan view of the position of these piezometers in the field.

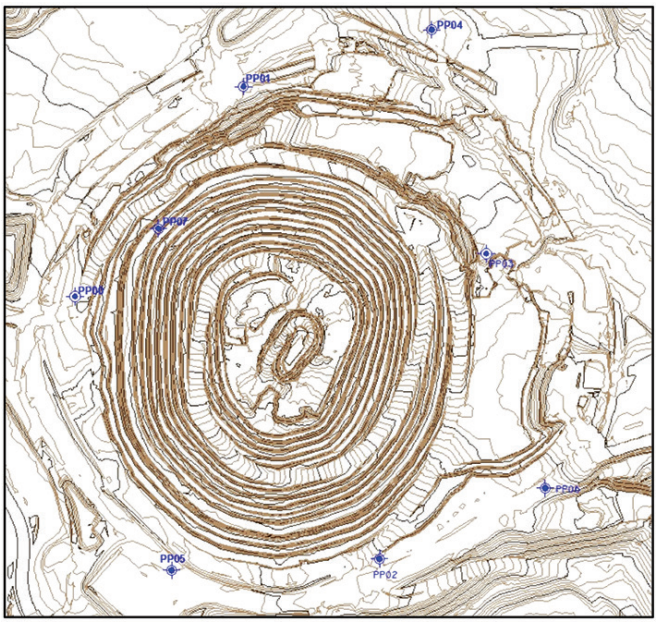

Figure 11—Location of piezometers in and around an early stage of the pit excavation, corresponding to those piezometers highlighted in Figure 10

Piezometer information is also utilized to monitor the effects of shutdown in sectors of the SDR system for maintenance purposes. Finally, the development of pore pressures during mining activities for over 10 years, as described previously, provided invaluable information for checking and calibrating the estimated pore pressures generated by the hydro-coupling process utilized in FLAC3D.

Conventional inclinometers

Predominant use was made of conventional inclinometer systems comprising continuous metal tubes installed to depths of up to 140 m. The distortions of these tubes were measured manually on a weekly or twice-weekly basis and compared with previous readings to calculate displacement velocities. Figure 12 shows a cross-section of the pit incorporating the south dump, showing the displacements detected within bedding planes at depth. Figure 13 shows an enlarged view of one of these inclinometer profiles indicating, for a perimetral location, the magnitude of displacements that manifested at bedding plane positions during pit excavation.

Real-time inclinometer readings

As well as conventional inclinometers, in key areas of the pit, technically more advanced inclinometers were installed. These systems enabled continuous information to be gathered as well as displacement exceedance alerts to be sent directly to the geotechnical engineers´ mobile telephone (a functional tool also available for the topographical prism system). Figure 14 shows the cumulative displacements detected with a real-time inclinometer. This inclinometer was placed in the southwest of the phase 2 area for vigilance purposes during the extraction of high-grade mineralization adjacent to the mine´s less competent footwall shales. Figure 15 shows the location of this particular real-time inclinometer with respect to the pit´s phase 1 area.

These inclinometers were more costly than conventional systems but provided far more information with respect to the evolution of movement and reaction of the substrata in real time during mining activity in that particular area; for example, deepening of an adjacent excavation. Given the extra costs involved, the most optimal form of implementation was to

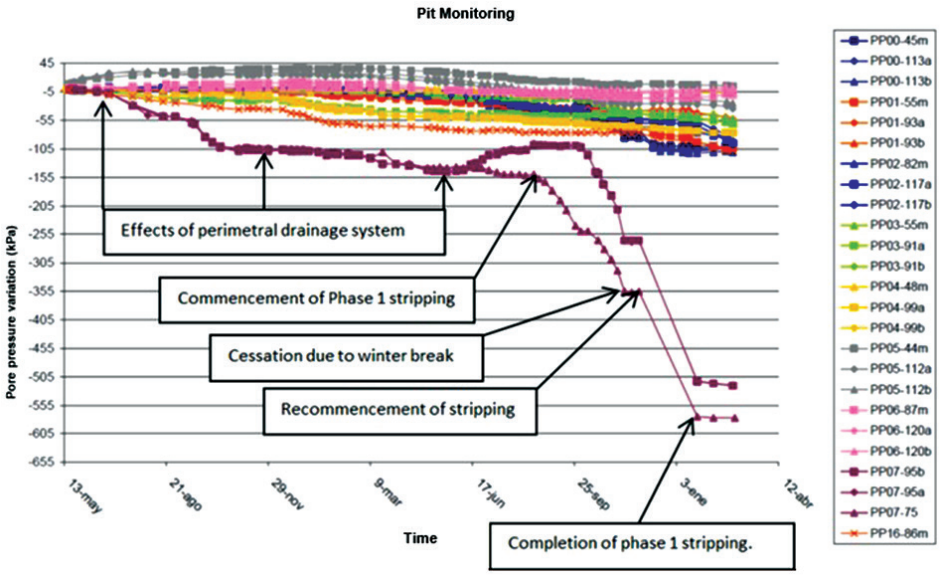

Figure 10—Ongoing piezometer monitoring during excavation showing clear relationship between pore pressures and stripping activities

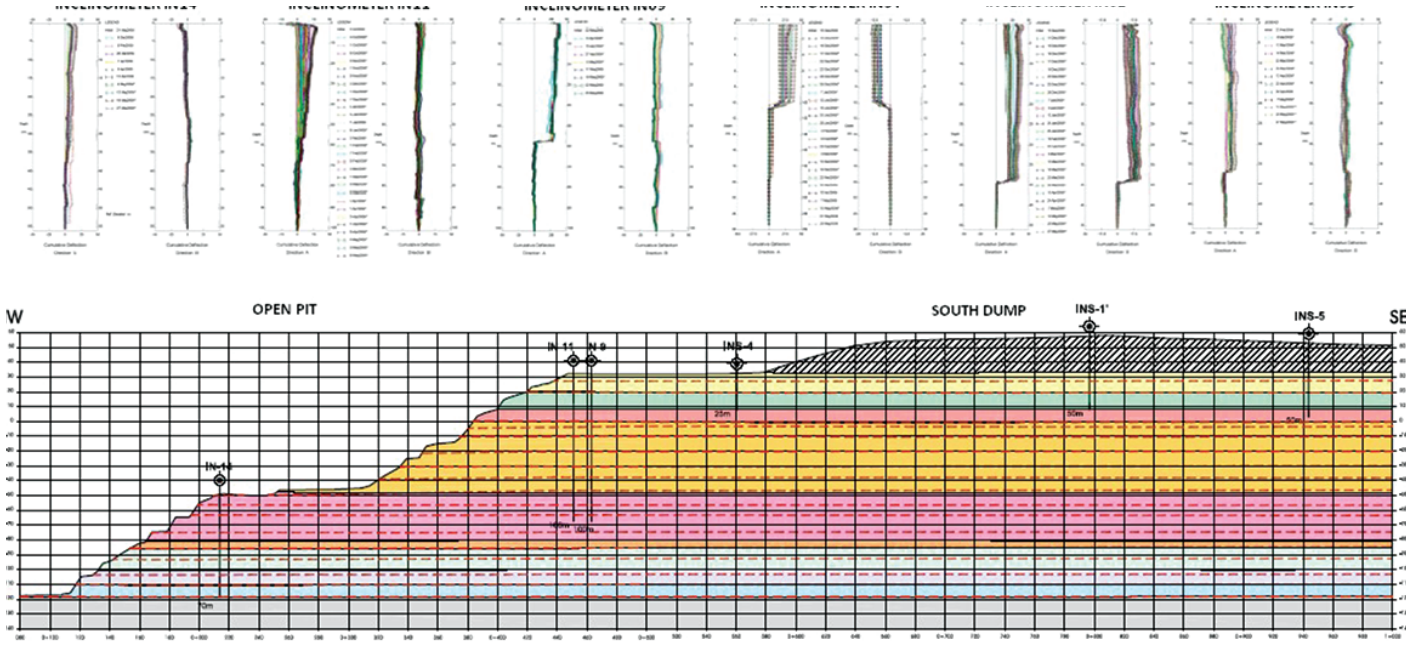

Figure 12—Cross-section of pit with key inclinometers, showing displacement in continuous bedding planes at depth

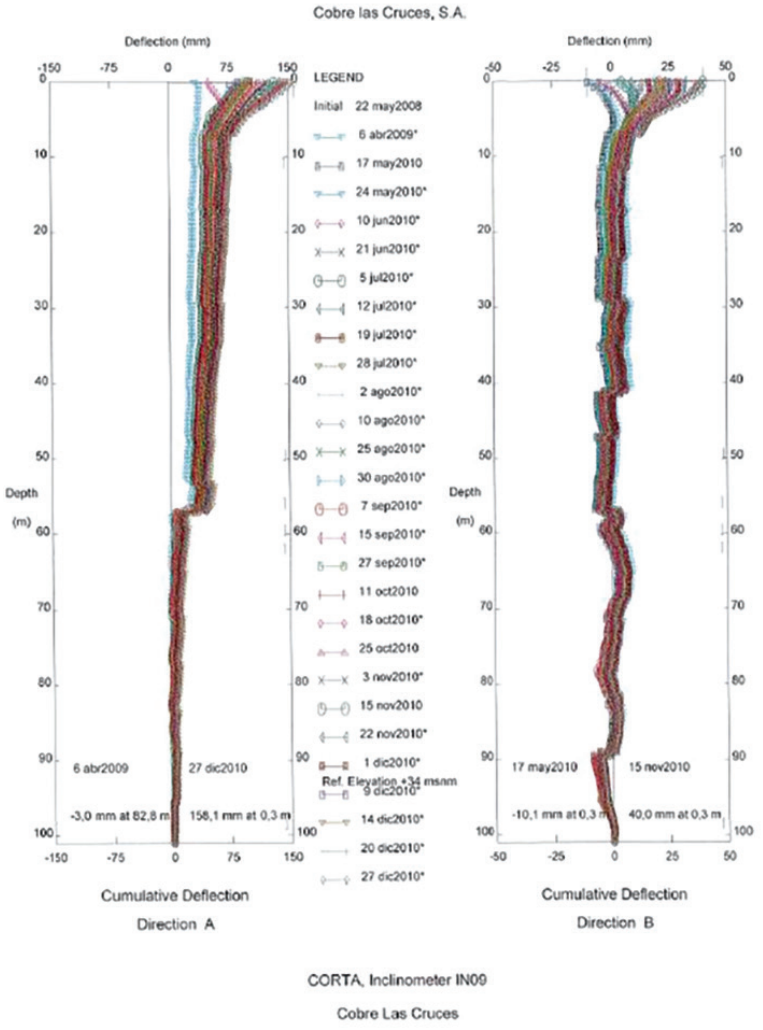

Figure 13— Detail of one inclinometer(IN09) showing displacement at 55 m depth corresponding with a known major bedding plane

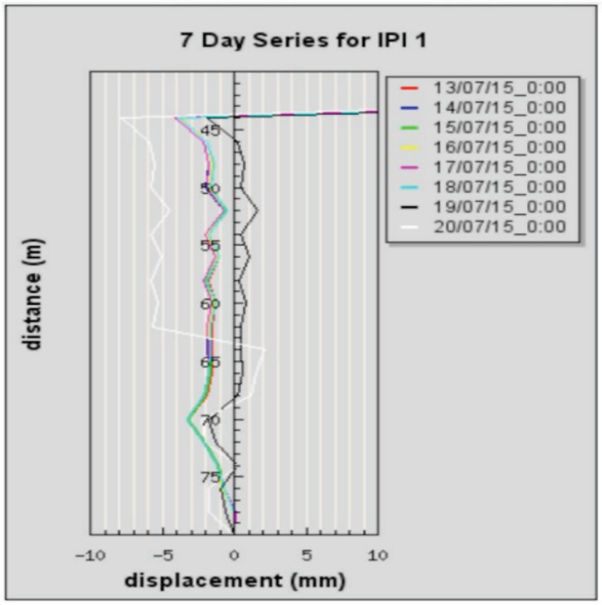

Figures 14—Cumulative movement down-hole for real-time inclinometer IPI1 installed adjacent to the footwall shales

begin with a localized analysis of the slope of concern and the commencement of monitoring with conventional inclinometer systems to understand where instability was most likely to occur. Once this was firmly established, the zones with higher risk of instability were then targeted with real-time sensors. This continues to be the installation philosophy employed at Las Cruces Mine.

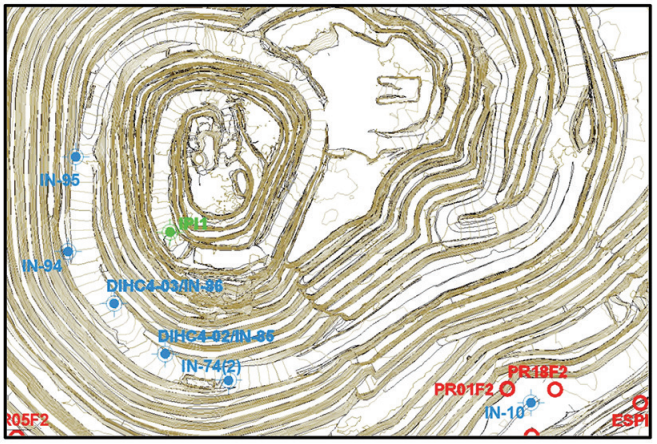

Figures 15—Plan view of phase 2 showing the location of real-time inclinometer IPI1 in the pit

Visual inspections and geotechnical mapping

All the above instrumental vigilance was complemented by solid and ongoing in-the-field observation. This varied from simple but regular slope inspections undertaken to ensure short-term stability in operative areas, through to complex geotechnical reconciliation cartography to determine the quality and condition of the blasting and excavation works in comparison. Figure 16 shows a typical geotechnical mapping of a mine bench using conventional methods as well as stereographical photo methods. The mine employed 3D photography complemented with structural observations carried out on site. Post-processing of the photographs also provided an opportunity to encounter structures not accessible during the mapping due to safety

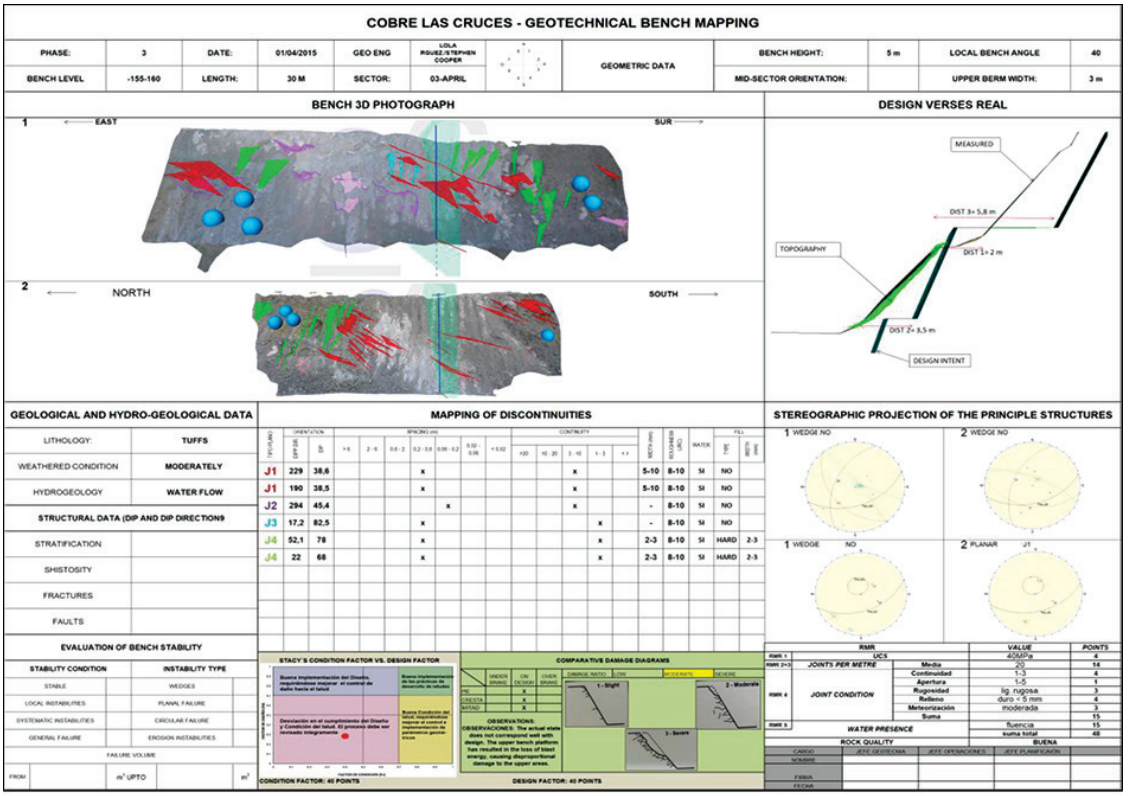

Figure 16—Formalized geotechnical cartography providing slope reconciliation following blast and excavation

considerations. The mapping as usual detailed the rocks' lithological and structural characteristics (orientation, weathering condition, roughness, fill *etc.*). In addition, the mapping attempts to undertake an objective evaluation of the efficiency of the blast utilizing factors associated with blast condition, and conformity to intended design.

Summary of design stages

Over the first 10 years, during stripping and ore extraction, the initial geotechnical model and design were modified and refined, culminating in additional investigation and geotechnical parameter characterization in 2012.

The work in 2012 was initially undertaken for due diligence purposes to complement an ongoing geological infill drilling campaign. Nevertheless, from the outset focus was placed on the possibility of increasing pit angles in the more competent lower marls. This possibility seemed reasonable, given increases observed in resistance parameters with depth, as calculated from bulk samples (considered less disturbed) obtained during the pit excavation. Additionally, during stripping a notable transition in strength at around 75 m depth was observed, which promoted the transition from mechanical free digging to the use of blasting to 'loosen' these lower marls prior to excavation.

Thus, along with an improved definition of the lithological variability of the Palaeozoic, the aim of further pit characterization was to improve knowledge of this marl sub-stratum. The additional information obtained indicated a small, but significant, increase in resistance parameters that were initially fed into a more refined SLIDE limit state analysis to justify increases in pit angles in those marls (from 28° to 31°). The same characterization information was also used subsequently in a three-dimensional finite difference tenso-deformational model which simultaneously incorporated the hydromechanical coupling for final pit geometrical configuration.

This evolution also had a basis in observations of reasonable behaviour of the slopes generally over a number of years, particularly at depth, which including the deformation results of the pit monitoring described in the previous section.

Using FLAC3D, attempts were made to model the hydrological complexities introduced by the pit decompression, low permeability of the overlying marls, and the use of a system of water extraction and reinjection put in place to obtain a drawdown on the water table, improving overall stability and minimizing environmental effects.

This section describes key phases in the evolution of the pit design.

First design refinement (2007)

During 2007 the first detailed hydromechanical calibration in 3D of the pore pressure after completion of the pre-stripping of the marls was undertaken. The result of this work was described in Galera *et al.* (2009a). Figure 17 shows the cohesion values utilized in the block model in this first iteration of mine excavation (highlighting just the circular phase 1 and 2 condition). Figure 18 shows the results of the pore pressure comparison for some of the piezometers that had been installed at that early stage and which were indicating a reduction in pore pressure due to the decompression and aforementioned drainage system.

Key points of 2007 design stage

- Axisymmetrical FLAC3D analysis utilized to match pore pressures in design with those observed in vibrating-wire piezometers during the initial phases of stripping (pore pressure calibration process)
- Modelling of pressure drawdowns induced by the ring of perimetral drainage wells that formed part of the drainage and reinjection system (SDR)
- Incorporation in pit design of pore pressure drops due to a volumetric expansion associated with the excavation of the pit, achieved by the use of hydromechanical coupling to model the reaction of the soil/water mass as the principal stress rotated during pit excavation and slope formation.

A paper on that analysis (Galera *et al.* 2009b) highlighted that coupling of hydrogeological and mechanical behaviour indeed provides a rationale to incorporate piezometers as part of the pit monitoring system. In addition, the authors suggested the possibility of applying the same technique not just to soil slopes, but also to hard rock slopes with high permeability values, although clearly hydrologic recharge would set a limit to this aspect. Further work was recommended at other mine sites in this respect.

In general, this first work in FLAC3D was undertaken early in the mine life with less data build-up prior to the analysis. The determination of global safety factors in FLAC3D is also achieved *via* the summation of a series of local safety factors on each block (strength reduction factors). This process in itself can be subjective as appropriate slip planes need to be established

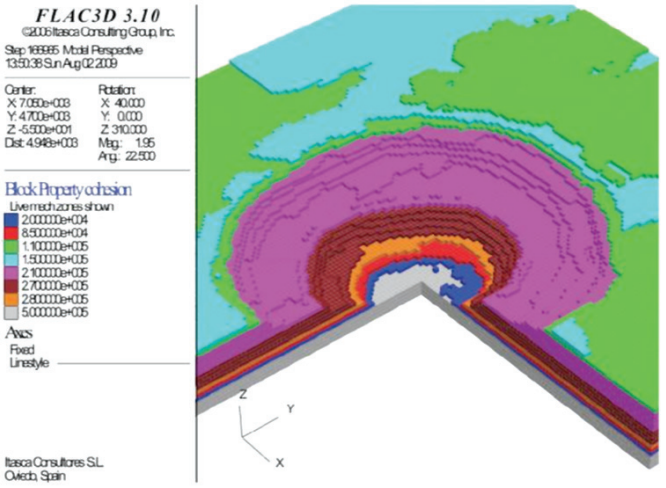

Figure 17—Initial FLAC3D pit analysis, showing cohesion values, utilized in the first attempt to analyse the 3D effects of stripping activities

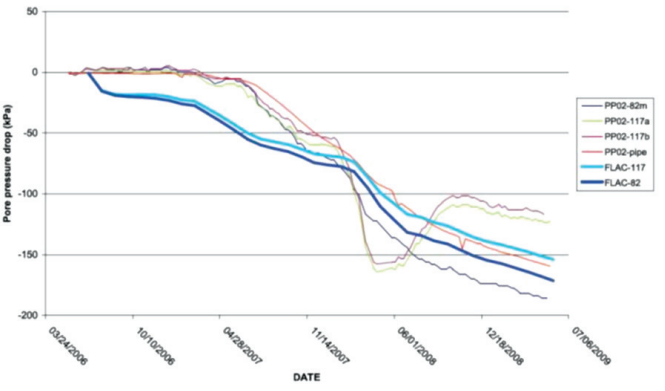

Figure 18—Pore pressure calibration attempts for the first FLAC3D pit analysis

for the summation process. Thus, the objective at that early stage was not to steepen slope angles, but rather confirm, *via* an alternative evaluation process, the angles approved previously by the more traditional limit state analysis methodology.

Global pit optimization (2012)

In 2012, during an operational optimization of the pit for resource model modifications, ongoing geological drilling was further complemented with geotechnical drilling and an associated refinement of the geotechnical pit model. Figure 19 shows the re-analysis of the pit slope stability undertaken using 2D limit state methods, while Figure 20 shows the aspect of the pit at the end of 2012.

Substantial refinements were made in the following areas.

- *Marls*—Desktop studies of excavations in the marls in the region (incorporating observations at an adjacent marl quarry operation) indicated that a relatively homogeneous and isotropic marl packet could be expected, and this was corroborated with regional information supplied by the Spanish Geological Institute. Early analysis incorporated those generic assumptions and focused on large-scale mass failure mechanisms. However, during the initial stripping operations, geotechnical mapping and a number of localized failures clearly demonstrated that any large instability was likely to be significantly structurally dominated. Thus a series of modifications was considered necessary for the marls, consisting of:
  - Incorporation of bedding planes and subvertical structures observed in geotechnical mapping of slopes during seven years of excavation (Figures 21 and 22). Minor movements had been observed in bedding planes by inclinometer monitoring. Distortions in the range of 100 mm to 200 mm (total cumulative movement) were typical, with decompression velocities of 0.1 to 0.3 mm/d observed in newly opened excavation zones. Although few instabilities were associated with these bedding planes at that stage, it was evident that these structures, along with other subvertical (apparently tectonically induced) joint sets, could play a pivotal role in future stability, and thus required consideration in design refinement. Analysis of bedding-plane displacements observed in inclinometers was therefore included in the global analysis (Cooper *et al.*, 2011).

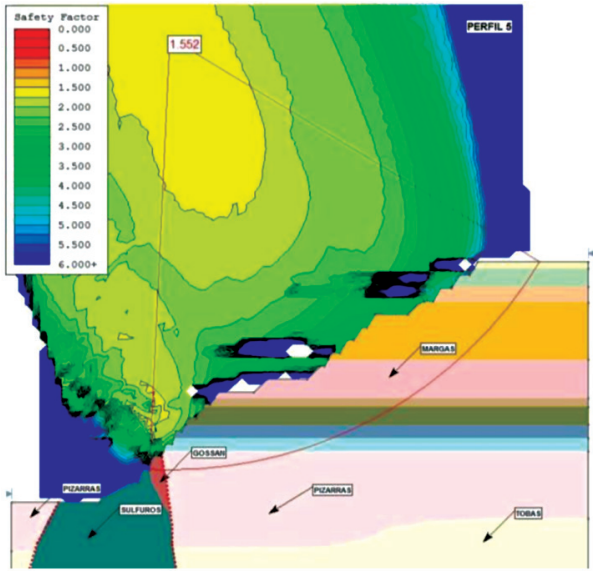

Figure 19—Example profile from 2012 analysis showing incorporation of Palaeozoic lithological variation

Figure 20—Configuration of the pit in late 2012. Note the weathered condition of the older phase 1 area in comparison to the more recently constructed slopes on the right

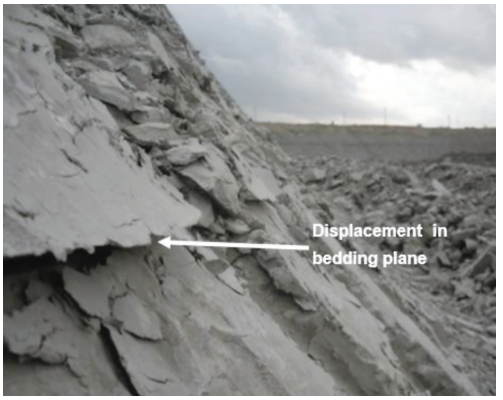

Figure 21—Movement observed in one of the major bedding planes. Horizontal displacements of up to 30 mm were noted and corroborated to deformations within perimetral inclinometers

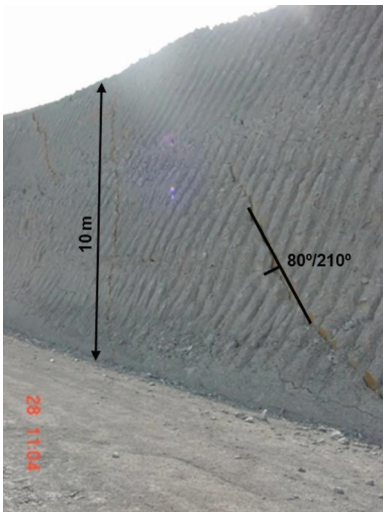

Figure 22—Subvertical tectonic structure observed in freshly exposed marls in phase 4 at 50 m depth

These bedding planes in marls were observable both implicitly *via* movement within inclinometers and explicitly following geological mapping of the slopes. They were generally observed to be closed, with no significant fill material, and close to the horizontal (with dip direction around 3° towards the south). In general, bedding planes occurred every 5 m to 6 m, some of which represent transition interfaces between the distinct marl bands

- Acknowledgement in design of a significant transition in geotechnical resistance parameters between the upper and lower marls (with a transition zone at around 80 m depth in Blue Marls LEVEL 1 to LEVEL 2). This transition, which was observed in laboratory testing and was also confirmed in the field, marked the depth at which blasting of the marls for excavation purposes became economically viable
- Modification of the resistive strength parameters (cohesion and friction angle, correlated with depth) for the lower marls. This implied a re-analysis of all information, incorporating additionally bulk samples that were less disturbed, with reduced scatter in the test results.

The incorporation of these three concepts led to a better understanding of a number of bench and multi-bench failures that had occurred nearer to the crest of the pit, as well as the recommendation to increase slope angle at depths between 80 m and 140 m from 28° to 31°.

➤ *Palaeozoic*—Improved analysis process on the Palaeozoic, which was assumed initially to be relatively intact and competent, included:

- Incorporation of geotechnical mapping. Mapping of the pit slopes had been conducted bench-by-bench since stripping commenced and represented a significant and useful information database
- Specific analysis of problematic footwall shales. This analysis was predominantly kinematic to determine the likely severity and scale of planer instabilities
- Variation in slope angle recommendations depending on lithology and favourability/unfavourability of tectonic structures. Previous universal 45° slope recommendations became litho-specific and varied between 32° and 51°, depending on the above factors.

Further developments up to 2015

Information from the 2012 pit optimization was incorporated into a FLAC3D analysis of the pit in order to ensure that modifications, newly proposed in 2014, did not adversely affect pit slope stability. These modifications consisted of:

➤ Minor changes to the geometric configuration of the dumps near the northern perimeter of the pit
➤ Geometric modifications of the pit required for ore extraction near problematic footwall shales in the southern areas of the pit.

Figures 23 and 24 show the configuration of the block model for the FLAC3D analysis of the north and south pit areas.

Key elements of the design were:

➤ Alignment of coordinate system with the geological block model for future data re-incorporation
➤ Division of analysis into distinct zones (southern and northern aspects) to reduce demand on processing power and speed up the analysis
➤ Reduction of analysis block size with 10 m × 10 m blocks in the pit. Enlargement of block size with distance from pit. This block size corresponds better to the individual bench sizes, allowing an evaluation of individual bench/berm stability. This block size was considered a sensible medium, given that the alternative, a 5 m × 5 m, block size, would have required greater computer processing power and longer time
➤ Remapping of piezometric data up to 2014 to improve hydromechanical coupling calibration
➤ Analysis of individual phases of the pit within FLAC3D to arrive at final pit configuration.

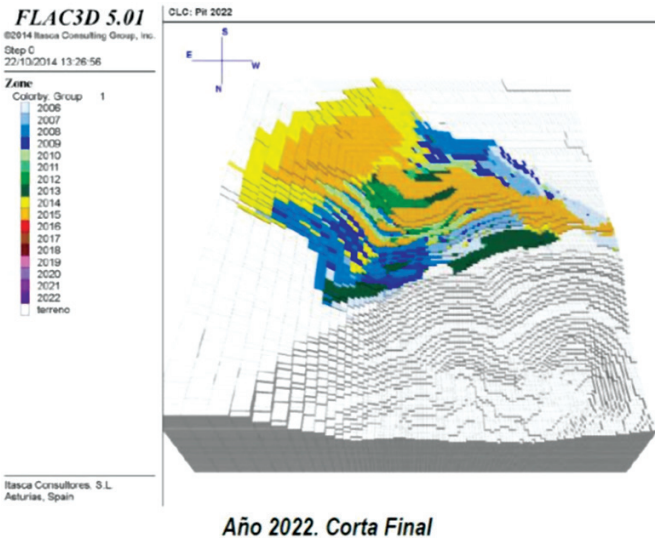

Figure 23—South side analysis in FLAC3D (Cooper *et al.*, 2014). The colours indicate the year-on-year increases in southern perimetral dump height assumed in analysis. Reduction in block size can also be observed within the pit where the analysis required higher block resolution

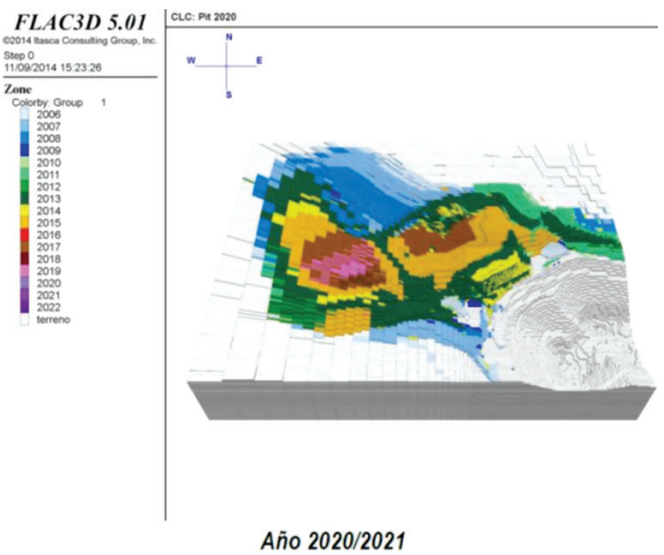

Figure 24—Northern pit slope analysis in FLAC3D (Cooper *et al.*, 2014). Again, block colours represent yearly increase in heights (in this case associated with tipping activities within the north dump tailings facility)

Stability considerations for slopes excavated in fine hard soils/soft rocks

Given the amount of work undertaken between the re-characterization and optimization process and the subsequent FLAC3D analysis, a method was needed for effectively communicating these changes to the mining team for ease of practical adoption during mine development. This was achieved with the mine operations visualization software VULCAN, enabling easy visualization of the various distinct geotechnical zones. Figures 25 and 26 show screenshots of the information placed in VULCAN, with two key aspects highlighted:

- Block modelling containing lithology and rock quality rating. The incorporation of both lithotype and rock quality rating (the Bieniawski RMR rock classification system) was considered useful for planning purposes when undertaking proposed pit configuration modifications
- Refinement of the 10 m × 10 m grid to 5 m × 5 m sub-blocks utilizing VULCAN interpolation software subroutines. The use of the interpolation tools built into the VULCAN software allowed an effective increase in resolution of the available information, which again was useful for pit configuration modification, given the use of 10 m benches.

Excavation optimization

During the various stages of excavation, operational activities were optimized in an attempt to best preserve the slope conditions. Highlighted among these are:

- A reduction in bench height from 20 m to 10 m. This was implemented early in the mine life, after attempts to achieve stable 20 m bench heights, stipulated in design, resulted in berm loss. This swift action to reduce bench heights to 10 m immediately improved stability, especially in the initial, highly weathered and less competent upper marls. However, the improved stability needed to be balanced against an associated reduction in the safety berm widths
- Rendering the benches impermeable utilizing plastic and topsoil emplacement. Along with incorporation of a slight berm angle towards the pit in later years, this formed part of an effort to improve rainfall runoff from the benches and avoid this rainwater ingressing into the marls through fissures. Figure 27 shows an example of toppling which occurred on early slopes that were not rendered impermeable
- Improvement of blasting process, double benching in 5 m separate stages, significantly reducing the energy imparted to slopes
- Optimization of blasting patterns in the Palaeozoic, implementing a wall blast procedure with modified blast patterns to improve bench preservation and reduce slope rock fragmentation
- Slope smoothing and bench-to-bench knitting to reduce wall promontories (pit bullnoses) between phases.

Figure 28 shows an analysis of the energy distribution of a test blast, while in Figure 29 the improvements in bench and slope preservation using the described optimization can be clearly seen.

Conclusions

There is no single solution to achieve stable slopes in an open pit mine such as Las Cruces. Although any activity can entail potential risks, the mine operates with an ALARA (As Low As Reasonably Achievable) risk policy and an objective of zero harm. In order to achieve this objective, over the years sturdier and more refined designs have been implemented to determine where the predominant risks in the mine lie and to what extent. Aside from minor instabilities observed over the years (typically wedge failures associated with localized geological structures), we have provided two examples of instabilities observed during mining that necessitated further work (toppling in the upper marls and planar failures in the footwall shales). Once higher risk areas had been identified, critical vigilance systems were subsequently put in place to manage the risk appropriately and on occasion, localized pushbacks prescribed in order to achieve

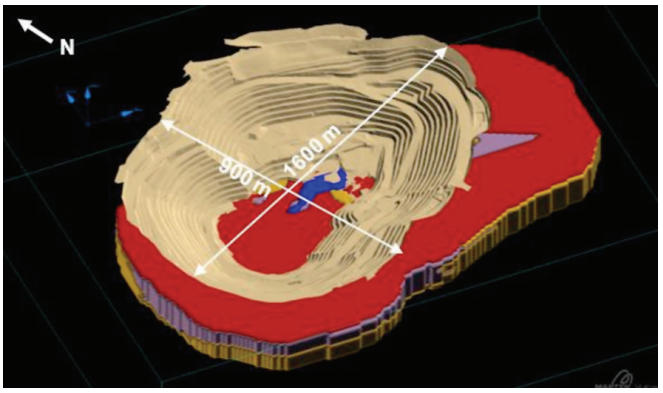

Figures 25—Screenshot from the VULCAN visualization program showing smoothed wireframes derived and interpolated from the geotechnical block model (lithological model)

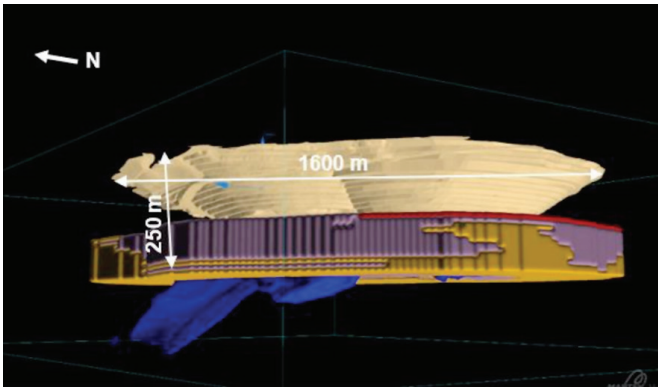

Figures 26—A screenshots from the VULCAN visualization program showing the extention of lithological wireframes at depth

Figure 27—Toppling in 2010 following heavy rains. The installation of topsoil and plastic sealing can be seen in the lower benches in the distance

Figure 28—Blast design simulation undertaken to ensure correct energy distribution (Rocha *et al*., 2015)

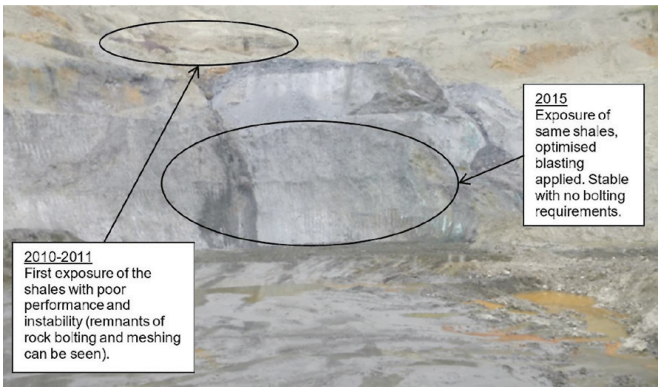

Figure 29—Result of lessons learnt during geotechnical optimization of blasting on the footwall shales

a slope geometry more appropriate to the ground conditions. In some circumstances, ore extraction has only been possible with heightened local analysis, instrumentation, and vigilance.

In addition, in the case of Las Cruces, early mine development occurred during a period where significant technical advances were being made in monitoring systems – in particular the development of direct slope scanning topographical systems, 3D photography as a cartography aid, and even more recently, the incorporation of high-definition (4K) drone photography, which facilitates visual evaluations of large pits. If the mine had commenced in 2015 rather than 2005, it is likely that most of these systems would have been used from the outset rather than as part of a continuous improvement methodology.

Nonetheless, is it not always possible economically, nor appropriate technically, to implement all vigilance measures at the start of mining operations. Any pit design and vigilance plan needs to develop hand-in-hand with the mine's evolution, increasing in its refinement in preparation for the mine's most precarious stages (usually, but not always when the mine is at its deepest configuration) and finally winding down, changing from new investment to ongoing maintenance later in the mine life, when closure and restoration beckons.

References

Alonso, E.E. and Gens, A. 2006. Aznalcóllar dam failure, part 1: field observations and material properties. *Géotechnique*, vol. 56, no. 3. pp. 165–183.

Burland, J.B. 1989. Small is beautiful -The stiffness of soils at small strains. *Canadian Geotechnical Journal*, vol. 26. pp. 499–516.

Chandler, R.J., Leroueil, S., and Trenter, N.A. 1990. Engineering in Mercia Mudstone. *Report* C570. CIRIA. London.

Cooper, S., Pérez, C., Vega, L., Galera, J.M., and Pozo, V. 2011. The role of bedding planes on the slope stability in Cobre Las Cruces open pit. *Proceedings of the International Symposium on Slope Stability in Open Pit Mining and Civil Engineering*, Vancouver, Canada, 18–21 September 2011. Eberhardt, E. and Stead, D. (eds). Canadian Rock Mechanics Association.

Cooper, S., Rodríguez M.D., Pozo, V., and Galera J.M. 2014. Advanced 3D geotechnical modeling of Las Cruces Open pit.. *Proceedings of the 2013 ISRM European Rock Mechanics Symposium (EUROCK 2014)*, Vigo, Spain, 27–29 May 2014. International Society for Rock Mechanics and Rock Engineering, Lisbon, Portugal.

Dindarloo, S.R. 2015. Peak particle velocity prediction using support vector machines: a surface blasting case study. *Journal of the Southern African Institute of Mining and Metallurgy*, vol.115. pp. 637–643.

Galera, J.M., Álvarez, M., and Bieniawski, Z.T. 2006. Evaluation of the deformation modulus of rock mass using RMR. Comparison with dilatometer tests. *Proceedings of the ISRM Workshop W1, Underground Works under Special Conditions*. International Society for Rock Mechanics and Rock Engineering, Lisbon, Portigal. pp. 71–77.

Galera, J.M., Montero, J., Pérez, C., Vega, L., and Varona, P. 2009a. Coupled hydromechanical analysis of Cobre Las Cruces Open Pit. *Proceedings of the International Symposium on Slope Stability in Open Pit Mining and Civil Engineering*, Santiago, Chile. Gecamin Ltda. http://subterra-ing.com/wp-content/uploads/2012/10/2009.-Coupled-hydromechanical-analysis-of-Cobre-Las-Cruces-Open-Pit.pdf

Galera, J.M, Checa, M., Pérez, and C., and Pozo, V. 2009b. Enhanced characterization of a soft marl formation using in situ and lab tests, for the prestripping phase of Cobre Las Cruces open pit mine. *Proceedings of the International Symposium on Slope Stability in Open Pit Mining and Civil Engineering*, Santiago, Chile. Gecamin Ltda. http://subterra-ing.com/wp-content/uploads/2012/10/2009.-Characterization-of-soft-marl-formation-using-in-situ-lab-test-Cobre-las-Cruces-pit-mine.pdf

Gens, A. and Alonso, E.E. 2006. Aznalcóllar dam failure. Part 2: Stability conditions and failure. *Géotechnique*, vol. 56, no. 3. pp. 185–201.

Gens, A. and Alonso, E.E. 2006. Aznalcóllar dam failure. Part 3: Dynamics of the motion. *Géotechnique*, vol. 56, no. 3. pp. 203–210.

Hoek, E. and Karzulovic, A. 2000. Rock mass properties for surface mines. *Slope Stability in Surface Mining*. Hustralid, W.A., McCarter, M.K., and van Zyl, D.J.A. (eds.). Society for Mining, Metallurgy and Exploration, Littleton, CO. pp. 59–70.

Hoek, E., Carranza-Torres, C., and Corkum, B. 2002. Hoek-Brown failure criterion - 2002 edition. *Proceedings of the Fifth North American Rock Mechanics Symposium*, Toronto, Canada. Vol. 1. American Rock Mechanics Association, Alexandria, VA. pp. 267–73.

Hoek, E. and Diederichs, M.S. 2006. Empirical estimation of rock mass modulus. *International Journal of Rock Mechanics & Mining Sciences*, vol. 43. pp. 203–215.

Hoek, E. 2012. Blast Damage Factor D. *Technical note. RocNews*, 2 February 2012. Winter 2012.

Kalamaras, G.S and Bieniawski, Z.T. 1995. A rock mass strength concept incorporating the effect of time. *Proceedings of 8th ISRM Congress*, Tokyo. Japan, 25-29 September 1995. Balkema. pp. 295–302.

Rocha, M., Carrasco, I., Castilla, J., Cooper, S., and Rodríguez, M.D. 2012. Wall control by blasting optimization at Las Cruces open pit copper mine (Spain). *FRAGBLAST 10. Proceedings of the 10th International Symposium on Rock Fragmentation by Blasting*. New Delhi, India, 26-29 November, 2012. Sing, P.K. and Sinha, A. (eds). CRC Press, Leiden, The Netherlands. pp. 715–724.

Shen, J., Karakus, M., and Xu, C. 2013. Chart-based slope stability assessment using the Generalized Hoek–Brown criterion. *International Journal of Rock Mechanics and Mining Sciences*, vol. 64. pp. 210–219.

Skempton, A.W. 1954. The pore pressure coefficients A and B. *Géotechnique*, vol. 4, no. 4. pp. 143–147.

Sönmez, H. and Ulusay, R. 2002. Discussion on the Hoek-Brown failure criterion and suggested modifications to the criterion verified by slope stability case studies. *Bulletin of Earth Sciences*. Application and Research Centre of Hacettepe University. *Yerbilimleri*. vol. 26. pp. 77–99.

Spain. 2002. Royal Decree 997/2002, Norma de Construcción Sismorresistente: Parte General y de Edificación (NCSE-02). Ministerio de Fomento. (Spanish Seismic Legislation). 27 September 2002.

Spain. 1985. Royal Decree 863/1985. Reglamento General de Normas Básicas de Seguridad Minera. (Boletín oficial del estado, número 140, de 12- 06- 1985). (Spanish Mining Legislation). 2 April 1985.

Terzaghi, K. and Peck, R.B. 1948. Soil Mechanics in Engineering Practice. Wiley, New York.

Tsige, M. 1999. Microfábrica y mineralogía de las arcillas azules del Guadalquivir y su relación con las propiedades geotécnicas. *Monografía 67*. Ministerio de Fomento, CEDEX, Madrid, Spain. ◆

SIGRA ESTABLISHES IN AFRICA

WWW.SIGRA.CO.ZA

Sigra is a 25 year old Australian company that operates in the areas of civil, mining and petroleum geomechanics. It also deals with fluids in the ground. Using each industry's jargon this range of work includes geotechnical engineering, rock mechanics, strata control, hydrogeology and reservoir engineering. The fluids may be water or hydrocarbon liquids, especially gasses. This cross disciplinary exposure has brought many benefits to our clients' operations.

To do this work Sigra has built up a suite of field and laboratory tools. These are backed by analysis techniques and software. Many items of the equipment and techniques it uses have been developed in house. These have been built to do something far better than anything available commercially or taken from a standard.

Sigra works in several modes. It can simply provide a measurement service, such as that for rock stress, or it can undertake total exploration and mine design operations. Sigra designs longwall coal mines. It has also been involved in the exploration and design of metalliferous mines, civil tunnels, hydroelectric power projects and gas fields. In all of these processes Sigra is prepared to bring the benefits of innovation to our clients.

The essence of what Sigra does is founded on establishing a sound understanding of the geology. This is backed by good measurement of the field parameters which typically include, rock stress, fluid pressure, permeability and fluid type. In the laboratory Sigra measures a suite of parameters including rock moduli, poroelastic behaviour, strength gas content and gas adsorption behaviour. This is then followed by a capability to design whatever is required. Sigra also has a strong instrumentation capability that enables it to measure what happens in the ground after construction or during mining. This can be applied to deformation measurement around underground openings or to pressure decline in gas reservoirs.

Another one of Sigra's strengths is a good knowledge of drilling, including directional drilling. This has uses in collecting samples, draining fluids or placing services.

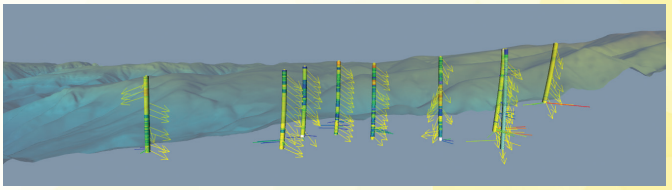

EXAMPLES OF SOME OF SIGRA'S PROJECTS ARE:

Multi-seam longwall exploration and design at Moura in Central Queensland for Vale. This work involved drilling, geology, rock mechanics and gas characterisation. This was followed by a total mine design.

Site investigation for a 1000 m deep pumped storage power station in New South Wales as part of the Snowy 2.0 project for Snowy Hydro. This involved stress measurement, structural geological assessment, groundwater measurement (using drill stem test techniques derived from the petroleum industry) and rock property determination.

Stress measurement operations using Sigra's proprietary IST overcore tool for:

Lucara's Letlhakane diamond mine in Botswana

Sydney Metro Rail developments

Rio Tinto's Jadar lithium project in Serbia

LKAB's iron ore mine in Sweden

Anglo American's coal mines in Queensland

Debswana's Jwaneng mine in Bostwana

Rockburst and outburst research – major research projects commissioned by the Australian Coal Industry Research Program to provide solutions for that industry.

Sigra

The effects of froth depth and impeller speed on gas dispersion properties and metallurgical performance of an industrial self-aerated flotation machine

H. Naghavi[1], A. Dehghani[1], and M. Karimi[2]

Affiliation:
[1]Mining and Metallurgical Engineering Department, Yazd University, Yazd, Iran.
[2]Department of Chemistry and Chemical Engineering, Chalmers University of Technology, Sweden.

Correspondence to:
H. Naghavi

Email:
h.naghavi@stu.yazd.ac.ir

Dates:
Received: 28 Jul. 2018
Revised: 19 Dec. 2018
Accepted: 15 Feb. 2019
Published: July 2019

How to cite:
Naghavi, H., Dehghani, A., and Karimi, M.
The effects of froth depth and impeller speed on gas dispersion properties and metallurgical performance of an industrial self-aerated flotation machine.
The Southern African Insitute of Mining and Metallurgy

DOI ID:
http://dx.doi.org/10.17159/2411-9717/244/2019

ORCiD ID:
H. Naghavi
https://orchid.org/0000-0003-4979-5249

Synopsis

In self-aerated flotation machines, the gas rate depends on operational variables (*e.g.* froth depth and impeller speed), pulp properties (*e.g.* solid content and viscosity), and reagent addition (*e.g.* type and concentration of frother). The gas rate has a strong correlation with the flotation performance by influencing the gas dispersion properties and froth retention time. A factorial experimental design was used to study how the gas dispersion properties, the froth retention time, and the flotation performance respond to changes in froth depth and impeller speed (as the most common operational variables). An in-depth understanding of the effects of impeller speed and froth depth on the gas dispersion properties, especially the bubble surface area flux and froth retention time, is necessary to improve operating strategies for self-aerated flotation machines. All experiments were carried out in a 50 m³ self-aerated flotation cell in an iron ore processing plant. The results showed that the froth depth affected the metallurgical performance mostly via changing the froth retention time. The impeller speed had two important impacts on the metallurgical performance via varying both the froth retention time and the bubble surface area flux in the froth and pulp zones, respectively. The interaction effects of the froth depth and impeller speed were also established. This allowed us to develop a strategy for operating self-aerated flotation machines based on varying the froth depth and impeller speed with regard to the cell duty.

Keywords
self-aerated flotation machine, gas dispersion properties, metallurgical performance, impeller speed, froth depth.

Introduction

A mechanical flotation machine may be divided into two distinct zones. namely the pulp zone and the froth zone (Goodall and O'Connor, 1989; Yianatos, Bergh, and Cortes, 1998; Rahman, Ata, and Jameson, 2015a, 2015b). The overall flotation recovery, R_o, including the true flotation (particles attached to the bubble lamellae) and entrainment (particles recovered in water held in the bubble plateau boundaries), is a function of the recoveries in the two zones. It is calculated as follows (Dobby, 1984):

$$R_O = \frac{R_c R_f}{1 - R_c(1 - R_f)} \quad [1]$$

where R_c and R_f are the pulp and froth recoveries, respectively.

A schematic diagram of the pulp and froth recoveries is shown in Figure 1.

Equation [1] shows that neglecting the recovery in each zone can adversely affect the overall recovery. The froth recovery is primarily a function of the particle residence time in the froth zone (*i.e.*, froth retention time), such that increasing the froth retention time decreases the froth recovery (Mathe *et al.*, 1998). The froth retention time, τ_f, can be expressed as follows:

$$\tau_f = \frac{h.\varepsilon_f}{J_g} \quad [2]$$

where $h.\ \varepsilon_f$, and J_g are froth depth, gas holdup in the froth phase, and superficial gas velocity, respectively (Zheng, Franzidis, and Manlapig, 2004). If the liquid/solids holdup in the froth is negligible (*i.e.*, $\varepsilon_f = 1$), then Equation [2] can be simplified to:

$$\tau_f = \frac{h}{J_g} \quad [3]$$

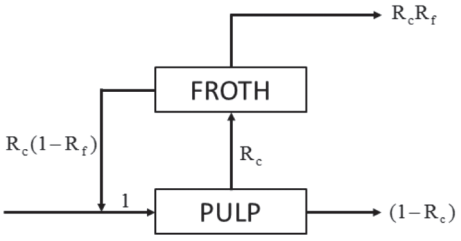

Figure 1—Schematic representation of recovery model for pulp and froth zones (Mathe *et al*., 1998)

where J_g is defined as the volumetric flow rate of air entering the cell (Q_g) divided by the cell cross-sectional area at the pulp-froth interface level (A) (Gorain, Franzidis, and Manlapig, 1997):

$$J_g = \frac{Q_g}{A} \quad [4]$$

The pulp recovery depends on a wide range of complex factors. For instance, the hydrodynamic conditions of a flotation cell are known to directly affect the flotation efficiency. Hydrodynamic parameters, especially gas dispersion properties, are responsible for controlling the particle-bubble contact as an essential part of the flotation process (Schubert and Bischofberger, 1978; Gorain, Franzidis, and Manlapig, 1995a, 1995b). The gas dispersion properties indicate the efficiency of the distribution of air bubbles across the cell volume (Schwarz and Alexander, 2006; Vinnett, Yianatos, and Alvarez, 2014). The bubble surface area flux, S_b, is an efficient measure of the hydrodynamic conditions in a flotation cell, certainly as far as gas dispersion properties are concerned (Gorain, Franzidis, and Manlapig, 1997). The bubble surface area flux is defined as a measure of bubble surface area rate rising through the cell per unit cross-sectional area. It can be described mathematically by Equation [5] (Gorain, Franzidis, and Manlapig, 1997):

$$S_b = 6\frac{J_g}{d_{32}} \quad [5]$$

where d_{32} represents the Sauter mean bubble diameter.

The bubble surface area flux has a strong correlation with the overall flotation rate constant, k, as shown in Equation [6] (Gorain, Franzidis, and Manlapig, 1999):

$$k = P.S_b.R_f \quad [6]$$

where P represents the ore floatability.

This equation implies that the greater the available surface area of bubbles, the greater the chance of particle-bubble contact in the pulp phase. Therefore, it results in a higher flotation rate constant (Gorain, Franzidis, and Manlapig, 1999).

In the flotation process, the gas rate is a key variable which provides the gas surface area required for selective transport of mineral particles (Yianatos, Contreras, and Diaz, 2010). This variable has a positive impact on recoveries of the pulp and froth zones by varying the gas dispersion properties and froth retention time, respectively (Vera, Franzidis, and Manlapig, 1999; Rahman, Ata, and Jameson, 2015a).

In self-aerated flotation machines, the gas rate depends on the pulp properties (*e.g.* viscosity and solid content), the chemical variables (*e.g.* type and concentration of frother), and the operational variables (*e.g.* froth depth and impeller speed) (Yianatos *et al.*, 2001; Girgin *et al.*, 2006). For example, it is increased by increasing the froth depth and the impeller speed. Increasing the impeller speed increases suction, whereas increasing the froth depth reduces back-pressure at the point of gas injection (Girgin *et al.*, 2006). It is obvious that manipulation of the gas rate in self-aerated flotation machines is more complicated than the in forced-aerated flotation machines in which the gas rate is an independent variable.

Froth depth and impeller speed are the most common operational variables in flotation plants and control of them is significant for adjusting the gas rate and improving the flotation performance (Venkatesan, Harris, and Greyling, 2014). Extensive work is reported in the literature on the study of operational variables. These studies generally showed that in pilot and industrial forced-aerated flotation machines, the impeller speed and gas rate have a distinct impact on the bubble size. The bubble size is decreased with increasing impeller speed, and increased with increasing gas rate (Gorain, Franzidis, and Manlapig, 1995a, 1995b; Grau and Heiskanen, 2005; Grau, Nousiainen, and Yanez, 2014). It was found that increasing the impeller speed generally has a positive effect on the rate of flotation, accompanied by a significant decrease in the concentrate grade. This decrease may be due to increases in entrainment or in the rate of flotation of poorly liberated (low grade) particles or floatable gangue (Gorain, Franzidis, and Manlapig, 1997; Deglon, 2005).

Also, it is suggested that the recovery and plant capacity could be increased by manipulating the froth depth and the gas rate, *i.e.* at a low froth depth and high gas rate, although the concentrate grade could be decreased (Vera, Franzidis, and Manlapig, 1999; Zheng, Johnson, and Franzidis, 2006; Ata and Jameson, 2013; Seguel *et al.*, 2015). Venkatesan, Harris, and Greyling (2014) found a significant interaction effect between gas rate and froth depth, highlighting the importance of testing these factors one at a time in any optimization work.

In recent years, with the growth of flotation control systems, the metallurgical targets of a flotation bank are automatically controlled by manipulating the froth depth, gas rate, and frother dosage, with regard to the monitoring concentrate and tailing grades (Yianatos, Henriquez, and Oroz 2006; Venkatesan, Harris, and Greyling, 2014). Also, the impact of 'gas management' in flotation banks is shown by a number of researchers, in which the gas rate profiling can affect the performance of a flotation bank significantly (Cooper *et al.*, 2004; Hernandez-Aguilar and Reddick, 2007; Smith, Neethling, and Cilliers, 2008; Hadler and Cilliers, 2009; Fournier *et al.*, 2015).

In the published literature, the importance of operational variables such as gas rate, froth depth, and impeller speed in determining the flotation performance has become increasingly recognized. However, the problem at the time is lack of technical and practical details. The effect of operational variables such as impeller speed and froth depth on the gas dispersion properties and froth retention time should be understood. This is a critical requirement for adjusting the gas rate and optimizing the operation in industrial self-aerated flotation cells. For example, it is unclear what happens to the froth retention time as the froth depth increases, because the gas rate and froth depth increase simultaneously while they have a reverse effect and a direct effect on the froth retention time, respectively.

The purpose of this paper is to investigate on the one hand the effects of impeller speed and froth depth on gas

dispersion properties and froth retention time, and on the other hand to study the relationship between these parameters and metallurgical performance with the aim of understanding how froth depth and impeller speed affect metallurgical efficiency. This allows us to develop an operating strategy based on the cell duty (*e.g.* rougher or cleaner) by use of only operational variables.

Materials and methods

Experimental

Industrial-scale experiments were carried out in a 50 m^3 self-aerated flotation cell the first cell of the desulphurization flotation bank of the Gol Gohar iron ore processing plant in Sirjan, Iran.

A central composite design (CCD) was used to investigate the effects of impeller speed and froth depth on the process responses (*i.e.*, the gas dispersion parameters, the froth retention time, and the metallurgical efficiency). The CCD is a factorial type of experimental design which enables the investigation of the effects of multiple variables simultaneously. The CCD design has the added benefit of requiring fewer experimental runs (Venkatesan, Harris, and Greyling, 2014).

The CCD experiments included 4-factorial, 4-centres, and 4-axial runs. The variable levels are given in Table I. The impeller speed is shown in revolutions per minute (r/min) (and as a percentage of the maximum speed) and the froth depth is shown in centimetres (and as a percentage of the maximum froth depth).

The flotation cell was operated for 20 minutes after changing the operational variables, including the impeller speed and the froth depth. This time is equivalent to three times the pulp residence time that ensures a steady-state operation. The gas dispersion measurements were then carried out along with sampling of the feed, concentrate, and tailings streams. The experiments were conducted based on CCD design and the results were analysed by Design-Expert software version 10.0.6.

Gas dispersion measurements

The gas dispersion properties are usually expressed in terms of superficial gas velocity, bubble size, gas holdup, and bubble surface area flux (Finch *et al.*, 2000; Vinnett, Yianatos, and Alvarez, 2014). The superficial gas velocity and the bubble size were measured in order to calculate the bubble surface area flux and the froth retention time.

Superficial gas velocity, J_g, is a measure of aeration ability (Gorain, Franzidis, and Manlapig, 1997). In order to measure J_g, a probe similar to those used by Gorain, Franzidis, and Manlapig (1996) and Power, Franzidis, and Manlapig (2000) was used. It consisted of a transparent tube with a pneumatic pinch valve at the bottom, and the other end was closed. The probe was completely filled with water, and placed in a proper position in the cell. The pinch valve was then opened to allow the air bubbles to move up the probe and displace the water. By measuring the water discharge time, T_d, between two points at distance L, the superficial gas velocity was calculated as:

$$J_g = \frac{L}{T_d} \quad [7]$$

Figure 2 shows the steps to measure superficial gas velocity by J_g probe.

The bubble size was measured using a bubble size analyser based on the design of Gomez and Finch (2007). Figure 3 shows a schematic of the bubble size analyser.

The device included a sampling tube connected to a sloped viewing chamber with rear illumination. The sloped view helps provide an approximately single plane of bubbles. The images of the bubble population were taken by a digital camera and analysed using ImageJ software version 1.50. A typical image of bubbles is shown in Figure 4. Each measurement was conducted at least twice and on average over 5000 bubbles were sized on each run.

The mean bubble diameter adopted was the Sauter mean bubble diameter, d_{32}. The d_{32} represents the size of a bubble with the same ratio of volume to surface as the total distribution, and is calculated as follows (Gorain, Franzidis, and Manlapig, 1997):

$$d_{32} = \frac{\sum_{i=1}^{n} d_i^3}{\sum_{i=1}^{n} d_i^2} \quad [8]$$

Table I

Selected parameters for CCD experimental design; actual and coded levels

Variables x	High axial level (+2)	High factorial level (+1)	Medium level (0)	Low factorial level (-1)	Low axial level (-2)
Impeller speed, r/min (%) Froth depth, cm (%)	179 (100%) 41 (55%)	170 (95%) 38 (51%)	152 (85%) 30 (43%)	134 (75%) 22 (34%)	125 (70%) 19 (30%)

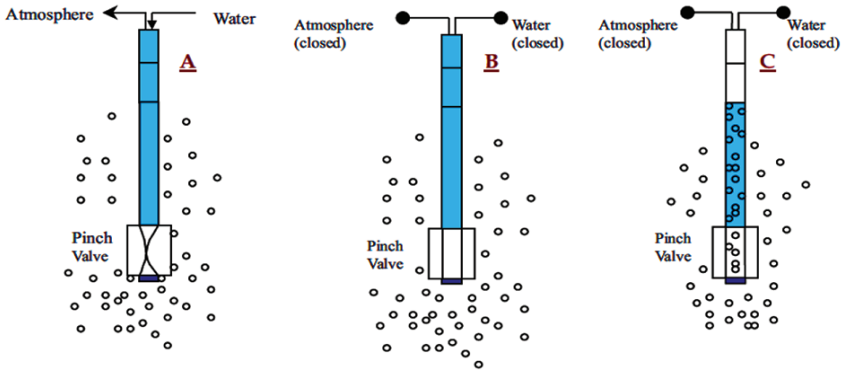

Figure 2—A schematic of steps to measure superficial gas velocity by J_g probe (Power, Franzidis, and Manlapig, 2000)

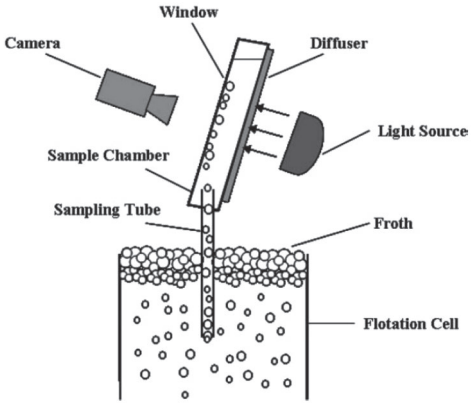

Figure 3—A schematic of the bubble size analyser (Girgin *et al.*, 2006)

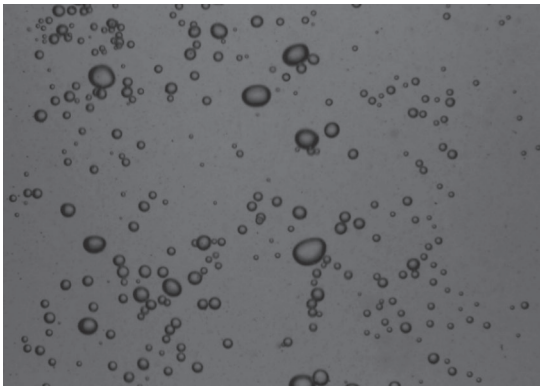

Figure 4—Image captured with the bubble size analyser device

where d_i is diameter of the bubble and n is total number of bubbles.

Similarly to the work of Gomez and Finch (2007) and Vinnett, Yianatos, and Alvarez (2014), the gas dispersion parameters were measured at the same position for all the tests, halfway between the cell wall and the froth crowder and just below the pulp-froth interface. In order to generate reliable measurements of J_g and d_{32}, multiple readings were averaged. The froth retention time and the bubble surface area flux were then calculated according to Equations [3] and [5], respectively.

Sampling for metallurgical evaluation

All experiments were carried out in two consecutive working shifts to limit the feed grade variations, while the feed rate, solid content, and chemical reagent dosages were kept constant. The enrichment ratio (Equation [9]) and the concentrate mass recovery (Equation [10], were used as the metallurgical parameters. This was similar to the work of Yianatos *et al.* (2001), who used these parameters for industrial rougher cell characterizations.

$$\text{Enrichment ratio} = \frac{c}{f} \qquad [9]$$

$$\text{Concentrate mass recovery} = 100\frac{f-t}{c-t} \qquad [10]$$

where t, c, and f are the grades of the tails, concentrate, and feed, respectively.

Samples of feed, concentrate, and tailings were taken at each operating condition and subjected to chemical analysis for sulphur content.

Results and discussion

Effect of froth depth and impeller speed on gas dispersion properties

Superficial gas velocity

Figure 5 shows that the superficial gas velocity, J_g, increased with increasing froth depth and impeller speed. The mechanism of impeller speed is simple, as it can be shown that the air suction increases with increasing impeller speed, and according to Equation [4], as a result the superficial gas velocity is also increased.

The flotation cell was provided with a froth crowder, with the shape of an inverted cone, to accelerate the froth discharge to the concentrate overflow. It had about 45 degrees of slope and it made the cell cross-sectional area at the pulp–froth interface level change by varying the froth depth. Therefore, it was impossible to predict the change in J_g with the froth depth variations, due to the simultaneous changes in gas rate and cross-sectional area at the pulp-froth interface level. The results show that the superficial gas velocity increases with increasing froth depth (Figure 5), indicating a dominant effect of the gas rate on J_g.

It can also be seen from Figure 5 that there is a dominant effect of impeller speed on J_g. It is clear that manipulating the froth depth is not a feasible option to improve J_g, because increasing the froth depth increases the cross-sectional area at the pulp-froth interface level, which then affects the J_g, inversely.

Bubble size

The Sauter mean bubble diameter, d_{32}, increases with increasing impeller speed and froth depth (Figure 6) due to the direct relationship between the superficial gas velocity and the Sauter mean bubble diameter (Gorain, Franzidis, and Manlapig, 1995a, 1995b; Nesset *et al.*, 2006; Grau, Nousiainen, and Yanez, 2014; Vinnett, Yianatos, and Alvarez, 2014).

Note that the effect of impeller speed on the bubble size might appear contradictory. In forced-air flotation machine, increasing the impeller speed decreases d_{32}, due to the increased shear

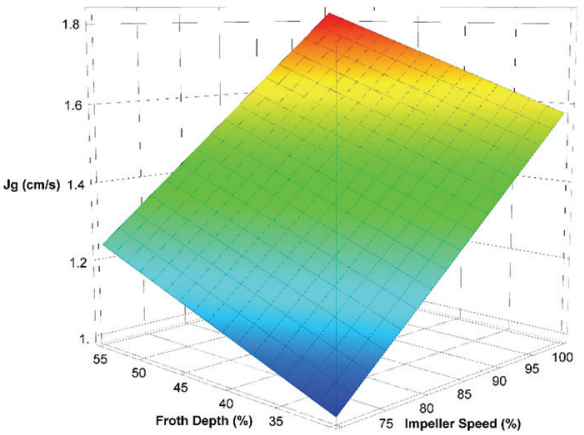

Figure 5—Effects of impeller speed and froth depth on the superficial gas velocity

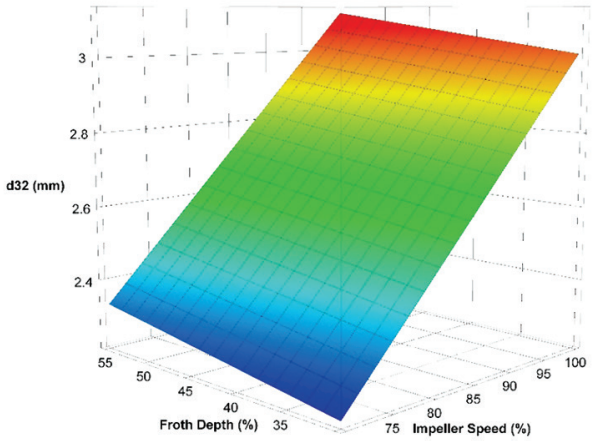

Figure 6—Effects of impeller speed and froth depth on the Sauter mean bubbles size

force (Gorain, Franzidis, and Manlapig, 1995a, 1995b; Grau and Heiskanen, 2005; Grau, Nousiainen, and Yanez, 2014). However, Nesset, Zhang, and Finch (2012) found that the impeller speed did not significantly impact the bubble size over a wide operating range of impeller speeds. On the other hand, in a self-aerated flotation machine, as Girgin *et al.* (2006) stated, increasing the impeller speed improves the bubble size, due to the increased gas rate. Their study was conducted in a laboratory-scale machine and in a two-phase system. The results obtained were confirmed in an industrial-scale flotation machine where three phases were present. It seems that in a self-aerated flotation machine, gas rate is more pronounced than the added shear, which results in a larger d_{32}.

The measured bubble sizes, as shown in Figure 6, are slightly larger than the common range in industrial flotation cells. The main reason is that the frother concentration was low in the operating cell.

Bubble surface area flux

As can be seen from Figure 7, the maximum bubble surface area flux, S_b, is obtained at the deepest froth depth and the highest impeller speed. As shown earlier, the impeller speed had a predominant effect on J_g and d_{32}, while Figure 6 shows that froth depth has a predominant effect on S_b. This means that the same S_b values can be obtained from different combinations of J_g and d_{32}, as was observed by Vinnett, Yianatos, and Alvarez (2014).

Furthermore, as shown in Figures 5, 6, and 7, increasing the impeller speed or froth depth increased J_g, d_{32} and S_b simultaneously. This means that there is a dominant effect of J_g on S_b. This finding implies that increasing the impeller speed and the froth depth could increase the overall flotation rate constant, due to the increased S_b (see Equation [6]). This is investigated in the next sections.

Effects of froth depth and impeller speed on the froth retention time

In each experiment, based on adjusted froth depth and measured J_g, the froth retention time, τ_f, was calculated. The effect of impeller speed on the froth retention time is shown on Figure 8. The froth retention time decreased with increasing impeller speed, due to the increased gas rate. On the other hand, despite the increased gas rate with increasing froth depth, the froth retention time increased, which indicated a major effect of froth depth in determining τ_f (see Equation [3]). This means that the superficial gas velocity variations, as a result of froth depth changing, have a less significant effect on the froth retention time.

Metallurgical performance evaluation

The metallurgical performance of the flotation cell was evaluated under various predetermined conditions of froth depth and impeller speed by using the enrichment ratio and the concentrate mass recovery, which indicate the flotation selectivity and flotation rate, respectively. The results show that the enrichment ratio is decreased with increasing impeller speed or decreasing froth depth, as can be seen from Figure 9, whereas the concentrate mass recovery is increased.

As can be seen from Figures 7, 8, and 9, the impeller speed and the froth depth affect the metallurgical performance by varying the froth retention time and the bubble surface area flux. This is discussed in detail below.

Effect of froth retention time

As can be seen from Figures 8 and 9a, the enrichment ratio increases with increasing froth depth and froth retention time. Deeper froths are generally associated with higher concentrate

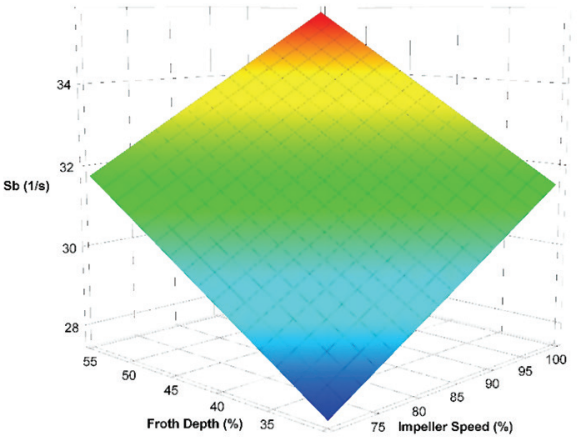

Figure 7—Effects of impeller speed and froth depth on the bubble surface area flux

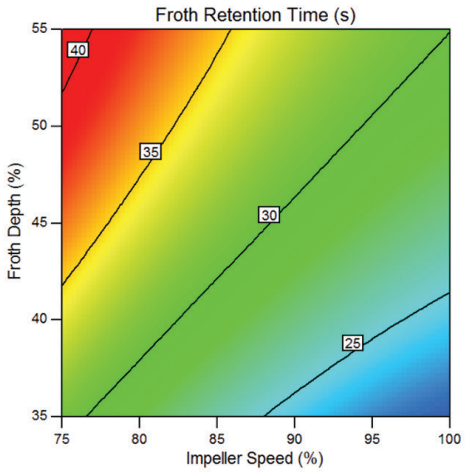

Figure 8—Effects of impeller speed and froth depth on the froth retention time

The effects of froth depth and impeller speed on gas dispersion properties

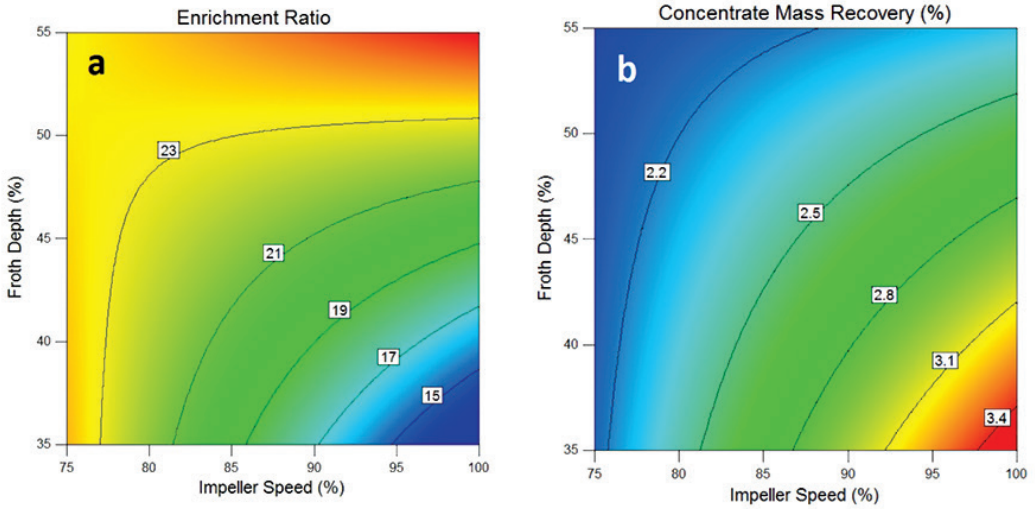

Figure 9—Effects of impeller speed and froth depth on the enrichment ratio (a) and the concentrate mass recovery (b)

grades, since deeper froths allow longer froth retention times, resulting in more time for coalescence of bubbles and drainage of unattached material, including entrained gangue or low-grade particles (Hadler *et al.*, 2012).

Bubble coalescence is one of the important froth phenomena that cause particle detachment in the froth zone (Ata, 2012), and drainage is also helpful to increase the quality of the final concentrate by rejecting the entrained hydrophilic fine particles to the pulp phase (Ata, Ahmed, and Jameson, 2004; Zheng, Franzidis, and Johnson, 2006). On the other hand, if the rate of coalescence is reduced, as a result of decreased froth retention time, the number of particles being lost from the froth and returning to the pulp zone will also be reduced (Rahman, Ata, and Jamson, 2015a).

The froth retention time affects the overall flotation recovery, mainly *via* changes in the froth phase recovery (Mathe *et al.*, 1998). Thus, the recovery in the froth zone could be improved as a result of the minimization of bubble coalescence in this zone with decreasing froth depth or increasing impeller speed.

Effect of bubble surface area flux

The bubble surface area flux, S_b, has a strong correlation with flotation rate constant (Gorain, Franzidis, and Manlapig, 1997; Hernandez, Gomez, and Finch, 2003), while on the other hand it has an inverse relationship with concentrate grade (Nesset *et al.*, 2006). This is because the greater the surface area of bubbles, the greater the probabilities of bubble-particle collision and attachment (Gorain, Franzidis, and Manlapig, 1999; Rahman, Ata, and Jameson, 2015a; Tabosa *et al.*, 2016). This increases the flotation rate of particles with weak hydrophobicity (Rahman, Ata, and Jameson, 2015a), and as a result the concentrate mass recovery increases.

As previously shown in Figure 7, increasing both the impeller speed and froth depth improved bubble surface area flux, and according to Equation [6] it is expected that the overall flotation rate constant would increase with increasing impeller speed and froth depth.

As can be seen from Figure 9b, increasing impeller speed improves concentrate mass recovery, due to increased S_b and decreased τ_f. Although increasing the froth depth increases S_b, the concentrate mass recovery is decreased, due to the increased τ_f (see Figures 7 and 8). Therefore, it can be concluded that in self-aerated flotation machines, the froth depth affects the overall flotation recovery mostly *via* the froth retention time. In other words, the froth depth has an insignificant effect on the overall flotation recovery by improving the bubble surface area flux. Thus, it is suggested that the froth depth should never be used to improve gas dispersion properties, whereas the impeller speed had two important impacts on the metallurgical performance by influencing both froth retention time and bubble surface area flux in the froth and pulp zones, respectively.

It should be noted that the impeller speed also affects the metallurgical performance through other mechanisms. For example, increasing the impeller speed improves solid suspension and bubble-particle collision efficiency in the pulp zone, resulting in an increase in the overall flotation recovery. However, in this study just the gas dispersion properties and the froth retention time were investigated.

Interaction effects of operational variables

The interaction effects of froth depth and impeller speed are more important than their individual effects. For example, at a high froth depth, the impeller speed has no effect on the enrichment ratio and increases the concentrate mass recovery only slightly, as seen in Figure 10. At a low froth depth, increasing the impeller speed improves the concentrate mass recovery. This suggests that deeper froths, due to the increased froth retention time, have a great effect on metallurgical performance, while the impeller speed has only a small effect on the overall recovery.

At low froth depth (low froth retention time) the metallurgical efficiency is influenced by the cell hydrodynamic conditions, especially gas dispersion properties. In this case, the froth recovery is almost 100%, due to low froth retention time, and the pulp recovery plays a major role in determining the flotation performance. It is obvious that increasing the impeller speed improves the gas dispersion and solid suspension efficiencies, resulting in an increase in the transfer of valuable and middling particles and some fine gangue particles to the froth phase and, as a result, the overall flotation recovery increases.

On the other hand, at high froth depth (high froth retention time) the froth recovery plays a major role in determining the flotation performance. However, this does not mean that the

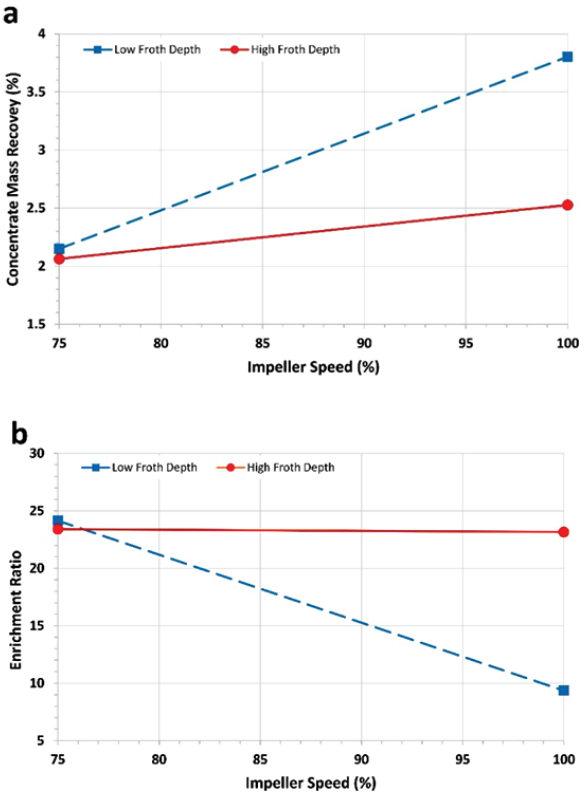

Figure 10—The interaction effects of impeller speed and froth depth on the concentrate mass recovery (a) and the enrichment ratio (b)

metallurgical performance is not influenced by the impeller speed. As Figure 10a shows, at high froth depth the concentrate mass recovery improves with increasing impeller speed. The main reason is that increasing the impeller speed increases the transfer of valuable and middling particles to the froth phase. Despite upgrading in the deep froth zone, the recovery of valuable particles increases, resulting in an improved concentrate mass recovery with no negative effect on enrichment ratio. Therefore, based on the results in Figure 10, it is suggested that with deeper froths, the impeller speed should be kept high to improve hydrodynamic conditions and, consequently, to maximize flotation performance.

Figure 11 shows the concentrate mass recovery against the enrichment ratio as a single curve. The overall trend is a decrease in enrichment ratio with increasing concentrate mass recovery. There are two areas of operating conditions. The upper part of the curve corresponds to a high impeller speed and a low froth depth, increasing the concentrate mass recovery. The lower part corresponds to deeper froths with a wide range of impeller speeds. This graph shows that by adjusting the operational variables alone, the metallurgical target can be achieved.

Operating strategies for self-aerated flotation machines

In this section a strategy for operating self-aerated flotation cell based on varying froth depth and impeller speed with regard to the cell duty, *e.g.* rougher, scavenger, or cleaner, is proposed. Depending on the type of ore being processed and the flotation duties, achieving a desirable recovery or high concentrate grade will be the main metallurgical target (Power, Franzidis, and Manlapig, 2000).

Rougher or scavenger duties

The main objective of rougher or scavenger flotation banks is to achieve maximum recovery at minimum acceptable concentrate grade (Yianatos, Henriquez, and Oroz, 2006). Thus, it is suggested that the flotation cell operates at low froth depth and high gas rate (Schwarz and Alexander, 2006; Hadler *et al.*, 2012; Rahman, Ata, and Jameson, 2015a). As previously mentioned, the low froth depth and the high gas rate decrease the froth retention time and improve the gas dispersion properties, which provides a maximum mass pull and high flotation recovery.

In a self-aerated flotation cell, it is impossible to achieve a low froth depth and high gas rate simultaneously by adjusting the froth depth alone, because decreasing the froth depth decreases the gas rate. Thus, it is necessary that the gas rate increases with increasing impeller speed. It is suggested that in rougher or scavenger duties, the impeller speed be increased to provide a high gas rate, then the froth depth decreases to provide the maximum recovery as the metallurgical target.

It should be noted that the impeller speed can be increased to a maximum allowable that prevents flooding conditions. Flooding conditions occurs at very high gas rates when the impeller is unable to disperse air properly, resulting in huge slugs of bubbles moving up near the shaft and giving a boiling appearance on the surface (Gorain, Franzidis, and Manlapig, 1999). This is undesirable as the flotation performance rapidly decreases. It has been found that coarser and denser particles need more turbulence to improve the collision rate and solid suspension efficiency (Rodrigues, Leal Filho, and Masini, 2001). Therefore, depending on the nature of flotation feed, including particle size and density, an optimum impeller speed and turbulence are required (Deglon, 2005).

Cleaner duty

Self-aerated flotation machines are commonly employed for rougher or scavenger duties (Shean and Cilliers, 2011). It is necessary to use a different operating strategy if they operate as cleaners in flotation banks.

The main objective of cleaner flotation banks is to achieve maximum concentrate grade at an acceptable recovery. Thus, it is suggested that the cleaner flotation cell operates at high froth depth and low gas rate to improve the froth retention time and upgrading in the froth zone (Cooper *et al.*, 2004; Schwarz and Alexander, 2006; Shean and Cilliers, 2011; Hadler *et al.*, 2012).

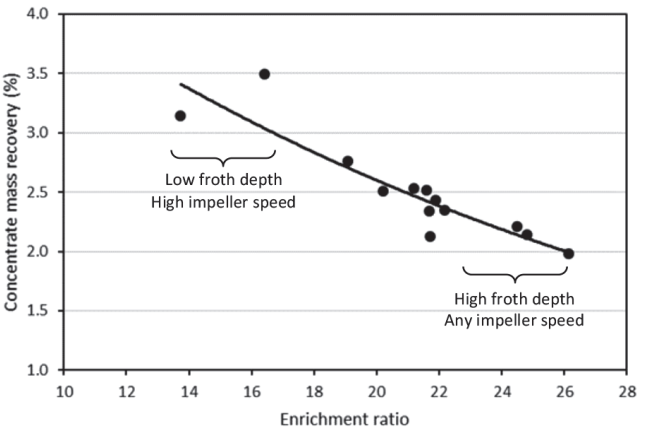

Figure 11—Concentrate mass recovery *versus* enrichment ratio

From a practical point of view, it is impossible to achieve a high froth depth and low gas rate simultaneously by adjusting the froth depth alone. Thus, it is necessary that the gas rate decreases with decreasing impeller speed. However, the impeller has some limitations related to minimum speed. The impeller is responsible for the gas dispersion, solid suspension, and bubble-particle collisions (Power, Franzidis, and Manlapig, 2000; Rodrigues, Leal Filho, and Masini, 2001; Deglon, 2005) and also, as mentioned earlier, flotation requires a certain degree of turbulence depending on the size and density of particles. Hence, an excessively reduced impeller speed causes a rapid decrease in metallurgical performance. It seems that in cleaner duty, decreasing the gas rate by changing the froth depth or impeller speed is a major issue.

With respect to the interaction effects between impeller speed and froth depth, in deeper froths, with increasing impeller speed, despite increasing the gas rate, there is no negative effect on enrichment ratio (see Figure 10b). Thus it is suggested that in cleaner flotation banks the cell be operated at high froth depth and high impeller speed. Although the high impeller speed provides a high gas rate and as a result increases the entrainment and the recovery of less hydrophobic particles to the froth phase, the high froth depth provides upgrading in the froth zone.

To achieve this, it is necessary to increase the impeller speed to a point where flooding conditions are prevented, then the froth depth should be increased to a point such that the amount of froth overflow product is acceptable and the target concentrate grade is achieved.

It seems that the strategy of decreasing the gas rate for cleaner duty is applicable only to forced-air flotation machines, because the gas rate is an independent variable and can be decreased without decreasing the impeller speed. In self-aerated flotation machines, it is impossible to decrease the gas rate by varying the impeller speed with no negative effect on the efficiencies of solid suspension and gas dispersion.

Conclusions

The effects of froth depth and impeller speed on gas dispersion parameters, froth retention time, and metallurgical performance were investigated in an industrial self-aerated flotation machine. The following conclusions can be drawn from the results presented in this paper.

- There was a positive relationship between the operational variables (froth depth and impeller speed) and the gas dispersion parameters (superficial gas velocity, bubble size, and bubble surface area flux).
- Froth depth had a small effect on the superficial gas velocity, due to the simultaneous changes in the gas rate and cross-sectional area at the pulp-froth interface level. Therefore it is suggested that varying the froth depth is not a feasible option to improve superficial gas velocity.
- With increasing impeller speed and froth depth, despite an increase in the superficial gas velocity, J_g, and the Sauter bubble mean diameter, d_{32}, the bubble surface area flux, S_b, increased. This means that there was a dominant effect of J_g on S_b.
- Despite the increased gas rate with froth depth, the froth retention time, τ_f, was increased, which indicated a major effect of froth depth on τ_f. In other words, increased superficial gas velocity with froth depth had a less significant effect on the froth retention time.
- The froth depth affected the metallurgical performance mostly *via* changing the froth retention time. In that, the froth depth had an insignificant effect on the flotation performance by improving the bubble surface area flux. The impeller speed had two important effects on the metallurgical performance *via* varying both froth retention time and bubble surface area flux in the froth and pulp zones, respectively.
- There was an interaction effect between impeller speed and froth depth. It was found that at a low froth depth the impeller speed plays a major role in determining the flotation efficiency, due to increased gas dispersion efficiency, while at a high froth depth the metallurgical performance was influenced mainly by increased froth retention time.
- A strategy for operating self-aerated flotation machines based on varying froth depth and impeller speed with regard to the cell duty, *e.g.* rougher, scavenging, or cleaner, is as proposed. It is suggested that operating under high gas rate, by increasing impeller speed alone, is the best strategy for obtaining high metallurgical performance, because it prevents the reduction of solid suspension and gas dispersion efficiencies. Then, depending on the cell duty, the froth depth should be manipulated to achieve the metallurgical target.

Acknowledgements

The authors thank Gol Gohar Iron Mining Complex for their support and collaboration throughout the course of this research.

References

Ata, S. 2012. Phenomena in the froth phase of flotation - A review. *International Journal of Mineral Processing*, vol. 102–103. pp. 1–12.

Ata, S., Ahmed, N., and Jameson, G.J. 2004. The effect of hydrophobicity on the drainage of gangue minerals in flotation froths. *Minerals Engineering*, vol. 17, no. 7–8. pp. 897–901.

Ata, S. and Jameson, G.J. 2013. Recovery of coarse particles in the froth phase – A case study. *Minerals Engineering*, vol. 45. pp. 121–127.

Cooper, M., Scott, D., Dahlke, R., Finch, J.A., and Gomez, C.O. 2004. Impact of air distribution profile on banks in a Zn cleaning circuit. *Proceedings of the 36th Annual Meeting of the Canadian Mineral Processors of CIM*, Ottawa, Ontario, Canada, October. CIM, Montreal. pp. 525–540.

Deglon, D.A. 2005. The effect of agitation on the flotation of platinum ores. *Minerals Engineering*, vol. 18, no. 8. pp. 839–844.

Dobby, G.S. 1984. A fundamental flotation model and flotation column scale-up. PhD thesis, Department of Mining and Metallurgical Engineering, McGill University, Montreal, Canada.

Finch, J.A., Xiao, J., Hardie, C., and Gomez, C.O. 2000. Gas dispersion properties: bubble surface area flux and gas holdup. *Minerals Engineering*, vol. 13, no. 4. pp. 365–372.

Fournier, J., Hardie, C., Torrealba, J., and Nesset, J.E. 2015. A review of gas dispersion studies in flotation plants. *Proceedings of the 47th Annual Canadian Mineral Processors Operators Conference*, Ottawa, Ontario, January. CIM, Montreal. pp. 207–233.

Girgin, E.H., Do, S., Gomez, C.O., and Finch, J.A. 2006. Bubble size as a function of impeller speed in a self-aeration laboratory flotation cell. *Minerals Engineering*, vol. 19, no. 2. pp. 201–203.

Goodall, C.M. and O'Connor, C.T. 1989. Residence time distribution studies of the solid and liquid phases in a laboratory column flotation cell. *Proceedings of the International Colloquium: Developments in Froth Flotation*, Cape Town, South Africa, 3–4 August 1989. Volume 2. Southern African Institute of Mining and Metallurgy, Johanneburg. http://www.saimm.co.za/Conferences/FrothFlotation/004-Goodall.pdf

Gomez, C.O. and Finch, J.A. 2007. Gas dispersion measurements in flotation cells. *International Journal of Mineral Processing*, vol. 84, no. 1–4. pp. 51–58.

Gorain, B.K., Franzidis, J.-P., and Manlapig, E.V. 1995a. Studies on impeller type, impeller speed and air flow rate in an industrial scale flotation cell. Part 1: Effect on bubble size distribution. *Minerals Engineering*, vol. 8, no. 6. pp. 615–635.

Gorain, B.K., Franzidis, J.P., and Manlapig, E.V. 1995b. Studies on impeller type, impeller speed and air flow rate in an industrial flotation cell. Part 2: Effect on gas hold-up. *Minerals Engineering*, vol. 8, no. 12. pp. 1557–1570.

Gorain, B.K., Franzidis, J.-P., and Manlapig, E.V. 1996. Studies on impeller type, impeller speed and air flow rate in an industrial scale flotation cell. Part 3: Effect on superficial gas velocity. *Minerals Engineering*, vol. 9, no. 6. pp. 639–654.

Gorain, B.K., Franzidis, J.-P., and Manlapig, E.V. 1997. Studies on impeller type, impeller speed and air flow rate in an industrial scale flotation cell. Part 4: Effect of bubble surface area flux on flotation performance. *Minerals Engineering*, vol. 10, no. 4. pp. 367–379.

Gorain, B.K., Franzidis, J.-P., and Manlapig, E.V. 1999. The empirical prediction of bubble surface area flux in mechanical flotation cells from cell design and operating data. *Minerals Engineering*, vol. 12, no. 3. pp. 309–322.

Grau, R. and Heiskanen, H. 2005. Bubble size distribution in laboratory scale flotation cells. *Minerals Engineering*, vol. 18, no. 12. pp. 1164–1172.

Grau, R., Nousiainen, M., and Yañez, A. 2014. Gas dispersion measurements in three Outotec flotation cells: TankCell 1, e300 and e500. *Proceedings of the 27th International Mineral Processing Congress*, Santiago, Chile, 20–24 October. Gecamin Ltda.

Hadler, K. and Cilliers, J.J. 2009. The relationship between the peak in air recovery and flotation bank performance. *Minerals Engineering*, vol. 22, no. 5. pp. 451–455.

Hadler, K., Greyling, M., Plint, N., and Cilliers, J.J. 2012. The effect of froth depth on air recovery and flotation performance. *Minerals Engineering*, vol. 36-38. pp. 248–253.

Hernandez, H., Gomez, C.O., and Finch, J.A. 2003. Gas dispersion and de-inking in a flotation column. *Minerals Engineering*, vol. 16, no. 8. pp. 739–744.

Hernandez-Aguilar, J.R. and Reddick, S. 2007. Gas dispersion management in a copper/molybdenum separation circuit. *Proceedings of the Sixth International Copper-Cobre Conference*, Toronto, Canada, 25-30 August 2007 Vol. 2. Del Villar, R., Nesset, J.E., Gomez , C.O., and Stradling, A.W. (eds.). CIM, Montreal. pp 173–184.

Mathe, Z.T., Harris, M.C., O'Connor, C.T., and Franzidis, J.-P. 1998. Review of froth modelling in steady state flotation systems. *Minerals Engineering*, vol.11, no. 5. pp. 397–421.

Nesset, J.E., Hernandez-Aguilar, J.R., Acuna, C., Gomez, C.O., and Finch, J.A. 2006. Some gas dispersion characteristics of mechanical flotation machines. *Minerals Engineering*, vol. 19, no. 6-8. pp. 807–815.

Nesset, J.E., Zhang, W., and Finch, J.A. 2012. A benchmarking tool for assessing flotation cell performance. *Proceedings of the 44th Annual Canadian Mineral Processors Operators Conference*, Ottawa, Ontario, Canada, 17–19 January. CIM, Montreal. pp. 183–209.

Power, A., Franzidis, J.-P., and Manlapig, E.V. 2000. The characterization of hydrodynamic conditions in industrial flotation cells. *Proceedings of the 7th Mill Operators' Conference*, Kalgoorlie, Western Australia, 12–14 October, Australasian Institute of Mining and Metallurgy, Melbourne. pp. 243–256.

Rahman, R.M., Ata, S., and Jameson, G.J. 2015a. Study of froth behavior in controlled plant environment – Part 1: Effect of air flow rate and froth depth. *Minerals Engineering*, vol. 81. pp. 152–160.

Rahman, R.M., Ata, S., and Jameson, G.J. 2015b. Study of froth behavior in controlled plant environment – Part 2: Effect of collector and frother concentration. *Minerals Engineering*, vol. 81. pp. 161–166.

Rodrigues, W.J., Leal Filho, L.S., and Masini, E.A. 2001. Hydrodynamic dimensionless parameters and their influence on flotation performance of coarse particles. *Minerals Engineering*, vol. 14, no. 9. pp. 1047–1054.

Schubert, H. and Bischofberger, C. 1978. On the hydrodynamics of flotation machines. *International Journal of Mineral Processing*, vol. 5, no. 2. pp. 131–142.

Schwarz, S. and Alexander, S. 2006. Gas dispersion measurements in industrial flotation cells. *Minerals Engineering*, vol. 19, no. 6–8. pp. 554–560.

Seguel, F., Soto, I., Krommenacker, N., Maldonado, M., and Becerra Yoma, N. 2015. Optimizing flotation bank performance through froth depth profiling: Revisited. *Minerals Engineering*, vol. 77. pp. 179–184.

Shean, B.J. and Cilliers, J.J. 2011. A review of froth flotation control. *International Journal of Mineral Processing*, vol. 100, no. 3–4. pp. 57–71.

Smith, C., Neethling, S.J., and Cilliers, J.J. 2008. Air-rate profile optimisation: From simulation to bank improvement. *Minerals Engineering*, vol. 21, no. 12–14. pp. 973–981.

Tabosa, E., Runge, K., Holtham, P., and Duffy, K. 2016. Improving flotation energy efficiency by optimizing cell hydrodynamics. *Minerals Engineering*, vol. 96–97. pp. 194–202.

Venkatesan, L., Harris, A., and Greyling, M. 2014. Optimization of air rate and froth depth in flotation using a CCRD factorial design – PGM case study. *Minerals Engineering*, vol. 66–68. pp. 221–229.

Vera, M.A., Franzidis, J.-P., and Manlapig, E.V. 1999. Simultaneous determination of collection zone rate constant and froth zone recovery in a mechanical flotation environment. *Minerals Engineering*, vol.12, no. 10. pp. 1163–1176.

Vinnett, L., Yianatos, J., and Alvarez, M. 2014. Gas dispersion measurements in mechanical flotation cells: Industrial experience in Chilean concentrators. *Minerals Engineering*, vol. 57. pp. 12–15.

Yianatos, J., Bergh, L., and Cortes, G. 1998. Froth zone modelling of an industrial flotation column. *Minerals Engineering*, vol. 11, no. 5. pp. 423–435.

Yianatos, J., Bergh, L., Condori, P., and Aguilera, J. 2001. Hydrodynamic and metallurgical characterization of industrial flotation banks for control purposes. *Minerals Engineering*, vol. 14, no. 9. pp. 1033–1046.

Yianatos, J., Henriquez, F.H., and Oroz, A.G. 2006. Characterization of large size flotation cells. *Minerals Engineering*, vol. 19, no. 6-8. pp. 531–538.

Yianatos, J., Contreras, F., and Díaz, F. 2010. Gas holdup and RTD measurement in an industrial flotation cell. *Minerals Engineering*, vol. 23, no. 2. pp. 125–130.

Zheng, X., Franzidis, J.-P., and Manlapig, E. 2004. Modelling of froth transportation in industrial flotation cells: Part I. Development of froth transportation models for attached particles. *Minerals Engineering*, vol. 17, no. 9–10. pp. 981–988.

Zheng, X., Franzidis, J.-P., and Johnson, N.W. 2006. An evaluation of different models of water recovery in flotation. *Minerals Engineering*, vol. 19, no. 9. pp. 871–882.

Zheng, X., Johnson, N.W., and Franzidis, J.-P. 2006. Modelling of entrainment in industrial flotation cells: water recovery and degree of entrainment. *Minerals Engineering*, vol. 19, no.11. pp. 1191–1203. ◆

Transforming ore bodies into valuable commodities

Jacinth-Ambrosia, Australia 2006

Metallurgical Services

Research and Development

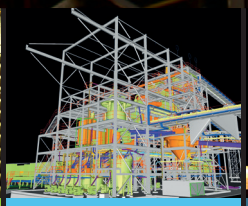

Process Plant Design

Process Plant Construction

Equipment Supply

Equipment Commissioning

Your go to partner for extracting maximum value from industrial minerals, iron ore, coal, chrome and heavy minerals across the project lifecycle

Mineral Technologies
A Downer Company

Downer
Relationships creating success

MT South Africa +27 35 797 3230
info@mineraltechnologies.com
www.mineraltechnologies.com

A proposed preliminary model for monitoring hearing conservation programmes in the mining sector in South Africa

N. Moroe, K. Khoza-Shangase, M. Madahana, and O. Nyandoro

Affiliation:
[1]University of the Witwatersrand, South Africa.

Correspondence to:
N. Moroe

Email:
Nomfundo.Moroe@wits.ac.za

Dates:
Received: 3 May 2018
Revised: 28 Jan. 2019
Accepted: 14 Mar. 2019
Published: July 2019

How to cite:
Moroe, N., Khoza-Shangase, K., Madahana, M., and Nyandoro, O. A proposed preliminary model for monitoring hearing conservation programmes in the mining sector in South Africa.
The Southern African Insitute of Mining and Metallurgy

DOI ID:
http://dx.doi.org/10.17159/2411-9717/18/016/2019

ORCiD ID:
N. Moroe
https://orchid.org/0000-0001-7186-5632

K. Khoza-Shangase
https://orchid.org/0000-0002-6220-9606

Synopsis

Occupational noise-induced hearing loss (ONIHL) is classified as the leading work-related disability in the mining industry. ONIHL has a negative impact, on not only the health and occupational productivity of affected individuals, but arguably also on the country's mining industry and economy. Hearing conservation programmes (HCPs) are an effective strategy in the management of ONIHL. However, current literature indicates that HCPs are not achieving the anticipated and desired outcomes in the South African mining sector despite the efforts focused on the management of ONIHL. Therefore, the purpose of this study is to propose the use of a feedback-based noise monitoring model as a tool for monitoring and managing ONIHL in the South Africa's mining sector. This model is a basic static feedback model with practical applications such as estimating, monitoring. and providing quantitative information to aid miners, mining administrators, and policy-makers in decision-making around HCPs. Additionally, the model could form part of an early intervention and management strategy for ONIHL in the workplace. The strength of this model, although currently static, is that it encompasses all the pillars of HCPs and takes into account the policies concerned with the management of ONIHL in the mining sector.

Keywords
occupational noise, hearing loss, feedback noise-monitoring model, risk management, mining sector.

Introduction

Hazardous noise levels (above 85 dBA) in the workplace place exposed employees at risk of developing a disabling occupational noise-induced hearing loss (ONIHL). ONIHL is the 'partial or complete hearing loss in one or both ears as a result of one's employment' (Nandi and Dhatrak, 2008, p. 1). This type of hearing loss develops gradually as a result of being exposed to continuous or intermittent high levels of noise over a long period of time (McBride, 2004; Patel *et al.*, 2010; Rappaport and Provencal, 2001). A hearing threshold below 40 dBs is classified as a disabling hearing loss (Yadav *et al.*, 2015), resulting in a hidden condition that does not readily manifest itself (Tye-Murray, 2009, p. 3). Dugan (2003) describes disabling hearing loss as the 'most prevalent, least recognized and least understood physical disability', while Copley and Frederichs (2010) and Hermanus (2007) argue that permanent disabling hearing loss is a major contributor to the global burden of disease on individuals, families, communities, and countries.

ONIHL is a prevalent condition in the mining industry and is classified as the leading work-related disability, and the second most common form of acquired hearing loss after presbycutic (age-related) hearing loss, with severe consequences for those exposed to high levels of noise (Ritzel and McCrary-Quarles, 2008). Although hearing loss is not life-threatening, the presence of a mild hearing loss (thresholds between 26-39 dBs), if unmanaged, may have a profound impact on the quality of life of the affected individual (Tye-Murray, 2009). Prolonged exposure to hazardous noise can potentially also lead to increased fatigue and decreased concentration, which ultimately increases human errors at work (Amjad-Sardrudi *et al.*, 2012; Picard *et al.*, 2008). ONIHL has a potential to significantly reduce workers' ability to perform or complete tasks that are dependent on auditory signals or verbal communication (Thorne, 2006). Furthermore, due to hearing loss sustained at work, which subsequently results in a communication handicap, workers may be regarded as incompetent or inactive, which ultimately, will impact on team work and group productivity (Momm and Geiecker, 2009). Moreover, hearing loss can negatively affect communication among workers, which can lead to safety concerns as workers may not be able to hear warning signals such as sirens since high-

frequency sounds are the most affected. Compromised ability to communicate may lead to increased risk of accidents (Kirchner *et al.*, 2012).

ONIHL can present a limitation on the kind of employment suitable for a person with hearing loss (Thorne, 2006), which may lead to economic burdens for developing countries in particular. Moreover, studies have shown that ONIHL contributes to occupational injuries, ill health, and absenteeism, which results in enormous social and economic implications for individuals, their families, communities, and the country at large (Amjad-Sardrudi *et al.*, 2012; Coderio *et al.*, 2005; Hermanus, 2007; Kramer, Kapteyn, and Houtgast, 2006).

ONIHL is a complex disease (Le *et al.*, 2017). Regardless of the amount of noise an individual is exposed to, some people are more prone to developing hearing loss than others subjected to the same level and amount of noise (Daniel, 2007; Sliwinska-Kowalska *et al.*, 2005). However, it is still not known why this is the case (Sliwinska-Kowalska and Davis, 2012). Individual susceptibility or risk factors associated with ONIHL can be either non-modifiable – outside one's control, or modifiable – within one's control (Daniel, 2007). Non-modifiable factors include age, race, and gender (Daniel, 2007). Modifiable factors include smoking, exposure to ototoxic agents, and ototoxic drugs (used to treat diseases like HIV/AIDS, TB, and cancer (Khoza-Shangase, 2013). These risk factors present a challenge to individuals who are exposed to occupational noise, as they undoubtedly lead to negative effects on ear care, health, and safety for individuals subjected to such excessive noise.

Economically, ONIHL has direct and indirect costs (Hermanus, 2007). Direct costs include compensation costs, costs associated with damage in the workplace, and the cost of interruption of production; while indirect costs include the cost of livelihood lost and loss of income to dependents (Hermanus, 2007). Statistics on the burden of ONIHL in developing countries are not readily available (Nelson *et al.*, 2005); however, Chadambuka, Mususa, and Muteti (2013) argue that 80% of individuals affected by ONIHL reside in low- and middle-income countries where ONIHL presents a 'much heavier burden than in developed regions of the world'.

In South Africa, in 2007, it was estimated that nearly half the mining industry's workforce was exposed to 'deafening noise, and of these workers more than 90% work in zones in which noise exceeds the 85 dBA time-weighted average, with 11% working in zones in which the noise levels are even higher' (Hermanus 2007, p. 534). In 2011, Edwards *et al.* (2011) reported that approximately 73.2% of the workforce was exposed to noise levels above the legislated occupational exposure level of 85 dBA. In 2012, the Chamber of Mines, as cited by Strauss *et al.* (2014), reported that 3.1 out of every 1000 workers have ONIHL.

According to Hong *et al.* (2013) although the impact of ONIHL on one's health and quality of life cannot be quantified in tangible measures or standards, the compensation cost for ONIHL is continually increasing. Rand Mutual Assurance (RMA) insures approximately 80% of mining industry workers. Approximately 12% of occupational injury and disease claims processed annually by RMA are due to ONIHL (Begley, 2004). In 2004, this cost was estimated at R15 000 per person (Begley, 2004), resulting to approximately R75 million paid out in compensation claims in that same year (Hermanus, 2007). Based on the analysis of the costs of NIHL claims in a study conducted by Edwards and Kritzinger (2012), RMA paid out several millions of rands in compensation for ONIHL in the period 1998-2007.

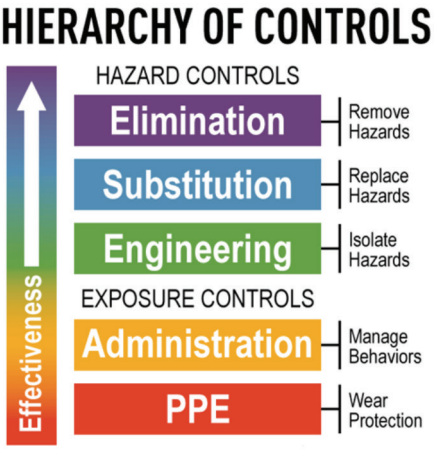

Figure 1—HCPs hierarchy of control (OSH Academy, 2018)

Reporting on the prevalence of ONIHL in the South African mining sector, Strauss *et al.* (2014) further stated that several factors, such as non-occupational noise exposure and vibration, as well as biological factors, increase the prevalence of ONIHL. These biological factors include smoking, age, gender, genetics, ototoxic drugs, and illnesses such as tuberculosis. These factors contribute to an individual's susceptibility to ONIHL.

Management of ONIHL

A review of literature on the management of ONIHL in the mining sector shows that hearing conservation programmes (HCPs) are the most effective way of managing excessive exposure to hazardous noise in the workplace (Amedofu, 2007; Feuerstein, 2001; Chadambuka, Mususa, and Muteti, 2013; Moroe, 2018). This is particularly so for the hierarchy of control, which if implemented correctly is reported to lead to desired outcomes that include the elimination of noise as depicted in Figure 1.

According to the hierarchy of control, engineering and administrative controls are the first line of defence in the management of hazardous noise in the workplace, after elimination and substitution of the noise source (McBride, 2004; Patel *et al.*, 2010; Rappaport and Provencal, 2001). However, evidence suggests that in practice, engineering and administrative controls are not given first priority (Suter, 2012). Locally, there is a slow uptake in implementing engineering controls as the chief strategy in the management of ONIHL (Moroe *et al.*, 2018). One of the main reasons for this is that machinery for engineering controls is reported to be very expensive (Rupprecht, 2017). Consequently, there is a heavy reliance on the use of hearing protection devices (HPDs), despite these being the last line of defence in the elimination of ONIHL, as indicated on the hierarchy of control.

Current international and local literature indicates that HPDs are the most widely used form of protection against high levels of noise, despite their proven inadequacy (discomfort, improper sizing, poor hygiene, and the inability to hear speech and warning signals when using them) (Bruce, 2007; Bruce and Wood, 2003; Hong *et al.*, 2013; Suter, 2012; Ntlhakana, Kanji, Khoza-Shangase, 2015; Steenkamp, 2007). Suter (2012) argues that although there is no doubt that HPDs are helpful in reducing

the impact of sound energy on the ear, they can be most effective when used in conjunction with engineering and administrative controls and other HCP pillars. Moroe *et al.* (2018) conducted a systematic literature review on the management of ONIHL in the mining sector in Africa. Their findings indicated that the majority of the studies conducted on the management of ONIHL focus on the use of HPDs. Furthermore, these studies were conducted in a piecemeal fashion, as specific individual pillars were targeted instead of a comprehensive, holistic HCP analysis. It is clear that ONIHL is a risk which needs to be eliminated or reduced through effective management strategies.

Risk is defined as 'the probability that a particular adverse event occurs during a stated period of time or results from a particular challenge' (Elmontsri, 2014, p. 50). Fiedler (2004) postulates that many workplaces have hazards – that is, anything presenting a threat to health and safety within an organization, which may put employees at risk of injury or harm to health, thereby necessitating systematic management such as a risk management matrix. Risk matrices have been used for years to rank various risks in the military (Donoghue, 2001). More recently, practitioners, academics, and the business community have shown an interest in risk management (Dabari and Saidin, 2014). Risk management has become a primary goal in every organization due to its ability to promote organizational outputs and create measureable value for stakeholders (Gates, Nicolas, and Walker, 2012). Specific to occupational health and safety, Hermanus (2007, p. 536) argues that 'the underlying premise of risk management is that improvements in health and safety can be made by correctly identifying and addressing hazards or factors (which may be underlying or direct) that contribute to occupational risk'. Fiedler (2004) complements this argument by stating that risk management is an integral and critical factor in the success of occupational health and safety programmes in that it serves to identify and assess risks resulting from hazards. This consequently leads to appropriate action to reduce or eliminate risk (Fiedler, 2004).

Risk management is defined as 'a systematic approach that aligns strategy, people, technology, processes and knowledge with the purpose of assessing, evaluating and managing the risk that an organisation faces' (Dabari and Saidin, 2014, p. 268). Central to the current study, Elmontsri (2014, p. 49) defines risk management as the process of 'reducing the risk to a level deemed tolerable by society and to assure control, monitoring, and public communication'. This definition acknowledges that in some contexts, such as the mining industry, risk of noise as a hazard cannot be entirely eliminated, thus, this definition fits aptly with the current study.

Locally, there is a dearth of studies focusing on risk management as a strategy tool in the management of ONIHL in the mining industry. Steenkamp has proposed a few models for the management of occupational noise. These models included a six sigma-based management model to eliminate noise-induced hearing loss (Steenkamp, 2007), new technology and re-engineering of HCPs (Steenkamp, 2008a), and effective second-level noise control through a personal approach to hearing conservation Steenkamp, (2008b). While these studies may be effective and relevant, they seem to mostly focus on the use of HPDs, where the burden of eliminating ONIHL rests with the employee with little emphasis on the involvement of the employer and other stakeholders such as policymakers who are involved in the management of ONIHL. There is therefore a need for

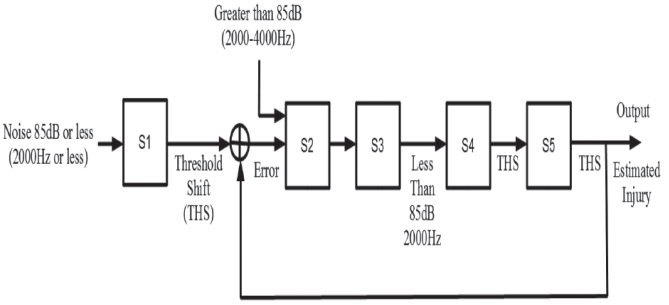

Figure 2—Overall system diagram for a feedback-based model for NIHL monitoring

studies that incorporate all stakeholders and policies concerned with ONIHL in the mining sector. The purpose of this study is to introduce a feedback-based noise monitoring model (see Figure 2) as a tool for managing ONIHL in the mining sector in South Africa. This tool was conceptualized from a risk management framework as discussed below.

Conversion of the risk management framework to the feedback-based noise monitoring model (FBNMM)

This feedback-based noise management model (FBNMM, see Figure 2) is comprised of five subsystems: S1 is the baseline or reference point, S2 is the control unit, which consists of the policies and mandatory code of practice (COP), together with the milestones, S3 is the actuator, which ensures compliance, S4 is the plant, which acts as the implementation phase through an individual exposed to noise, and S5 is the evaluation or checkup point, consisting of a sensor.

The FBNMM proposed in this paper is derived from the risk management framework (RMF) (Figure 3) adapted from ISO 31000. This RMF was further revised by the Australian Government's Department of Finance (Department of Finance, Australia, 2016) and is adopted as a conceptual framework for this paper. This framework comprises three core components which need to be implemented consistently in order to achieve a structured approach to the management of risk. These components are:

- Principles to describe the essential attributes of good risk management

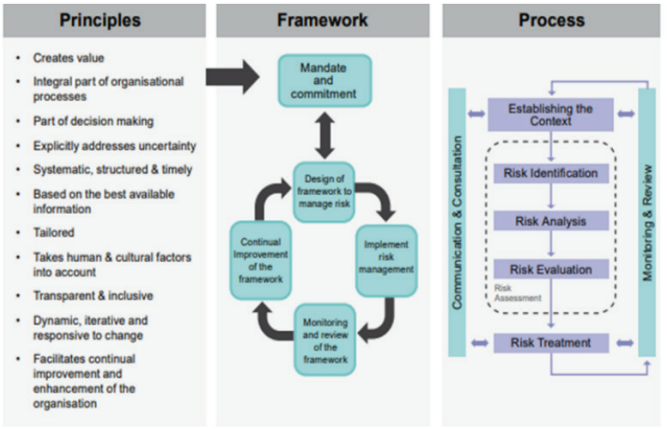

Figure 3—Risk management framework (Department of Finance, Australia, 2016)

A proposed preliminary model for monitoring hearing conservation programme

- Framework providing a structure for risk management
- Process which prescribes a tailored, structured approach to understanding, communicating, and managing risk in practice.

For the purpose of this study, the focus is on the third component, the process component. Drawing from the definition of risk as discussed earlier, in order to convert this process component into a feedback-based noise monitoring model, the risk is identified as noise. In converting the risk process component, all the processes are taken into consideration as discussed below.

- Establishing the context. In this study, the context is the mining industry where the presence of excessive noise has been identified as a hazardous risk. In order to address this risk, there need to be regulations, Acts, COPs, policies *etc.* which give background to the context of the mine. In relating this to the proposed FBNMM, these policies represent S2.
- Risk assessment, which comprises risk identification, analysis, and evaluation. This process relates to compliance with mandated policies and regulations in a given context. For this study, this applies to the COP, (Figure 4) and the 2014 Mine Health and Safety Council (MHSC) milestones (MHSC, 2014). This COP encompasses all the HCP pillars; however, it lacks a rapid monitoring system which can aid with early identification of possible ONIHL development. The COP is concerned with compliance, which is represented by S3 in the FBNMM. In order to evaluate compliance, there needs to be a checking system where the effectiveness of the implemented policies is measured. Therefore, S4 is concerned with the implementation of policies in order to check for compliance.
- Risk treatment. After implementing the processes mentioned in S2, S3, and S4, an output is obtained, which is then fed back to the baseline or reference point (S1) for comparison and benchmarking. At this stage, administrators are informed regarding a suitable action plan for intervention if needed. Hence this proposed model is called a feedback noise-monitoring model. Furthermore, in line with the RMF, this proposed model can serve to monitor and review policies, thereby implementing context-specific recommendations that influence risk assessments and evaluations.

This FBNMM is a basic feedback model, and still requires further refinement. At this stage it is used to provide preliminary results to illustrate its application. The potential value of this model can be measured in terms of possible significant savings in ONIHL compensation claims and also contribute towards the quality of life of people exposed to excessive noise in the workplace.

Fundamental to any control system is the capability to measure the output of the system and to take corrective action if its value digresses from some desired value (Burns and Grove, 2009). A system may be defined as a collection of materials, parts, components, or procedures which are included within some specified boundary. A system may be open loop or closed loop. A control system may be defined as an interconnection of varying units of a system in a configuration that provides a desired response (Burns and Robinson, 1970). In this configuration, one or more output variables may be tracked (follow a certain reference over time). A control engineering approach uses engineering and mathematics to investigate and predict the performance of systems. A feedback control system is a closed-loop system whose output is controlled using its output measurements as a feedback signal. This signal is compared with a reference signal to generate an error signal which is filtered by a controller to produce the system's control input (Boulet, 2000).

The risk management matrix was developed into a basic static feedback model by identifying the inputs and the outputs of the systems, the plant, the reference, controllers, the disturbance, and sensors and actuators of the system. As a result, the ONIHL monitoring model was developed using feedback or closed-loop configuration to allow for effective monitoring of mineworkers in

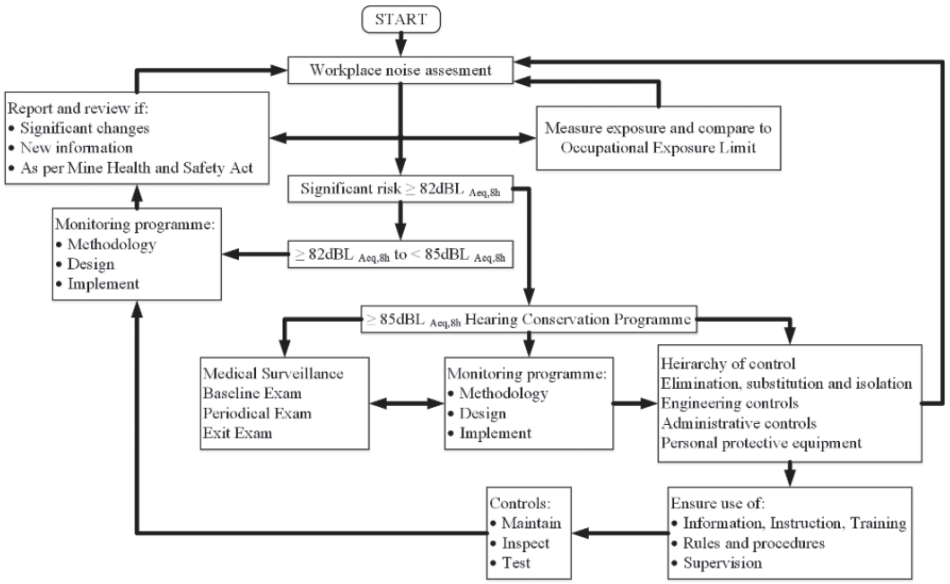

Figure 4—Summarized code of practice (Mine Health and Safet Inspectorate, 2003)

Table I

Values of U, V, L_0

Frequency (Hz)	U	v	L_0
500	-0.033	0.110	93
1000	-0.020	0.070	89
2000	-0.045	0.066	80
3000	0.012	0.037	77
4000	0.025	0.025	75
6000	0.019	0.024	77

Table II

K values

Q	K	Q	K
5	1.645	50	0
10	1.282	95	1.645
15	1.036	90	1.282
20	0.842	85	1.036
25	0.675	80	0.842
30	0.524	75	0.675
35	0.385	70	0.524
40	0.253	65	0.385
45	0.126	60	0.253
		55	0.126

the presence or absence of internal or external uncertainty. Figure 2 shows the different interconnected subsystems that form the overall system. The whole system may therefore be defined as a feedback-based, single-input single-output (SISO) nonlinear stochastic system. The ISO 1999 international standard statistical equations are used for the model (ISO 1999:2013).

The practical application of this model would be to estimate, monitor, and provide quantitative information on the temporary threshold shift (TTS), which eventually leads to the permanent threshold shift (PTS). Miners and mining administrators or policy-makers use this information in decision-making with regards to noise management in the workplace that could reduce the impact of ONIHL. Monitoring employees at shorter intervals, for instance monthly, would ensure that the employers are aware of the state of hearing of their employees and will thus provide an opportunity for early intervention. The model therefore forms part of the early intervention and prevention of ONIHL in the workplace.

The input to this model is the occupational noise exposure of a 'naïve person' (S1 – reference point or baseline) (person who has not been exposed to excessive occupational noise that has caused a permanent threshold shift). The occupational noise exposure is the disturbance to the system. The estimated ONIHL is the output.

Model description

Equations to be used in calculating model parameters of the subsystem are presented below prior to model descriptions. Given the following parameters:

H The hearing threshold level for a specified fraction of a population as a function of age
Y Age in years
Q Various ranges of the percentages of the population
a Coefficient used in the equation for calculation of hearing loss
S_u Standard deviation of the upper half of the distribution
S_1 Standard deviation of the lower half of the distribution
$H_{md,18}$ The median value of the hearing threshold of ontologically normal persons of the same sex aged 18 years, which for practical purposes is taken as zero, as specified in the ISO 389 series. Hence, H_Q is the hearing threshold level associated with age.

The values for the coefficient a and the multiplier are presented in Tables I and II. (ISO 1999: 2013).

The formulae applicable for the calculation of hearing threshold (H) as a function of age Y (years), for the various ranges of the percentage (Q), having hearing threshold levels exceeding the value H_Q are:

For Q = 50%:

$$H_{md,\,Y} = a(Y-18)^2 + H_{md;18} \quad [1]$$

For 5% ≤ Q <50%:

$$H_Q = H_{md,Y} + KS_u \quad [2]$$

For 50% < Q ≤ 95%:

$$H_Q = H_{md,Y} - KS_1 \quad [3]$$

$$S_u = b_u + 0.445\, H_{md,\,Y} \quad [4]$$

$$S_1 = b_1 + 0.356\, H_{md,y} \quad [5]$$

The values of b_1 and b_2 are listed in Tables III to V.

$$d = 20 \log_{10}(1 - C) \quad [6]$$

$$H' = H + N - \frac{HXN}{120} \quad [7]$$

Table III

Values of X_u, Y_u, X_l, and Y_l

Frequency (Hz)	X_u	Y_u	X_l	Y_l
500	0.044	0.016	0.033	0.002
1000	0.022	0.016	0.020	0.000
2000	0.031	0.016	0.016	0.000
3000	0.007	- 0.002	0.029	- 0.010
4000	0.005	0.009	0.016	- 0.002
6000	0.013	0.008	0.028	- 0.007

Table IV

Coefficient of *a* values

Frequency (Hz)	a (dB/year) Male	A (dB/year) Female
125	0.0030	0.0030
250	0.0030	0.0030
500	0.0035	0.0035
1000	0.0040	0.0040
1500	0.0055	0.0050
2000	0.0070	0.0060
3000	0.155	0.0075
4000	0.0160	0.0090
6000	0.0180	0.0120
8000	0.0220	0.0150

Table V

b_u and b_l values

Frequency Hz)	b_u (dB) Males	b_u (dB) Female	b_l (dB) Males	b_l (dB) Females
125	7.23	6.67	5.78	5.34
250	6.67	6.12	5.34	4.89
500	6.12	6.12	4.89	4.89
1000	6.12	6.12	4.89	4.89
1500	6.67	6.67	5.34	5.33
2000	7.23	6.67	5.78	5.34
3000	7.78	7.23	6.23	5.78
4000	8.34	7.78	6.67	6.23
6000	9.45	8.90	7.56	7.12
8000	10.56	10.56	8.45	8.45

H' = Hearing threshold level, in decibels, associated with age and noise (HTLAN)

H = Hearing threshold level, expressed in decibels, associated with age (HTLA)

N = Actual or potential noise induced permanent threshold shift (NIPTS), expressed in decibels.

N is calculated using the following equations:

$$N_{50}\ [uv\lg(t/t_0)]\left(L_{\mathrm{EX,8h}} -\right)^2 \quad [8]$$

$$N_{50,t<10} = N_{50,t=10} \quad [9]$$

$L_{EX,\ 8h}$ is the noise exposure level normalized to a nominal 8-hour working day, expressed in decibels

L_o is the sound pressure level, defined as a function of frequency, expressed in decibels, below which the effect on hearing is negligible

t is the exposure duration, expressed in years

t_o is 1 year

u and v are given as a function of frequency

Values of u, v, and L_0 used to determine the (noise-induced permanent threshold shifts) NIPTS for the median value of the population.

This formula applies to $L_{ex,\ 8h}$ greater than L_o. In cases where $L_{ex,\ 8h}$ is less than L_o, it shall be deemed equal to L_o so that N_{50} is zero.

Threshold shift for an individual not exposed to occupational noise

In Figure 2, S1 represents the threshold shift of an individual who has not been exposed to occupational noise. Equation [1] is used to determine the effects of age on the hearing ability of this individual. The input to this system is noise exposure which is less than 85 dB at 2000 Hz. At this level of exposure and frequency in the absence of any other factors; for instance, exposure to a sudden explosion (Burns and Robinson, 1970), then the only hearing loss that would occur is loss due to presbycusis. The output to this system is the hearing threshold shift. The hearing threshold level associated with age (HTLA) (ISO 1999: 2013) is calculated as shown in Equation [2].

Controllers (policy and intervention)

The Code of Practice (Figure 4) and the 2014 Mine Health and Safety Council (MHSC) Milestones for the elimination of ONIHL in the mining sector as published by Mine Health and Safety Inspectorate (2003) serve as policies and intervention strategies for the management of noise. Therefore, S2 is the sub-system that represents the mandatory code of conduct imposed in a mine for both surface and underground employees and anyone on site (Mine Health and Safety Inspectorate, 2003). S2 is simplified by amalgamating the policies (Code of Practice and 2014 Mine Health and Safety Milestones for the elimination of ONIHL in the mining sector) and the intervention (administrative controls and the use of hearing protection devices). Depending on the policy implemented by the mine, occupational noise is decreased. The system is therefore represented with an equation used by manufacturers in the industry in the design of noise reduction protective gear (Bannon and Kaputa, 2015), shown by Equation [6].

Sensors

S3 is the sensing unit of the model. The sensor used in this unit may be the National Institute for Occupational Safety and Health (NIOSH) Sound Level Meter mobile application tool or personal dosimeters (National Institute for Occupational Safety and Health, n.d). This sensor is used to measure sound levels in the mine and it outputs the noise intensity and the frequency.

Threshold shift for an individual exposed to occupational noise

S4 is defined by Equation [7] and it represents an individual who has been exposed to occupational noise while also suffering from presbycusis.

Checkup

When the hearing threshold shifts of an employee are monitored on a daily, weekly, or monthly basis, the company will be able to assess their state of hearing. Should a worker's threshold

shift significantly over a month, the mining administrator will be able to monitor and assess if the hearing protection is working properly or if there are other factors causing the shift, which will then be addressed. S5 represents the check subsystem. This can be monthly monitoring of the hearing threshold shifts. For annual and biannual checkups, an audiogram is used to establish if a temporary threshold shift has progressed into a permanent threshold shift, thus indicating damage to hearing resulting in ONIHL.

Illustration of the model – preliminary results

To demonstrate the use of the feedback model, the following fictitious scenario was created. Six mineworkers, comprising three females and three males, who started employment at the ages of 50, 40, and 25 years respectively are used as case studies (Figures 5–10). It is assumed that all subjects have hearing within normal limits, with no previous history of exposure to occupational noise, thus the baseline is not taken into account. They work in a deep mine with a maximum noise intensity of 107 dB at a frequency of 4000 Hz. The results show the pattern of threshold shift if the workers were without hearing protection for 15 years. This illustration demonstrates the significant shift in hearing threshold, thus highlighting the importance of the use of hearing protection devices in noisy environments. Furthermore, research indicates that most workers, although provided with HPDs, sometimes do not use them correctly or the HPD may be faulty.

From the graphs, it is observed that if left unprotected and unmonitored, all mineworkers, irrespective of their age, will have experienced a threshold shift of more than 25 dB from their given baseline in less than 10 years. The designed system currently offers a predictive model for the mine administrators, who should now take steps to monitor the mineworkers frequently to ensure that significant threshold shift does not occur, as stipulated by the Mine Health and Safety Council (MHSC, 2014).

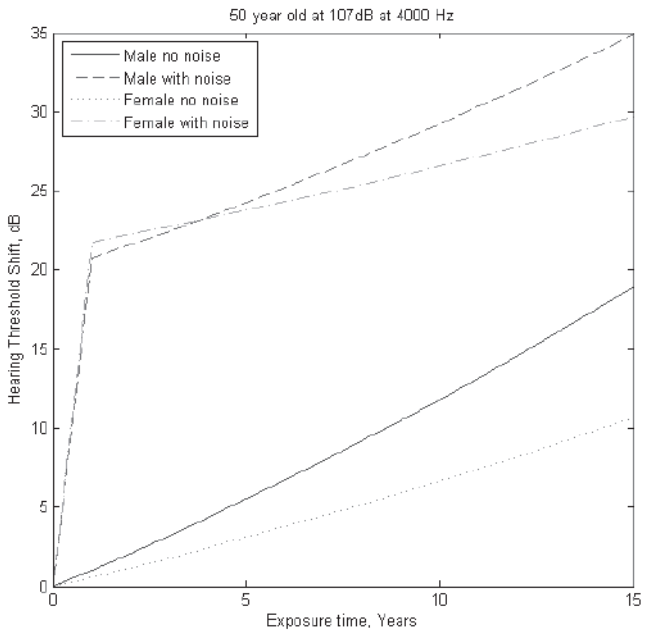

Figure 5—50-year-old mineworker's threshold shift without hearing protection

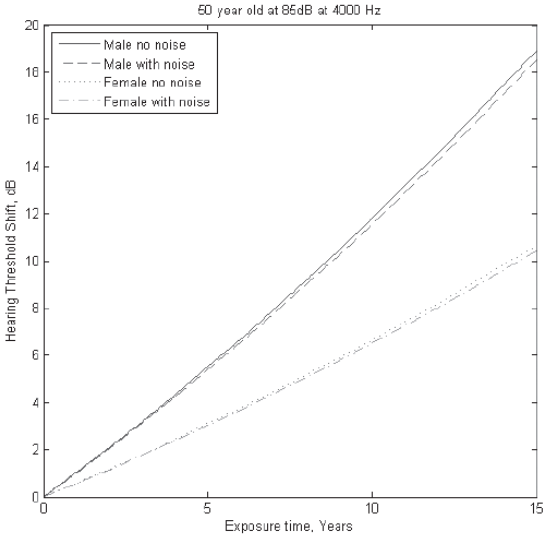

Figure 6—50-year-old mineworker's threshold shift with hearing protection

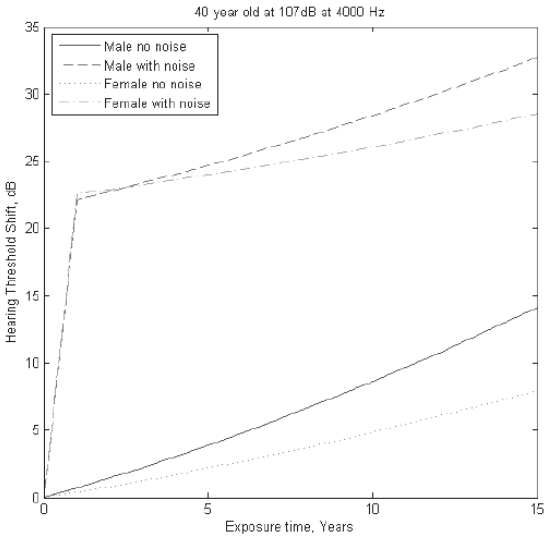

Figure 7—40-year-old mineworker's threshold shift without hearing protection

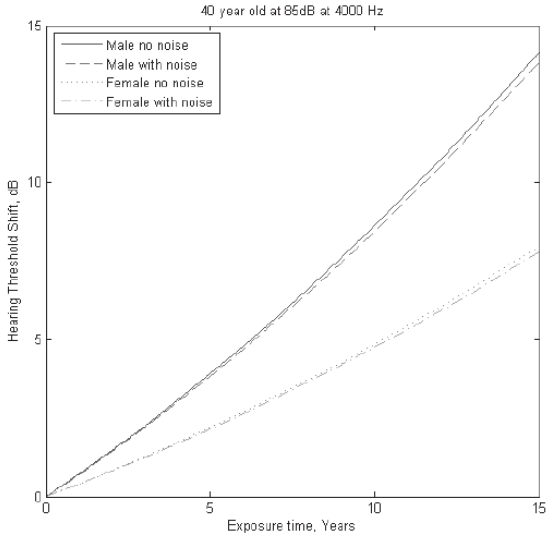

Figure 8—40-year-old mineworker's threshold shift with hearing protectio

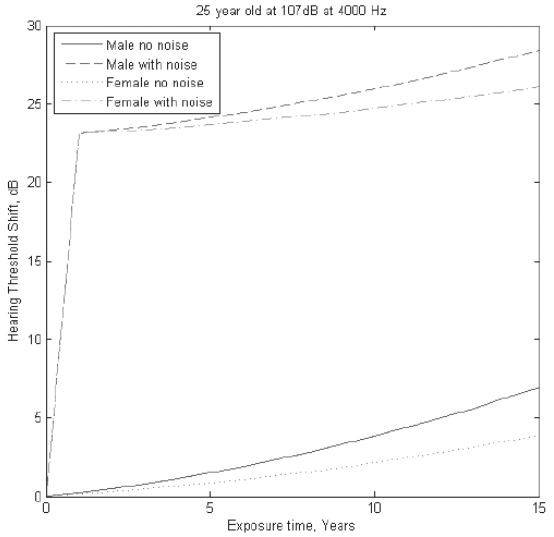

Figure 9—25-year-old mineworker's threshold shift without hearing protection

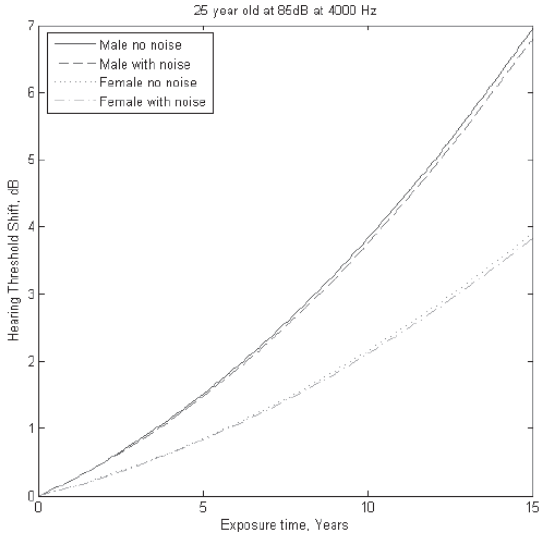

Figure 10—25-year-old mineworker's threshold shift with hearing protection

Limitations of the model

- The presented model is a static model and currently excludes the dynamic aspects. Future refinements will include the dynamic aspects, thus enabling the mine administrators to access the real-time hearing status of workers while at work.
- The current model does not include a controller. Future versions will include design of linear and nonlinear controllers for the system, thus allowing for interpretation of policies using control law.
- Model validation with real audiological patient data has not been performed. Therefore, the model will be validated using real data from the mines, and the results presented in a subsequent paper.
- The success of this model relies on the active involvement of different stakeholders. This may present complexities as multiple departments may have to work together. Current studies have indicated a lack of involvement of all stakeholders, which impacts on the success of any implemented programme.
- This model does not take into consideration non-modifiable factors when inputting data

Recommendations

- Model validation with real audiological patient data has not been performed. Therefore, the model needs to be validated using real data from the mines. This will be covered in a subsequent paper.
- Conversion of the current model from a static to a dynamic model by incorporating the model of the human ear as part of the plant.
- Interpretation of policy as a control law, hence the use of both basic and robust appropriate controllers for the system.

Conclusion

Successful elimination of ONIHL is the goal of any HCP. Efforts towards enhancing strategies to achieve this goal should be increased. Research into HCPs and their effectiveness with tangible recommendations on how to manage this occupational health risk should be prioritized. The model introduced in this paper aims to achieve this. This proposed model should be interpreted taking cognisance of the five identified limitations, which will be addressed in a subsequent paper.

References

AIRMIC. 2010. A structured approach to Enterprise Risk Management (ERM) and the requirements of ISO 31000. https://www.theirm.org/media/886062/ISO3100_doc.pdf

AMEDOFU. 2007. Effectiveness of hearing conservation program at a large surface gold mining company in Ghana. *African Journal of Health Science*, vol. 14. pp. 49–53.

AMJAD-SARDRUDI, H., DORMOHAMMADI, A., GOLMOHAMMADI, A. , and POOROLAJAL, J. 2012. Effect of noise exposure on occupational injuries: A cross-sectional study. *Journal of Research in Health Sciences,* vol. 12. pp. 101–104.

BANNON, M. and KAPUTA, F. 2015. Decibel drop and noise reduction coefficients for material combinations. Thermaxx Noise Insulation Jackets. https://www.thermaxxjackets.com/noise-reduction-coefficients-and-decibel-drop/

BOULET, B. 2000. Introducction to feedback control system. Coronado Systems. http://www.cim.mcgill.ca/~ialab/ev/Intro_control1.pdf

BRUCE, R.D. 2007. Engineering controls for reducing workplace noise. *Noise Engineering*, vol. 37, no. 3. pp. 33–39.

BRUCE, R.D. and WOOD, E.W. 2003. The USA needs a new national policy for occupational noise. *Noise Control Engineering*, vol. 51. pp. 162–165.

BURNS, N. and Grove, S.K. 2009. The Practice of Nursing Research : Appraisal, Synthesis, and Generation of Evidencei. Elsevier Saunders.

BURNS, W. and ROBINSON, D.W. 1970. Hearing and noise in industry. Her Majesty's Stationery Office, London.

CHADAMBUKA, A., MUSUSA, F., and MUTETI, S. 2013. Prevalence of noise induced hearing loss among employees at a mining industry in Zimbabwe. *African Health Science*, vol. 13. pp. 899–906.

CODERIO, R., CLEMENTA, A.P., DINIZ, C.S., and DIAS, A. 2005. Occupational noise as a risk factor for work-related injuries. *Rev Saude Publica*, vol. 39. pp. 1–5.

Department of Finance, Australia. 2016. An overview of the risk management process. COMCOVER Information sheet. https://www.finance.gov.au/sites/default/files/Risk-Management-Process.pdf

Copley, G.J. and Frederichs, N.B. 2010. An approach to hearing loss in children. *South African Family Practice*, vol. 52. pp. 34–39.

Dabari, I.J. and Saidin, S.Z. 2014. A theoratical framework on the level of risk management implemenattion in the Nigerian banking sector: The moderating effect of top management support. *Social and Behavioral Sciences*, vol. 164. pp. 627–634.

Donoghue, A.M. 2001. The design of hazard risk assessment matraces for ranking occupational health risks and thier application in mining and mineral processing. *Occupational Medicine*, vol. 51. pp. 118–123.

Dugan, M.B. 2003. Living with Hearing Loss. Gallaudet Press, Washington.

Edwards, A.L. and Kritzinger, D. 2012. Noise-induced hearing loss milestones: past and future. *Journal of the Southern African Institute of Mining and Metallurgy*, vol. 112. pp. 865–869.

Elmontsri, M. 2014. Review of the strengths and waeknesses of risk matrices. *Journal of Risk Analysis and Crisis Response*, vol. 4. pp. 49–57.

Feuerstein, J.F. 2001. Occupational hearing conservation. *Handbook of Clinical Audiology*.. 5th edn Katz, J. (ed.). Lippincott Williams & Wilkins, Philadelphia, PA.

Fiedler, A.e. 2004. The role of risk management for occupational health and safety: Benefiting from effective risk assessment. Northwest Controlling Corporation Ltd. https://www.noweco.com/download/wp_ohse.pdf

Gates, S., Nicolas, J.L., and Walker, P.L. 2012. Enterprise risk management: A process for enhanced management and improved performance. *Management Accounting Quarterly*, vol. 13. pp. 28–38.

Hermanus, M.a. 2007. Occupational health and safety in mining—status, new developments, and concerns. *Journal of the Southern African Institute of Mining and Metallurgy*, vol. 107. pp. 531–537.

Hong, O., Kerr, M.J., Poling, G.L., and Dhar, S. 2013. Understanding and preventing noise-induced hearing loss. *Disease-a-Month*, vol. 59. pp. 110–118.

ISO 1999. 2013. Acoustics — Estimation of noise induced hearing loss.

International Organization for Standardization, ISO 389 series. https://www.iso.org/search.html?q=ISO%20389%20series [accessed 20 January 2019].

Khoza-Shangase, K. 2013. Ototoxicity in tuberculosis treatment in South Africa: Views from healthcare workers involved in the management of TB. *African Journal of Pharmacy and Pharmacology*, vol. 7. pp. 2141–2145.

Kirchner, D.B., Evenson, E., Dobie, R.A., Rabinowitz, P., Crawford, J.,Kopke, R., and Hudson, T.W. 2012. Occupational noise-induced hearing loss. *Journal of Occupational and Environmental Medicine*, vol. 54. pp. 106–108.

Kramer, S.E., Kapteyn, T.S., and Houtgast, T. 2006. Occupational performance: Comparing normally-hearing and hearing-impaired employees using the Amsterdam Checklist for Hearing and Work. *International Journal of Audiology*, vol. 45. pp. 503–512.

Le, T.N., Straatman, L.V., Lea, J., and Westerberg, B. 2017. Current insights in noise-induced hearing loss: a literature review of the underlying mechanism, pathophysiology, asymmetry, and management options. *Journal of Otolaryngology - Head and Neck Surgery*, vol. 46. pp. 1–15.

Mcbride, D.I. 2004. Noise-induced hearing loss and hearing conservation in mining. *Occupational Medicine (London)*, vol. 54. pp. 290-296.

MHSC 2014. The road to zero harm - New milestones: *Proceedings of the 10th Anniversary of the 2003 Occupational Health and Safety*. Mine Health and Satety Council, johannesburg.

Mine Health and Safety Inspectorate. 2003. Guideline for the compilation of a mandatory code of practice for an occupational health programme (occupational hygiene and medical surveillance) for noise. Department of Minerals and Energy, Pretoria.

Momm, W. and Geiecker, O. 2009. Disability and work. *Encyclopaedia of Occupational Health and Safety*. International Labour Office. http://www.ilocis.org/documents/chpt17e.htm

Moroe, N.f. 2018. Occupational noise-induced hearing loss in South African large-scale mines: Exploring hearing conservation programmes as complex interventions embedded in a realist approach. *International Journal of Occupational Safety and Ergonomics*. pp. 1–9.

Moroe, N.f., Khoza-Shangase, K., Kanji, A., and Ntlhakana, L. 2018. The management of occupational noise induced hearing loss in the mining sector in Africa: A systematic review- 1994-2016. *Noise and Vibration Worlwide*, vol. 49. pp. 181–190.

Nandi, S.S. and Dhatrak, S.V. 2008. Occupational noise-induced hearing loss in India. *Indian Journal of Occupational Environmental Medicine*, vol. 12. pp. 53–56.

National Institute for Occupational Safety and Health. Not dated. Noise and hearing loss prevention: NIOSH Sound Level Meter App. https://www.cdc.gov/niosh/topics/noise/app.html

Nelson, D.I., Nelson, R.Y., Concha-Barrientos, M., and Fingerhut, M. 2005. The global burden of occupational noise-induced hearing loss. *American Journal of Industrial Medicine*, vol. 48. pp. 446–58.

Ntlhakana, L., Kanji, A., and Khoza-Shangase, K. 2015. The use of hearing protection devices in South Africa: Exploring the current status in a gold and a non-ferrous mine. *Occupational Health Southern Africa*, vol. 21. pp. 10–15.

Patel, D.S., Witte, K., Zuckerman, C., Murray-Johnson, L., Orrego, V., Maxfield, A.M., Meadows-Hogan, S., Tisdale, J., and Thimons, E.D. 2010. Understanding barriers to preventive health actions for occupational noise-induced hearing loss. *Journal of Health Communication*, vol. 6. pp. 155–68.

Picard, M., Girard, S.A., Simard, M., Larocque, R., Leroux, T., and Turcotte, F. 2008. Association of work-related accidents with noise exposure in the workplace and noise-induced hearing loss based on the experience of some 240,000 person-years of observation. *Accident Analysis & Prevention*, vol. 40. pp. 1644–1652.

Rappaport, J.M. and Provencal, C. 2001. Neurotology for audiologists. *Handbook of Clinical Audiology*. 5th edn. Katz, J. (ed.). Lippincott Williams & Wilkins, Philadelphia, PA.

Ritzel, D.O. and Mccrary-Quarles, A.R. 2008. Hearing loss prevention and noise control. *Umwelt und Gesundheit*, vol. 1. pp. 22–29.

Rupprecht, S.m. 2017. Bench mining utilizing manual labour and mechanized equipment – a proposed mining method for artisanal small-scale mining in Central Africa. *Journal of the Southern African Institute of Mining and Metallurgy*, vol. 117. pp. 25–31

Sliwinska-Kowalska, M., Zamyslowska-Szmytke, E., Szymczak, W., Kotylo, P., Fiszer, M., Wesolowski, W., and Pawlaczyk-Luszczynska, M. 2005. Exacerbation of noise induced hearing loss by co-exposure to workplace chemicals. *Environmental Toxicology and Pharmacology*, vol. 19, no. 3. pp . 547–553.

Sliwinski-Kowalska, M. and Davis, A. 2012. Noise induced hearing loss. *Noise and Health*, vol. 14. pp. 274–280.

Steenkamp, R.J. 2007. A six sigma-based management model to eliminate the noise-induced hearing loss pandemic in South African mines. *Southern African Business Review*, vol. 11, no. 1. pp. 104–124.

Steenkamp, R.J. 2008a. Effectve hearing conservation demands new technology and re-engineering. *South African Journal of Industrial Engineering*, vol. 19. pp. 215–229.

Steenkamp, R.J. 2008b. A personal approach to hearing conservation: the key to effective second-level noise control. *South African Journal of Industrial Engineering*, vol. 19. pp. 215–229.

Suter, A.H. 2012. Engineering controls for occupational noise exposure: The best way to save hearing. *Sound and Vibrations*, vol. 45. pp. 21–31.

Thorne, P. 2006. Best practice in noise-induced hearing loss management and prevention: A review of literature, practices and policies for the New Zealand context. Accident Compensation Corporation, New Zealand.

Tye-Murray, N. 2009. Foundations of Aural Rehabilitation: Children, Adults, and their Family Members. Delmar Cengage Learning, Clifton Park, NY.

Yadav, M., Yadav, K.s., Netterwala, A., Khan, B., and Desai, N.S. 2015. Noise induced hearing loss (nihl) and its correlation with audiometric observations in heavy vehicle operators suffering with metabolic disorders. *International Journal of Medical and Clinical Research*, vol. 6. pp. 315–320. ◆

New Concept Mining

Powered by Epiroc

Coal pillar strength analysis based on size at the time of failure

J.N. van der Merwe

Affiliation:
Visiting Professor, School of Mining Engineering, University of the Witwatersrand.

Correspondence to:
J.N. van der Merwe

Email:
nielen@stablestata.co.za

Dates:
Received: 8 Jan. 2019
Revised: 14 Apr. 2019
Accepted: 25 Apr. 2019
Published: July 2019

How to cite:
van der Merwe, J.N.
Coal pillar strength analysis based on size at the time of failure.
The Southern African Insitute of Mining and Metallurgy

DOI ID:
http://dx.doi.org/10.17159/2411-9717/566/2019

ORCiD ID:
J.N. van der Merwe
https://orchid.org/0000-0002-3709-5520

Synopsis

A major shortcoming of the statistical back-analysis of coal pillar strength is that it relies on the as-mined pillar dimensions, not taking into account time-related pillar scaling with subsequent reduction in pillar width. The paper describes an investigation where the rate of pillar scaling was applied to the pillars in the databases of failed and unfailed pillars. The reduced pillar sizes were then used in the same method of statistical back-analysis that had been used in the past.

This resulted in an equation for pillar strength which predicts significantly greater pillar strength than the previous statistical analyses, which is similar to the strength which had been found earlier by direct testing of large specimens underground. It is concluded that the lower strengths found by previous statistical analyses are due to the incorrect pillar width being used and that by adjusting the pillar sizes to compensate for scaling, more credible results that correspond to direct testing are obtained.

As the newly derived strength equation is time-dependent, it follows that the safety factors and probabilities of failure are likewise time-dependant. An equation to determine the probability of failure is also developed. This results in the safety factor being close to unity at a probability of failure of 50%, which is aligned to statistical expectation.

Keywords
coal pillars, time dependency, pillar failure, failure probability.

Introduction

Since the Coalbrook mine disaster, caused by massive pillar collapse, there have been several attempts at analysing and defining the strength of coal pillars. It was realized in the very beginning that performing classical strength tests on coal specimens in a laboratory and then transferring those results to real coal pillars could not be successful. The scatter of results is one problem and, more seriously, there is a size effect (at least for small specimens) that made the transformation of strength results to much larger coal pillars underground all but impossible.

Two main schools of thought then emerged. Some researchers preferred to perform direct strength tests on large specimens underground, while others relied on statistical back-analysis of failed and unfailed pillar cases, attempting to determine the differences in size and shape that would allow a satisfactory prediction of failure. The latter school of thought resulted in the method that was widely accepted by the South African coal mining industry, described in the landmark publication by Salamon and Munro (1967).

Since that time there have been a number of re-analyses, prompted by more failures occurring, resulting in larger and hence more reliable databases, the realization that there are meaningful differences in the pillar strength characteristics in different coalfields, and alternative methods of analysis. By and large, all of these attempts can be seen as updates of the original work by Salamon and Munro (1967).

One of the difficulties with statistical methods is that the effects of time on pillar strength are not taken into account. A pillar case in the databases is merely classified as either failed or unfailed, meaning that pillars of different ages at their time of failure (and consequently having undergone different magnitudes of size reduction) are all treated the same. Only the as-mined dimensions are considered.

This paper describes an attempt to overcome that difficulty by basing the statistical analysis on the expected sizes of the pillars at their time of collapse. The outcome is a new pillar strength formula, based on dimensions as well as age, which is then further developed to result in a time-related probability of failure.

The paper first summarizes the historical developments that led up to the present analysis in order to provide the required context. It then describes the methodology that was used and presents the final outcomes.

Note that where mention is made of 'pillar failure' in this paper it means the collapse of relatively large groups of pillars, and not the collapse of individual pillars. The collapse cases had to be sufficiently wide to result in subsidence of the surface, substantially greater than would be caused by elastic compression of the pillars, in order to be included in the database.

Following the suggestion by Salamon, Canbulat, and Ryder (2006), the term 'unfailed' is used throughout to refer to the database of pillars that had not failed. It is interesting to note that one of the motivations for using the term (as opposed to 'stable' cases) was that the pillars in that database may fail at some time in the future.

Historical developments

It is not the aim of this paper to provide a comprehensive overview of coal pillar strength developments. Only those developments that have relevance to the present study and that could be seen as milestones leading up to the present work are briefly described in order to provide the historical context.

The cornerstone work by Salamon and Munro (1967)

Following the Coalbrook disaster in 1960, described by van der Merwe (2000), it was realized that a method to define coal pillar strength was urgently required, as no satisfactory method existed at the time. It was soon seen that laboratory tests on coal specimens would not result in an acceptable outcome. The main problem was that strength is size-dependent and transforming the laboratory test results to real coal pillars was not sufficiently accurate.

It has been shown since the very early times that the strength of a rock pillar, σ_P, can be described by the following fundamental equation:

$$\sigma_P = k w^{\alpha} h^{\beta}, \quad [1]$$

where
k = constant related to the material strength
w = pillar width
h = pillar height
α and β are constants related to material type.

The constant β consistently has negative value. The strength of a pillar is thus directly proportional to its width and inversely proportional to height.

Salamon and Munro (1967) overcame the size obstacle by using cases of failed pillars underground in a statistical analysis to determine the critical parameters. What they essentially did was to set up two databases: one for failed cases (27 cases) and one for unfailed cases (98 cases). The selection criteria are described in the reference. The analysis was thus based on real pillars and not laboratory-sized specimens. Note that the database of failed cases represented the full population of known failures, while the unfailed database was a representative sample of the unfailed cases.

It was reasoned that if both the strength of pillars and the loads imposed on them, σ_L, are known, it would be possible to have a measure of stability. The simplest measure of stability is merely the ratio of pillar strength to the load imposed on it, the safety factor (SF):

$$\mathrm{SF} = \frac{\sigma_P}{\sigma_L} \quad [2]$$

The pillar load is simply assumed to be caused by the weight of the overlying strata, distributed equally over the pillars, or

$$\sigma_L = \rho g H \frac{(w+B)^2}{w^2} \quad [3]$$

where H = depth to floor of the workings
B = bord width.

(Note for clarification – in the context of this paper, ρg is often replaced by 0.025 MN/m^3, and $w + B$ by the pillar centre distance, C).

The maximum likelihood estimation method was used to determine the parameters k, α, and β to be used in Equation [1]. The maximum likelihood function as it was used is based on the assumption that pillars failed at a load equal to their strength, *i.e.* at SF = 1. The method then results in values for k, α, and β that cause the frequency distribution of SF to be as densely concentrated around a value of unity as possible.

The maximum likelihood function also takes account of the existence of unfailed pillars in the sense that the two fundamental requirements in the calculation are that for the failed database, SF = 1 and for the unfailed data base, SF > 1. Yet, the method is much more reliant on the failed cases than the unfailed ones as the first requirement dominates the process.

Although this is not claimed by the authors, criticism of the method includes the salient assumption that at the time of mining, the pillars contained in the failed database had dimensions resulting in SF = 1 – either intentionally or by chance. This is not the case, as pillar sizes were determined by operational requirements more than stability and pillars could thus have any size suiting those operational requirements as long as failure did not occur during the mining operation.

It furthermore assumes that pillar dimensions remained constant over the period until they failed, which is also known not to be the case. It does not explain why pillars fail at vastly different ages, ranging from just a few months to more than 50 years. The authors also noted that it was very likely for different coal seams or regions to have different strength constants, but there was simply not sufficient data to perform the analysis for different areas.

Nonetheless, the constants that Salamon and Munro determined were successfully used in the mining industry for several decades, and while more pillar failures have occurred since the introduction of the formula, there has not been a repeat of the Coalbrook disaster. The additional failures that occurred do not imply that the formula as it was used was incorrect. If anything, they demonstrate the nature of variability, and with that, the power of using a probability of failure approach to pillar design.

Salamon and Munro found the following:

k = 7.2 MPa
α = 0.46
β = –0.66

It has to be noted that while k in terms of the equation equals the strength of a cubic metre of coal, it is not a laboratory-determined unit strength: it is a statistically determined number related to the material strength. For this reason, k should be seen against the background of the linked group of constants. It is

incorrect to develop a new strength formula by merely changing the value of k without at least investigating the impact on α and β.

The early direct strength tests

A comprehensive overview of the attempts to base pillar strength on tests performed underground on larger specimens than can be tested in a laboratory is provided by van Heerden (1975). Although these outcomes did not find application in the South African coal mining industry, they did elsewhere, notably in the USA and Australia.

Direct tests have distinct advantages over the statistically based methods. The most important advantage is that the exact dimensions of the specimen are known at the time of testing. The outcomes are also site-specific and therefore not contaminated by the inclusion of weaker or stronger pillars from other areas or seams. This is confirmed by the fact that different strengths were indeed found for different geographical areas, even within the same coalfield.

The latter advantage is also perhaps the most important disadvantage in the sense that results from one set of tests cannot be summarily applied elsewhere; separate tests will be required for different mines. A summary of the results reported by van Heerden (1975) is given in Table I.

It is noteworthy that in all three cases, it was found that α and β have values of 0.5 and –0.5 respectively, and that two of the three tests resulted in substantially higher values of k than found by Salamon and Munro (1967). It is possible that the tests at Witbank Colliery cannot be directly compared to the other two, as the tests were carried out by ensuring uniform loading across the specimens as opposed to uniform displacement for the other two sets of tests.

Note should also be taken of the work by Wagner (1974), who performed the tests at Usutu Colliery. For the purposes of this paper one of the important conclusions is that large specimens fail by a process of progressive spalling of the pillar sides from the edges towards the core.

Subsequent updates

Over the years following the initial work, updates have been provided at different times although they were not necessarily used by the industry. The updates were prompted primarily by changes in the databases as more information became available from failures that continued to occur. Over time, the database of failed cases increased in size and therefore could be expected to yield more reliable results. By 2012, the database of failed cases had grown from the 27, which was available to Salamon and Munro, to a total of 86 cases. Differentiation of the coalfields and alternative methods of analysis also motivated re-analysis at different times. Table II summarizes the important outcomes over the period after the initial work.

Table I

Results from direct strength tests on large specimens

Colliery	Number of tests	k (MPa)	α	β
New Largo	10	13.3	0.5	–0.5
Usutu	10	11.0	0.5	–0.5
Witbank Colliery	19	4.5	0.5	–0.5

Table II

Summary of updates using statistical back-analysis after 1967

Year	Reason for update	k (MPa)	α	β
1991[1]	New data	5.24	0.63	–0.78
1993[2]	Differentiation (Vaal Basin)	4.5	0.46	–0.66
2003[3]	Differentiation, alternative method of analysis	3.5	1	–1
2006[4]	New data, differentiation	6.19	.67	–0.87
2013[5]	New data, differentiation	6.61	0.5	–0.7
2013[5]	New data, differentiation, alternative method of analysis	5.47	0.8	–1

1 Madden and Hardman (1992)
2 Van der Merwe (1993)
3 Van der Merwe (2003)
4 Salamon, Canbulat, and Ryder (2006) – only the outcomes for the Witbank seams were selected for comparison
5 Van der Merwe and Mathey (2013a)

The alternative method of analysis referred to in Table II is the overlap reduction (OR) method. This method is based on the requirement for a SF that it has to allow the maximum possible separation between the databases of failed and unfailed cases, seeing that the primary purpose of having a SF is to ensure that failure is prevented. It is a standard statistical method that merely calculates the area of overlap between two normal distributions.

It does not pose the requirement that pillars had to be mined with the intention of having a SF of unity and it makes full use of the database of unfailed cases. Nonetheless, it also results in the average SF of failed cases equal to unity, the major difference between this method and the maximum likelihood function being that it does not result in the minimum scatter of SF around a value of unity. It was seen that the outcome from the OR method results in better separation of the databases. It therefore serves the primary function of the safety factor concept, which is to better distinguish between failed and unfailed pillars.

There were two other significant developments that led up to the analysis described in this paper. The first was an attempt to determine the rate of pillar scaling in order to predict the time at which failure can be expected. This was based on the understanding that the reason for delayed pillar failure is that all pillars scale to greater or lesser degrees and that failure will occur only when the pillars have scaled to some critical size. This method was first proposed in 2003 and updated in 2016 (van der Merwe, 2016).

The second development was the establishing of a link between the SF and probability of failure (van der Merwe and Mathey, 2013b). The basis for this development was a comparison of failed cases to the total number of cases in each interval of safety factor, making use of the full population of unfailed cases which was found by extension of the sample database. The reason for the development was to find a more rational way to quantify the measure of stability than can be done with the SF on its own.

Current situation

The current situation as compared to that in 1967 can be summarized as follows:

- The database of failed cases has grown from 27 to 86
- There is now sufficient data to allow differentiation of some coalfields, in particular the Witbank no. 2 and 4 seams and the Highveld seams

- There is a more suitable method of analysis;
- There is a method to determine the amount of pillar scaling over time for the Witbank no. 2 and 4 seams and the Highveld seams
- There is a method to determine the probability of failure for the Witbank no. 2 and 4 seams and the Highveld seams.

However, there is at least one major missing item. The pillar strength, as well as the probability of failure, are still based on the as-mined dimensions of the pillars. It is proposed that this is the cause of some deviations from expectations that still exist, such as the fact that the probability of failure is not 50%, but close to 8%, at SF = 1 using the probabilistic approach as proposed by van der Merwe and Matthey (2013c). The reason for this is that by using the as-mined dimensions and the full population of unfailed pillar cases, there are a number of surviving low safety factor cases in the unfailed database that cannot be ignored. The rest of the paper is devoted to an attempt to overcome this problem.

The existence of those unfailed pillars cannot be explained by using the safety factor concept as the only indicator of pillar stability. This is just another indication that the probabilistic approach should be used in the evaluation of stability.

Basis of the new analysis

The analysis described in this paper is based on a simple concept. The pillar sizes in the database of failed cases were reduced by using the expected scaling rate and applying that over the period between mining and failure. This resulted in the expected pillar sizes at the time of failure. Likewise, the pillar sizes in the unfailed database were reduced by applying the same scaling rates over the period since the time of mining and the year 2012, when the database was created.

The pillar strength was then determined by applying the overlap reduction method to the two adjusted databases. This resulted in pillar strength based on the dimensions of pillars at the time of failure, and not at the time of mining.

The full population of unfailed cases was next determined by extending the sample database by the most reasonable estimate of the number of 'panel units' that exist. The notion of a 'panel unit' was introduced to break up the entire mined area into standardized areas. It has been seen that initial pillar collapse areas are circular, with a diameter approximately equal to the panel width. It is then reasoned that collapses separated by more than 2.5 times the panel width would likely be considered as separate collapses. The 'panel unit' is thus an area described by the panel width and length equal to 2.5 times the panel width.

Finally, the probability of failure was determined by comparing the failed cases in each interval of SF with the total number of panel units in the same intervals.

All this was done by considering the Witbank no. 2 and 4 seams and the Highveld Coalfield only. The outcomes are thus restricted for applicability to those two areas.

The databases

As statistical procedures were used, it is important to describe the databases. The first filter that was applied to the full databases of failed and unfailed cases, as recorded in van der Merwe and Mathey (2013b), was to eliminate all but the Witbank and Highveld no. 2 and 4 seams. From those two remaining collections only those with recorded dates of mining (and failure for the failed database) could be used. This resulted in substantial reduction of the databases.

The database of failed cases then contained 32 cases and the sample database of unfailed cases, 157. This was considered to be sufficient for statistical analysis. The resulting database is contained in the Appendix.

Creating the database for the full population of unfailed cases, which is required to determine the probability of failure, was more challenging. The method described in van der Merwe and Mathey (2013c) was based on firstly estimating the total coal production over time in South Africa using the bord and pillar method. The average extraction ratio was then determined and this resulted in an estimate of the total number of pillars left *in situ*. The next step was to estimate the number of 'panels' by determining the average number of pillars in a panel by simply counting the pillars in typical panels on a number of sample mines. Note that for this investigation, the concept of 'panel units' was used instead of counting pillars on selected mines. At all stages in the previous investigation the average numbers were used.

For this investigation the same basic procedure was used, but given that using average values, especially for lognormal distributions, can result in skewed outcomes, statistically more reliable methods were used. All the variables were subjected to a series of Monte Carlo analyses. The statistical parameters for each were determined from the combined sample databases, since at the time of mining it was not known whether the pillars would fail. For all cases the natural logarithms were used since the distributions were lognormal in nature. Table III summarizes the input values.

The total tons left underground in the form of pillars, T_L, was found by

$$T_L = \frac{T_M(1-e)}{e} \quad [4]$$

where e = extraction ratio
T_M = total tons mined.

The total number of pillars left, P_T, is then T_L divided by the average tons per pillar, based on the distributions of the two items. The number of pillars per panel, P_P is found by

$$P_P = \frac{2.5L_P^2}{C^2} \quad [5]$$

where L_P is the panel width and C is the pillar centre distance.

Finally, the number of panel units, N_P, is simply P_T / P_P.

The final outcome was that a total of 14 500 panel units, based on the median of the resulting lognormal distribution (Figure 1), are likely in existence. The full database contained

Table III

Input used for the Monte Carlo analyses

Parameter	Mean of logs	Standard deviation of dogs
Pillar width	2.19	0.46
Bord width	1.8	0.1
Mining height	1.03	0.39
Extraction ratio	-0.47	0.23
Pillars per panel	5.83	0.86
Panel width	5.20	0.86
Tons per pillar	5.77	1.06

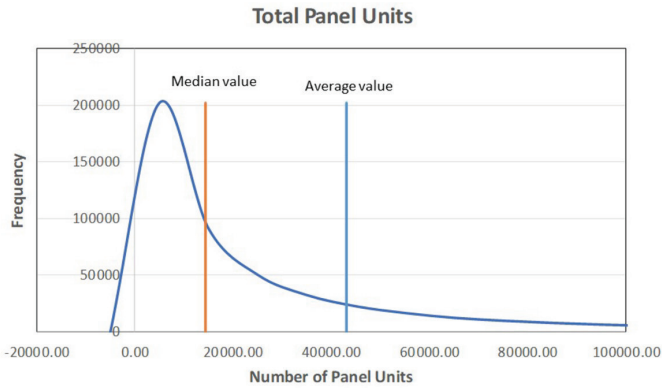

Figure 1—Frequency distribution of total number of 'panel units'. The median value was selected as the indicator of central tendency

65% of all cases in the Witbank and Highveld no. 2 and 4 seams, and this then resulted in the final estimate of 9 400 panel units for the purposes of determining the probability of failure, as described later.

Pillar strength analysis

It has to be emphasized that in this and following sections, all analyses are based on the reduced pillar sizes and comparisons with previous results should be made with great caution.

From van der Merwe (2016) the amount of scaling by which pillar width is reduced, dT, after a time T, is:

$$dT = mh^{x}T^{1-x}, \quad [6]$$

where h = mining height (m)
m = constant, 0.1799
x = constant, 0.7549
T = age of pillars (years).

At any given point in time the reduced pillar width, w_T, is then

$$w_T = w_0 - dT \quad [7]$$

where w_0 is the as-mined pillar width.

Equations [6] and [7] were then applied to the pillars in the databases. For the failed database, the ages of the pillars at the time of collapse were used. For the unfailed database, the year 2012 was used as the base since the database was set up in 2012.

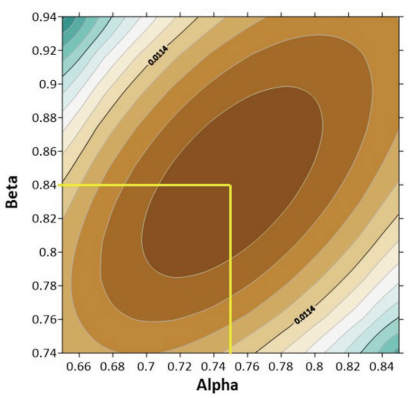

Figure 2—Contours of overlap area for variations of α and β

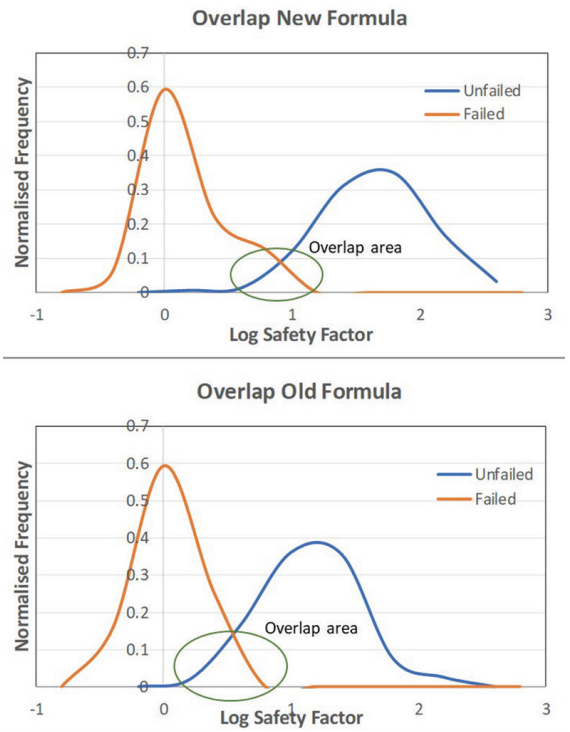

Figure 3—Comparison of distributions of safety factors in the failed and unfailed data bases

The pillar strength was determined by using the OR method, described in van der Merwe and Mathey (2013a). In essence, the values for the parameters α and β are found by iteration to result in the combination that displays the smallest overlap between the frequency distributions of the logarithms of the failed and unfailed cases. Figure 2 is a contour plot of the areas of overlap for the final round of iterations. It was seen that $\alpha = 0.74$ and $\beta = 0.85$ were the optimal values. It was then found that $k_T =$ 10.2 MPa satisfied the criterion that the median of the SF of failed cases should be unity. It is important to note that the material strength constant, k, is in the same range as that found by the direct strength tests (Table I) for which the dimensions at the time of failure were exactly known.

Figure 3 shows the normalized frequency distributions of the logs of the safety factors in the failed and unfailed databases for the previous strength equation as well as the one found in this investigation, indicating the areas of overlap.

The σ-value (standard deviation of the logarithms of SF) is 0.34, which indicates a wider scatter of the SF than with previous investigations. The frequency distributions of the logarithms of the safety factors in the failed database are shown in Figure 4. Note that for the OR method, separation of the databases is the more important criterion. The overlap area between the databases was reduced by 8% compared to the previous investigation (see van der Merwe and Mathey, 2013a).

The equation for pillar strength, which now incorporates the effects of time, is then as follows:

$$\sigma_{S,T} = k_T \frac{w_T^{\alpha}}{h^{\beta}} \quad \text{MPa} \quad [8]$$

In the expanded form the full equation can be written as

$$\sigma_{S,T} = k_T \frac{\left(w_0 - mh^{x}T^{1-x}\right)^{\alpha}}{h^{\beta}} \quad \text{MPa} \quad [9]$$

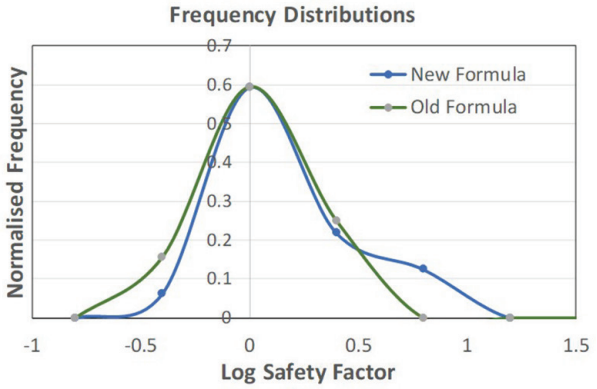

Figure 4—Frequency distributions of the logarithms of the safety factors in the failed database

Note that the pillar load to be used in conjunction with Equation [3] for the determination of the safety factor, should also be based on the reduced pillar width. The load is then expressed by

$$\sigma_{L,T} = \frac{0.025HC^2}{w_T^2} \text{ MPa} \quad [10]$$

where H is the depth to the floor of mining and C is the pillar centre distance, which is not affected by time. The safety factor at any given point in time is then

$$SF_T = \frac{\sigma_{S,T}}{\sigma_{L,T}} \quad [11]$$

Comparison with other pillar strength equations

Figure 5 shows a comparison with other equations for pillar strength. To facilitate comparison, the strength as obtained with Equation [4] was taken at time zero, *i.e.* the as-mined pillar sizes before scaling had taken place was used. The equations selected for comparison are from Wagner (1974), van Heerden (1975), Salamon, Canbulat, and Ryder (2006), and van der Merwe and Mathey (2013a). The mining height used for the comparison was 3.2 m.

The figure clearly shows two distinct groups of curves. The group comprising Salamon, Canbulat, and Ryder (2006) and van der Merwe and Mathey (2013a) predicts significantly lower strength than the group comprising Wagner (1974), van Heerden (1975), and the proposed strength based on Equation [4].

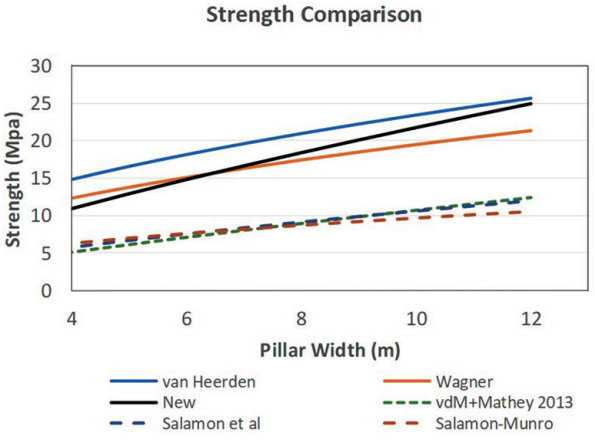

Figure 5—Comparison of pillar strength predicted by different equations

Table IV

Characteristics of the distributions

Database	Mean (logs)	Standard deviation (logs)
Failed	0.07	0.35
Unfailed	1.37	0.44

The most significant difference between the two groups is that for the latter group the actual pillar strength at the time of failure was used in the derivation, while for the former group there was no allowance made for the reduction in pillar width. It is considered significant that the statistical back-analysis based on reduced pillar width at the time of failure is in close agreement with the large-scale direct strength tests.

The implication of this finding is that coal pillars are significantly stronger than predicted by the equations currently in use, but that the strength reduces over time as the pillar width decreases.

Probability of failure

It is well known that the probability of failure is a more rational indicator of pillar stability than the safety factor.

The best way to determine the probability of failure is to compare the number of failed cases in the database to the total number of cases in each interval of safety factor. The full population of the unfailed cases was found by extending the sample database by the ratio of the total number of panel units to the number of recorded cases in the sample database.

For this investigation this proved to be a problem since there was a scarcity of recorded cases in the important part of the distributions, which is the overlap area between the databases of failed and unfailed cases.

The problem was overcome by creating idealized numbers of failed and unfailed cases from the lognormal distributions of those databases. Table IV contains the characteristics of the databases of failed and unfailed cases.

The final result is shown in Figure 6, the probability of failure as a function of the safety factor. The resulting equation is:

$$\text{PoF} = \exp\left(-0.93SF_T^{4.28}\right) \quad [12]$$

According to Equation [12], the PoF has a value of 0.5 at a safety factor of 0.93, which is close to the statistical expectation of 1.0.

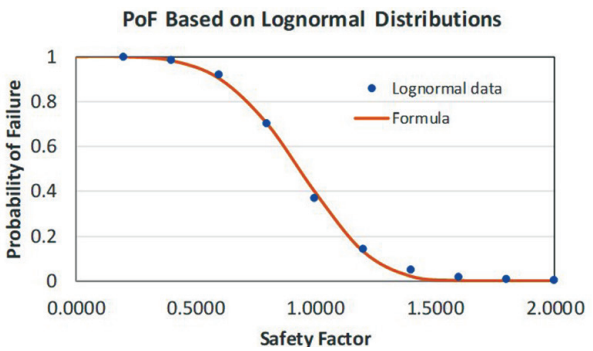

Figure 6—Probability of failure as a function of safety factor

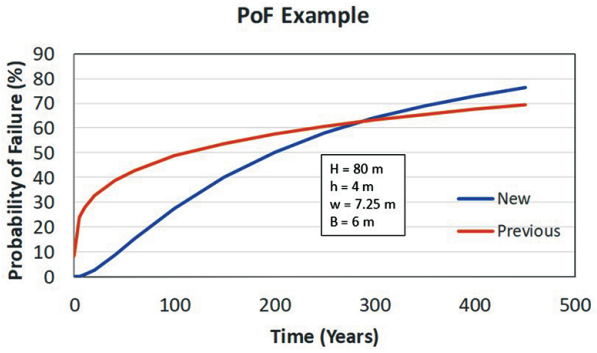

Figure 7—Example of comparison of the increase in probability of failure over time. The as-mined dimensions for the example were chosen such that the initial safety factor was 1.0 as calculated with the van der Merwe and Mathey (2013) pillar strength

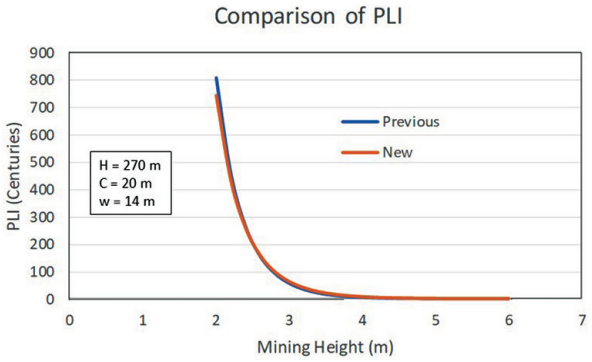

Figure 8—An example showing the similarities between the PLI values for varying mining height obtained with the old and new equations

Equation [12] should not be confused with the equation given for probability of failure in van der Merwe and Mathey (2013c). That equation was based on the as-mined pillar dimensions and does not include the effect of time on pillar sizes. Equation [12], in contrast, is based on the ever-reducing pillar width due to ongoing pillar scaling. It therefore results in the probability of failure at any given point in time. The probability of failure increases over time as the pillar width reduces.

This aspect has been addressed in van der Merwe (2016), but the time-related decay in strength in that publication was based on the strength derived from the as-mined pillar sizes. Figure 7 is an example comparing the previous increase in probability of failure with that obtained from this analysis.

Impact on pillar life index

With the new equation for pillar strength and the more realistic value of safety factor at the point where a failure probability of 50% is reached, the equations for the critical scaling distance had to be adapted. This will have a downstream effect on the pillar life index as reported by van der Merwe (2016).

Following the same line of argument as in van der Merwe (2016), the new equation for the critical scaling distance should calculate the scaling distance that will result in a failure probability of 50%, which implies a safety factor of 0.93. The equation which is then derived from Equations [9] and [10] and with substitution of $\alpha = 0.74$, $\beta = 0.85$, and $k_T = 10.2$ MPa is:

$$d_c = w - [0.002279 H h^{0.85} C^2]^{0.365} \qquad [13]$$

The other equations will remain the same, repeated here for convenience. The pillar life index, PLI, is:

$$\text{PLI} = \left[\frac{d_c}{m h^x}\right]^{(1/1-x)} \qquad [14]$$

where m = constant, 0.1799
x = constant, 0.7549.

The PLI values with the new equation are not substantially different from the ones obtained with the previous equation, see Figure 8 for a comparison.

Number of pillar failures

There is no direct way to compare the expected number of pillar failures with the actual failures, because none of the equations predict definite failure, only the probability of it occurring. However, as a very rough estimate, it could be expected that over a period of time and with a sufficiently large database, it may not be unreasonable to expect that half of the pillars with a failure probability of more than 0.5 would have failed. This means that there is an expectation that if the *pro rata* number of cases with failure probability greater than 0.5 in the combined database of failed and unfailed cases is extended to half of the number of panel units currently in existence to account for the age of the database, there should be some resemblance with the actual number of failures.

On that basis, the following was found:

- Salamon and Munro's equations predicted 149 failures
- The van der Merwe and Matthey equations, after adjusting for pillar scaling, predicted 261 failures
- The equations in this paper also predicted 149 failures.

The actual number of recorded failures in the Witbank and Highveld coalfields was 45, indicating that all three the methods over-estimate the number of failures. This conclusion should be viewed with caution as the method of derivation described above relies on very broad estimates. It should also be borne in mind that pillar failures are rare events (45 recorded cases out of 9 400 panel units) and if, for instance, the assumptions on which the calculation of panel units change only slightly, the predicted outcomes would be different. The only meaningful conclusion that can be reached in this respect is that the equations, as well as reality, indicate that pillar failures are rare events.

Conclusions

Research to find the most suitable way of evaluating coal pillar strength has been ongoing in South Africa since the Coalbrook collapse of 1960. Initially there were two main methods of determination; namely direct strength tests performed on large specimens underground and statistical back-analysis based on recorded cases of pillar failure.

Statistical back-analysis, pioneered by Salamon and Munro (1967), proved to be the preferred method and direct strength tests were not used, or even referred to, for several decades.

The realization that coal pillars scale over time revealed an important disadvantage of the statistical methods as applied previously, namely that the pillar sizes used for the analyses were not correct. Only the as-mined dimensions could be used as the actual pillar sizes at the time of collapse could not be established. By contrast, the actual pillar sizes for the direct tests were known and used.

The real pillars at the time of failure were in fact smaller than the as-mined dimensions used for the statistical analyses.

Therefore, the resulting equations for strength predicted lower values because the pillar sizes used for the analyses were greater than they actually were.

The quantification of the rate of pillar scaling opened the possibility to estimate the pillar sizes at the time of failure. In this investigation, the reduction in pillar size, based on the rates of pillar scaling, was used in the statistical analysis.

The result was that greater pillar strengths than previously determined with the statistical back-analyses were found. Furthermore, the predicted strengths corresponded more to the initial *in-situ* tests than they did to the previous statistical analyses. This correspondence between the *in-situ* tests and the statistical back-analysis based on expected pillar sizes at the time of failure is seen as confirmation that the approach used in this investigation is correct.

The probability of failure, based on the expected real pillar sizes, is linked to the safety factor. It is also shown that now, the safety factor at a 50% probability of failure is very close to the statistical expectation of 1.0. This finding overcomes the apparent anomaly in previous publications, where the safety factor at a probability of failure of 50% is significantly lower.

It is also indicated that the pillar strength reduces and the probability of failure increases over time. The previous considerations were all based on the inherent assumption that pillar sizes are static and do not reduce over time – which is incorrect.

It should always be borne in mind in investigations of this nature that far fewer than 1% (estimates range between 0.3% and 0.5%) of all pillars have failed. The pillar strength and the probability of failure are based on this very small part of the overall database. The data is not perfect and some degree of scatter will always be present in the outcomes. However, it is held that incremental improvement is better than delayed perfection, and the industry can only use the best information available.

In this light, it is recommended that similar analyses be repeated at suitable time intervals, to be determined when new insights into pillar mechanics, better methods of analysis, and more data become available. Pillar stability is not a static consideration and neither should the procedures used for evaluation be. There has to be a process of continual renewal.

References

Madden, B.J. and Hardman, D.R. 1992. Long term stability of bord and pillar workings. *Proceedings of Construction Over Mined Areas, the 5th Conference of the South African Institute of Civil Engineering*.

Salamon, M.D.G. and Munro, A.H. 1967. A study of the strength of coal pillars. *Journal of the South African Institute of Mining and Metallurgy*, vol. 68, no. 2. pp. 55–67.,

Salamon, M.D.G., Canbulat, I., and Ryder, J.A. 2006. Development of seam-specific strength formulae for South African collieries. *Final Report Task 2.16, Coaltech2020*. Coaltech, Johannesburg.

Van der Merwe, J.N. 1993. Revised strength factor for coal in the Vaal Basin. *Journal of the South African Institute of Mining and Metallurgy*, vol. 93, no. 3. pp. 71–77.

Van der Merwe, J.N. 2003. A new coal pillar strength formula for South Africa. *Journal of the South African Institute of Mining and Metallurgy*, vol. 103, no. 5. pp. 281–292.

Van der Merwe, J.N. and Mathey, M. 2013a. Update of coal pillar strength formulae for South African coal using two methods of analysis. *Journal of the Southern African Institute of Mining and Metallurgy*, vol. 113, no. 11. pp. 841–847.

Van der Merwe, J.N. and Mathey, M. 2013b. Update of coal pillar database for South African coal mining. *Journal of the Southern African Institute of Mining and Metallurgy*, vol. 113, no. 11. pp. 825–840.

Van der Merwe, J.N. and Mathey, M. 2013c. Probability of failure of South African coal pillars. *Journal of the Southern African Institute of Mining and Metallurgy*, vol. 113, no. 11. pp. 849–857.

Van der Merwe, J.N. 2016. Review of coal pillar lifespan prediction for the Witbank and Highveld coal seams. *Journal of the Southern African Institute of Mining and Metallurgy*, vol. 116, no. 11. http://dx.doi.org/10.17159/2411-9717/2016/v116n11a11

Van Heerden, W.L. 1975 In situ complete stress-strain characteristics of large coal specimens. *Journal of the South African Institute of Mining and Metallurgy*, March 1975. pp. 207–217

Wagner, H. 1974. Determination of the complete load-deformation characteristics of coal pillars. *Proceedings of the 3rd Congress of the International Society for Rock Mechanics*, Denver, CO. Vol. 2. pp. 1076–1081. ◆

Appendix. Data Bases of failed and unfailed cases.

Failed cases

Seam	Coalfield	Depth [m]	Pillar width [m]	Bord width [m]	Mining height [m]	Year of mining	Year of collapse
H4	Highveld	55.5	7.43	6.62	3.8	1981	2007
H4	Highveld	78.2	10.53	6.47	5.16	1980	2003
H4	Highveld	65	8.38	6.82	3.3	1981	2012
W2	Witbank	86.4	7.5	6.5	4.6	1953	2002
W2	Witbank	102	7.6	6.2	4.5	1954	2005
W1	Witbank	25.9	3.66	8.53	3.05	1917	1921
W2	Witbank	90	7.5	6	4.8	1959	1968
W2	Witbank	62	7.5	6.4	4	1931	1971
W2	Witbank	62	7.3	6.2	4	1930	1982
W2	Witbank	62	6.1	6.1	4	1930	1976
W2	Witbank	62	6.1	6.1	4	1930	1968
W2	Witbank	41	6.4	6.4	6.2	1944	1966
W2	Witbank	41	6.4	6.4	6.2	1944	1988
W2	Witbank	41	6.4	6.4	6.2	1944	1990
W2	Witbank	61	6.1	6.1	4.57	1932	1964
W2	Witbank	57.9	6.1	7.62	3.96	1932	1964
W2	Witbank	21.3	3.96	8.23	4.57	1922	1947
W2	Witbank	29.6	5.18	7.01	5.49	1945	1959

Coal pillar strength analysis based on size at the time of failure

Seam	Coalfield	Depth [m]	Pillar width [m]	Bord width [m]	Mining height [m]	Year of mining	Year of collapse
W2	Witbank	33.5	6.1	6.71	5.49	1946	1950
W2	Witbank	30.5	4.57	7.62	3.66	1915	1919
W2	Witbank	88.4	7.16	6.55	4.88	1959	1962
W2	Witbank	38	6.1	7.6	6.5	1932	2016
W4	Witbank	28.5	3.8	5.8	2.7	1952	1968
W4	Witbank	34	3.5	6.7	2.7	1952	1968
W4	Witbank	34	3.5	6.7	2.7	1952	1971
W4	Witbank	56	5.1	6.5	3.3	1957	1976
W4	Witbank	32	3.3	6.4	2.3	1954	2000
W4	Witbank	32.5	3.2	6.5	2.1	1954	1991
W4	Witbank	43	4.8	6.2	2.8	1965	1991
W4	Witbank	41.1	4.27	6.4	3.05	1955	1959
W4	Witbank	61	4.72	6.86	3.51	1957	1959
W4	Witbank	30.5	3.35	6.4	2.59	1952	1963

Unfailed cases

Seam	Coalfield	Depth [m]	Pillar width [m]	Bord width [m]	Mining height [m]	Year of mining
B Seam	Ermelo	52.5	5.66	6.38	1.7	2003
B Seam	Ermelo	55.7	6.85	6.13	1.7	1999
2	Witbank	122	15.4	6.6	2.5	1997
2	Witbank	122	15.4	6.6	2.5	1997
2	Witbank	82	12	6	3	1997
4	Highveld	68	12.9	7.1	4.06	1997
4	Highveld	72	12.89	7.11	4.15	1997
4	Highveld	81	13.01	6.99	4.31	1997
4	Highveld	84	12.97	7.03	4.31	1997
4	Highveld	79	13.58	6.42	5.89	1997
4	Highveld	71	12.32	6.68	5.84	1997
4	Highveld	73	10.21	6.79	3.93	1997
4	Highveld	83	13.66	6.34	6.13	1997
4	Highveld	77	10.22	6.78	4.05	1997
4C-Lower	Highveld	122	21	6.71	3.29	1997
4C-Lower	Highveld	122	21.2	6.71	3.29	1997
B Seam	Ermelo	35.73	5	6.12	1.73	1997
2	Highveld	93.8	14.7	6	3.2	1996.8
1	Witbank	87.6	12	6	2.8	1996.75
2	Highveld	93.8	14.92	6	3	1996.7
4-Upper	Highveld	203.42	19	6	1.7	1996.6
4-Upper	Highveld	203.42	19	6	1.7	1996.6
2	Witbank	50	10	6	3.8	1996
2	Witbank	122.17	12	6	2.8	1996
2	Witbank	44.55	6	6	3.3	1996
2	Witbank	87.53	12	6	3.6	1996
4	Highveld	66	10.92	7.08	6.45	1996
4	Highveld	76	8.85	7.15	3.48	1996
4	Witbank	36.3	8	6	3.7	1996
4C-Lower	Highveld	92.28	17.07	6.93	3.87	1996
4-Upper	Highveld	178.49	19	6	2.3	1996
4-Upper	Highveld	195.15	20	6	2.1	1996

Coal pillar strength analysis based on size at the time of failure

Seam	Coalfield	Depth [m]	Pillar width [m]	Bord width [m]	Mining height [m]	Year of mining
1	Witbank	83.92	11.47	6	3	1995.75
2	Witbank	98.72	13	6	4	1995
2	Witbank	121.02	13	6	3.5	1995
2	Witbank	68.9	12.9	6	3	1995
4C-Lower	Highveld	151	23.85	6.15	3.34	1995
B Seam	Ermelo	35.5	4.6	6.81	2	1995
2	Witbank	53.86	7	6	5	1994.75
2	Witbank	70.1	12	6	3.35	1994.6
CL	East.Tvl	140.72	15	6	2.7	1994.25
2	Witbank	111.91	13.4	6	3	1994
2	Witbank	108.63	18.5	6	3.65	1994
2	Witbank	108.63	12.5	6	3.38	1993.5
2	Witbank	37.36	10	6	2.8	1993
2	Witbank	70.76	14	6	2.6	1993
4C-Lower	Highveld	171.7	21.19	6.81	2.9	1993
4C-Lower	Highveld	110	17.82	6.18	3.46	1993
4C-Lower	Highveld	146.2	19.89	6.29	2.91	1993
B Seam	Ermelo	25.15	4.39	6.54	1.65	1993
2	Witbank	56.11	7.5	6	3.5	1992
4	Highveld	58.3	8.47	6	3.8	1992
4	Highveld	59.3	11	6	3.7	1992
4C-Lower	Highveld	106	16.47	7.5	3.5	1992
CL	East. Tvl	130.75	15	6	2	1991.92
2	Witbank	108.75	14	6	3	1991.75
2	Witbank	40.07	7.5	6	3.2	1991
2	Witbank	44.55	12	6	3	1991
2	Witbank	40.3	8	6	2.1	1991
4	Highveld	50	9.3	5.7	3.65	1991
4C-Lower	Highveld	109	17.5	6.48	3.67	1991
4C-Lower	Highveld	124.9	18.27	5.73	2.67	1991
CU-CL	East. Tvl	104.76	12	6	4.8	1991
No. 4	Highveld	55.2	8.98	6.96	3.95	1991
4	Highveld	169	21.81	6.19	2.58	1990.5
2	Witbank	77.65	12	5.84	3.8	1990
2	Witbank	40.07	8	6	3.2	1990
2	Witbank	44.55	12	6	2.5	1990
2	Witbank	52.8	11.3	6	3	1990
4	Highveld	46.1	7.1	6.9	3.8	1990
4	Highveld	54	8.52	6.48	3.69	1990
4C-Lower	Highveld	154	21.37	6.26	2.72	1990
2	Highveld	93.8	14	6	3.6	1989.9
CU-CL	East. Tvl	114.3	12	6	2.6	1989.67
CU-CL	East. Tvl	119.41	15	6	2.3	1989.17
2	Witbank	36.53	7	6	3	1989
4	Highveld	70	10.68	6.32	3.25	1989
4	Highveld	49	8.57	6.43	3.69	1989
4	Highveld	56	8.59	6.41	3.63	1989
4C-Lower	Highveld	170	22	6	2.6	1989
4C-Lower	Highveld	106	15.84	6.35	3.16	1989
CU-CL	East. Tvl	83.43	12	6	2.8	1988.92
CU-CL	East. Tvl	114.35	12	6	2.3	1988.42

Coal pillar strength analysis based on size at the time of failure

Seam	Coalfield	Depth [m]	Pillar width [m]	Bord width [m]	Mining height [m]	Year of mining
2	Witbank	34.6	12.21	5.6	3.4	1988
2	Witbank	34.15	8	6	3	1988
2	Witbank	38.37	8.1	6.4	5.9	1988
4	Witbank	67.8	11	6	4	1988
4	Witbank	67.8	11.73	6	4	1988
B Seam	Ermelo	80.5	6.58	6.39	1.65	1988
No. 4	Highveld	30.35	8.96	6.06	3.85	1988
4	Highveld	57	9.35	6.65	3.65	1987
4	Highveld	64.92	9	6	3.72	1987
4C-Lower	Highveld	137	21.82	5.84	2.84	1987
B Seam	Ermelo	54.6	5.67	6.37	1.6	1987
B Seam	Ermelo	40.33	4.53	6.52	1.83	1987
4	Highveld	64.92	20.57	6	3.5	1986.8
4	Highveld	64.92	9	6	3.6	1986.8
2	Witbank	52.8	8	6	3	1986
CU-CL	East. Tvl	101.21	12	6	2.3	1985.75
4	Highveld	55	11.8	6.2	3.41	1985
2	Highveld	94	10.22	6.78	3	1984
2	Highveld	94	10.2	6.8	2.8	1984
2	Witbank	70	15	6	3	1984
4	Highveld	65	10.98	6.02	3.2	1984
No. 4	Witbank	36.5	7.25	6.3	2.68	1984
2	Witbank	79.92	9	6	2.9	1983
4	Highveld	68	11.66	6.34	3.4	1983
4	Highveld	46	8.6	6.4	3.55	1983
4	Highveld	51	8.65	6.35	3.64	1983
No. 4	Highveld	57.34	9.07	5.99	3.84	1983
No. 4	Witbank	25.7	6.15	6.17	2.6	1983
4	Highveld	68	10.87	6.13	3.37	1982
4	Highveld	75	10.7	6.3	3.41	1982
4	Highveld	74	9.9	7.1	3.33	1982
4	Witbank	42.8	7	6	2.2	1982
4	Highveld	51.8	10.98	6.02	2.88	1981.5
4	Highveld	51	8.89	6.11	3.27	1981
4	Highveld	74	11.31	5.69	3.41	1981
4	Highveld	54	8.92	6.08	3.58	1981
4	Highveld	77	10.04	5.96	2.94	1981
4	Highveld	78	10.7	6.3	3.35	1981
4	Highveld	73	10.63	6.37	3.85	1981
4	Highveld	75	11.03	5.97	5.5	1981
4	Highveld	71	10.7	6.3	5.5	1981
4	Highveld	76	10.8	6.2	5.5	1981
4	Witbank	62.48	10	6	2.2	1981
4	Witbank	62.48	15	6	2.1	1981
4	Witbank	62.48	9	6	2.25	1981
No. 4	Highveld	41.35	8	5.98	3.6	1981
No. 4	Witbank	24.15	6.1	6.25	2.65	1981
2	Witbank	118.62	15	6	3.5	1980.25
2	Witbank	64.47	9	6	1.89	1980
2	Witbank	33.8	8	6	2.4	1980
4	Highveld	75	10.03	6.97	3.07	1980

Coal pillar strength analysis based on size at the time of failure

Seam	Coalfield	Depth [m]	Pillar width [m]	Bord width [m]	Mining height [m]	Year of mining
4	Highveld	77	9.81	7.19	4.86	1980
No. 4	Highveld	36.2	5.7	6.27	3.8	1980
No. 4	Highveld	39.95	6.89	6.08	3.7	1980
2	Witbank	55.75	11	6	3	1978.7
2	Witbank	55.75	10.28	6	2.8	1978
No. 4	Witbank	39.1	6.63	6.36	2.6	1978
2	Witbank	34.5	5.5	6.5	5.5	1977
2	Witbank	70.79	12	6	2.2	1975.5
2	Witbank	84.84	7	6	2.26	1974
2	Witbank	84.84	7	6	2.26	1974
2	Witbank	84.84	7	6	2.26	1974
2	Witbank	63.64	14	6	3	1972.75
No. 4	Witbank	18.58	4.86	6.16	2.78	1970
No. 4	Witbank	21.5	5.09	5.96	2.75	1969
No. 4	Witbank	30.55	8.07	7.11	3.2	1968
No. 4	Witbank	66.95	7.77	7.5	3	1968
No. 4	Witbank	26.51	4.32	6.68	2.65	1967
No. 2	Witbank	64.79	13.03	5.37	3.08	1965
No. 4	Witbank	47.07	8.29	6.89	3.37	1965
No. 4	Witbank	44.95	5.03	6.01	2.68	1965
No. 4	Witbank	40.86	7.55	7.63	2.92	1957
No. 2	Witbank	98.15	12.56	5.23	2.65	1956
No. 4	Witbank	49.82	7.63	7.67	3.05	1953

Diamonds – Source to Use — 2020 Conference

Innovation and Technology

9 June 2020 — A technical and economic guide to diamond process engineering workshop and Technical Visits

10 June 2020 — Conference

11 June 2020 — Conference and Site Visit (SAB World of Beer)

The Birchwood Hotel & OR Tambo Conference Centre, Johannesburg

BACKGROUND

The *Diamonds – Source to Use* conference series targets the full spectrum of the diamond pipeline, from exploration through to sales and marketing. The 2020 conference, the eighth in the series, will focus on advances in the mining and metallurgical aspects as well as many of the downstream and related industries

KEYNOTE SPEAKER

L. Hockaday, *Mintek – Renewable Energy Technology*

D. Collins
Mac Consulting

OBJECTIVE

The objective of the conference is to provide a forum for the dissemination of information relating to the latest tools and techniques applicable to all stages of the diamond industry, from exploration through mine design, processing, to cutting, marketing, and sales.

WHO SHOULD ATTEND

- Geologists
- Mineral (diamond) resource managers
- Mining engineers
- Process engineers
- Consultants
- Suppliers
- Sales/marketing
- Diamantaires
- Mine managers
- Mining companies
- Students

2 ECSA CPD points,
24 GSSA CPD points and
3 SACNASP CPD points
will be allocated to
all attending delegates

TOPICS

- Geology and exploration
- Mine expansion projects
- Mining, metallurgy, and processing technology
- Rough diamond sales and marketing
- Cutting, polishing, and retail
- Synthetic diamonds
- Financial services and industry analysis
- Industry governance, beneficiation, and legislation
- Mine-specific case-studies

Site visits

- **Epiroc South Africa**
- **Multotec South Africa**
- **SAB World of Beer Tour & Tasting**

For further information contact:
Camielah Jardine • Head of Conferencing · SAIMM
P O Box 61127 • Marshalltown 2107 • Tel: (011) 834-1273/7 • Fax: (011) 833-8156 or (011) 838-5923
E-mail: camielah@saimm.co.za • Website: http://www.saimm.co.za

SAIMM
THE SOUTHERN AFRICAN INSTITUTE OF MINING AND METALLURGY

SAIMM
THE SOUTHERN AFRICAN INSTITUTE OF MINING AND METALLURGY

Hydrometallurgy Colloquium

Impurity removal in hydrometallurgy

17–18 September 2019

Glenhove Conference Centre, Melrose Estate, Johannesburg

BACKGROUND

Removal of impurity metals plays a very important role in the final grade and quality of the target metals recovered in hydrometallurgical processes. From base to precious metals, a proper consideration of a metal separation and impurity removal circuit can have a huge impact on the success of an operation. This course aims to enhance knowledge in the separation and removal of metal ions in solution, with focus being on solvent extraction, ion exchange, precipitation cementation, membrane separation. Selected current practice and new technologies applicable to base metals, precious metals, uranium etc. will be considered.

WHO SHOULD ATTEND

> Process engineers (chemical, metallurgical) who would like a refresher course or enhance their knowledge on techniques used for impurity removal in hydrometallurgy.

> Graduates from other disciplines such as chemistry or environmental science, who are involved in related work.

> Plant operators who wish to enhance their skills and knowledge.

> University postgraduate students.

SPEAKERS

Allan Nesbitt
Tibsen Technologies

Simon Pitts
DuPont

Peter Cole
Peter Cole Metallurgical Services

Alison Lewis
University of Cape Town

FOR FURTHER INFORMATION CONTACT:
Camielah Jardine • Head of Conferencing • Saimm
Tel: +27 11 834-1273/7 • Fax: +27 11 833-8156
E-mail:camielah@saimm.co.za •Website: http://www.saimm.co.za

NATIONAL & INTERNATIONAL ACTIVITIES

2019

18–21 August 2019 — Copper 2019
Vancouver Convention Centre, Canada
Contact: Brigitte Farah
Tel: +1 514-939-2710 (ext. 1329), E-mail: metsoc@cim.org
Website: http://com.metsoc.org

19–22 August 2019 — Southern African Coal Processing Society 2019 Conference and Networking Opportunity
Graceland Hotel Casino and Country Club, Secunda
Contact: Johan de Korte, Tel: 079 872-6403
E-mail: dekorte.johan@gmail.com
Website: http://www.sacoalprep.co.za

28–30 August 2019 — IFAC MMM 2019 Symposium
Stellenbosch Institute for Advanced Studies Conference Centre, Stellenbosch, Cape Town
Email: info@ifacmmm2019.orgWebsite: https://www.ifacmmm2019.org

4–5 September 2019 — Surface Mining Masterclass 2019
Birchwood Hotel & OR Tambo Conference Centre, Johannesburg
Contact: Camielah Jardine
Tel: +27 11 834-1273/7, Fax: +27 11 838-5923/833-8156
E-mail: camielah@saimm.co.za, Website: http://www.saimm.co.za

11–12 September 2019 — Revitalising exploration activity in southern Africa
'Potential for Exploration'
Misty Hills Country Hotel & Conference Centre, Muldersdrift, Johannesburg
Contact: Camielah Jardine
Tel: +27 11 834-1273/7, Fax: +27 11 838-5923/833-8156
E-mail: camielah@saimm.co.za, Website: http://www.saimm.co.za

17–18 September 2019 — Hydrometallurgy Colloquium 2019
'Impurity removal in hydrometallurgy'
Glenhove Conference Centre, Melrose Estate, Johannesburg
Contact: Camielah Jardine
Tel: +27 11 834-1273/7, Fax: +27 11 838-5923/833-8156
E-mail: camielah@saimm.co.za, Website: http://www.saimm.co.za

31 October–1 November 2019 — International Mine Health and Safety Conference 2019
Misty Hills Country Hotel & Conference Centre, Muldersdrift, Johannesburg
Contact: Camielah Jardine
Tel: +27 11 834-1273/7, Fax: +27 11 838-5923/833-8156
E-mail: camielah@saimm.co.za, Website: http://www.saimm.co.za

1 November 2019 — SAIMM YPC Namibia Technical Conference 2019
Roof of Africa Hotel and Conference Cente, Namibia
Contact: Camielah Jardine
Tel: +27 11 834-1273/7, Fax: +27 11 838-5923/833-8156
E-mail: camielah@saimm.co.za, Website: http://www.saimm.co.za

13–15 November 2019 — XIX International Coal Preparation Congress & Expo 2019
New Delhi, India
Contact: Coal Preparation Society of India
Tel/Fax: +91-11-26136416, 4166 1820
E-mail: cpsidelhi. india@gmail.com, president@cpsi.org. inrksachdev01@gmail.com, hi.sapru@monnetgroup.com

18-22 November 2019 — Coal Pillar Design Course 2019
The Estuary Hotel, South Coast, KwaZulu-Natal
Contact: Camielah Jardine
Tel: +27 11 834-1273/7, Fax: +27 11 838-5923/833-8156
E-mail: camielah@saimm.co.za, Website: http://www.saimm.co.za

2020

12–13 February 2020 — Tailing Storage Conference 2019
'Investing in a Sustainable Future'
Birchwood Hotel & OR Tambo Conference Centre, Johannesburg
Contact: Camielah Jardine
Tel: +27 11 834-1273/7, Fax: +27 11 838-5923/833-8156
E-mail: camielah@saimm.co.za, Website: http://www.saimm.co.za

25–26 February 2020 — SAMCODES Conference 2020
'Good Practice and Lessons Learnt Industry Reporting Standards'
The Birchwood Hotel & OR Tambo Conference Centre, Johannesburg
Contact: Camielah Jardine
Tel: +27 11 834-1273/7, Fax: +27 11 838-5923/833-8156
E-mail: camielah@saimm.co.za, Website: http://www.saimm.co.za

25–29 May 2020 — The 11th International Conference on Molten Slags, Fluxes and Salts 2020
The Westin Chosun Seoul Hotel, Seoul, Korea
Tel: +82-2-565-3571
Email: secretary@molten2020.org
http://www.molten2020.org

9–11 June 2020 — Diamonds – Source to Use — 2020 Conference
'Innovation and Technology'
Birchwood Hotel & OR Tambo Conference Centre, Johannesburg
Contact: Camielah Jardine
Tel: +27 11 834-1273/7, Fax: +27 11 838-5923/833-8156
E-mail: camielah@saimm.co.za, Website: http://www.saimm.co.za

14–17 June 2020 — 2nd European Mineral Processing and Recycling Congress – EMPRC 2020
Aachen, Germany
Contact: Jürgen Zuchowski
Email: gdmb@gdmb.de
Website: https://emprc.gdmb.de

22 June 2020 — Renewable Solutions for Energy Intensive Industry Colloquium 2020
Kathu, Northern Cape
Contact: Camielah Jardine
Tel: +27 11 834-1273/7, Fax: +27 11 838-5923/833-8156
E-mail: camielah@saimm.co.za, Website: http://www.saimm.co.za

24-25 June 2020 — 3rd School on Manganese Ferroalloy Production 2020
Kathu, Northern Cape
Contact: Camielah Jardine
Tel: +27 11 834-1273/7, Fax: +27 11 838-5923/833-8156
E-mail: camielah@saimm.co.za, Website: http://www.saimm.co.za

4–7 October 2020 — Massmin2020 Eight International Conference on Mass Mining
Santiago, Chile
Contact: J.O. Gutiérrez
Tel: (56-2) 2978 4476, www.minas.uchile.cl

18–22 October 2020 — IMPC XXX International Mineral Processing Congress 2020
Cape Town International Convention Centre, Cape Town
Contact: Camielah Jardine
Tel: +27 11 834-1273/7, Fax: +27 11 838-5923/833-8156
E-mail: camielah@saimm.co.za, Website: http://www.saimm.co.za

Company affiliates

The following organizations have been admitted to the Institute as Company Affiliates

3M South Africa (Pty) Limited
AECOM SA (Pty) Ltd
AEL Mining Services Limited
Air Liquide (PTY) Ltd
Alexander Proudfoot Africa (Pty) Ltd
AMEC Foster Wheeler
AMIRA International Africa (Pty) Ltd
ANDRITZ Delkor(pty) Ltd
Anglo Operations Proprietary Limited
Anglogold Ashanti Ltd
Arcus Gibb (Pty) Ltd
ASPASA
Atlas Copco Holdings South Africa (Pty) Limited
Aurecon South Africa (Pty) Ltd
Aveng Engineering
Aveng Mining Shafts and Underground
Axis House Pty Ltd
Bafokeng Rasimone Platinum Mine
Barloworld Equipment -Mining
BASF Holdings SA (Pty) Ltd
BCL Limited
Becker Mining (Pty) Ltd
BedRock Mining Support Pty Ltd
BHP Billiton Energy Coal SA Ltd
Blue Cube Systems (Pty) Ltd
Bluhm Burton Engineering Pty Ltd
Bouygues Travaux Publics
CDM Group
CGG Services SA
Coalmin Process Technologies CC
Concor Opencast Mining
Concor Technicrete
Council for Geoscience Library
CRONIMET Mining Processing SA Pty Ltd
CSIR Natural Resources and the Environment (NRE)
Data Mine SA
Digby Wells and Associates
DRA Mineral Projects (Pty) Ltd
DTP Mining - Bouygues Construction
Duraset
Elbroc Mining Products (Pty) Ltd
eThekwini Municipality
Expectra 2004 (Pty) Ltd
Exxaro Coal (Pty) Ltd
Exxaro Resources Limited
Filtaquip (Pty) Ltd
FLSmidth Minerals (Pty) Ltd
Fluor Daniel SA (Pty) Ltd
Franki Africa (Pty) Ltd-JHB
Fraser Alexander (Pty) Ltd
G H H Mining Machines (Pty) Ltd
Geobrugg Southern Africa (Pty) Ltd
Glencore
Hall Core Drilling (Pty) Ltd
Hatch (Pty) Ltd
Herrenknecht AG
HPE Hydro Power Equipment (Pty) Ltd
Immersive Technologies
IMS Engineering (Pty) Ltd
Ingwenya Mineral Processing
Ivanhoe Mines SA
Joy Global Inc.(Africa)
Kudumane Manganese Resources
Leco Africa (Pty) Limited
Longyear South Africa (Pty) Ltd
Lull Storm Trading (Pty) Ltd
Maccaferri SA (Pty) Ltd
Magnetech (Pty) Ltd
Magotteaux (Pty) Ltd
Maptek (Pty) Ltd
MBE Minerals SA Pty Ltd
MCC Contracts (Pty) Ltd
MD Mineral Technologies SA (Pty) Ltd
MDM Technical Africa (Pty) Ltd
Metalock Engineering RSA (Pty)Ltd
Metorex Limited
Metso Minerals (South Africa) Pty Ltd
Micromine Africa (Pty) Ltd
MineARC South Africa (Pty) Ltd
Minerals Council of South Africa
Minerals Operations Executive (Pty) Ltd
MineRP Holding (Pty) Ltd
Mintek
MIP Process Technologies (Pty) Limited
Modular Mining Systems Africa (Pty) Ltd
MSA Group (Pty) Ltd
Multotec (Pty) Ltd
Murray and Roberts Cementation
Nalco Africa (Pty) Ltd
Namakwa Sands(Pty) Ltd
Ncamiso Trading (Pty) Ltd
New Concept Mining (Pty) Limited
Northam Platinum Ltd - Zondereinde
Opermin Operational Excellence
Optron (Pty) Ltd
PANalytical (Pty) Ltd
Paterson & Cooke Consulting Engineers (Pty) Ltd
Perkinelmer
Polysius A Division of Thyssenkrupp Industrial Sol
Precious Metals Refiners
Ramika Projects (Pty) Ltd
Rand Refinery Limited
Redpath Mining (South Africa) (Pty) Ltd
Rocbolt Technologies
Rosond (Pty) Ltd
Royal Bafokeng Platinum
Roytec Global (Pty) Ltd
RungePincockMinarco Limited
Rustenburg Platinum Mines Limited
Salene Mining (Pty) Ltd
Sandvik Mining and Construction Delmas (Pty) Ltd
Sandvik Mining and Construction RSA (Pty) Ltd
SANIRE
Schauenburg (Pty) Ltd
Sebilo Resources (Pty) Ltd
SENET (Pty) Ltd
Senmin International (Pty) Ltd
Smec South Africa
Sound Mining Solution (Pty) Ltd
Speciality Construction Products (Pty) Ltd
SRK Consulting SA (Pty) Ltd
Time Mining and Processing (Pty) Ltd
Timrite Pty Ltd
Tomra (Pty) Ltd
Ukwazi Mining Solutions (Pty) Ltd
Umgeni Water
Webber Wentzel
Weir Minerals Africa
Welding Alloys South Africa
Worley Parsons RSA (Pty) Ltd

UNIVERSITY STUDENT BODIES

The SAIMM YPC Career and Leadership Conference is aimed at enhancing students' leadership skills and to provide them with an opportunity to interact with various stakeholders. The conference fulfils a need for students to acquire additional soft skills that will serve them well in their future career paths. These student bodies organise the conference on a rotational basis.

UNISA	UNISA	**UNISA Mining Society (UMS)** is a structure which exists within the University of South Africa (UNISA). UMS which is an acronym for UNISA Mining Society acknowledges its existence as an autonomous substructure of Science Engineering and Technology Student Association (SETSA). UMS represents students in Mining Engineering and Mine Survey.
UP	MYNBOU TUKS MINING	**The Tuks Mining Society (TMS)** is a student led society and the sub-house of mining department; which forms part of Engineering Built-Environment and Information Technology (EBIT). It is under the supervision of the mining department and aims not only at enhancing students social and leadership skills, but also creates a platform for students to network with other students, lecturers, alumni members and industry professionals. It was founded in the 1990's with the initial purpose of addressing the social needs of its members.
	Metallurgical Engineering	The **Metallurgical Sub-house** is a student organisation of the Department of Material Science and Metallurgical Engineering at the University of Pretoria. The main objectives of the Sub-House are to serve as a communication link between students in the Department of Materials Science and Metallurgical Engineering and the staff members, to assist in organizing academic, social and other events for the department and to assist in marketing Metallurgical Engineering as a career and a study field.
WITS	SCHOOL OF CHEMICAL AND METALLURGICAL ENGINEERING	The **CHMT (Chemical and Metallurgy) School Council** is an extension and operates under the governance of the SRC. We are here to voice out our students' concerns, interests and suggestions.
	SCHOOL OF MINING ENGINEERING	The **Mining Engineering Student Council (MESC)** is committed to exemplary student leadership in defining competent Mining Engineer that the Wits School of Mining Engineering is producing for the mining industry and the country at large. To this end, it aims to encourage academic excellence and promote equality of opportunity through effective, accountable and transparent student leadership.
	S.M.E.S	The **Student in Mining Engineering Society (SMES)** is a student body recognised by Wits University with the main objective to represent and address the social needs of its members (mainly consisting of Wits Mining Engineering Students). It is concerned with linking students to the school, alumni and the industry through different events.
UJ	MINING FORUM	We, the school of mines students of the University of Johannesburg, drawn from various cultural, religious, social, economic and political backgrounds, conscious of the historic disparities within the South African mining industry in general; and committed to the building and sustenance of a non-racial, non-sexist and democratic institution.
	Metallurgical Engineering Student Organisation MESO EXTRACT AND CAST YOUR FUTURE	**MESO** is an organisation concerned with the holistic development of its constituents. Academic excellence combined with social development is a goal that is to be reached. MESO seeks to create an environment that will allow for an improved relationship between students and the Metallurgical department. Our aim is also to build a bridge between students and the institution (University of Johannesburg) and industry.
	UJ 2016 WOMEN IN MINING	**Women in Mining** of the University of Johannesburg is a constituency of female students in mining related courses (namely; Mining Engineering, Mineral Surveying and Metallurgical Engineering). We are the flowers of our nation, springing from different roots of cultures, religion and race. In unity, we stand through our diversity with the main aim to empower each other.

The Southern African Institute of Mining and Metallurgy

is proud to present the

16th Annual Student Colloquium

Embracing Technology and Innovation in the Minerals Industry

YOUNG PROFESSIONALS COUNCIL

THE SOUTHERN AFRICAN INSTITUTE OF MINING AND METALLURGY

Supported by

UNIVERSITY OF JOHANNESBURG

UNIVERSITEIT VAN PRETORIA
UNIVERSITY OF PRETORIA
YUNIBESITHI YA PRETORIA
Denkleiers • Leading Minds • Dikgopolo tša Dihlalefi

NAMIBIA UNIVERSITY OF SCIENCE AND TECHNOLOGY

NWU®
NORTH-WEST UNIVERSITY
NOORDWES-UNIVERSITEIT
YUNIBESITI YA BOKONE-BOPHIRIMA

Tshwane University of Technology
We empower people

VUT
Vaal University of Technology
Your world to a better future

UNISA university of south africa

UNIVERSITY OF THE WITWATERSRAND, JOHANNESBURG

Date: 16 October 2019

Venue: The Canvas Riversands, Fourways, Johannesburg

The Southern African Institute of Mining and Metallurgy has been organizing and presenting the annual Student Colloquium since 2002, to afford the best final-year mining and metallurgical students an opportunity to present their final year projects to an audience of mining and metallurgical industry experts.

These students are our future young professionals and will be fundamentally affected by how the industry operates. We have to support and assist our future young professionals! As Nelson Mandela observed: 'Education is the most powerful weapon which you can use to change the world'.

The SAIMM cordially invites our experts in the field to meet the fine calibre of young professionals who are about to embark on their careers in industry. There are 11 mining and 11 metallurgical presentations planned for the event, to be held at Johannesburg on 16 October 2019 . The top five in each discipline will have the opportunity to be published in the prestigious SAIMM Journal in April 2020. The presentations selected will be required to be submitted in the form of draft papers before 8 October 2019.

Our strategy is: To contribute to the nurturing of prosperous and empowered young professionals.

FOR FURTHER INFORMATION CONTACT:
Camielah Jardine | Head of Conferencing | SAIMM
E-mail: camielah@saimm.co.za | Tel: +27 11 834 1273/7 | Website: www.saimm.co.za